



Checkliste Habilitation

Einreichung Unterlagen bei der Beförderungskommission

- Ausführlicher Lebenslauf, inklusive Facharzt-Diplom, Dissertationsurkunde(n) oder Promotionsurkunde(n), PhD-Abschlüsse, etc.**
 - Angabe des Bürgerortes (Schweizer/in), ansonsten Geburtsort
 - Privat- und Geschäftsadresse mit E-Mail-Adresse und Telefon, aktuelle Funktion
- Nachweis Lehre**
 - Nachweis von mindestens 14 Stunden im Rahmen der Aus-, Weiter- und Fortbildung in der Humanmedizin in den letzten drei Jahren, mit Formular „Nachweis der geleisteten Lehrveranstaltungen“.
- Publikationsliste**
 - Mit Angabe des Impact Factors (im aktuellen Jahr) pro Publikation für die Originalarbeiten.
 - Die 3 Publikationen von hohem wissenschaftlichen Wert markieren.
 - Bei Einreichung noch unveröffentlichter Artikel: Bestätigungsschreiben des Journals muss beigelegt sein – und diese Artikel müssen ebenfalls markiert werden.
 - Bei kumulativer Habilitationsschrift: in Publikationsliste markieren, welche Artikel in Habilitationsschrift behandelt werden. Diese Artikel in Habilitationsschrift einbinden und die besten 3 behandelten Artikel zusätzlich in Publikationsliste markieren.
- Abstract der Habilitationsschrift mit Deckblatt**
 - maximal 1 Seite und Deckblatt, zusammengeheftet
- Fachvertretergutachten**
- Formular „Besprechung an Fachbereichssitzung“ mit allen Unterschriften**
- Vorschlag von 4 Gutachtern und Gutachterinnen**
 - 2 Professuren der UZH, 2 externe Professuren
- Kopie der Kurs- oder Weiterbildungsbestätigung im Bereich der Hochschuldidaktik (Didaktikkurs)**
- 3 Themenvorschläge für die Probevorlesung**
 - 1 Vorschlag aus dem engen Gebiet, 2 Vorschläge aus dem weiteren Gebiet
- Habilitationsschrift**
 - Es darf keine Überlappung zwischen Habilitationsschrift und eigenen Dissertationen (MD, PhD) bestehen.
 - A4 Format, gebunden gemäss Vorschriften zur Bindung
 - Deckblatt oder Etikette vorhanden
 - korrekte Gliederung des Inhalts
- 3 Publikationen von hohem wissenschaftlichen Wert**
 - Diese 3 Artikel dürfen nicht für die kumulative Habilitationsschrift verwendet werden
- alle Unterlagen elektronisch (PDF) senden an olga.zalesko@dekmmed.uzh.ch**

Datum: 7.11.2018

Unterschrift: [Signature]



**Universität
Zürich^{UZH}**

**Habilitation
Besprechung an Fachbereichssitzung**

**Medizinische Fakultät
Dekanat**

Universität Zürich
Medizinische Fakultät, Dekanal
Bereich Fakultätsgeschäfte
Pestalozzistrasse 3/5
CH-8091 Zürich
www.med.uzh.ch

Dieses Formular muss ausgefüllt und von der Fachvertreterin / vom Fachvertreter unterzeichnet werden. Danach wird es zusammen mit den weiteren Unterlagen zur nächsten Fachbereichssitzung beim Sekretariat der Leiterin / dem Leiter des entsprechenden Fachbereichs eingereicht (mind. 10 Tage vor Sitzungsdatum und in 1 PDF-Datei zusammengefasst).

Nach der Besprechung an der Fachbereichssitzung wird das von der Fachbereichsleiterin / vom Fachbereichsleiter unterzeichnete Formular der Habilitandin / dem Habilitanden ausgehändigt.

Die Habilitandin / der Habilitand kann ab dem Moment, wo sie / er dieses Formular von allen Stellen unterzeichnet zurückhält ihre / seine Unterlagen bei der Beförderungskommission einreichen, gemäss Checkliste auf www.med.uzh.ch/Habilitation.

Angaben zur Fachvertreterin / zum Fachvertreter:

Wer meldet die Habilitandin / den Habilitanden an?
Prof. Dr. Erich Seifritz

Angaben zur Habilitandin / zum Habilitanden:

Vollständiger Name und akademische Titel:
Dr. med. univ. Philipp Homan, PhD

Tätigkeit:
Oberarzt

Arbeitsort:
Universitätsklinik für Psychiatrie, Zürich

Lehrgebiet, deutsche Bezeichnung:
Psychiatrie und Psychotherapie

Lehrgebiet, englische Bezeichnung:
Psychiatry and Psychotherapy

Bürgerort:
bei Schweizer Staatsbürgern Bürgerort,
ansonsten bitte Geburtsort:
Regensburg

Geburtsdatum:
13.02.1980

Wohnort:
Zürich

Total der Originalpublikationen:
29

Unterschrift der Fachvertreterin / des Fachvertreters: 

Datum Besprechung im Fachbereich:
10.09.2019
v20180723

Postfach 1931, 8032 Zürich

Universität Zürich
Medizinische Fakultät, Dekanat
Prof. Dr. Rainer Weber
Dekan
Pestalozzistrasse 3/5
8091 Zürich

Psychiatrische Universitätsklinik Zürich
**Klinik für Psychiatrie, Psychotherapie und
Psychosomatik**
Lenggstrasse 31, Postfach 1931
8032 Zürich
Telefon +41 (0)44 384 23 12
Telefax +41 (0)44 384 27 19
Zentrale +41 (0)44 384 21 11
sekretariat.seifritz@bli.uzh.ch
www.pukzh.ch

Direktor Klinik für Psychiatrie, Psychotherapie und
Psychosomatik:
Prof. Dr. med. Erich Seifritz

Zürich, 30. August 2019

**Habitationsantrag von Herrn Dr. med. univ. Philipp Homan, PhD, geb.
13.02.1980**

Sehr geehrter Herr Dekan, lieber Rainer

Gerne möchte ich Herrn Homan zur Habilitation an der MeF der UZH anmelden.

Beruflicher Werdegang

Philipp Homan ist in Wien aufgewachsen, wo er auch von 2002 bis 2008 Humanmedizin studiert hat. Danach begann er seine Facharztausbildung sowie ein PhD-Studium an der Universitätsklinik für Psychiatrie in Bern bei Prof. Dr. Werner Strik und Prof. Dr. Thomas Dierks und arbeitete dort auch als Oberarzt, bevor er 2015 mit einem Stipendium des Schweizer Nationalfonds für insgesamt vier Jahre ans Mount Sinai Hospital und ans Zucker Hillside Hospital nach New York ging.

Unter Supervision von Prof. Dr. Thomas Dierks lernte Herr Homan während seines PhD-Studiums die nichtinvasive Hirnstimulation als neues Behandlungsverfahren bei persistierenden Positivsymptomen der Schizophrenie kennen, und konnte dazu mehrere hochrangige Studien veröffentlichen. Diese Arbeiten wurden mit dem Hans-Heimann-Preis der Deutschen Gesellschaft für Psychiatrie, Psychotherapie und Nervenheilkunde (DGPPN) 2014 sowie dem Frutiger Preis 2014 ausgezeichnet. Sein PhD schloss er 2013 an der Universität Bern mit summa cum laude ab.

Begleitend absolvierte Herr Homan seine dreijährige psychotherapeutische Weiterbildung in psychodynamischer Psychotherapie am Sigmund-Freud-Institut in Bern, welche er 2011 erfolgreich abschloss. Im Jahre 2014 erlangte Herr Homan den Facharzttitel für Psychiatrie und Psychotherapie FMH. Seit Juli 2019 ist Herr Homan als Oberarzt an der KPPP der PUK Zürich tätig.

Persönlichkeit

Herr Homan hat in den Jahren seiner Tätigkeit als Arzt und Forscher fundierte Fachkenntnisse über das gesamte Spektrum der klinischen Psychiatrie und Psychotherapie erworben. Er zeichnet sich durch ein hohes Talent in der Führung von interdisziplinären Teams sowie in der spezialisierten psychotherapeutischen und pharmakologischen Behandlung von schwer kranken psychiatrischen Patienten aus. Herr Homan wird von den Patienten für seine Empathie und Kompetenz geschätzt, und ist auch ein allerseits geschätzter Kollege, der sich nebst seiner Fachkompetenz auch durch seine Hilfsbereitschaft und Sozialkompetenz und einen herausragenden Einsatz für die Lehre und Forschung auszeichnet. Ein wichtiges Anliegen ist für Herrn Homan die ärztliche Nachwuchsförderung, welche er durch seine Funktion als Arbeitsgruppenleiter an der PUK Zürich mit grossem Engagement unterstützt.

Wissenschaftliche Qualifikation

Herr Homan legt insgesamt 29 Originalpublikationen in erstklassigen wissenschaftlichen Fachzeitschriften vor, ausserdem drei Übersichtsarbeiten (Reviews), zwei Fallstudien (Case Reports) und zwei Editorials. Bei 15 der 29 Originalpublikationen war er Erstautor, bei vier davon Letztautor. Hervorzuheben ist, dass seine Arbeiten in hochrangigen Journalen publiziert worden sind, unter anderem in *Nature Neuroscience*, *JAMA Psychiatry*, *American Journal of Psychiatry*, *Biological Psychiatry* und *Neuropsychopharmacology*. Somit sind aus meiner Sicht die Anforderungen an die Publikationsstätigkeit für die Habilitation an der UZH ohne Zweifel erfüllt. Die wissenschaftliche Arbeit von Herrn Homan zeichnet sich einerseits durch sein Interesse in der Erforschung der neurobiologischen und psychologischen Mechanismen der Positivsymptomatik bei Schizophrenie aus; andererseits hat er sich mit der Frage der Möglichkeit einer personalisierten Medizin in der Psychiatrie beschäftigt und hierzu hochrangige Beiträge als Erstautor (*Nature Neuroscience*) und Letztautor (*JAMA Psychiatry*) vorgelegt.

Durch die in der hier vorgelegten kumulativen Habilitationsschrift beschriebenen Studienergebnisse konnte Herr Homan neuartige Erkenntnisse in Bezug auf die Möglichkeiten und Grenzen einer individualisierten Psychiatrie aufzeigen. Diese Erkenntnisse könnten im Verlauf der nächsten Jahre in klinischen Populationen eingesetzt und überprüft werden. Damit leistet Herr Homan einen wichtigen Beitrag zum Verständnis von neurobiologischen diagnostischen und prognostischen Biomarkern.

Insgesamt zeichnet sich die wissenschaftliche Tätigkeit von Herrn Homan durch Originalität und einen methodisch hohen Anspruch aus. Er besitzt ausgeprägtes Talent in der Anwendung von verschiedenen methodologischen Ansätzen, sowie höchste wissenschaftliche Kompetenz in der Planung und Leitung von wissenschaftlichen Projekten.

Die von Herrn Homan geleiteten Forschungsprojekte wurden durch verschiedene nationale und internationale Stiftungen finanziell gefördert. Zudem ist er Homan als Gutachter (Peer reviewer) für zahlreiche internationale Journale tätig, unter anderem *JAMA Psychiatry*, *Current Biology* und *Neuroimage*.

Didaktik und Lehre

Herr Homan engagiert sich seit dem Beginn seiner Karriere konstant und erfolgreich in der neurowissenschaftlichen und psychiatrischen Lehre, und hat gleich bei Stellenantritt an der Universität Zürich zahlreiche Vorlesungen und Seminare übernommen, weil ihm die Lehre besonders wichtig ist. Er vermittelt Medizinstudenten die biowissenschaftlichen Grundlagen in der psychiatrischen Forschung allgemein und zu Psychose und Positivsymptomatik im Besonderen. Im Rahmen der klinisch-psychiatrischen Lehre ist er Lehrdozent für den klinischen Kurs Psychiatrie, in welchem Medizinstudenten die Erhebung und Interpretation des psychopathologischen Befundes am psychiatrischen Patienten vermittelt werden. Zudem hält Herr Homan Vorlesungen zur Pathophysiologie und Klinik von psychiatrischen Erkrankungen. Herr Homan engagiert sich ausserdem in der Ausbildung von Medizinstudierenden und an der Weiterbildung von Assistenzärzten. Herr Homan hat ausserdem mehrere Kurse für Didaktik besucht und erfüllt damit auch alle Voraussetzungen für erfolgreiche Lehre.

Aus meiner Sicht erfüllt Herr Homan damit aufgrund seiner wissenschaftlichen und didaktischen Leistungen ganz klar die Voraussetzungen für die Venia Legendi an der MeF der UZH; er ist für die Forschung und Lehre hervorragend geeignet.

Entwicklungspotential

Herr Homan ist ein hervorragender Psychiater und klinischer Wissenschaftler mit beeindruckendem Leistungsausweis und einer gewinnenden, loyalen, kollegialen und leistungsorientierten Persönlichkeit. Er hat sich national und international stetig weiterentwickelt und bereits mehrere Stufen seiner klinischen und wissenschaftlichen Karriere absolviert. Seine Forschungsthemen und Projekte hat er sich über viele Jahre selbstständig erarbeitet und ist national und international gut vernetzt, was er mit zahlreichen Kooperationen im Sinne des Standortes PUK Zürich nützt. Herr Homan vertritt mit seinem translationalen und methodisch vielfältigen Schwerpunkt in der Erforschung Psychosen einen unverzichtbaren Bereich der klinischen Neurowissenschaften und der Psychiatrie.

Aus all den genannten Gründen kann ich aus voller Überzeugung bestätigen, dass Herr Homan aufgrund seiner wissenschaftlichen, klinischen und didaktischen Leistungen sowie seiner Persönlichkeit bestens geeignet ist und alle Voraussetzungen für die Venia Legendi an der MeF der UZH erfüllt.

Antrag

Als Fachvertreter unterstütze ich den Antrag von Herrn Homan zur Habilitation vollumfänglich und ohne Vorbehalt.

Für Rückfragen stehe ich gerne zur Verfügung und verbleibe mit freundlichen Grüßen



Prof. Dr. med. Erich Seifritz
Direktor KPPP

Philipp Homan, MD, PhD

Personal information

Date of birth	13.02.1980
Place of birth	Regensburg
Nationality	Austrian
Address	University Hospital of Psychiatry Lenggstrasse 31 8032 Zurich Switzerland
Private address	Weinbergstrasse 37 8006 Zurich Switzerland
ORCID	0000-0001-9034-148X
Email	philipp.homan@bli.uzh.ch
Mobile	+41 79-379-6097
Twitter	@philipphoman
Web	https://homanlab.github.io

Education

11/2015	Board certification (Facharzt). Psychiatry and Psychotherapy, Swiss Medical Association (FMH)
04/2013	PhD, Neuroscience (Dr. phil.). University of Bern, Switzerland. Advisor: Thomas Dierks, MD
07/2008	MD (Dr. med.). Medical University of Vienna, Austria. Thesis defense: 6/4/2008. Advisor: Michael Hubenstorf, MD, PhD
10/1999 - 06/2002	Study of business and computer science. Technical University of Vienna, Austria

Employment history

07/2019 - present	Attending Physician and Group Leader. University Hospital of Psychiatry (Head: Erich Seifritz, MD), University of Zurich, Zurich, Switzerland.
08/2017 - 06/2019	Assistant Professor. Feinstein Institute for Medical Research and Zucker School of Medicine, New York, NY, USA.
08/2015 - 07/2017	Postdoctoral Research Fellow. Schiller Laboratory of Affective Neuroscience (Head: Daniela Schiller) at Friedman Brain Institute (Head: Eric Nestler), Icahn School of Medicine at Mount Sinai, New York, NY, USA. Funded by Swiss National Science Foundation (SNF 161077). Advisor: Daniela Schiller, PhD
07/2013 - 07/2015	Group Leader. Non-invasive Brain Stimulation Unit, Translational Research Center at the University Hospital of Psychiatry, University of Bern, Switzerland. Advisor: Thomas Dierks, MD
09/2013 - 07/2015	Attending Physician (Oberarzt). University Hospital of Psychiatry, University of Bern, Switzerland. Advisor: Werner Strik, MD
09/2008 - 08/2013	Resident. University Hospital of Psychiatry and Department of Endocrinology, Diabetology & Clinical Nutrition, Inselspital, University of Bern, Switzerland. Advisors: Werner Strik, MD and Peter Diem, MD

Supervision of junior researchers

- Stephanie Winkelbeiner, PhD, postdoc

- Maria Neumeier, doctoral student
- Werner Surbeck, MD, PhD, postdoc
- Nils Kallen, MD, postdoc
- Noemi Dannecker, MSc, graduate student
- Rahel Horisberger, MSc, doctoral student
- Nikolaos Marousis, MD, postdoc
- Marialuisa Cavelti, PhD, postdoc
- Taylor Marzuk, research assistant
- Qi Lin, research assistant
- Jingchu Hu, PhD, graduate student

Scientific reviewing

Adhoc reviewer JAMA Psychiatry; Biological Psychiatry; Current Biology; Schizophrenia Bulletin; Psychoneuroendocrinology; eNeuro; Human Brain Mapping; NeuroImage; Neuropsychologia; Translational Psychiatry; Psychophysiology; Neuropsychobiology; Psychiatry Research: Neuroimaging; Journal of Neuroscience Methods; World Journal of Biological Psychiatry; Frontiers in Psychiatry; Cognitive Affective and Behavioral Neuroscience; Brain Imaging and Behavior; Nutrients; Scientific Reports; Clinical and Experimental Pharmacology and Physiology; Computational Psychiatry; Journal of Psychopharmacology; Neuroscience; PLOS One; Psychiatry Research; Progress in Neuro-Psychopharmacology and Biological Psychiatry; BMC Psychiatry; Bioinformatics

Editorial Board The British Journal of Psychiatry

Organisation of conferences

- 06/2016** Organized a 2-day training course in transcranial magnetic stimulation for physicians and PhD-students together with Dr. Yosuke Morishima. Graduate School of Health Sciene, University of Bern, Switzerland
- 04/2015** Organized a 4-week training course in transcranial magnetic stimulation for physicians. University Hospital of Psychiatry Bern, Switzerland

Funding

- 09/2019** NARSAD Young Investigator Grant from the Brain & Behavior Research Foundation (BBRF), USA. Duration: 2 years. Role: PI.
- 06/2015** Advanced Postdoc.Mobility Fellowship from the Swiss National Science Foundation, Switzerland (SNF 161077). Duration: 2 years. Role: PI.

Awards

- 10/2019** Young Investigator Award from the Swiss Society of Biological Psychiatry (SSBP), Switzerland
- 03/2019** Young Investigator Award from the World Federation of Societies of Biological Psychiatry (WFSBP), Germany
- 04/2018** Travel Award from the Schizophrenia International Research Society, USA
- 05/2016** Poster Award from the Friedman Brain Institute at the 8th Annual Neurosciene Retreat, New York Academy of Medicine, USA
- 11/2014** Hans Heimann Dissertation Award from the Deutsche Gesellschaft für Psychiatrie, Psychotherapie und Nervenheilkunde (DGPPN), Germany

09/2014 Frutiger Award from the Foundation Adrian and Simone Frutiger, Switzerland

11/2011 Poster Award from the Deutsche Gesellschaft für Psychiatrie, Psychotherapie und Nervenheilkunde (DGPPN), Germany

Conference talks

- American College of Neuropsychopharmacology (ACNP)
- Schizophrenia International Research Society (SIRS)
- Winter Conference for Brain Research (WCBR)
- Society of Research in Psychopathology (SRP)
- World Federation of Societies of Biological Psychiatry (WFSBP)
- German Federation of Psychiatry and Psychotherapy (DGPPN)
- European Conference of Schizophrenia Research (ECSR)

Invited talks

- Laureate Institute for Brain Research, Tulsa, Oklahoma
- National Institute of Mental Health (NIMH)
- IBM Watson, York Town Heights, New York
- University of Geneva
- Mount Sinai School of Medicine, New York
- Zucker Hillside Hospital, New York
- Medical University of Vienna
- University of Zurich
- University of Toronto

NOTIFICATION
on Conferment an Academic Degree

D I C T U M

Pursuant to § 87 para 1 i.c.w. § 124 para 1 University Act 2002 [Fed. Act I N°. 120/2002 i.i.p.f.] and Z 4 of annex 1 to the University Studies Act [Fed. Act I Nr. 48/1997 a.l.a.], the Curriculumsdirektorin for the diploma programme Medicine at the Medizinische Universität Wien herewith confers upon

Mr. Philipp Homan,
born 13 February 1980, registration number 9925118,
citizenship Austria,
the academic degree of
Doktor der gesamten Heilkunde (Dr.med.univ.)

G R O U N D S

Upon completion of the diploma programme Medicine following positive assessment of all curricular exams legally required for the diploma programme Medicine (notification bulletin of the Universität Wien, piece XXX, No. 308 dated 24 July 2002, i.i.p.f.), the pre-requisites for conferment of the academic degree of "Doktor der gesamten Heilkunde" have been fulfilled on 01 July 2008.
Hence the decision was in accordance with the ruling.

I N F O R M A T I O N O N T H E R I G H T T O A P P E A L

§ 25 para 1 Z 12 University Act 2002 provides the legal right to appeal against this notification to the Senate of the Medizinische Universität Wien. The appeal has to be filed within two weeks after delivery to the responsible Curriculumsdirektorin of the Medizinische Universität Wien (c/o Studien- und Prüfungsabteilung der Medizinischen Universität Wien) with reference to the notification and enclosure of a well-founded petition.

Vienna, this 24 July 2008

Die Curriculumsdirektorin
Univ.Prof. Dr.med.univ. Anita Rieder

UNIVERSITÄT BERN

The Graduate School for Health Sciences

hereby certifies that

Philipp Homan

from Austria, born on February 13, 1980

having submitted the thesis

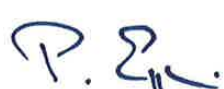
On the neurobiology of hallucinations

and having passed the thesis defence, is awarded the degree of

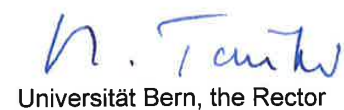
PhD in Health Sciences (Neurosciences)

with the mark **summa cum laude**

Bern, April 29, 2013



The Dean of the
Faculty of Medicine


The Dean of the
Faculty of Human Sciences
Universität Bern, the Rector



Schweizerische Eidgenossenschaft
Confédération suisse
Confederazione Svizzera
Confederaziun svizra
Swiss Confederation

Eidgenössisches Departement des Innern EDI
Département fédéral de l'intérieur DFI
Dipartimento federale dell'Interno DFI
Departamento federal de l'Intern DFI
Federal Department of Home Affairs FDHA

SIWF
ISFM  FMH

WEITERBILDUNGSDIPLOM

Philipp Homan
von Österreich

erhält den eidgenössischen Weiterbildungstitel als

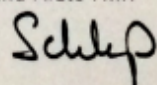
FACHARZT FÜR PSYCHIATRIE UND PSYCHOTHERAPIE

aufgrund des absolvierten akkreditierten Weiterbildungsganges gemäss
Bundesgesetz vom 23. Juni 2006 über die universitären Medizinalberufe.

Bern, 27. November 2015
GLN 7601000919823



Verbindung der Schweizer Ärztinnen
und Ärzte FMH

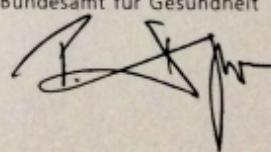


Schweizerisches Institut für ärztliche
Weiter- und Fortbildung SIWF



Eidgenössisches Departement des Innern
Bundesamt für Gesundheit





List of publications

Philipp Homan, MD, PhD*

1 Original investigations¹

1. **Homan P**, Argyelan M, Fales CL, DeRosse P, Szeszko PR, Robinson DG, Lencz T, Malhotra AK. Striatal volume and functional connectivity correlate with weight gain in early-phase psychosis. *Neuropsychopharmacology*, 2019. doi: 10.1038/s41386-019-0464-y. IF: 7.2. ♦
2. Winkelbeiner S, Leucht S, Kane JM, **Homan P**. Evaluation of differences in individual treatment response in schizophrenia spectrum disorders. *JAMA Psychiatry*, 2019. doi: 10.1001/jamapsychiatry.2019.1530. IF: 15.9. ♦
3. **Homan P**, Argyelan M, DeRosse P, Szeszko P, Gallego JA, Hanna L, Robinson D, Kane JM, Lencz T, Malhotra AK. Structural similarity networks predict clinical outcome in early-phase psychosis. *Neuropsychopharmacology*, 2019. <https://dx.doi.org/10.1038/s41386-019-0322-y>. IF: 7.2. ♦
4. **Homan P**, Levy I, Feltham E, Gordon C, Hu J, Li J, Pietrzak RH, Southwick S, Krystal JH, Harpaz-Rotem I, Schiller D. Neural computations of threat in the aftermath of combat trauma. *Nature Neuroscience*, 2019. <https://dx.doi.org/10.1038/s41593-018-0315-x>. IF: 21.1. ♦
5. Gaillard C, Guillod M, Ernst M, Torrisi S, Federspiel A, Schoebi D, Recabarren R, Ouyang X, Mueller-Pfeiffer C, Horsch A, **Homan P**, Wiest R, Hasler G, Martin-Soelch C. Striatal responsiveness to reward under threat-of-shock and working memory load: A preliminary study. *Brain and Behavior*. IF: 2.1.
6. Cavelti M, Winkelbeiner S, Federspiel A, Walther S, Stegmayer K, Giezendanner S, Laimboeck K, Strik W, Horn H, **Homan P**. Formal thought disorder in schizophrenia and white matter abnormalities: A tract-based spatial statistics analysis. *Psychiatry Research: Neuroimaging*, (279): 40–50, 2018. <https://dx.doi.org/10.1016/j.pscychresns.2018.05.011>. IF: 2.3. ♦
7. Winkelbeiner S, Cavelti M, Federspiel A, Dierks T, Strik W, Horn H, **Homan P**. Decreased blood flow in the right insula and middle temporal gyrus predicts negative formal thought disorder in schizophrenia. *Schizophrenia Research*, 201: 432–434, 2018. <https://dx.doi.org/10.1016/j.schres.2018.06.009>. IF: 4.6. ♦
8. Kunzelmann K, Grieder M, van Swam C, **Homan P**, Hubl D, Dierks T. Am I hallucinating or is my fusiform cortex activated? Functional activation differences in schizophrenia patients with and without hallucinations. *The European Journal of Psychiatry*, 33: 1–7, 2019. <https://dx.doi.org/10.1016/j.ejpsy.2018.06.002>. IF: 0.7.
9. Viviano JD, Buchanan RW, Calarco N, Gold JM, Foussias G, Bhagwat N, Stefanik L, Hawco C, DeRosse P, Argyelan M, Turner J, Chavez S, Kochunov P, Kingsley P, Zhou X, Malhotra AK, Voineskos AN, Carpenter W, Zaranski J, Arbach E, August S, Remington G, Dickie E, Kwan J, Plagiannakos C, Mason M, Boczułak M,

*philipp.homan@bli.uzh.ch

¹Contributions forming the Habilitation are marked with ♦, contributions of high scientific value are marked with ♦♦, equal contributions with #.

- Miranda D, **Homan P**, DeRosse P, Iacoboni M, Green M. Resting-state connectivity biomarkers of cognitive performance and social function in individuals with schizophrenia spectrum disorder and healthy control subjects. *Biological Psychiatry*, 84(9): 665–674, 2018. <https://dx.doi.org/10.1016/j.biopsych.2018.03.013>. IF: 11.5.
10. Cavelti M, Kircher T, Nagels A, Strik W, Horn H, **Homan P**. Neuroimaging of formal thought disorder in schizophrenia: A systematic review. *Schizophrenia Research*, (199): 2–16, 2018. <https://dx.doi.org/10.1016/j.schres.2018.02.051>. IF: 4.6.
 11. Hu J, Wang W, **Homan P**, Wang P, Zheng X, Schiller D. Reminder duration determines threat memory modification in humans. *Scientific Reports*, 8: 8848, 2018. <https://dx.doi.org/10.1038/s41598-018-27252-0>. IF: 4.0.
 12. **Homan P**, Lin Q, Murrough JW, Soleimani L, Bach DR, Clem RL, Schiller D. Prazosin during threat discrimination boosts memory of the safe stimulus. *Learning & Memory*, 24(11): 597–601, 2017. <https://dx.doi.org/10.1101/lm.045898.117>. IF: 2.4.
 13. **Homan P**, Ely BA, Yuan M, Brosch T, Ng J, Trope Y, Schiller D. Aversive smell associations shape social judgment. *Neurobiology of Learning and Memory*, 144: 86–95, 2017. <https://dx.doi.org/10.1016/j.nlm.2017.07.004>. IF: 3.0.
 14. **Homan P**, Reddan MC, Brosch T, Koenigsberg HW, Schiller D. Aberrant link between empathy and social attribution style in borderline personality disorder. *Journal of Psychiatric Research*, 94: 163–171, 2017. <https://dx.doi.org/10.1016/j.jpsychires.2017.07.012>. IF: 3.9.
 15. Cavelti M, **Homan P**, Vauth R. The impact of thought disorder on therapeutic alliance and personal recovery in schizophrenia and schizoaffective disorder: An exploratory study. *Psychiatry Research*, 239: 92–98, 2016. <https://dx.doi.org/10.1016/j.psychres.2016.02.070>. IF: 2.2.
 16. Kindler J, Jann K, **Homan P**, Hauf M, Walther S, Strik W, Dierks T, Hubl D. Static and dynamic characteristics of cerebral blood flow during the resting state in schizophrenia. *Schizophrenia Bulletin*, 41: 163–70, 2015. <https://dx.doi.org/10.1093/schbul/sbt180>. IF: 7.3.
 17. **Homan P**, Grob S, Milos G, Schnyder U, Eckert A, Lang U, Hasler G. The role of BDNF, leptin, and catecholamines in reward learning in bulimia nervosa. *International Journal of Neuropsychopharmacology*, 18(5), 2015. <https://dx.doi.org/10.1093/ijnp/pyu092>. IF: 4.2.
 18. **Homan P**, Neumeister A, Nugent A, Charney D, Drevets WC, Hasler G. Serotonin versus catecholamine deficiency: behavioral and neural effects of experimental depletion in depression. *Translational Psychiatry*, 5: e532, 2015. <https://dx.doi.org/10.1038/tp.2015.25>. IF: 5.2.
 19. **Homan P**#, Vermathen P#, Van Swam C, Federspiel A, Boesch C, Strik W, Dierks T, Hubl D, Kreis R. Magnetic resonance spectroscopy investigations of functionally defined language areas in schizophrenia patients with and without auditory hallucinations. *Neuroimage*, 94: 23–32, 2014. <https://dx.doi.org/10.1016/j.neuroimage.2014.03.009>. IF: 5.8. ♦
 20. **Homan P**, Drevets WC, Hasler G. The effects of catecholamine depletion on the neural response to fearful faces in remitted depression. *International Journal of Neuropsychopharmacology*, 17(9): 1419–28, 2014. <https://dx.doi.org/10.1017/s1461145714000339>. IF: 4.2.
 21. **Homan P**, Drevets WC, Hasler G. Neural correlates of free t3 alteration after catecholamine depletion in subjects with remitted major depressive disorder and in controls. *Psychopharmacology (Berl)*, 231(2): 409–17, 2014. <https://dx.doi.org/10.1007/s00213-013-3250-2>. IF: 3.4.

22. Woodward T, Jung K, Hwang H, Yin J, Taylor L, Menon M, Peters E, Kuipers E, Waters F, Lecomte T, Sommer I, Daalman K, van Luterveld R, Hubl D, Kindler J, **Homan P**, Badcock J, Chhabra S, Cella M, Keedy S, Allen P, Mechelli A, Preti A, Siddi S, Erickson D. Symptom dimensions of the psychotic symptom rating scales in psychosis: A multi-site study. *Schizophrenia Bulletin*, 40 Suppl 4: S265–74, 2014. <https://dx.doi.org/10.1093/schbul/sbu014>. IF: 7.3.
23. **Homan P**, Drevets WC, Hasler G. Growth hormone response to catecholamine depletion in unmedicated remitted subjects with major depressive disorder and healthy controls. *Journal of Clinical Psychopharmacology*, 33: 621–626, 2013. <https://dx.doi.org/10.1097/JCP.0b013e31829a8284>. IF: 3.0.
24. **Homan P**, Grob S, Milos G, Schnyder U, Hasler G. Reduction in total plasma ghrelin levels following catecholamine depletion. Relation to bulimic and depressive symptoms. *Psychoneuroendocrinology*, 38: 1545–1552, 2013. <https://dx.doi.org/10.1016/j.psyneuen.2012.12.024>. IF: 4.0. ♦
25. **Homan P**, Kindler J, Hauf M, Walther S, Hubl D, Dierks T. Repeated measurements of cerebral blood flow in the left superior temporal gyrus reveal tonic hyperactivity in patients with auditory verbal hallucinations: A possible trait marker. *Frontiers in Human Neuroscience*, 7: 304, 2013. <https://doi.org/10.3389/fnhum.2013.00304>. IF: 2.9.
26. Kindler J, **Homan P**, Flury R, Strik W, Dierks T, Hubl D. Theta burst transcranial magnetic stimulation for the treatment of auditory verbal hallucinations: Results of a randomized controlled study. *Psychiatry Research*, 209(1): 114–117, 2013. <https://dx.doi.org/10.1016/j.psychres.2013.03.029>. IF: 2.2.
27. Kindler J, **Homan P**, Jann K, Federspiel A, Flury R, Hauf M, Strik W, Dierks T, Hubl D. Reduced neuronal activity in language-related regions after transcranial magnetic stimulation therapy for auditory verbal hallucinations. *Biological Psychiatry*, 73(6): 518–24, 2013. <https://dx.doi.org/10.1016/j.biopsych.2012.06.019>. IF: 11.5.
28. **Homan P#**, Kindler J#, Hauf M, Hubl D, Dierks T. Cerebral blood flow identifies responders to transcranial magnetic stimulation in auditory verbal hallucinations. *Translational Psychiatry*, 2: e189, 2012. <https://dx.doi.org/10.1038/tp.2012.114>. IF: 5.2.
29. Walther S, Schüpbach B, Seifritz E, **Homan P**, Strik W. Randomized, controlled crossover trial of dronabinol, 2.5 mg, for agitation in 2 patients with dementia. *Journal of Clinical Psychopharmacology*, 31(2): 256–258, 2011. <https://dx.doi.org/10.1097/jcp.0b013e31820e861c>. IF: 3.0.

2 Case reports

1. Winkelbeiner S, Suker S, Bachofner H, Eisenhardt S, Steinau S, Walther S, Federspiel A, Dierks T, Strik W, **Homan P**. Targeting obsessive-compulsive symptoms with rTMS and perfusion imaging. *The American Journal of Psychiatry*, 175: 81–83, 2018. <https://dx.doi.org/10.1176/appi.ajp.2017.17060634>. IF: 13.7.
2. **Homan P**, Kindler J, Federspiel A, Flury R, Hubl D, Hauf M, Dierks T. Muting the voice: a case of arterial spin labeling-monitored transcranial direct current stimulation treatment of auditory verbal hallucinations. *American Journal of Psychiatry*, 168(8): 853–4, 2011. <https://dx.doi.org/10.1176/appi.ajp.2011.11030496>. IF: 13.7.

3 Reviews

1. Marzouk T, Winkelbeiner S, Malhotra AK, **Homan P**. Transcranial magnetic stimulation for positive symptoms in schizophrenia: A systematic review. *Neuropsychobiology*, 2019. IF: 1.7.

2. Cavelti M, Thompson KN, Hulbert C, Betts J, Jackson H, Francey S, **Homan P**, Chanen AM. Exploratory comparison of auditory verbal hallucinations and other psychotic symptoms among youth with borderline personality disorder or schizophrenia spectrum disorder. *Early Intervention in Psychiatry*, 2018. <https://dx.doi.org/10.1111/eip.12763>. IF: 3.3.
3. **Homan P**, Kindler J, Hubl D, Dierks T. Auditory verbal hallucinations: imaging, analysis, and intervention. *European Archives of Psychiatry and Clinical Neuroscience*, 262 Suppl 2: 91–5, 2012. <https://dx.doi.org/10.1007/s00406-012-0355-2>. IF: 3.2.

4 Editorials, essays, and preprints

1. **Homan P**, Kane J. Clozapine as an early-stage treatment. *Acta Psychiatrica Scandinavica*, 138: 279–280, 2018. <https://dx.doi.org/10.1111/acps.12965>. IF: 4.7.
2. **Homan P**, Schiller D. Neuroscience: This is not a spider. *Current Biology*, 26(19): R898–R900, 2016. <https://dx.doi.org/10.1016/j.cub.2016.08.037>. IF: 9.1.
3. Munkholm K, Winkelbeiner S, **Homan P**. Individual response to antidepressants for depression in adults - a simulation study and meta-analysis. *PsyArXiv*, 2019. doi: 10.31234/osf.io/m4aqc.
4. **Homan P**, Schooler NR, Brunette MF, Rotondi A, Ben-Zeev D, Gottlieb JD, Mueser KT, Achtyes ED, Ginderich S, Marcy P, Meyer-Kalos P, Hauser M, John M, Robinson DG, Kane JM. Psychosis relapse prevention through health technology program reduces rehospitalization. *bioRxiv*, 2019. doi: 10.1101/626663.
5. **Homan P**, Lau H, Levy I, Raio C, Bach D, Carmel D, Schiller D. Affective flexibility without perceptual awareness. *bioRxiv*, 2018. <https://dx.doi.org/10.1101/505545>.



Habilitation / Nachweis der geleisteten Lehrveranstaltungen von:

Akademischer Titel: Dr. med. univ., PhD
Name: Homan
Vorname: Philipp
Institut/Klinik: Psychiatrische Universitätsklinik Zürich
Strasse: Lenggstrasse 31
PLZ/Ort: 8032 Zürich

Bitte erwähnen Sie hier alle Lehrveranstaltungen, bei denen Sie in den letzten drei Jahren insgesamt mindestens 14 Stunden im Rahmen der Aus-, Weiter- und Fortbildung in der Humanmedizin erbracht haben (Habilitationssordnung § 5 lit. e).

Datum: 20.8.2019

Unterschrift:



UZH, Medizinische Fakultät, Pestalozzistrasse 3/5, CH-8091 Zürich

Herr
Dr. med. Philipp Homan, PhD
PUK
Universität Zürich
Lenggstrasse 31
8032 Zurich

Olga Zalesko B.A.
Beförderungskommission, USMLE
Telefon +41 44 634 40 41
olga.zalesko@dekmmed.uzh.ch

Zürich, 24.07.2019 /oz

Anrechnung von Weiterbildungen in der Hochschuldidaktik für die Habilitation

Sehr geehrter Herr Dr. Homan

Vielen Dank für die Information zum Nachweis einer Weiterbildung im Bereich der Hochschuldidaktik, die Sie uns zugestellt haben.

Folgende Weiterbildungen wurden von Ihnen besucht:

- Zucker Hillside Hospital Northwell Health, Weiterbildung «Effectively Presenting Neuroscience», 03/2018-06/2018 (8 Stunden)
Kursleitung: Dr. John Young und Dr. David Ross
- Universitäre Psychiatrische Dienste Bern (UPD), Weiterbildungskurs «Recovery praktisch – paritäre Einführung und Schulung», 23./29.08.2013, 7./15.11.2013 und 13./21.02.2014 (6 Tage)
Kursleitung: René Hadorn und Sandra Gelormini
- Universitäre Psychiatrische Dienste Bern (UPD), Mitarbeit an der Konzeption und dem Aufbau des Recovery Trialogs Bern, 2012-2013 (20 Stunden)

Die oben aufgeführten Weiterbildungen erfüllen die Anforderung der Didaktik Ausbildung für die Habilitation und können angerechnet werden.

Wir wünschen Ihnen weiterhin alles Gute für Ihre berufliche Laufbahn.

Freundliche Grüsse

Olga Zalesko B.A.
Beförderungskommission, USMLE

Abstract der Habilitationsschrift

**Individual differences and
the scope of precision medicine in psychiatry**

Zur Erlangung der Venia Legendi der Universität Zürich

Verfasst von
Philipp Homan

Zürich, 20. August 2019

Abstract

More than any other field in medicine, psychiatry has faced major theoretical and practical challenges – challenges which most likely reflect the complexity of both the brain and the environment. Individual differences between patients is one aspect of this complexity. Patients with the same diagnosis and with exposition to a similar environment may vary considerably in the way they process information on the algorithmic and the neural level. The detection of such differences may benefit from computational models that reduce the high dimensional data to theoretically meaningful parameters which may reflect individual correlates of clinical symptoms. Whether such differences translate directly into differences in response to treatment is an open question. Our own evaluation of individual differences in treatment response suggested that we tend to overestimate the heterogeneity in treatment effects, simply because a clear distinction of the relevant variance components is not possible from common randomized controlled trials. Elaborated study designs such as N-of-1 trials or advanced statistical modeling is needed to estimate the personal element of treatment response or side effects. Together, this suggests that a realistic evaluation of the need for precision medicine in psychiatry requires complex study designs together with computational modeling and advanced statistical techniques.

Habilitationsschrift

**Individual differences and
the scope of precision medicine in psychiatry**

Zur Erlangung der Venia Legendi der Universität Zürich

Verfasst von
Philipp Homan

Zürich, 20. August 2019

Contents

1 Abstract	3
2 Introduction	4
2.1 Individual differences: the challenge of psychiatry	4
2.1.1 Views from inside the field	4
2.1.2 Views from outside the field	5
2.1.3 Appreciating individual differences between patients	6
2.2 Individual differences in clinical symptoms	7
2.3 Individual differences in treatment response	8
2.4 Individual differences in side effects	9
3 Summary of included papers	11
3.1 Study 1: Homan et al. 2019a, Neuropsychopharmacology	11
3.2 Study 2: Homan et al. 2019b, Neuropsychopharmacology	11
3.3 Study 3: Homan et al. 2019c, Nature Neuroscience	12
3.4 Study 4: Winkelbeiner et al. 2019, JAMA Psychiatry	12
3.5 Study 5: Winkelbeiner et al. 2018, Schizophrenia Research	13
4 Conclusion	14
5 Appendix: Discussed papers	26
5.1 Homan et al. 2019a, Neuropsychopharmacology	26
5.2 Homan et al. 2019b, Neuropsychopharmacology	47
5.3 Homan et al. 2019c, Nature Neuroscience	59
5.4 Winkelbeiner et al. 2019, JAMA Psychiatry	86
5.5 Winkelbeiner et al. 2018, Schizophrenia Research	101

1 Abstract

More than any other field in medicine, psychiatry has faced major theoretical and practical challenges – challenges which most likely reflect the complexity of both the brain and the environment. Individual differences between patients is one aspect of this complexity. Patients with the same diagnosis and with exposition to a similar environment may vary considerably in the way they process information on the algorithmic and the neural level. The detection of such differences may benefit from computational models that reduce the high dimensional data to theoretically meaningful parameters which may reflect individual correlates of clinical symptoms. Whether such differences translate directly into differences in response to treatment is an open question. Our own evaluation of individual differences in treatment response suggested that we tend to overestimate the heterogeneity in treatment effects, simply because a clear distinction of the relevant variance components is not possible from common randomized controlled trials. Elaborated study designs such as N-of-1 trials or advanced statistical modeling is needed to estimate the personal element of treatment response or side effects. Together, this suggests that a realistic evaluation of the need for precision medicine in psychiatry requires complex study designs together with computational modeling and advanced statistical techniques.

2 Introduction

2.1 Individual differences: the challenge of psychiatry

2.1.1 Views from inside the field

More than any other field in medicine, psychiatry is still facing major theoretical and practical challenges. These are acknowledged by leaders in the field. The theoretical challenges include pathogenesis and aetiology while the practical challenges include classification and diagnosis as well as prognosis and treatment (Stephan *et al.*, 2016a,b). What makes diagnoses a major problem is that they are still primarily based on subjective symptoms that lack objective biological correlates. The idea that mental disorders are brain disorders is already more than 150 years old (Griesinger, 1867) and is being questioned regularly (Borsboom, 2017; Fried *et al.*, 2017; Borsboom *et al.*, 2018); and indeed, patients' self reports are still the major source for diagnosing mental disorders. One reason why it has been difficult to confirm the hypothesis that mental disorders must have a neural basis might be that patients with the same diagnosis may have very different underlying neurobiology. In other words, a symptom-based diagnosis might not always map onto the same neurobiological disease mechanism. This means that the underlying biological mechanisms may vary between patients reporting the same symptoms, and a purely symptom-based diagnosis might blur biological differences and for the same reason might also lack the ability to guide treatment decisions. Thus, such diagnosis lacks biological validity and prognostic utility (Stephan *et al.*, 2016a; Insel, 2014; Schumann *et al.*, 2014; Krystal and State, 2014; Owen, 2014; Kapur *et al.*, 2012). It is therefore hardly surprising that developing new pharmacological treatments based on these diagnoses without a clear neural underpinning and novel treatment targets has largely been unsuccessful (Stephan *et al.*, 2016a; Sarter and Tricklebank, 2012).

More than any other field of medicine, psychiatry has also been subject to strong criticism from within and outside the field. One example from within the field was the recently published statement of the former director of the National Institute of Mental Health (NIMH), Thomas Insel. Given that one attempt to address the theoretical challenge of symptom-based diagnoses had been the transdiagnostic Research Domain Criteria introduced by NIMH under his leadership, a leadership that was meant to promote neurobiological research across diagnostic boundaries (Insel, 2013, 2014; Insel and Cuthbert, 2015), the lack of breakthroughs that have translated into clinical practice might have been the reason why Insel has recently voiced the following self-criticism: "I spent 13 years at NIMH really pushing on the neuroscience and genetics of mental disorders, and when I look back on that I realize that while I succeeded at getting lots of really cool papers published by cool scientists at fairly large costs – I think \$20 billion – I don't think we moved the needle in reducing suicide, reducing

hospitalizations, improving recovery for the tens of millions of people who have mental illness. I hold myself accountable for that (Rogers, 2017)."

2.1.2 Views from outside the field

In addition to comments on the challenges of psychiatry from within the field of psychiatry, there have been comments from outside the field as well. They often have similar objections against current practices in clinical psychiatry and psychiatric research. One important example was a widely discussed essay in the New York Review of Books by the former editor of the New England Journal of Medicine – one of the most prestigious scientific journals in the whole field of medicine. The essay included several arguments against the current state of affairs in psychiatry and deserves a literal quote since it recapitulates recurrent themes in the criticism of psychiatry. It argued that publication bias, industry sponsorship, and questionable withdrawal studies are the main reason why psychiatric drug efficacy should be contested: "The industry-sponsored studies usually cited to support psychoactive drugs – and they are the ones that are selectively published – tend to be short-term, designed to favor the drug, and show benefits so small that they are unlikely to outweigh the long-term harms. The problem with relapse studies ... is that they don't distinguish between a true relapse and withdrawal symptoms that result from the abrupt cessation of drugs (Angell, 2011c)." According to this view, efficacy of psychoactive drugs is overstated while the potential harm they cause is suppressed.

Similar criticism have been stated regularly in recent years (Angell, 2011a,b; Gøtzsche, 2014; Harrington, 2019; Korducki, 2019; Moncrieff and Kirsch, 2005; Frances and Widiger, 2012; Frances, 2012; Hengartner and Moncrieff, 2018; Moncrieff, 2018; Braillon *et al.*, 2019), and the subsequent exchanges between critiques and defenders of psychiatry are often redundant in nature (Angell, 2011c; Nutt *et al.*, 2014). Nevertheless, it might be useful to summarize the main objections, as in a book by Peter Gotzsche, the former director of the Nordic Cochrane Centre (Gøtzsche, 2015). The author concludes that psychiatric diagnoses are unreliable; biological explanations do not reduce but increase the stigma against mental illness; monoamine and dopamine hypotheses do not explain depression and psychosis; long term psychopharmacological treatment does not prevent recurrences of the illnesses; antidepressants may cause severe withdrawal symptoms; schizophrenia and other illnesses do not lead to brain damage; and psychoactive drugs do not prevent but cause brain damage. While these objections may sound exaggerated they have indeed been used in these or similar phrasing by critics of current psychiatric practice. Questioning not only commonly identified problems such as diagnosis and classification, they also raise doubt about biological correlates of mental illnesses such as depression (Homan *et al.*, 2015) and schizophrenia (Kapur and Seeman, 2001).

One could add another problem, not mentioned in this list, and not specific to psychiatry research but biomedical research in general: replication of scientific research findings. Not only in psychology do findings often not replicate (Open Science Collaboration, 2015), the same is true for major neurobiological findings in psychiatry as well (Drysdale *et al.*, 2016; Dinga *et al.*, 2018). In summary, respected professionals from within and outside the field have agreed that the major breakthroughs for patients based on a mainly neurobiological research agenda have not happened yet. One reason that they have not happened yet might be that the true appreciation of individual differences between patients was potentially more often claimed rather than actually considered. It might also be true that the consideration of individual differences is harder than initially believed. In the current work we try to summarize our own attempts to shed some light on such individual differences and to thereby gauge the scope for more precision in psychiatry.

2.1.3 Appreciating individual differences between patients

That patients differ from one another is by no means a controversial position to hold. On the contrary, the assumption is widely shared that much of what is done in medicine and psychiatry does not work, simply because it is based on average treatment effects; and that medicine should shift its focus on individual, not average, effects of treatment. A recent editorial in *Nature* summarized this accordingly: “Every day, millions of people are taking medications that will not help them. The top ten highest-grossing drugs in the United States help between 1 in 25 and 1 in 4 of the people who take them ... For some drugs, such as statins – routinely used to lower cholesterol – as few as 1 in 50 may benefit. There are even drugs that are harmful to certain ethnic groups because of the bias towards white Western participants in classical clinical trials (Schork, 2015).”

The problem is that while it might be true that different disease mechanisms may underly the same diagnoses, it is not clear whether this automatically translates into individual differences in how patients respond to the same treatment. Indeed, rather than disease mechanisms it is not unlikely that part of what has driven the attempt to personalize drug treatment is the sobering perspective that currently there are no new drugs for serious mental illness on the horizon. It follows that for the near future, psychiatry will likely have to live with the treatments that have already been established and have been shown to be as effective as treatments in general medicine (Leucht *et al.*, 2012). Although critical voices have often disagreed with the efficacy (Gøtzsche, 2014; Kirsch *et al.*, 2008; Moncrieff and Kirsch, 2005), tolerability (Davies *et al.*, 2019), and necessity (Wunderink *et al.*, 2013) of pharmacological treatment (especially with respect to antidepressants (Munkholm *et al.*, 2019)), clinical psychiatry will have to keep offering pharmacological treatment to patients with severe mental disorders in

the near future, and the drugs will likely be the same as they have been.

To address the rather sobering aspect of drug development one idea has been that the available treatments could at least be tailored to the individual (Schork, 2015). As we mentioned above, the rationale behind this idea is the assumption that there are individual differences between patients in terms of neurobiological disease mechanisms (Brodersen *et al.*, 2013; Deserno *et al.*, 2012; Demjaha *et al.*, 2012, 2014; Howes, 2010; Howes *et al.*, 2012; Stephan *et al.*, 2016a; Drysdale *et al.*, 2016) that require a corresponding adjustment of the pharmacological or somatic treatment in question. Importantly, such individual differences may be apparent already at the high risk state, before conversion to psychosis has occurred (Schmidt *et al.*, 2013; Schmidt and Borgwardt, 2013; Schmidt *et al.*, 2014; Koutsouleris *et al.*, 2014). For example, if psychosis patients who have been classified as treatment-resistant do indeed differ neurobiologically (in terms of a relatively undisturbed dopaminergic neurotransmission compared to controls) from patients that respond well to antipsychotic treatment (Vanes *et al.*, 2018), then antipsychotics that are mainly aimed at blocking the dopamine D2 receptor might not be the right treatment for patients who show this alteration even before starting any treatment.

Computational modeling has been proposed as one promising attempt to dissect individual differences in disease mechanisms (Adams *et al.*, 2016; Huys *et al.*, 2016; Stephan *et al.*, 2017b,a). In addition, a more data driven machine learning approach might complement theory driven computational models and improve classification of diseases and prediction of clinical outcome (Huys *et al.*, 2016). Thus, computational modeling and machine learning, sometimes summarized under the umbrella term 'computational psychiatry' (Huys *et al.*, 2016), have been proposed as part of the solution for the current challenges in psychiatry.

2.2 Individual differences in clinical symptoms

Differences between patients with the same diagnosis have often been highlighted (Fisher *et al.*, 2018) and are readily apparent to clinicians and researchers alike. For example, why is it that only some individuals who have been exposed to similar traumatic events later develop posttraumatic stress disorder? In a series of studies, we assessed different aspects of associative learning using computational and neuroimaging methods in healthy controls and in patients (Homan *et al.*, 2017a,b,c, 2018, 2019c). We showed that a specific learning component, prediction error weight, may explain individual differences in combat veterans. Indeed, highly symptomatic veterans assigned more weight to prediction errors, suggesting that they exaggerated their attention adjustment to unreliable stimuli. This finding was intriguing because it was based on a more fine-grained computational analysis that a conventional summary statistic approach might have easily missed (Daw, 2011; Wilson and Collins, 2019). It suggests that in

order to capture individual differences in patients' behavior one has to apply computational tools that exploit prior knowledge on learning behavior together with Bayesian statistics (Homan *et al.*, 2019c).

2.3 Individual differences in treatment response

Thus, individual differences in learning that map onto psychopathology are detectable with computational tools. Ultimately, these differences could inform treatment decisions if it can be shown that they also map onto differences in response to treatment. Although we have shown that these differences in treatment response require careful assumptions (Winkelbeiner *et al.*, 2019), previous work suggests that such differences (although detected here with more conventional imaging methods) may indeed correlate with treatment outcome. Given that brain stimulation has shown some promise in the treatment of persistent positive symptoms (Homan *et al.*, 2011; Brunelin *et al.*, 2012; Slotema *et al.*, 2010; Lefaucheur *et al.*, 2014), we investigated psychosis patients with persistent positive symptoms (Homan *et al.*, 2012b, 2013, 2014; Kindler *et al.*, 2015) and showed that individuals who would later respond well to a treatment with transcranial magnetic stimulation had a higher regional blood flow in the target area in the left temporal cortex (Homan *et al.*, 2012a). Notably, we also showed that patients stimulated at this area had a decrease of regional blood flow after treatment that was correlated with symptom improvement (Kindler *et al.*, 2013a,b).

Given that positive symptoms also include the understudied domain of thought disturbance, we aimed at characterizing this syndrome more comprehensively in terms of brain structure and function (Cavelti *et al.*, 2018a,b; Winkelbeiner *et al.*, 2018) because of the potential impact of thought disorder on real life outcome including recovery (Cavelti *et al.*, 2016). Moreover, we have also shown that thought disturbance is the syndrome of which we can predict the improvement during antipsychotic treatment using baseline imaging predictors (Homan *et al.*, 2019a). Importantly, we characterized individual treatment response using a comprehensive approach with mixed models which allowed us to separate random variation from actual treatment variation in each participant (Senn, 2016; Hecksteden *et al.*, 2018). In addition, we could estimate individual treatment response more efficiently by using all available data and more conservatively by applying shrinkage (Hedeker and Gibbons, 2006; Gelman *et al.*, 2013). Using this method, we showed that individual differences in structural brain similarity predicted treatment response in first episode psychosis (Homan *et al.*, 2019a), suggesting that these networks capture biologically and clinically meaningful correlates of psychosis.

2.4 Individual differences in side effects

Psychotic disorders are prevalent in about 3% of the population and add to both morbidity and mortality (Olfson *et al.*, 2015). They involve positive and negative symptoms as well as cognitive dysfunction (Howes and Murray, 2014). Antipsychotic drugs act on dopamine D2 receptors and are essential in the treatment of psychosis (McCutcheon *et al.*, 2019; Kapur and Seeman, 2001; Seeman and Lee, 1975; Seeman *et al.*, 1976). Clinical response, however, is variable and often poor. Indeed, 30-40% of patients with psychosis (Lindenmayer, 2000; Mortimer *et al.*, 2010) fail to respond to antipsychotics at recommended doses and duration – despite proper occupancy of dopamine D2 receptors (Wolkin and Barouche, 1989; Coppens *et al.*, 1991). It is thus essential that we improve outcome in those patients – particularly during their first illness episode, as relapses may delay response during the next episode (Takeuchi *et al.*, 2018). Importantly (and mirroring the heterogeneity of psychosis), there might be a different neurochemical deficit involved in cases of treatment-resistance. Alternatively, the dopaminergic dysfunction could be even higher in those cases, so that antipsychotic dopamine blockade is insufficient to improve symptoms. Importantly, clozapine has shown to be effective in such cases where other antipsychotics had failed (Kane *et al.*, 1988), highlighting that there does exist a treatment for such treatment-resistant psychoses. It is also known, however, that clozapine is under-utilized (Kane, 2012), which underscores the need of prospective biomarkers that may guide treatment (Homan *et al.*, 2019a). An important goal of current research is thus to prospectively test circuit-based markers of antipsychotic treatment response and to see if biomarker-informed treatment decisions may improve clinical outcome. This may allow to tailor treatments to subgroups of patients (Kapur *et al.*, 2012) and to identify novel treatment targets for the next generation of effective treatments (Insel, 2013).

Of similar importance, however, is the consideration of side effects of antipsychotic treatments. They add to the considerable burden of the illness and promote cardiovascular and metabolic diseases. The seminal framework by Davis *et al.* (1991) set the stage for considering striatal hyperdopaminergic neurotransmission as the key substrate of psychosis. Since then, numerous functional imaging studies have found corticostriatal abnormalities in psychosis. For example, an early PET study showed that positive symptoms were correlated with activity in the ventral striatum (Liddle and Wands, 1992). Studies using tasks during functional magnetic resonance imaging (fMRI) have found a correlation between reduced striatal activity and positive symptoms in medicated patients with psychosis (Juckel *et al.*, 2006; Menon *et al.*, 2011; Sorg *et al.*, 2013; Jensen *et al.*, 2008) and in first episode patients (Nielsen *et al.*, 2012a). In bipolar patients, the striatum has also shown decreased activation (Pavuluri *et al.*, 2011; Pompei *et al.*, 2011; Liu *et al.*, 2012; Yip *et al.*, 2015), although these studies also included non-

psychotic patients. More recent evidence comes from studies in chronic patients that examined striatal connectivity with limbic and prefrontal brain areas (Yoon *et al.*, 2012; Orliac *et al.*, 2013; Quidé *et al.*, 2013; Tu *et al.*, 2013; Khadka *et al.*, 2013; Mamah *et al.*, 2013), and our own group has expanded these examinations to patients with a first episode of psychosis (Sarpal *et al.*, 2015). Transcending mere striatal dysfunction, striatal dysconnectivity is thus a robust finding in psychosis. Notably, these findings are based on resting state fMRI, a measure that can be obtained relatively easily in a population such as first episode patients. Task-based fMRI, on the other hand, offers more experimental control over the measurement and the testing of specific mechanistic hypotheses with advanced computational modeling techniques (Homan *et al.*, 2019c). The trade-off is the challenge that task-based fMRI may impose on psychiatric patients. Nevertheless, a growing literature suggests that the striatum can indeed be studied with task-based fMRI in psychosis (Schlagenhauf *et al.*, 2009; Deserno *et al.*, 2012), and reinforcement learning is a reliable way to activate it.

Given the crucial role of the striatum in psychosis, it is reasonable to assume that effects of treatment should be reflected by striatal activity and connectivity. Support for this assumption comes from research in healthy controls and in patients. In controls, dopamine agonism increased whereas dopamine depletion decreased striatal connectivity with cortical targets (Cole *et al.*, 2013; Nagano-Saito *et al.*, 2008), supporting a correlation between dopamine receptor availability and frontostriatal connectivity (Ghahremani *et al.*, 2012). In psychosis patients, corticostriatal activity and connectivity may reflect response to antipsychotic treatment. Indeed, striatal activation before and blood flow after antipsychotic treatment correlated with positive symptom improvement in schizophrenia (Lahti *et al.*, 2009; Nielsen *et al.*, 2012b). In addition, striatal activation increased after antipsychotic treatment in pediatric mania (Pavuluri *et al.*, 2012), supporting a cross-diagnostic effect. In first episode psychosis, our group found that baseline striatal connectivity distinguished responders from nonresponders (Sarpal *et al.*, 2016), a result that was replicated in an independent cohort of patients (Sarpal *et al.*, 2016). Striatal connectivity changes from baseline to follow-up also correlated with the improvement in positive symptoms in a subsample of those patients (Sarpal *et al.*, 2015) and in a similar study from a different group (Anticevic *et al.*, 2015). Together, these results suggest that striatal connectivity is a marker of treatment effects in psychosis.

Given that overall outcome is not only shaped by symptom improvement but also absence of severe side effects, we also studied one of the most common side effects in antipsychotic treatment, namely weight gain (Correll *et al.*, 2009). Focusing on the reward circuitry in the striatum, we showed that both striatal volume and frontostriatal connectivity predicted weight gain in first episode psychosis patients Homan *et al.* 2019b. This suggests that patients might not only benefit from the prediction of treatment response but also from the predic-

tion of severe side effects. Combining these two predictors may help calculating personalized risk-benefit profiles, where each patient's likelihood to respond is weighted by their likelihood to experience severe side effects.

3 Summary of included papers

3.1 Study 1: Homan et al. 2019a, Neuropsychopharmacology

In this study, we calculated structural similarity networks in each participant and hypothesized that the hubness, i.e., the number of edges connecting a node to the rest of the network, would be associated with clinical outcome. The study included 82 patients with early psychosis (defined as a cumulative life time exposure to antipsychotic treatment of less than 2 years) and 58 healthy controls. Medications were administered in a double-blind randomized manner, and patients were scanned at baseline prior to treatment with second-generation antipsychotics. Symptoms were assessed with the Brief Psychiatric Rating Scale at baseline and over the course of 12 weeks. Nodal degree of structural similarity networks was computed for each subject and entered as a predictor of individual treatment response into a partial least squares regression. We found that the first two partial least squares regression components explained 29% of the variance in treatment response after cross-validation. Nodes loading strongly on the first component were primarily located in the orbito- and prefrontal cortex, whereas nodes loading strongly on the second PLS component were primarily located in the superior temporal, precentral, and middle cingulate cortex. We interpreted these findings as suggesting link between brain network morphology and clinical outcome in early-phase psychosis.

3.2 Study 2: Homan et al. 2019b, Neuropsychopharmacology

This study was based on the clinical rationale that second-generation antipsychotic drugs are essential in the treatment of psychotic disorders while also being well-known for inducing substantial weight gain and obesity. Critically, weight gain may reduce life expectancy for up to 20-30 years in patients with psychotic disorders, and prognostic biomarkers are generally lacking. Even though other receptors are also implicated, the dorsal striatum, rich in dopamine D2 receptors, which are antagonized by antipsychotic medications, plays a key role in the human reward system and in appetite regulation, suggesting that altered dopamine activity in the striatal reward circuitry may be responsible for increased food craving and weight gain. We measured striatal volume and striatal resting-state

functional connectivity at baseline, and weight gain over the course of 12 weeks of antipsychotic treatment in 81 patients with early-phase psychosis. We also included a sample of 58 healthy controls. Weight measurements were completed at baseline, and then weekly for 4 weeks, and every 2 weeks until week 12. We used linear mixed models to compute individual weight gain trajectories. Striatal volume and whole-brain striatal connectivity were then calculated for each subject, and used to assess the relationship between striatal structure and function and individual weight gain in multiple regression models. Patients had similar baseline weights and body mass indices (BMI) compared with healthy controls. There was no evidence that prior drug exposure or duration of untreated psychosis correlated with baseline BMI. Higher left putamen volume and lower sensory motor connectivity correlated with the magnitude of weight gain in patients, and these effects multiplied when the structure-function interaction was considered in an additional exploratory analysis. Together, we concluded that the results provide evidence for a correlation of striatal structure and function with antipsychotic-induced weight gain. Lower striatal connectivity was associated with more weight gain, and this relationship was stronger for higher compared with lower left putamen volumes.

3.3 Study 3: Homan et al. 2019c, Nature Neuroscience

In this study we combined computational, morphological, and functional analyses to assess latent markers of associative threat learning with computational modeling combat veterans. We then estimated correlations of these markers with overt post-traumatic stress disorder. Using reversal learning, we found that symptomatic veterans showed greater physiological adjustment to cues that did not predict what they had expected, indicating greater sensitivity to prediction errors for negative outcomes. This exaggerated weighting of prediction errors shapes the dynamic learning rate (associability) and value of threat predictive cues. The degree to which the striatum tracked the associability partially mediated the positive correlation between prediction-error weights and PTSD symptoms, suggesting that both increased prediction-error weights and decreased striatal tracking of associability independently contribute to PTSD symptoms. Furthermore, decreased neural tracking of value in the amygdala, in addition to smaller amygdala volume, independently corresponded to higher PTSD symptom severity. We interpreted these results as providing evidence for distinct neurocomputational contributions to the symptoms of posttraumatic stress disorder.

3.4 Study 4: Winkelbeiner et al. 2019, JAMA Psychiatry

This study combined data from simulations and from a meta analysis of antipsychotic drug trials. We started out from the assumption that patients vary consid-

erably in their response to antipsychotic drugs in randomized controlled trials which is a widely shared belief. We assumed that a personal element of response should be reflected by a clinically relevant increase in overall variance in the treatment compared to the control group and analyzed 53 trials from the last 25 years resulting in 75 comparisons of antipsychotics with placebo. Surprisingly, we found that the average difference in Positive and Negative Symptoms Score variances was not larger but slightly smaller under treatment compared to control. Thus, in this study, we found no evidence that antipsychotic drugs increased the outcome variance, suggesting no personal element of response to treatment but instead indicating that the variance was slightly lower in the treatment group than in the control group. We concluded that although the study cannot rule out that subsets of patients respond differently to treatment, it suggests that the average treatment effect is a more reasonable assumption for the individual patient than often assumed.

3.5 Study 5: Winkelbeiner et al. 2018, Schizophrenia Research

In this study, we analyzed individual differences in formal thought disorder, a major contributor to positive symptoms in psychosis and a cause of severe communication disturbances that may ultimately affect therapeutic reliance and clinical recovery. On the neural level, a range of associated brain areas have been found which might reflect the heterogeneity of formal thought disorder itself. Thus, we hypothesized that a differentiation into positive (such as unanticipated, bizarre, or inappropriately expressed speech) and negative (such as speech reduced in quantity, content, or fluency) thought disorder might help at characterizing the neural basis of thought disorder. Since this patient population is particularly difficult to recruit because of the communication difficulty, we included a relatively small sample of only twenty-four patients with psychosis. We assessed the severity of symptoms with the Thought, Language, and Communication, where the subscales Disorganization and Emptiness provided measures of positive and negative formal thought disorder. Using structural and perfusion imaging as readouts of the neurobiology, we found that negative thought disorder moderately correlated with decreased blood flow in the right insula and in the right middle temporal gyrus. We did not find evidence that positive thought disorder symptoms correlated with structural or perfusion measures. We interpreted these findings as providing preliminary evidence that abnormal blood perfusion might contribute to negative thought disorder and that studies investigating larger samples should elucidate whether positive and negative FTD indeed reflect distinct entities of thought disorder with different neurophysiological characteristics.

4 Conclusion

In summary, this work has shown that individual differences between patients constitute a major challenge for psychiatry. Patients with the same diagnosis and with exposition to a similar environment may vary considerably in the way they process information on the algorithmic and the neural level. The detection of such differences may benefit from computational models that reduce the high dimensional data to theoretically meaningful parameters. These parameters (such as the prediction error weight showed above) provide a representation of the data on a much lower dimension (Huys *et al.*, 2016) and may reflect individual differences that correlate with clinical symptoms. Whether such differences translate directly into differences in response to treatment is an open question. Our own evaluation of individual differences in antipsychotic treatment response suggested that we tend to overestimate the heterogeneity in treatment effects, simply because a clear distinction of the relevant variance components is not possible from classic randomized controlled trials. Elaborated study designs such as N-of-1 trials or advanced statistical modeling is needed to estimate the personal element of treatment response. Together, this indicates that a realistic evaluation of the need for precision medicine in psychiatry requires complex study designs together with computational modeling and advanced statistical techniques.

References

- Adams RA, Huys QJ, Roiser JP (2016). Computational psychiatry: towards a mathematically informed understanding of mental illness. *Journal of Neurology, Neurosurgery and Psychiatry*, **87**(1): 53–63.
- Angell M (2011a). The Epidemic of Mental Illness: Why? *The New York Review of Books*, pp. 20–23. June 23.
- Angell M (2011b). The Illusions of Psychiatry. *The New York Review of Books*, pp. 20–23. July 14.
- Angell M (2011c). 'The Illusions of Psychiatry': An Exchange. *The New York Review of Books*, p. 23. August 18.
- Anticevic A, Hu X, Xiao Y, Hu J, Li F, Bi F, Cole MW, Savic A, Yang GJ, Repovs G, Murray JD, Wang XJ, Huang X, Lui S, Krystal JH, Gong Q (2015). Early-course unmedicated schizophrenia patients exhibit elevated prefrontal connectivity associated with longitudinal change. *Journal of Neuroscience*, **35**(1): 267–286.
- Borsboom D (2017). A network theory of mental disorders. *World Psychiatry*, **16**(1): 5–13.
- Borsboom D, Cramer A, Kalis A (2018). Brain disorders? not really... why network structures block reductionism in psychopathology research. *Behavioral and Brain Sciences*, pp. 1–54.
- Braillon A, Lexchin J, Blumsohn A, Hengartner MP (2019). The "pharmaceuticalisation" of life. *BMJ*, **365**: l1972.
- Brodersen KH, Daunizeau J, Mathys C, Chumbley JR, Buhmann JM, Stephan KE (2013). Variational bayesian mixed-effects inference for classification studies. *Neuroimage*, **76**: 345–61.
- Brunelin J, Mondino M, Gassab L, Haesebaert F, Gaha L, Suaud-Chagny MF, Saoud M, Mechri A, Poulet E (2012). Examining transcranial direct-current stimulation (tDCS) as a treatment for hallucinations in schizophrenia. *American Journal of Psychiatry*, **169**(7): 719–24.
- Cavelti M, Homan P, Vauth R (2016). The impact of thought disorder on therapeutic alliance and personal recovery in schizophrenia and schizoaffective disorder: An exploratory study. *Psychiatry Research*, **239**: 92–98.
- Cavelti M, Kircher T, Nagels A, Strik W, Horn H, Homan P (2018a). Neuroimaging of formal thought disorder in schizophrenia: A systematic review. *Schizophrenia Research*, (199): 2–16.

- Cavelti M, Winkelbeiner S, Federspiel A, Walther S, Stegmayer K, Giezendanner S, Laimboeck K, Strik W, Horn H, Homan P (2018b). Formal thought disorder is related to aberrations in language-related white matter tracts in patients with schizophrenia. *Psychiatry Research: Neuroimaging*, (279): 40–50.
- Cole DM, Beckmann CF, Oei NY, Both S, van Gerven JM, Rombouts SA (2013). Differential and distributed effects of dopamine neuromodulations on resting-state network connectivity. *NeuroImage*, **78**: 59–67.
- Coppens HJ, Slooff CJ, Paans AM, Wiegman T, Vaalburg W, Korf J (1991). High central d2-dopamine receptor occupancy as assessed with positron emission tomography in medicated but therapy-resistant schizophrenic patients. *Biological Psychiatry*, **29**(7): 629–634.
- Correll CU, Manu P, Olshanskiy V, Napolitano B, Kane JM, Malhotra AK (2009). Cardiometabolic risk of second-generation antipsychotic medications during first-time use in children and adolescents. *JAMA*, **302**(16): 1765.
- Davies J, Read J, Hengartner MP, Cosci F, Fava G, Chouinard G, van Os J, Nardi A, Gøtzsche P, Groot P, Offidani E, Timimi S, Moncrieff J, Spada M, Guy A (2019). Clinical guidelines on antidepressant withdrawal urgently need updating. *BMJ*, **365**.
- Davis KL, Kahn RS, et al. (1991). Dopamine in schizophrenia: a review and reconceptualization. *American Journal of Psychiatry*, **148**(11): 1474–1486.
- Daw ND (2011). *Trial-by-trial data analysis using computational models*, pp. 3–38. Oxford University Press, New York.
- Demjaha A, Egerton A, Murray RM, Kapur S, Howes OD, Stone JM, McGuire PK (2014). Antipsychotic treatment resistance in schizophrenia associated with elevated glutamate levels but normal dopamine function. *Biological Psychiatry*, **75**(5): e11–e13.
- Demjaha A, Murray RM, McGuire PK, Kapur S, Howes OD (2012). Dopamine synthesis capacity in patients with treatment-resistant schizophrenia. *American Journal of Psychiatry*, **169**(11): 1203–1210.
- Deserno L, Sterzer P, Wustenberg T, Heinz A, Schlagenhauf F (2012). Reduced prefrontal-parietal effective connectivity and working memory deficits in schizophrenia. *Journal of Neuroscience*, **32**(1): 12–20.
- Dinga R, Schmaal L, Penninx B, van Tol MJ, Veltman DJ, van Velzen L, van der Wee N, Marquand A (2018). Evaluating the evidence for biotypes of depression: attempted replication of drysdale et.al. 2017. *bioRxiv*.

- Drysdale AT, Gosenick L, Downar J, Dunlop K, Mansouri F, Meng Y, Fetcho RN, Zebley B, Oathes DJ, Etkin A, Schatzberg AF, Sudheimer K, Keller J, Mayberg HS, Gunning FM, Alexopoulos GS, Fox MD, Pascual-Leone A, Voss HU, Casey B, Dubin MJ, Liston C (2016). Resting-state connectivity biomarkers define neurophysiological subtypes of depression. *Nature Medicine*, **23**(1): 28–38.
- Fisher AJ, Medaglia JD, Jeronimus BF (2018). Lack of group-to-individual generalizability is a threat to human subjects research. *Proceedings of the National Academy of Sciences*, **115**(27): E6106–E6115.
- Frances AJ (2012). Diagnosing the dsm. *The New York Times*.
- Frances AJ, Widiger T (2012). Psychiatric diagnosis: Lessons from the dsm-iv past and cautions for the dsm-5 future. *Annual Review of Clinical Psychology*, **8**(1): 109–130.
- Fried EI, van Borkulo CD, Cramer AOJ, Boschloo L, Schoevers RA, Borsboom D (2017). Mental disorders as networks of problems: a review of recent insights. *Social Psychiatry and Psychiatric Epidemiology*, **52**(1): 1–10.
- Gelman A, Carlin J, Stern H, Dunson D, Vehtari A, Rubin D (2013). *Bayesian Data Analysis (Third Edition)*. CRC Press, Boca Raton, FL.
- Ghahremani DG, Lee B, Robertson CL, Tabibnia G, Morgan AT, Shetler ND, Brown AK, Monterosso JR, Aron AR, Mandelkern MA, Poldrack RA, London ED (2012). Striatal dopamine d2/d3 receptors mediate response inhibition and related activity in frontostriatal neural circuitry in humans. *Journal of Neuroscience*, **32**(21): 7316–7324.
- Gøtzsche P (2015). *Deadly Psychiatry and Organised Denial*. ArtPeople.
- Gøtzsche PC (2014). Why i think antidepressants cause more harm than good. *The Lancet Psychiatry*, **1**(2): 104–106.
- Griesinger W (1867). *Die Pathologie und Therapie der psychischen Krankheiten: Für Aerzte und Studirende*. Krabbe.
- Harrington A (2019). *Mind Fixers: Psychiatry's troubled Search for the Biology of Mental Illness*. W.W. Norton Company.
- Hecksteden A, Pitsch W, Rosenberger F, Meyer T (2018). Repeated testing for the assessment of individual response to exercise training. *Journal of Applied Physiology*, **124**: 1567–1579. PMID: 29357481.
- Hedeker D, Gibbons RD (2006). *Longitudinal data analysis*, volume 451. John Wiley & Sons, Hoboken, NJ.

- Hengartner MP, Moncrieff J (2018). Inconclusive evidence in support of the dopamine hypothesis of psychosis: Why neurobiological research must consider medication use, adjust for important confounders, choose stringent comparators, and use larger samples. *Frontiers in Psychiatry*, **9**: 174.
- Homan P, Argyelan M, DeRosse P, Szeszko PR, Gallego JA, Hanna L, Robinson DG, Kane JM, Lencz T, Malhotra AK (2019a). Structural similarity networks predict clinical outcome in early-phase psychosis. *Neuropsychopharmacology*, **44**(5): 915–922.
- Homan P, Argyelan M, Fales CL, DeRosse P, Szeszko PR, Robinson DG, Lencz T, Malhotra AK (2019b). Striatal volume and functional connectivity correlate with weight gain in early-phase psychosis. *Neuropsychopharmacology*. doi: 10.1038/s41386-019-0464-y.
- Homan P, Ely BA, Yuan M, Brosch T, Ng J, Trope Y, Schiller D (2017a). Aversive smell associations shape social judgment. *Neurobiology of Learning and Memory*, **144**: 86–95.
- Homan P, Kindler J, Federspiel A, Flury R, Hubl D, Hauf M, Dierks T (2011). Muting the voice: a case of arterial spin labeling-monitored transcranial direct current stimulation treatment of auditory verbal hallucinations. *American Journal of Psychiatry*, **168**(8): 853–4.
- Homan P, Kindler J, Hauf M, Hubl D, Dierks T (2012a). Cerebral blood flow identifies responders to transcranial magnetic stimulation in auditory verbal hallucinations. *Translational Psychiatry*, **2**: e189.
- Homan P, Kindler J, Hauf M, Walther S, Hubl D, Dierks T (2013). Repeated measurements of cerebral blood flow in the left superior temporal gyrus reveal tonic hyperactivity in patients with auditory verbal hallucinations: A possible trait marker. *Frontiers in Human Neuroscience*, **7**: 304.
- Homan P, Kindler J, Hubl D, Dierks T (2012b). Auditory verbal hallucinations: imaging, analysis, and intervention. *European Archives of Psychiatry and Clinical Neuroscience*, **262 Suppl 2**: 91–5.
- Homan P, Lau H, Levy I, Raio C, Bach D, Carmel D, Schiller D (2018). Affective flexibility without perceptual awareness. *bioRxiv*. doi: 10.1101/505545.
- Homan P, Levy I, Feltham E, Gordon C, Hu J, Li J, Pietrzak RH, Southwick S, Krystal JH, Harpaz-Rotem I, Schiller D (2019c). Neural computations of threat in the aftermath of combat trauma. *Nature Neuroscience*, **22**: 470–476. doi: 10.1038/s41593-018-0315-x.

- Homan P, Lin Q, Murrough JW, Soleimani L, Bach DR, Clem RL, Schiller D (2017b). Prazosin during threat discrimination boosts memory of the safe stimulus. *Learning & Memory*, **24**(11): 597–601.
- Homan P, Neumeister A, Nugent A, Charney D, Drevets WC, Hasler G (2015). Serotonin versus catecholamine deficiency: behavioral and neural effects of experimental depletion in depression. *Translational Psychiatry*, **5**: e532.
- Homan P, Reddan MC, Brosch T, Koenigsberg HW, Schiller D (2017c). Aberrant link between empathy and social attribution style in borderline personality disorder. *Journal of Psychiatric Research*, **94**: 163–171.
- Homan P, Vermathen P, Van Swam C, Federspiel A, Boesch C, Strik W, Dierks T, Hubl D, Kreis R (2014). Magnetic resonance spectroscopy investigations of functionally defined language areas in schizophrenia patients with and without auditory hallucinations. *NeuroImage*, **94**: 23–32.
- Howes O (2010). Dopamine dysregulation: Pathophysiology or endophenotype? *Schizophrenia Research*, **117**(2-3): 136.
- Howes OD, Murray RM (2014). Schizophrenia: an integrated sociodevelopmental-cognitive model. *The Lancet*, **383**(9929): 1677–1687.
- Howes OD, Vergunst F, Gee S, McGuire P, Kapur S, Taylor D (2012). Adherence to treatment guidelines in clinical practice: Study of antipsychotic treatment prior to clozapine initiation. *British Journal of Psychiatry*, **201**(06): 481–485.
- Huys QJ, Maia TV, Frank MJ (2016). Computational psychiatry as a bridge from neuroscience to clinical applications. *Nature Neuroscience*, **19**(3): 404–413.
- Insel T (2013). Transforming Diagnosis. NIMH Director's Blog. <http://www.nimh.nih.gov/about/director/index.shtml>. Accessed: 10.02.2015.
- Insel TR (2014). The nimb research domain criteria (rdoc) project: precision medicine for psychiatry. *American Journal of Psychiatry*, **171**(4): 395–397.
- Insel TR, Cuthbert BN (2015). Brain disorders? precisely. *Science*, **348**(6234): 499–500.
- Jensen J, Willeit M, Zipursky RB, Savina I, Smith AJ, Menon M, Crawley AP, Kapur S (2008). The formation of abnormal associations in schizophrenia: Neural and behavioral evidence. *Neuropsychopharmacology*, **33**(3): 473–479.
- Juckel G, Schlagenhauf F, Koslowski M, Wustenberg T, Villringer A, Knutson B, Wräse J, Heinze A (2006). Dysfunction of ventral striatal reward prediction in schizophrenia. *NeuroImage*, **29**(2): 409–416.

- Kane J, Honigfeld G, Singer J, Meltzer H (1988). Clozapine for the treatment-resistant schizophrenic: a double-blind comparison with chlorpromazine. *Archives of General Psychiatry*, **45**(9): 789–796.
- Kane JM (2012). Clozapine is underutilized. *Shanghai Archives of Psychiatry*, **24**(2): 114.
- Kapur S, Phillips AG, Insel TR (2012). Why has it taken so long for biological psychiatry to develop clinical tests and what to do about it? *Molecular Psychiatry*, **17**(12): 1174–1179.
- Kapur S, Seeman P (2001). Does fast dissociation from the dopamine d₂receptor explain the action of atypical antipsychotics?: A new hypothesis. *American Journal of Psychiatry*, **158**(3): 360–369.
- Khadka S, Meda SA, Stevens MC, Glahn DC, Calhoun VD, Sweeney JA, Tamminga CA, Keshavan MS, O’Neil K, Schretlen D, Pearlson GD (2013). Is aberrant functional connectivity a psychosis endophenotype? a resting state functional magnetic resonance imaging study. *Biological Psychiatry*, **74**(6): 458–466.
- Kindler J, Homan P, Flury R, Strik W, Dierks T, Hubl D (2013a). Theta burst transcranial magnetic stimulation for the treatment of auditory verbal hallucinations: Results of a randomized controlled study. *Psychiatry Research*, **209**(1): 114–117.
- Kindler J, Homan P, Jann K, Federspiel A, Flury R, Hauf M, Strik W, Dierks T, Hubl D (2013b). Reduced neuronal activity in language-related regions after transcranial magnetic stimulation therapy for auditory verbal hallucinations. *Biological Psychiatry*, **73**(6): 518–24.
- Kindler J, Jann K, Homan P, Hauf M, Walther S, Strik W, Dierks T, Hubl D (2015). Static and dynamic characteristics of cerebral blood flow during the resting state in schizophrenia. *Schizophrenia Bulletin*, **41**: 163–70.
- Kirsch I, Deacon BJ, Huedo-Medina TB, Scoboria A, Moore TJ, Johnson BT (2008). Initial severity and antidepressant benefits: a meta-analysis of data submitted to the food and drug administration. *PLoS Medicine*, **5**(2): e45.
- Korducki KM (2019). It’s not just a chemical imbalance. *The New York Times*.
- Koutsouleris N, Riecher-Rossler A, Meisenzahl EM, Smieskova R, Studerus E, Kambeitz-Illankovic L, von Salder S, Cabral C, Reiser M, Falkai P, Borgwardt SJ (2014). Detecting the psychosis prodrome across high-risk populations using neuroanatomical biomarkers. *Schizophrenia Bulletin*, **41**(2): 471–482.

- Krystral JH, State MW (2014). Psychiatric disorders: diagnosis to therapy. *Cell*, **157**(1): 201–214.
- Lahti AC, Weiler MA, Holcomb HH, Tamminga CA, Cropsey KL (2009). Modulation of limbic circuitry predicts treatment response to antipsychotic medication: A functional imaging study in schizophrenia. *Neuropsychopharmacology*, **34**(13): 2675–2690.
- Lefaucheur JP, André-Obadia N, Antal A, Ayache SS, Baeken C, Benninger DH, Cantello RM, Cincotta M, de Carvalho M, De Ridder D, et al. (2014). Evidence-based guidelines on the therapeutic use of repetitive transcranial magnetic stimulation (rTMS). *Clinical Neurophysiology*, **125**(11): 2150–2206.
- Leucht S, Hierl S, Kissling W, Dold M, Davis JM (2012). Putting the efficacy of psychiatric and general medicine medication into perspective: review of meta-analyses. *The British Journal of Psychiatry*, **200**(2): 97–106.
- Liddle AR, Wands D (1992). There is a big-bubble problem in extended inflation. *Phys Rev D Part Fields*, **46**(8): 3655–3658.
- Lindenmayer JP (2000). Treatment refractory schizophrenia. *Psychiatric Quarterly*, **71**(4): 373–384.
- Liu CH, Ma X, Wu X, Li F, Zhang Y, Zhou FC, Wang YJ, Tie CL, Zhou Z, Zhang D, Dong J, Yao L, Wang CY (2012). Resting-state abnormal baseline brain activity in unipolar and bipolar depression. *Neuroscience Letters*, **516**(2): 202–206.
- Mamah D, Barch DM, Repovš G (2013). Resting state functional connectivity of five neural networks in bipolar disorder and schizophrenia. *Journal of Affective Disorders*, **150**(2): 601–609.
- McCutcheon RA, Abi-Dargham A, Howes OD (2019). Schizophrenia, dopamine and the striatum: From biology to symptoms. *Trends in Neurosciences*.
- Menon M, Schmitz TW, Anderson AK, Graff A, Korostil M, Mamo D, Gerretsen P, Addington J, Remington G, Kapur S (2011). Exploring the neural correlates of delusions of reference. *Biological Psychiatry*, **70**(12): 1127–1133.
- Moncrieff J (2018). Against the stream: Antidepressants are not antidepressants - an alternative approach to drug action and implications for the use of antidepressants. *BjPsych Bulletin*, **42**(1): 42–44.
- Moncrieff J, Kirsch I (2005). Efficacy of antidepressants in adults. *BMJ*, **331**(7509): 155–157.

- Mortimer A, Singh P, Shepherd C, Puthiryackal J (2010). Clozapine for treatment-resistant schizophrenia: National institute of clinical excellence (nice) guidance in the real world. *Clinical Schizophrenia & Related Psychoses*, **4**(1): 49–55.
- Munkholm K, Paludan-Müller AS, Boesen K (2019). Considering the methodological limitations in the evidence base of antidepressants for depression: a reanalysis of a network meta-analysis. *BMJ Open*, **9**(6).
- Nagano-Saito A, Leyton M, Monchi O, Goldberg YK, He Y, Dagher A (2008). Dopamine depletion impairs frontostriatal functional connectivity during a set-shifting task. *Journal of Neuroscience*, **28**(14): 3697–3706.
- Nielsen MO, Rostrup E, Wulff S, Bak N, Broberg BV, Lublin H, Kapur S, Glenthøj B (2012a). Improvement of brain reward abnormalities by antipsychotic monotherapy in schizophrenia. *Archives of General Psychiatry*, **69**(12): 1195.
- Nielsen MO, Rostrup E, Wulff S, Bak N, Lublin H, Kapur S, Glenthøj B (2012b). Alterations of the brain reward system in antipsychotic naive schizophrenia patients. *Biological Psychiatry*, **71**(10): 898–905.
- Nutt DJ, Goodwin GM, Bhugra D, Fazel S, Lawrie S (2014). Attacks on antidepressants: Signs of deep-seated stigma? *The Lancet Psychiatry*, **1**(2): 102–104.
- Olfson M, Gerhard T, Huang C, Crystal S, Stroup TS (2015). Premature mortality among adults with schizophrenia in the united states. *JAMA Psychiatry*, **72**(12): 1172.
- Open Science Collaboration (2015). Estimating the reproducibility of psychological science. *Science*, **349**(6251): aac4716.
- Oliac F, Naveau M, Joliot M, Delcroix N, Razafimandimbisoa A, Braza P, Dollfus S, Delamillieure P (2013). Links among resting-state default-mode network, salience network, and symptomatology in schizophrenia. *Schizophrenia Research*, **148**(1-3): 74–80.
- Owen MJ (2014). New approaches to psychiatric diagnostic classification. *Neuron*, **84**(3): 564–571.
- Pavuluri MN, Passarotti AM, Fitzgerald JM, Wegbreit E, Sweeney JA (2012). Risperidone and divalproex differentially engage the fronto-striato-temporal circuitry in pediatric mania: A pharmacological functional magnetic resonance imaging study. *Journal of the American Academy of Child & Adolescent Psychiatry*, **51**(2): 157–170.e5.
- Pavuluri MN, Passarotti AM, Lu LH, Carbray JA, Sweeney JA (2011). Double-blind randomized trial of risperidone versus divalproex in pediatric bipolar disorder: fMRI outcomes. *Psychiatry Research: Neuroimaging*, **193**(1): 28–37.

- Pompei F, Dima D, Rubia K, Kumari V, Frangou S (2011). Dissociable functional connectivity changes during the stroop task relating to risk, resilience and disease expression in bipolar disorder. *NeuroImage*, **57**(2): 576–582.
- Quidé Y, Morris RW, Shepherd AM, Rowland JE, Green MJ (2013). Task-related fronto-striatal functional connectivity during working memory performance in schizophrenia. *Schizophrenia Research*, **150**(2-3): 468–475.
- Rogers A (2017). Star Neuroscientist Tom Insel Leaves the Google-Spawned Verily for ... a Startup? *Slate*, **Nov. 5**.
- Sarpal DK, Argyelan M, Robinson DG, Szeszko PR, Karlsgodt KH, John M, Weissman N, Gallego JA, Kane JM, Lencz T, et al (2016). Baseline striatal functional connectivity as a predictor of response to antipsychotic drug treatment. *American Journal of Psychiatry*, **173**(1): 69–77.
- Sarpal DK, Robinson DG, Lencz T, Argyelan M, Ikuta T, Karlsgodt K, Gallego JA, Kane JM, Szeszko PR, Malhotra AK (2015). Antipsychotic treatment and functional connectivity of the striatum in first-episode schizophrenia. *JAMA Psychiatry*, **72**(1): 5.
- Sarter M, Tricklebank M (2012). Revitalizing psychiatric drug discovery. *Nature Reviews Drug Discovery*, **11**(6): 423.
- Schlagenhauf F, Sterzer P, Schmack K, Ballmaier M, Rapp M, Wräse J, Juckel G, Gallinat J, Heinz A (2009). Reward feedback alterations in unmedicated schizophrenia patients: relevance for delusions. *Biological Psychiatry*, **65**(12): 1032–9.
- Schmidt A, Borgwardt SJ (2013). Abnormal effective connectivity in the psychosis high-risk state. *NeuroImage*, **81**: 119–120.
- Schmidt A, Smieskova R, Aston J, Simon A, Allen P, Fusar-Poli P, McGuire PK, Riecher-Rössler A, Stephan KE, Borgwardt SJ (2013). Brain connectivity abnormalities predating the onset of psychosis. *JAMA Psychiatry*, **70**(9): 903.
- Schmidt A, Smieskova R, Simon A, Allen P, Fusar-Poli P, McGuire P, Bendfeldt K, Aston J, Lang U, Walter M, Radue E, Riecher-Rössler A, Borgwardt SJ (2014). Abnormal effective connectivity and psychopathological symptoms in the psychosis high-risk state. *Journal of Psychiatry Neuroscience*, **39**(4): 239–248.
- Schork NJ (2015). Personalized medicine: time for one-person trials. *Nature*, **520**: 609–611.

- Schumann G, Binder EB, Holte A, de Kloet ER, Oedegaard KJ, Robbins TW, Walker-Tilley TR, Bitter I, Brown VJ, Buitelaar J, et al. (2014). Stratified medicine for mental disorders. *European Neuropsychopharmacology*, **24**(1): 5–50.
- Seeman P, Lee T (1975). Antipsychotic drugs: Direct correlation between clinical potency and presynaptic action on dopamine neurons. *Science*, **188**(4194): 1217–1219.
- Seeman P, Lee T, Chau-Wong M, Wong K (1976). Antipsychotic drug doses and neuroleptic/dopamine receptors. *Nature*, **261**(5562): 717–719.
- Senn S (2016). Mastering variation: Variance components and personalised medicine. *Statistics in Medicine*, **35**(7): 966–977.
- Slotema CW, Blom JD, Hoek HW, Sommer IE (2010). Should we expand the toolbox of psychiatric treatment methods to include repetitive transcranial magnetic stimulation (rtms)? a meta-analysis of the efficacy of rtms in psychiatric disorders. *Journal of Clinical Psychiatry*, **71**(7): 873–84.
- Sorg C, Manoliu A, Neufang S, Myers N, Peters H, Schwerthöffer D, Scherr M, Mühlau M, Zimmer C, Drzezga A, Förstl H, Bäuml J, Eichele T, Wohlschläger AM, Riedl V (2013). Increased intrinsic brain activity in the striatum reflects symptom dimensions in schizophrenia. *Schizophrenia Bulletin*, **39**(2): 387–395.
- Stephan K, Schlagenhauf F, Huys Q, Raman S, Aponte E, Brodersen K, Rigoux L, Moran R, Daunizeau J, Dolan R, Friston K, Heinz A (2017a). Computational neuroimaging strategies for single patient predictions. *NeuroImage*, **145**: 180–199.
- Stephan KE, Bach DR, Fletcher PC, Flint J, Frank MJ, Friston KJ, Heinz A, Huys QJ, Owen MJ, Binder EB, Dayan P, Johnstone EC, Meyer-Lindenberg A, Montague PR, Schnyder U, Wang XJ, Breakspear M (2016a). Charting the landscape of priority problems in psychiatry, part 1: classification and diagnosis. *Lancet Psychiatry*, **3**(1): 77–83.
- Stephan KE, Binder EB, Breakspear M, Dayan P, Johnstone EC, Meyer-Lindenberg A, Schnyder U, Wang XJ, Bach DR, Fletcher PC, Flint J, Frank MJ, Heinz A, Huys QJM, Montague PR, Owen MJ, Friston KJ (2016b). Charting the landscape of priority problems in psychiatry, part 2: Pathogenesis and aetiology. *The Lancet Psychiatry*, **3**(1): 84–90.
- Stephan KE, Siemerkus J, Haker H (2017b). Zeitschrift für Psychiatrie, Psychologie und Psychotherapie. **65**: 9–19.

- Takeuchi H, Siu C, Remington G, Fervaha G, Zipursky RB, Foussias G, Agid O (2018). Does relapse contribute to treatment resistance? antipsychotic response in first- vs. second-episode schizophrenia. *Neuropsychopharmacology*, **44**(6): 1036–1042.
- Tu PC, Lee YC, Chen YS, Li CT, Su TP (2013). Schizophrenia and the brain's control network: Aberrant within- and between-network connectivity of the frontoparietal network in schizophrenia. *Schizophrenia Research*, **147**(2-3): 339–347.
- Vane LD, Mouchlianitis E, Collier T, Averbeck BB, Shergill SS (2018). Differential neural reward mechanisms in treatment-responsive and treatment-resistant schizophrenia. *Psychological Medicine*, **48**(14): 2418–2427.
- Wilson RC, Collins A (2019). Ten simple rules for the computational modeling of behavioral data. *PsyArxiv*. doi: 10.31234/osf.io/46mbn.
- Winkelbeiner S, Cavelti M, Federspiel A, Dierks T, Strik W, Horn H, Homan P (2018). Decreased blood flow in the right insula and middle temporal gyrus predicts negative formal thought disorder in schizophrenia. *Schizophrenia Research*, **201**: 432–434.
- Winkelbeiner S, Leucht S, Kane JM, Homan P (2019). Evaluation of differences in individual treatment response in schizophrenia spectrum disorders. *JAMA Psychiatry*. doi: 10.1001/jamapsychiatry.2019.1530.
- Wolkin A, Barouche F (1989). Dopamine blockade and clinical response: evidence for two biological subgroups of schizophrenia. *American Journal of Psychiatry*, **146**(7): 905–908.
- Wunderink L, Nieboer RM, Wiersma D, Sytema S, Nienhuis FJ (2013). Recovery in remitted first-episode psychosis at 7 years of follow-up of an early dose reduction/discontinuation or maintenance treatment strategy: long-term follow-up of a 2-year randomized clinical trial. *JAMA psychiatry*, **70**(9): 913–920.
- Yip SW, Worhunsky PD, Rogers RD, Goodwin GM (2015). Hypoactivation of the ventral and dorsal striatum during reward and loss anticipation in antipsychotic and mood stabilizer-naïve bipolar disorder. *Neuropsychopharmacology*, **40**(3): 658–666.
- Yoon JH, Nguyen DV, McVay LM, Deramo P, Minzenberg MJ, Ragland JD, Niendham T, Solomon M, Carter CS (2012). Automated classification of fmri during cognitive control identifies more severely disorganized subjects with schizophrenia. *Schizophrenia Research*, **135**(1-3): 28–33.

5 Appendix: Discussed papers

5.1 Homan et al. 2019a, Neuropsychopharmacology



ARTICLE

Structural similarity networks predict clinical outcome in early-phase psychosis

Philipp Homan ^{1,2,3}, Miklos Argyelan ^{1,2,3}, Pamela DeRosse ^{1,2,3}, Philip R. Szczek ⁴, Juan A. Gallego ^{1,2,3}, Lauren Hanna ^{1,2,3}, Delbert G. Robinson ^{1,2,3}, John M. Kane ^{1,2,3}, Todd Lencz ^{1,2,3} and Anil K. Malhotra ^{1,2,3}

Despite recent advances, there is still a major need for prediction of treatment success in schizophrenia, a condition long considered a disorder of dysconnectivity in the brain. Graph theory provides a means to characterize the connectivity in both healthy and abnormal brains. We calculated structural similarity networks in each participant and hypothesized that the "hubness", i.e., the number of edges connecting a node to the rest of the network, would be associated with clinical outcome. This prospective controlled study took place at an academic research center and included 82 early-phase psychosis patients (23 females; mean age [SD] = 21.6 [5.5] years) and 58 healthy controls. Medications were administered in a double-blind randomized manner, and patients were scanned at baseline prior to treatment with second-generation antipsychotics. Symptoms were assessed with the Brief Psychiatric Rating Scale at baseline and over the course of 12 weeks. Nodal degree of structural similarity networks was computed for each subject and entered as a predictor of individual treatment response into a partial least squares (PLS) regression. The model fit was significant in a permutation test with 1000 permutations ($P = 0.006$), and the first two PLS regression components explained 29% (95% CI: 27; 30) of the variance in treatment response after cross-validation. Nodes loading strongly on the first PLS component were primarily located in the orbito- and prefrontal cortex, whereas nodes loading strongly on the second PLS component were primarily located in the superior temporal, precentral, and middle cingulate cortex. These data suggest a link between brain network morphology and clinical outcome in early-phase psychosis.

Neuropsychopharmacology (2019) 0:1–8; <https://doi.org/10.1038/s41386-019-0322-y>

INTRODUCTION

Finding predictors of response to antipsychotic drug treatment is of critical importance to improving outcomes for psychotic disorders [1, 2]. A priori identification of patients who are not likely to respond to a specific treatment strategy could reduce the number and length of ineffective treatment trials. Moreover, understanding the biological underpinnings of effective treatments may lead to the detection of malleable central nervous system targets for the development of new treatment strategies—a current imperative because of the long-standing dearth of novel antipsychotic treatments.

Although parallel group trials cannot determine treatment response for individual patients in a definite manner, we have previously applied rigorous a priori criteria to distinguish likely responders from non-responders [3, 4] and have shown that functional striatal connectivity was higher in non-responders compared with responders [5] and normalized with antipsychotic treatment [6].

The fact that we found that brain connectivity was related to treatment outcome is not surprising. Schizophrenia has long been considered a disorder involving dysconnectivity in the human brain [7, 8], and graph theory has provided means to characterize the connectivity in the healthy and abnormal human brain [9].

Briefly, graph theory describes brain networks abstractly as a set of nodes and edges, and quantifies their patterns of connectivity [7]. Although normal brain graphs have typical properties (i.e., they are more organized than random graphs), brain graphs of schizophrenia patients may have specific abnormalities.

For example, highly connected nodes in the brain that are also densely connected with one another, so-called rich clubs, are present in schizophrenia but less prominent compared with healthy controls [10]. Other structural imaging studies using graph theory found evidence for less information integration and more clustering of nodes across brain regions [10–12]. Similar findings have emerged in other structural studies [13, 14], but studies based on functional connectivity have not always converged with these structural findings [15–17], and only a minority of studies have demonstrated relevance of these graph metrics for clinical outcome.

Although two prior studies [18, 19] computed group-wise graph metrics in responders and non-responders, we here tested how individual network architecture relates to individual clinical outcome. Previous work has shown that this can be achieved by comparing, in each individual, the statistical similarity between brain regions [20–22] or by assessing their correlations across different imaging domains [23]. Although still speculative, previous studies suggest that statistical similarity networks might

¹Center for Psychiatric Neuroscience, Feinstein Institute for Medical Research, Manhasset, NY, USA; ²Division of Psychiatry Research, Zucker Hillside Hospital, Northwell Health, New York, NY, USA; ³Department of Psychiatry, Zucker School of Medicine at Northwell/Hofstra, Hempstead, NY, USA and ⁴James J. Peters Veterans Affairs Medical Center, Bronx, NY, USA
Correspondence: Philipp Homan (phoman1@northwell.edu)

Received: 18 September 2018 Revised: 17 December 2018 Accepted: 16 January 2019
Published online: 24 January 2019

capture biologically meaningful correlates of development, aging, and brain disorders [24].

Statistical similarity between brain regions can be used to build similarity matrices across the whole brain for each individual from which a binary graph of nodes and edges can be constructed. This gives a similarity network (or connectome) for each participant, which can then serve as a predictor for individual treatment outcome. This was the approach we used in the current study (Fig. 1). Based on ample evidence that schizophrenia brain abnormalities are primarily located in highly connected nodes in the human connectome [25], we focused our analysis on the hubness (or nodal degree) graph metric, which can be computed from the similarity networks. We hypothesized that the hubness of cortical nodes would be associated with individual treatment outcome in two concatenated early psychosis cohorts. Treatment outcome of positive symptoms was computed using mixed models [26–30].

MATERIALS AND METHODS

Participants

We used two early-phase psychosis cohorts from two separate 12-week clinical trials on second-generation antipsychotics with a similar design and similar treatment effects (Fig. S1). Details have been published previously [31] and are summarized in Table 1, as well as in the Supplementary Information. Importantly, there were no significant differences between studies in duration of untreated psychosis ($t(62.48) = 0.72$, $P = 0.473$) and in the proportion of medication naïve participants ($\chi^2(1) = 2.66$, $P = 0.103$). Written informed consent was obtained from adult participants and the legal guardians of participants younger than 18 years. All participants under the age of 18 provided written informed assent. The study was approved by the Institutional Review Board (IRB) of Northwell Health, which served as the central IRB for all clinical sites. To replicate previously reported group differences in cortical thickness [32], we also included a sample of 58 healthy controls (Table 1). Healthy controls were recruited at the Zucker Hillside Hospital during the CIDAR trial.

Patients had a current DSM-IV-defined diagnosis of schizophrenia, schizophriform, schizoaffective disorder, or psychotic disorder not otherwise specified, and bipolar disorder with psychotic features and could have had up to 2 years of antipsychotic treatment. Many but not all subjects were first-episode patients. Note that excluding the patients with a diagnosis of bipolar disorder with psychotic features ($N = 3$) did not alter the results.

Symptom assessments using the anchored version of the Brief Psychiatric Rating Scale (BPRS-A) were done at baseline, weekly for 4 weeks, every 2 weeks until week 12. To obtain a measure of positive symptoms, we defined thought disturbance [3] as the sum of the following items: conceptual disorganization, grandiosity, hallucinatory behavior, and unusual thought content.

Structural magnetic resonance imaging and analysis
 Magnetic resonance imaging (MRI) exams were conducted on a 3-T scanner (GE Signa HDx). All participants were measured on the same scanner. We acquired anatomical scans in the coronal plane using an inversion-recovery prepared 3D fast spoiled gradient sequence (TR = 7.5 ms, TE = 3 ms, TI = 650 ms matrix = 256 × 256, FOV = 240 mm), which produced 216 contiguous images (slice thickness = 1 mm) through the whole brain. Image processing and segmentation were conducted with the FreeSurfer 5.1.0 recon-all pipeline and the Desikan-Killiany cortical atlas [33]. All image processing, parcellation, and quality control procedures were conducted while blinded to participants' demographic and clinical characteristics. Visual inspections for quality assurance were conducted and no manual interventions were necessary. Details

on the processing pipeline can be found in the Supplementary Information. We then tested for group differences in cortical thickness for each of the 68 regions as derived from the FreeSurfer recon-all pipeline and adjusted this analysis for age, sex, and intracranial volume.

Individual treatment response estimation

Rather than categorizing participants to responders and non-responders, which is statistically inefficient [29], we focused on treatment response as a continuous measure and used mixed models to make efficient use of the full sample and the repeated measures [26, 30, 34, 35].

Individual response was estimated using mixed models with restricted maximum likelihood and used as outcome measure in subsequent analyses. With mixed models, individual responses are estimated to be closer to the average treatment response, an effect that is well known as partial pooling or shrinkage [36]. The partial pooling effect for the two psychosis cohorts can be visualized by showing how individual treatment effects are pulled toward the average treatment effect (Fig. 2). Partial pooling makes the analysis less susceptible to individual outliers by attenuating the impact of participants with only few assessments (Fig. 2), which is of particular importance in estimating treatment response in relatively small samples. Although only 82 participants had MRI baseline data available, the full sample of 248 participants was used to obtain more precise estimates of the individual treatment response slopes. A more detailed description can be found in the Supplementary Information.

Graph theoretic analysis

Individual network graphs were computed following a new method that estimates statistical similarity across brain regions in each individual participant [20, 21]. The analysis flowchart is shown in Fig. 1. After cortical parcellation into 68 brain regions through the FreeSurfer recon-all pipeline, statistical similarity between all pair-wise brain regions was computed in each individual. First, probability density functions were estimated for the cortical thickness distribution in each region, using a Gaussian kernel and 512 sampling points. We followed the comprehensive characterization of structural similarity networks by Wang and colleagues [22] who also investigated the diminishing influence of increasing numbers of sampling points for the probability density function estimation. We then chose a more conservative resolution that the one used by Wang and colleagues [22] of 512 sampling points. This resulted in probability distributions for each of the 68 brain regions. Statistical similarity between each possible pair of distributions was then computed by calculating the Kullback-Leibler (KL) divergence between them [20–22]. The KL divergence measures the difference between two probability distributions (i.e., the loss of information when one distribution is used to approximate another). The KL divergence is thus defined as

$$D_{KL}(P||Q) = \sum_{i=1}^n P(i) \log \frac{P(i)}{Q(i)} \quad (1)$$

with P and Q being two probability distribution functions and n the number of sample points. Since $D_{KL}(P||Q)$ is not equal to $D_{KL}(Q||P)$, a symmetric variation of the KL divergence can be derived as follows:

$$D_{KL}(P, Q) = \sum_{i=1}^n \left(P(i) \log \frac{P(i)}{Q(i)} + Q(i) \log \frac{Q(i)}{P(i)} \right). \quad (2)$$

Finally, the following transformation was used to limit the measure to a range from 0 to 1:

$$KLS(P, Q) = e^{-D_{KL}(P, Q)}. \quad (3)$$

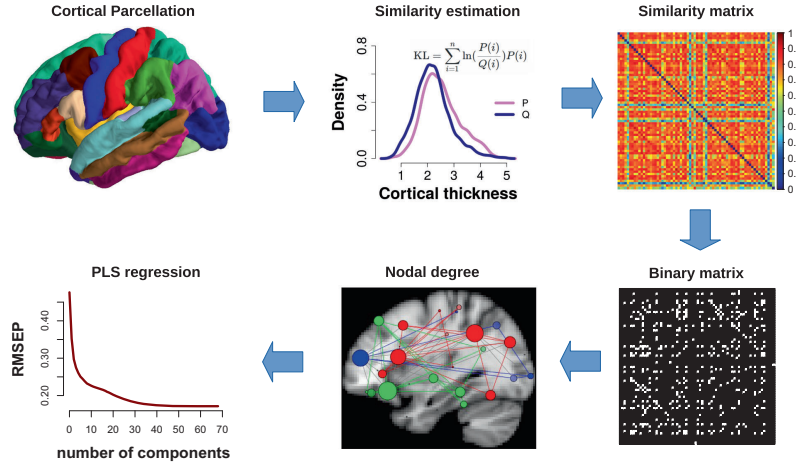


Fig. 1 Analysis flowchart. Computation of similarity networks in each participant by calculating the statistical similarity between brain regions. First, Freesurfer cortical parcellation was conducted for each individual participant. Cortical thickness was extracted for each vertex within each region and used to estimate the probability distribution function. The similarity between any pair of region was then estimated by calculating the KL divergence of their probability distributions, resulting in a 68×68 similarity matrix. The KL divergence computes the loss of information when one distribution is used to approximate another. The similarity matrix was then thresholded into a binary matrix to create a network graph. Graph-based degree (or hubness) for each node was then calculated for each individual participant. Nodal degrees were then entered as predictors into a partial least squares regression, using individual treatment response slopes as outcome measure. KL Kullback–Leibler divergence, PLS partial least squares regression, RMSEP root mean square error of prediction

Table 1. Sample characteristics						
Characteristic	PSY	Mean	SD	HC	Mean	SD
Males	59			25		
Females	23			33		
Age, years	82	21.6	5.5	58	28.1	11.9
Schizophrenia	57					
Schizopreniform disorder	15					
Psychotic disorder NOS	5					
Schizoaffective disorder	2					
Bipolar I disorder (with psychotic features)	3					
Prior medication exposure	75	8.4		29.4		
Medication naive	28					
Medication 2 weeks or less	71					
Education, years	77	12.2	2.2	58	13.7	2.9
IQ	69	97.9	13.2	49	102.2	10
BPRS total	82	42.7	7.5	0		
BPRS TD	82	14.3	3.1	0		
DUP, weeks	77	110.9	176.2	0		

PSY patients with early psychosis, HC healthy controls, BPRS Brief Psychiatric Rating Scale, BPRS TD Brief Psychiatric Rating Scale Thinking Disturbance, DUP duration of untreated psychosis, NOS not otherwise specified, IQ intelligence quotient

We thus computed the KLS values for all possible pairs of brain regions in each individual participant, resulting in a 68×68 similarity matrix S_{ij} for each subject (Fig. 1). Individual similarity matrices were then binarized by employing a sparsity threshold τ (number of actual edges divided by the maximum possible number of edges in a network), which ensured the same number of nodes and edges for the networks across participants. This resulted in a binary adjacency matrix A_{ij} [22]:

$$A_{ij} = [a_{ij}] = \begin{cases} 1, & \text{if } s_{ij} > KLS_{th}; \\ 0, & \text{otherwise,} \end{cases} \quad (4)$$

with KLS_{th} being a subject-specific KLS threshold that ensured that all networks had the same number of nodes and edges across participants. Following previous work [23], we chose a sparsity threshold of $\tau = 0.1$ for our analysis but also repeated calculations for a range of thresholds (0.1–0.7, with intervals of 0.05). The binary matrices allowed us to construct graphs of nodes and edges.

The graph theoretic measure of primary interest was nodal degree or hubness. The degree, $k(i)$, of a node is the number of edges connecting the i -th region to the rest of the network:

$$k(i) = \sum_{j=1}^n A_{ij}, \quad (5)$$

where A_{ij} is the binary adjacency matrix, which was computed by thresholding the similarity matrix, S_{ij} .

Statistical analyses

We used multivariate partial least squares (PLS) regression to test the relationship between nodal degree and individual treatment

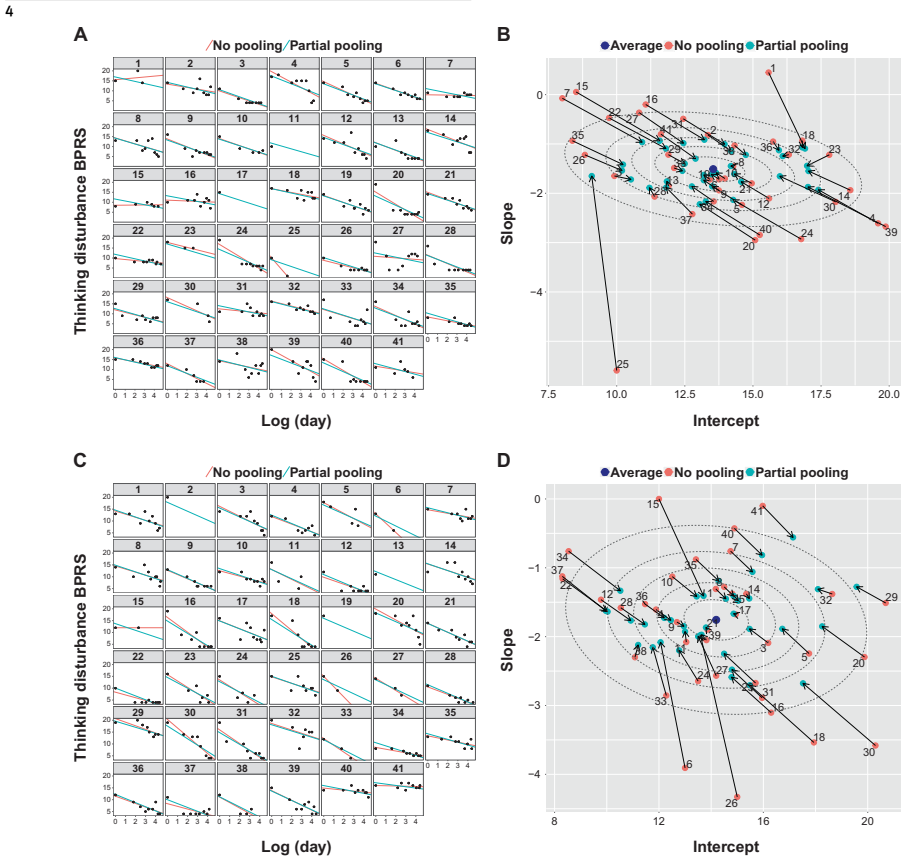


Fig. 2 Partial pooling to regularize individual response slopes. **a** Individual time courses for all participants from the first schizophrenia cohort. A log-linear relationship between time as measured in days from baseline and thinking disturbance symptoms was evident. Partial pooling regularized the individual slopes, i.e., the influence of outliers with only few assessments was attenuated. **b** The partial pooling effect is demonstrated by the individual responses being pulled toward the average treatment effect. As a consequence, outliers are less influential, as is particularly striking for those participants with few assessments. **c, d** The same is shown for the second schizophrenia cohort. Dotted ellipses indicate confidence regions for the average treatment effect (10, 30, 50, 70, 90%, respectively)

response. This method is particularly suited for a set of highly correlated predictors. In PLS, the optimal low-dimensional solution for a relationship between a set of correlated predictor variables and a response variable is computed. The 82×68 predictor variable matrix comprised estimates of degree (calculated at 10% connection density) for each of 68 nodes in each of 82 participants.

The (82×1) response vector comprised individual treatment response slopes. To account for unspecific inter-individual differences, the predictor matrix and the response vector were regressed on potential confounds, including study cohort (CIDAR, OMEGA3), baseline value of thinking disturbance, intracranial

volume, age, gender, and age \times gender interaction. Residuals of this regression were then used in the actual PLS analysis.

To rank each cerebral node according to its correlation with each PLS component, we used bootstrapping, i.e., drawing 1000 samples with replacement of the 82 individual participants, to compute the error on the PLS weights. A similar procedure has been used in recent graph theoretic work [23, 37, 38].

All analyses were conducted with R version 3.3.2 (2016-10-31) [39]. Mixed models were estimated using the lme4 library [40]. PLS regression were computed with the pls library [41], bootstrapping was performed with the boot library [42], and brain graph metrics were computed with the brainGraph [43] and igraph [44] libraries.

Python 2.7.15rc1 and pySurfer (0.8.0) were used for visualizing the imaging results.

RESULTS

Nodal degree predicts treatment response

The first two PLS regression components explained 29% (95% confidence interval (CI): 27, 30) of the variance in treatment response after cross-validation, with 1000 sets of five participants held out from the sample. This model fit was significant in a permutation test with 1000 permutations ($P = 0.006$). Notably, statistical significance ($P < 0.05$) was maintained when repeating the PLS regression across connection densities (0.1–0.7). The PLS components were positively correlated with treatment response slopes (first PLS component: $r = 0.66$, $P < 0.001$; second PLS component: $r = 0.4$, $P < 0.001$; Fig. 3). To assess their contribution, we ranked the 68 nodes of the individual networks according to their bootstrap standardized weight on each PLS component [23, 37, 38]. Most importantly, since the sign of the correlation between PLS components and treatment response slopes was positive (Fig. 3), nodes that correlated strongly with PLS scores had a negative relationship with treatment response. We found that they were primarily located in the orbito- and prefrontal cortices and posterior cingulate cortex for the first PLS component and in the superior temporal, precentral, and middle cingulate brain areas for the second PLS component (Fig. 3).

In summary, these findings suggest that individual differences in the configuration of structural similarity networks explain a significant proportion of the variance in treatment response.

We then also tested for group differences in nodal degree between psychosis patients and a cohort of healthy controls. Using permutation tests with 1000 permutations for each of the 68 nodes, we found a significant increase in nodal degree in the left orbitofrontal cortex ($P < 0.05$; Fig. S2).

Validation of results

To verify that our findings held up when using a different cortical parcellation scheme, we repeated the analysis using the Destrieux atlas [45], which comprises 148 nodes. We again found that the first two PLS components explained 30% (95% CI: 28, 31) of the variance in treatment response after cross-validation. In addition, excluding the patients with a diagnosis of bipolar disorder with psychotic features ($N = 3$) did not alter the results.

Group differences in cortical thickness

For completeness, we also assessed how the psychosis cohorts differed from the control cohort in terms of cortical thickness in all 68 cortical nodes. Confirming previous reports [32], cortical thickness was reduced in patients compared with controls most prominently in the left paracentral and parahippocampal gyrus and increased in the right rostral anterior cingulate cortex (Fig. S3). However, these alterations did not survive correction for multiple comparisons using false discovery rate ($q < 0.05$).

DISCUSSION

Here we showed that individual differences in structural similarity networks predicted treatment response in early-phase psychosis. The importance of this finding is twofold. First, we used the continuous scale to define treatment response, thereby increasing statistical sensitivity and avoiding power loss through dichotomization [29]. Second, and related, we computed networks for each participant, which allowed us to predict treatment response on the individual level.

We focused our analysis on a specific graph theoretic parameter, namely nodal degree or hubness. The rationale for this decision was that brain networks contain only a minority of highly connected nodes acting as hubs. Hubs are considered to be

functionally valuable by supporting information integration [25] but their value comes at a high biological cost due to increased metabolic demand and long-distance connections. Their prominent role suggests that schizophrenia-relevant brain abnormalities should be concentrated in hubs, a prediction that was indeed supported by a large body of meta-analytic evidence [25], where schizophrenia lesions were found most dominantly in frontal and temporal cortical hubs. In line with this notion, we found that nodal degree in orbito- and prefrontal areas contributed most strongly to the prediction of treatment response, with additional contributions from superior temporal regions. Importantly, nodes in the right orbitofrontal cortex have showed reduced degree compared with controls in functional networks in schizophrenia [15]. Our work extends this finding by showing that orbitofrontal nodes appear to impact clinical outcome in early-phase psychosis.

Although previous studies indicated the usefulness of brain morphology and machine learning in predicting response to treatment [46, 47], only one study has investigated the relationship between anatomical networks and clinical outcome [48]. That study used structural covariance of cortical folding to predict treatment response in first-episode psychosis, and found higher segregation, poorer integration, and vulnerable gyration covariance in non-responders. Specifically, non-responders showed reduced centrality of the left insula and anterior cingulate cortex. In addition, they were also more vulnerable to simulated lesions, i.e., covariance disintegrated after removal of high-degree hubs, supporting the relevance of nodal degree for treatment response [48]. A comparable study that used resting state functional connectivity found reduced global efficiency and increased clustering in patients with schizophrenia that normalized with response to antipsychotic treatment [19].

What is the biological meaning of structural similarity networks? It has been hypothesized that brain regions that grow together should display strong structural covariance across individuals [48, 49]. In line with this hypothesis, previous work has shown that structural networks of regions that grow together share similar global and nodal topological properties [50]. Thus, a likely interpretation is that structural similarity networks reflect "synchronized developmental change in distributed cortical regions" [50]. Accordingly, structural covariance networks show reorganization during normal development [24, 49, 51], aging [21, 52–54], and disease [12, 55, 56]. This suggests that structural similarity networks capture biologically meaningful correlates of development, aging, and brain disorders. Speculatively, then, these processes may impact distributed and treatment-relevant brain areas.

How can brain regions, similar in their thickness patterns and potentially growing synchronously, influence treatment outcome? Although still speculative, a potential mechanism is through the relationship with cognition. We have previously shown that higher scores in general cognition and reasoning capacity in particular were positive predictors of treatment response [4]. However, since that study did not include any brain imaging data, we could not characterize a potential neural correlate of this effect. Since brain network properties have been shown to be positively correlated with cognition [57], it is possible that they are the biological correlate underlying both cognition and improved treatment outcome.

An important difference between our study and previous attempts to characterize individual treatment response is that we did not dichotomize our sample into responders and non-responders. Although such dichotomization may be appealing and particularly relevant to clinicians, it is statistically inefficient to binarize a continuous measure [29, 58, 59]. The argument that binary decisions are what clinicians ultimately need to make, and therefore research should provide them with binary classifications, can easily be refuted. Indeed, if a binary decision must be made, it must be made at the point of actual clinical care, when all costs

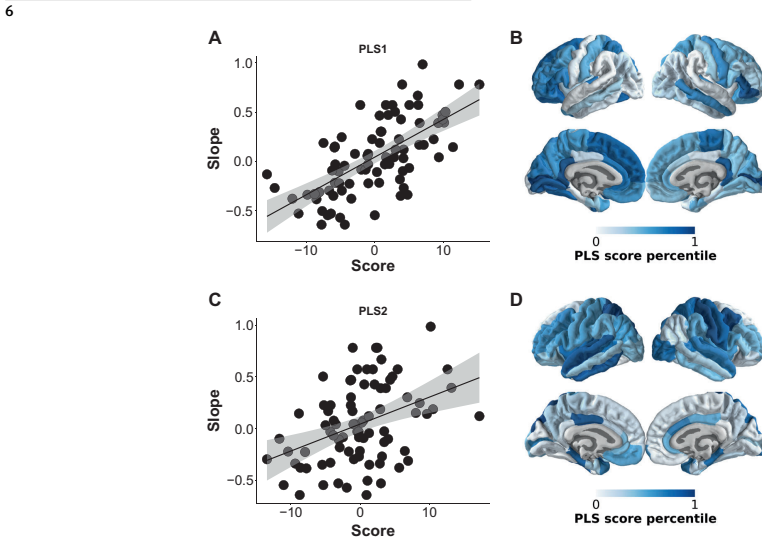


Fig. 3 Correlations of partial least squares (PLS) scores with individual treatment response and contribution of cortical nodes in the psychosis cohort ($N = 82$). Nodal degree for each of the 68 was entered into a PLS regression, with individual treatment response slopes as outcome measure. The first two PLS components explained a significant proportion of variance in treatment response. **a, b** The first PLS component correlated most strongly with nodal degree of orbito- and prefrontal cortices and posterior cingulate cortex. Note that more negative slopes meant better treatment response. **c, d** The second PLS component correlated most strongly with superior temporal, precentral, and middle cingulate brain areas

and potential benefits are known [59]. For example, the clinician may decide that a probable non-responder may still undergo treatment if the potential benefit outweighs the risk for that particular case. Furthermore, it is generally under-appreciated that it is often difficult to determine whether or not an individual patient responded to the treatment. The reason for this is that one does not know how the patient would have done under placebo. This is often overlooked and can limit attempts at classifying patients based on observed response. Thus, treatment response prediction based on a single-criterion classification in responders and non-responders should be treated with caution [75].

What is thus the potential clinical meaning and application of the current study's findings? With an approach such as this, the ultimate goal is to provide the clinician with an estimate of response probability for a given patient. As we have just shown, this is different from classifying the patient as a responder or non-responder. After taking all available information into account, it is the clinician (and not the researcher) who ultimately decides whether to treat even a likely non-responder. A study such as this can thus inform the clinician's decision process by providing individual predictions of treatment response.

The mixed model approach employed in this study is one way to address this problem; it separates random variation from actual treatment variation in each participant [29, 30]. In addition, individual treatment response is estimated more efficiently by utilizing the full data set and more conservatively by applying shrinkage [34, 36].

A few limitations merit comment. First, we did not include a placebo control group, which would have allowed us to compare the overall variability in response between the treatment and the

control groups. In principle, such a comparison would need to show that the variability in the treatment arm is higher than the one in the placebo arm, and that the difference is clinically relevant [60, 75]. However, placebo-controlled trials in early-phase psychosis have rarely been conducted. In addition, since the neurobiological underpinnings of graph metrics are still unknown, pathophysiological inferences must be made with caution. Next, we did not include functional connectivity [5] or other potentially predictive data in this study, which means that our findings may not be predictive when other predictors are included in the model. Finally, graph metrics may also vary depending on the parcellation scheme. However, in this study we repeated our analysis with an additional atlas of 148 nodes and found essentially the same results.

In conclusion, this study showed that advanced statistical modeling of treatment response and a relatively novel [20] computation of structural similarity networks established a potential link between brain network morphology and clinical outcome in early-phase psychosis.

FUNDING AND DISCLOSURE

This study was presented first at the European Conference of Schizophrenia Research 2017, Berlin, Germany. This work was supported by NIMH grant P50MH080173 to Dr. Malhotra, grant P30MH090590 to Dr. Kane, grant R01MH060004 to Dr. Robinson, grant R01MH076995 to Dr. Szeszko, and grant R21MH101746 to Drs. Robinson and Szeszko. Dr. Homan had full access to all the data in the study and takes responsibility for the integrity of the data and the accuracy of the data analysis. Dr. Robinson has

served as a consultant for Asubio, Otsuka, and Shire and has received grants from Bristol-Myers Squibb, Janssen, and Otsuka. Dr. Kane has served as a consultant for Alkermes, Eli Lilly, Forest, Forum, Genentech, Intracellular Therapies, Janssen, Johnson & Johnson, Lundbeck, Otsuka, Reviva, Roche, Sunovion, and Teva; he has received honoraria for lectures from Genentech, Janssen, Lundbeck, and Otsuka; and he is a shareholder in MedAvante and Vanguard Research Group. Dr. Lenzc has served as a consultant for Genomind. Dr. Malhotra has served as a consultant for Forum Pharmaceuticals and has served on a scientific advisory board for Genomind. The remaining authors declare no competing interests.

ACKNOWLEDGEMENTS

The authors acknowledge their patients, their patients' families, and their psychiatry research support staff. They thank Robert Gibbons, Ph.D., and Stephen Senn, Ph.D., for feedback regarding the statistical approaches used in this study.

DATA AND CODE AVAILABILITY

The data and code supporting the findings of this study are available online at <https://github.com/philiploman/ssn>. To ensure reproducibility we included a Makefile, which reflects the dependencies between different analysis modules and allows to run the analysis using the "make" command from the Unix command line.

ADDITIONAL INFORMATION

Supplementary Information accompanies this paper at (<https://doi.org/10.1038/s41386-019-0322-y>).

REFERENCES

- Stephan KE, Binder EB, Breakpear M, Dayan P, Johnstone EC, Meyer-Lindenberg A, et al. Charting the landscape of priority problems in psychiatry, part 2: pathogenesis and aetiology. *Lancet Psychiatry*. 2016;3:84–90.
- Dazzan P, Arango C, Fleischacker W, Galderisi S, Glenthoj B, Leucht S, et al. Magnetic resonance imaging and the prediction of outcome in first-episode schizophrenia: a review of current evidence and directions for future research. *Schizophr Bull*. 2015;41:574–83.
- Robinson DG, Gallego JA, John M, Petrides G, Hassoun Y, Zhang JP, et al. A randomized comparison of aripiprazole and risperidone for the acute treatment of first-episode schizophrenia and related disorders: 3-month outcomes. *Schizophr Bull*. 2015;41:1227–36.
- Trampush JW, Lenzc T, DeRosse P, John M, Gallego JA, Petrides G, et al. Relationship of cognition to clinical response in first-episode schizophrenia spectrum disorders. *Schizophr Bull*. 2015;41:1237–47.
- Sarpal DK, Argyelan M, Robinson DG, Szczesko PR, Karlsgodt KH, John M, et al. Baseline striatal functional connectivity as a predictor of response to anti-psychotic drug treatment. *Am J Psychiatry*. 2016;173:69–77.
- Sarpal DK, Robinson DG, Lenzc T, Argyelan M, Ikuta T, Karlsgodt K, et al. Antipsychotic treatment and functional connectivity of the striatum in first-episode schizophrenia. *JAMA Psychiatry*. 2015;725.
- Bullmore E, Vértes P. From Lichtenbaum to rich club. *JAMA Psychiatry*. 2013;70:780.
- Friston K, Brown HR, Siemerikus J, Stephan KE. The dysconnection hypothesis (2016). *Schizophr Res*. 2016;176:83–94.
- Bullmore E, Sporns O. Complex brain networks: graph theoretical analysis of structural and functional systems. *Nat Rev Neurosci*. 2009;10:186–98.
- van den Heuvel MP, Sporns O, Collin G, Schewe T, Mandl RC, Cahn W, et al. Abnormal rich club organization and functional brain dynamics in schizophrenia. *JAMA Psychiatry*. 2013;70:783–92.
- van den Heuvel MP, Mandl RCW, Stam CJ, Kahn RS, Hulshoff Pol HE. Aberrant frontal and temporal complex network structure in schizophrenia: a graph theoretical analysis. *J Neurosci*. 2010;30:15915–26.
- Zhang Y, Lin L, Liu CP, Zhou Y, Chou KH, Lo CY, et al. Abnormal topological organization of structural brain networks in schizophrenia. *Schizophr Res*. 2012;141:109–18.
- Bassett DS, Bullmore E, Verchinski BA, Mattay VS, Weinberger DR, Meyer-Lindenberg A. Hierarchical organization of human cortical networks in health and schizophrenia. *J Neurosci*. 2008;28:9239–48.
- Collin G, de Reus MA, Cahn W, Hulshoff Pol HE, Kahn RS, van den Heuvel MP. Disturbed grey matter coupling in schizophrenia. *Eur Neuropsychopharmacol*. 2013;23:46–54.
- Lynall ME, Bassett DS, Kerwin R, McKenna PJ, Kitzbichler M, Muller U, et al. Functional connectivity and brain networks in schizophrenia. *J Neurosci*. 2010;30:9477–87.
- Alexander-Bloch AF, Gogtay N, Meunier D, Birn R, Clasen L, Lalonde F, et al. Disrupted modularity and local connectivity of brain functional networks in childhood-onset schizophrenia. *Front Syst Neurosci*. 2010;4:147.
- Evans AC. Networks of anatomical covariance. *NeuroImage*. 2013;80:489–504.
- Palaniappan L, Marques TR, Taylor H, Mondelli V, Reinders AATS, Bonacorso S, et al. Globally efficient brain organization and treatment response in psychosis: a connectome study of gyration. *Schizophr Bull*. 2016;42:1446–56.
- Hadley JA, Kruglak NV, White DM, Ver Hoef L, Tabors J, Lahti AC. Change in brain network topology as a function of treatment response in schizophrenia: a longitudinal resting-state fMRI study using graph theory. *NPJ Schizophr*. 2016;2:16014.
- Kong X, Wang X, Huang L, Pu Y, Yang Z, Dang X, et al. Measuring individual morphological relationship of cortical regions. *J Neurosci Methods*. 2014;237:102–7.
- Kong X, Liu Z, Huang L, Wang X, Yang Z, Zhou G, et al. Mapping individual brain networks using statistical similarity in regional morphology from mri. *PLoS ONE*. 2015;10:e0141840.
- Wang H, Jin X, Zhang Y, Wang J. Single-subject morphological brain networks: connectivity mapping, topological characterization and test-retest reliability. *Brain Behav*. 2016;6:e00448.
- Seidlitz J, Vasa F, Shin M, Romero-Garcia R, Whitaker KJ, Vértes PE, et al. Morphometric similarity networks detect microscale cortical organisation and predict inter-individual cognitive variation. *Neuron*. 2018;97:231–47.
- Alexander-Bloch A, Giedd JN, Bullmore E. Imaging structural co-variance between human brain regions. *Nat Rev Neurosci*. 2013;14:322–36.
- Crossley NA, Mechelli A, Scott J, Carletti F, Fox PT, McGuire P, et al. The hubs of the human connectome are generally implicated in the anatomy of brain disorders. *Brain*. 2014;137:2382–95.
- Chen H, Cohen P. Using individual growth model to analyze the change in quality of life from adolescence to adulthood. *Health Qual Life Outcomes*. 2006;4:10.
- Senn S. Julius S. Measurement in clinical trials: a neglected issue for statisticians? *Stat Med*. 2009;28:189–209.
- Adkins DE, Åberg K, McClay JL, Hettema JM, Kornstein SG, Bukszár J, et al. A genome-wide association study of citalopram response in major depressive disorder—a psychometric approach. *Biol Psychiatry*. 2016;86:e25–7.
- Senn S. Mastering variation: variance components and personalised medicine. *Stat Med*. 2016;35:966–77.
- Hecksteden A, Pitsch W, Rosenberger F, Meyer T. Repeated testing for the assessment of individual responses to exercise training. *J Appl Physiol*. 2018;124:1567–79.
- Sarpal DK, Robinson DG, Fales C, Lenzc T, Argyelan M, Karlsgodt KH, et al. Relationship between duration of untreated psychosis and intrinsic corticostriatal connectivity in patients with early phase schizophrenia. *Neuropsychopharmacology*. 2017;42:2214–21.
- van Erp TG, Walton E, Hibar DP, Schmaal L, Jiang W, Glahn DC, et al. Cortical brain abnormalities in 4474 individuals with schizophrenia and 5098 control subjects via the enhancing neuro imaging genetics through meta analysis (enigma) consortium. *Am J Psychiatry*. 2018;175:644–54.
- Desikan RS, Ségonne F, Fischl B, Quinn BT, Dickerson BC, Blacker D, et al. An automated labeling system for subdividing the human cerebral cortex on mri scans into gyral based regions of interest. *Neuroimage*. 2006;31:968–80.
- Hedeker D, Gibbons RD. Longitudinal data analysis, Vol. 451. John Wiley & Sons; Hoboken, NJ, 2006.
- Norman G, Streiner D. Biostatistics: the bare essentials. Pmpb USA Ltd Series, B.C. Decker; Hamilton, Ontario. 2008.
- Gelman A, Carlin J, Stern H, Dunson D, Vehtari A, Rubin D. Bayesian data analysis, Third ed. Boca Raton: FL: CRC Press; 2013.
- Vértes PE, Rittman T, Whitaker KJ, Romero-Garcia R, Vásá F, Kitzbichler MG, et al. Gene transcription profiles associated with inter-modular hubs and connection distance in human functional magnetic resonance imaging networks. *Philos Trans R Soc B: Biol Sci*. 2016;371:20150362.
- Whitaker KJ, Vértes PE, Romero-Garcia R, Vásá F, Moutoussis M, Prabhu G, et al. Adolescence is associated with genetically patterned consolidation of the hubs of the human brain connectome. *Proc Natl Acad Sci USA*. 2016;113:9105–10.
- R Core Team. R: a language and environment for statistical computing. Vienna, Austria: R Foundation for Statistical Computing; 2016.
- Bates D, Maechler M, Bolker B, Walker S. Fitting linear mixed-effects models using lme4. *J Stat Softw*. 2015;67:1–48.

41. Mevik BH, Wehrens R, Liland KH. PLS: partial least squares and principal component regression. R package version2.6.0; 2016. <https://CRAN.R-project.org/package=pls>.
42. Carty A, Ripley BD. Boot: bootstrap R (S-Plus) functions. R package version1.3-20; 2017.
43. Watson CG, Stopp C, Newburger JW, Rivkin MJ. Graph theory analysis of cortical thickness networks in adolescents with d-transposition of the great arteries. *Brain Behav*. 2018;8:e00834.
44. Csardi G, Nepusz T. The iGraph software package for complex network research. *Inter-Journal* 2006; Complex Systems: 1695.
45. Destrieux C, Fischl B, Dale A, Halgren E. Automatic parcellation of human cortical gyri and sulci using standard anatomical nomenclature. *Neuroimage*. 2010;53:1–15.
46. Hasan A, Wobrock T, Guse B, Langguth B, Landgrebe M, Eichhammer P, et al. Structural brain changes are associated with response of negative symptoms to prefrontal repetitive transcranial magnetic stimulation in patients with schizophrenia. *Mol Psychiatry*. 2016;22:857–64.
47. Koutsouleris N, Wobrock T, Guse B, Langguth B, Landgrebe M, Eichhammer P, et al. Predicting response to repetitive transcranial magnetic stimulation in patients with schizophrenia using structural magnetic resonance imaging: a multisite machine learning analysis. *Schizophr Bull*. 2018;44:1021–34.
48. Palaniyappan L, Mahmood J, Balain V, Mougin O, Gowland PA, Liddle PF. Structural correlates of formal thought disorder in schizophrenia: an ultra-high field multivariate morphometry study. *Schizophr Res*. 2015;168:305–12.
49. Zieliński B, Gennatas ED, Zhou J, Seeley WW. Network-level structural covariance in the developing brain. *Proc Natl Acad Sci USA*. 2010;107:18191–6.
50. Alexander-Bloch A, Raznahan A, Bullmore E, Giedd J. The convergence of maturational change and structural covariance in human cortical networks. *J Neurosci*. 2013;33:2889–99.
51. Fan Y, Shi F, Smith JK, Lin W, Gilmore JH, Shen D. Brain anatomical networks in early human brain development. *NeuroImage*. 2011;54:1862–71.
52. Chen ZJ, He Y, Rosa-Neto P, Gong G, Evans AC. Age-related alterations in the modular organization of structural cortical network by using cortical thickness from MRI. *NeuroImage*. 2011;56:235–45.
53. Wu K, Taki Y, Sato K, Kinomura S, Goto R, Okada K, et al. Age-related changes in topological organization of structural brain networks in healthy individuals. *Human Brain Mapp*. 2011;33:552–68.
54. Zhu W, Wen W, He Y, Xia A, Anstey KJ, Sachdev P. Changing topological patterns in normal aging using large-scale structural networks. *Neurobiol Aging*. 2012;33:899–913.
55. He Y, Chen Z, Evans A. Structural insights into aberrant topological patterns of large-scale cortical networks in alzheimer's disease. *J Neurosci*. 2008;28:4756–66.
56. Seeley WW, Crawford RK, Zhou J, Miller BL, Greicius MD. Neurodegenerative diseases target large-scale human brain networks. *Neuron*. 2009;62:42–52.
57. Baggio HC, Segura B, Junque C, de Reus MA, Sala-Llonch R, den Heuvel MPV. Rich club organization and cognitive performance in healthy older participants. *J Cogn Neurosci*. 2015;27:1801–10.
58. Senn S. Disappointing dichotomies. *Pharm Stat*. 2003;2:239–40.
59. Harrell FE. Regression modeling strategies: with applications to linear models, logistic and ordinal regression, and survival analysis. Springer Series in Statistics, Springer International Publishing; Switzerland, 2015.
60. Cortes J, Gonzalez JA, Medina MN, Vogler M, Vilardo M, Elmore M, et al. Does evidence support the high expectations placed in precision medicine? A bibliographic review (version 2), p. 30. F1000Research. 7.
61. Wroclawski KM, Averill LA, Cobb Scott J, Averill CL, Schweinsburg B, Trejo M, et al. Cortical thickness reduction in combat exposed U.S. veterans with and without PTSD. *Eur Neuropsychopharmacol*. 2017;27:515–525.
62. Reuter M, Rosas HD, Fischl B. Highly accurate inverse consistent registration: a robust approach. *NeuroImage*. 2010;53:1181–96.
63. Ségonne F, Dale AM, Busa E, Glessner M, Salat D, Hahn HK, et al. A hybrid approach to the skull stripping problem in mri. *NeuroImage*. 2004;22:1060–75.
64. Fischl B, Salat D, Busa E, Albert M, Dieterich M, Haselgrave C, et al. Whole brain segmentation: automated labeling of neuroanatomical structures in the human brain. *Neuron*. 2002;33:341–55.
65. Fischl B, Salat DH, van der Kouwe AJ, Makris N, Ségonne F, Quinn BT, et al. Sequence-independent segmentation of magnetic resonance images. *NeuroImage*. 2004;23:569–584.
66. Fischl B, Liu A, Dale AM. Automated manifold surgery: constructing geometrically accurate and topologically correct models of the human cerebral cortex. *IEEE Trans Med Imaging*. 2001;20:70–80.
67. Ségonne F, Pachet J, Fischl B. Geometrically accurate topology-correction of cortical surfaces using nonseparating loops. *IEEE Trans Med Imaging*. 2007;26:518–29.
68. Dale AM, Fischl B, Sereno MI. Cortical surface-based analysis: I. segmentation and surface reconstruction. *NeuroImage*. 1999;9:179–94.
69. Fischl B, Dale AM. Measuring the thickness of the human cerebral cortex from magnetic resonance images. *Proc Natl Acad Sci USA*. 2000;97:11050–5.
70. Fischl B, Sereno MI, Dale AM. Cortical surface-based analysis: II: inflation, flattening, and a surface-based coordinate system. *NeuroImage*. 1999;9:195–207.
71. Fischl B, Van Der Kouwe A, Destrieux C, Halgren E, Ségonne F, Salat DH, et al. Automatically parcellating the human cerebral cortex. *Cereb Cortex*. 2004;14:11–22.
72. Kuperberg GR, Broome MR, McGuire PK, David AS, Eddy M, Ozawa F, et al. Regionally localized thinning of the cerebral cortex in schizophrenia. *Arch General Psychiatry*. 2003;60:878–88.
73. Han X, Jovicich J, Salat D, van der Kouwe A, Quinn B, Czanner S, et al. Reliability of MRI-derived measurements of human cerebral cortical thickness: the effects of field strength, scanner upgrade, and manufacturer. *NeuroImage*. 2006;32:180–94.
74. Reuter M, Schmansky NJ, Rosas HD, Fischl B. Within-subject template estimation for unbiased longitudinal image analysis. *NeuroImage*. 2012;61:1402–18.
75. Winkelbeiner S, Leucht S, Kane JM, Homan P. Often claimed, rarely tested: differences in individual drug response. *PsyArxiv*. 2018; <https://doi.org/10.31234/osf.io/5unfj>.

Supplementary Information

First cohort: CIDAR trial

Settings

The study was conducted at eight area facilities in New York City and one facility each in San Antonio, TX and Calgary, Alberta, Canada. All sites were not-for-profit institutions (either academic centers, community facilities, or public hospitals) located in urban or suburban areas, serving diverse communities in terms of economic status and racial/ethnic composition. Imaging data was acquired only for participants from the site in New York City. Data were collected from December 2005 until April 2013.

Participants

Enrolled patients had a current DSM-IV-defined diagnosis of schizophrenia, schizophreriform, schizoaffective disorder, or psychotic disorder Not Otherwise Specified (NOS) and were between 15-40 years of age. At baseline, patients had 2 weeks or less of a lifetime exposure to antipsychotic medication treatment (at any dose) and current positive symptoms of at least 4 (moderate) on one or more of the Brief Psychiatric Rating Scale-Anchored version (BPRS-A) 7 items: conceptual disorganization, grandiosity, hallucinatory behavior, or unusual thought content. For women, a negative pregnancy test and agreement to use a medically accepted birth control method was required.

Exclusion criteria were (1) meeting DSM-IV criteria for current substance-induced psychotic disorder, psychotic disorder due to a general medical condition, delusional disorder, brief psychotic disorder, shared psychotic disorder, or mood disorder (major depression or bipolar) with psychotic features; (2) serious neurological or endocrine disorder or medical condition/treatment known to affect

the brain; (3) medical conditions requiring treatment with a medication with psychotropic effects; (4) medical contraindications to risperidone or aripiprazole treatment; (5) significant risk of suicidal or homicidal behavior; (6) any factor (eg, language limitations) that would preclude informed consent or participation in study procedures; (7) diagnosis of diabetes (defined as fasting plasma glucose >126 mg/dl) or the metabolic syndrome (defined as 3 or more of the following: high blood pressure (>130/85 mm Hg), truncal obesity (waist circumference >40 inches for men and >35 for women), elevated fasting glucose (>110 mg/dl), low, high-density lipoprotein (HDL) cholesterol (<40 mg/dl for men and <50 mg/dl for women), and elevated triglycerides (>150 mg/dl); and (8) requiring antidepressant or mood stabilizer treatment.

Written informed consent was obtained from adult participants and the legal guardians of participants younger than 18 years. All participants under the age of 18 provided written informed assent. The study was approved by the Institutional Review Board (IRB) of Northwell Health, which served as the central IRB for all clinical sites.

Treatment

The acute trial of aripiprazole vs risperidone treatment lasted 12 weeks. Participants were stratified by site, previous antipsychotic exposure (none vs any), and diagnosis (psychotic disorder NOS vs other eligible diagnoses) and were randomly assigned on a 1:1 basis to double-masked treatment with either aripiprazole (5-30 mg/d) or risperidone (1-6 mg/d). Inclusion criteria required all participants to have very limited prior antipsychotic exposure (less than 2 weeks, see above); any antipsychotics being taken at study entry were discontinued.

The initial daily dose was 1 study capsule (ie, 5 mg of aripiprazole or 1 mg of risperidone). Medication doses were advanced according to a titration schedule (level 2 at day 4, level 3 at week 1,

two level 2 capsules at week 4, a level 2 and level 3 capsule at week 6, and two level 3 capsules at week 8) until response criteria were achieved or dose-limiting side effects occurred. Study psychiatrists could advance or slow the titration schedule for clinical needs.

Assessments

Initial diagnostic eligibility was established with the Structured Clinical Interview for DSM-IV Axis I Disorders (SCID). These data were later reviewed in a consensus conference for final diagnostic assignment. Symptom assessments using the BRPS-A were done at baseline, weekly for 4 weeks, every 2 weeks until week 12. To obtain a measure of positive symptoms, we defined thought disturbance [3] as the sum of the following items: conceptual disorganization, grandiosity, hallucinatory behavior, and unusual thought content. Assessments were performed by a team of central raters that traveled to New York area sites in person or used secure teleconferencing elsewhere. The same rater performed assessments with each participant throughout that individual's study participation. Intraclass correlation coefficients for the BPRS items were generally high (> 0.9) [3]. At baseline, trained psychometricians administered the MCCB and adhered to procedures described in the test manual.

Structural magnetic resonance imaging and analysis

Magnetic resonance imaging exams were conducted on a 3-T scanner (GE Signa HDx). We acquired anatomical scans in the coronal plane using an inversion-recovery prepared 3D fast spoiled gradient (IR-FSPGR) sequence (TR = 7.5 ms, TE = 3 ms, TI = 650 ms matrix = 256 × 256, FOV = 240 mm) which produced 216 contiguous images (slice thickness = 1 mm) through the whole brain. Image processing and segmentation were conducted with the Freesurfer 5.1.0 recon-all pipeline and the Desikan-Killiany cortical atlas [31]. Of note, this pipeline includes two surface smoothing steps with 10 curvature

averaging iterations and 10 smoothing iterations. All image processing, parcellation, and quality control procedures were conducted while blinded to participants' demographic and clinical characteristics. Visual inspections for quality assurance were conducted and no manual interventions were necessary.

Second cohort: OMEGA3 trial

Participants

For this cohort, we additionally included participants with bipolar disorder with psychotic features and participants could have had up to 2 years of antipsychotic treatment. Many but not all subjects were first episode patients. Apart from that, we applied the same inclusion and exclusion criteria as in the CIDAR trial (see above). After complete description of the study, written informed consent was obtained from adult participants and legal guardians of participants younger than 18 years who provided written assent. The study was approved by the Institutional Review Board (IRB) of the Feinstein Institute for Medical Research.

Assessments

Initial diagnostic eligibility was established with the Structured Clinical Interview for DSM-IV Axis I Disorders (SCID). These data were later reviewed in a consensus conference for final diagnostic assignment. Assessments of BRPS-A were done at baseline, weekly for 4 weeks, every 2 weeks until week 12. Thought disturbance was defined as the sum of unusual thought content, hallucinations, and conceptual disorganization from the BPRS-A. Assessments were performed by trained clinical raters at the Zucker Hillside Hospital. The same rater performed assessments with each participant throughout that individual's study participation.

Structural magnetic resonance imaging and analysis

Magnetic resonance imaging and analysis was conducted similarly as in the CIDAR trial (see above).

Freesurfer processing details

Briefly, and following a recent thorough description of the procedure [61], this freesurfer processing includes motion correction and averaging [62] of two volumetric T1 weighted images. Non-brain tissue is then removed with a hybrid deformation method [63], followed by a Talairach transformation and segmentation of subcortical white matter and deep gray matter volumetric structures [64, 65]. intensity normalization, tessellation of the gray matter white matter boundary, and automated correction of topology [66, 67]. The next step is surface deformation, guided by intensity gradients for optimal placement of gray/white and gray/cerebrospinal fluid borders, using the location where the greatest shift in intensity defines the transition to the other tissue class [68, 69].

After completion of the cortical models, final processing steps include surface inflation [68], registration to a spherical atlas based on individual cortical folding patterns [70], and parcellation of the cerebral cortex into units with respect to gyral and sulcal structure [33, 71]. Importantly, cortical thickness is then measured as the Euclidean distance from the gray/white boundary to the gray/CSF boundary at each vertex on the tessellated surface [69]. Procedures for the measurement of cortical thickness have been validated against manual measurements [72] and have shown high test-retest reliability [73, 74].

Individual response estimation

Assuming linear improvement over time, individual treatment response can be modeled as

$$Y_{ij} = \beta_{0j} + \beta_{1j} X_{ij} + \epsilon_{ij}, \quad (6)$$

where Y is the outcome measure (i.e., the symptoms) at time i for patient j , β_{0j} is the intercept and β_{1j} is the slope for patient j , X_{ij} is a vector of the time predictor (measured in log-transformed days from baseline), while ϵ is the error term, which is assumed to be normally distributed with mean zero and some unknown variance,

$$\epsilon_{ij} \sim \mathcal{N}(0, \sigma^2). \quad (7)$$

This level-1 model thus indicates each patient's treatment response over time. It can be extended to a level-2 model by including sample averages for intercept and slope,

$$\beta_{0j} = \gamma_{00} + U_{0j} \quad (8)$$

$$\beta_{1j} = \gamma_{10} + U_{1j} \quad (9)$$

with

$$\begin{pmatrix} U_{0j} \\ U_{1j} \end{pmatrix} \sim \mathcal{N} \begin{pmatrix} 0, & \tau_{00}^2 & \tau_{01} \\ 0, & \tau_{01} & \tau_{10}^2 \end{pmatrix}, \quad (10)$$

where U_{0j} is the random intercept and U_{1j} is the random slope, that is, the individual deviances from the sample intercepts and slopes, respectively, both with zero mean and some unknown variances. Note that the random slope, U_{1j} , was the measure of interest in this study and used as primary outcome.

The covariance between the random intercept and the random slope is indicated with τ_{01} . This hierarchical unconditional growth model describes the average symptom trajectory while accounting for individual deviances from both the intercept and the slope.

Due to the well-known challenges in assessing this specific patient population, missed assessments and minor variations in rating intervals were to be expected. We dealt with them by calculating the exact days from baseline when the ratings were performed, and used days rather than weeks as the time variable in our analysis. To account for the log-linear decrease of symptoms over time (Fig. S1) we used the log-transformed number of days.

An important difference from previous strategies to characterize individual treatment response is that we did not distinguish, *a priori*, between patients who met or did not meet a defined response criterion.

Rather, our method allowed for the estimation of individual treatment response. While only 82 participants had MRI baseline data available, the full sample of 248 participants was utilized to obtain more precise estimates of the individual treatment response slopes. The rationale for this approach is that information from the full sample can be used to estimate individual slopes more conservatively because the average treatment effect of the full sample provides a reasonable prior assumption for each individual response slope [34]. Thus, similar to full Bayesian estimation, a prior enters the statistical calculation; however, here the prior is derived empirically from the data, hence this method bears similarity with Empirical Bayes. The result is that individual responses are estimated to be closer to the average treatment response, an effect that is well-known as partial pooling or shrinkage. [36]. The partial pooling effect for the two schizophrenia cohorts can be visualized by showing how individual treatment effects are pulled toward the average treatment effect (Fig. 2). Partial pooling makes the analysis less susceptible to individual outliers by attenuating the impact of participants with only few assessments (Fig. 2), which is of particular importance in estimating treatment response in relatively small samples.

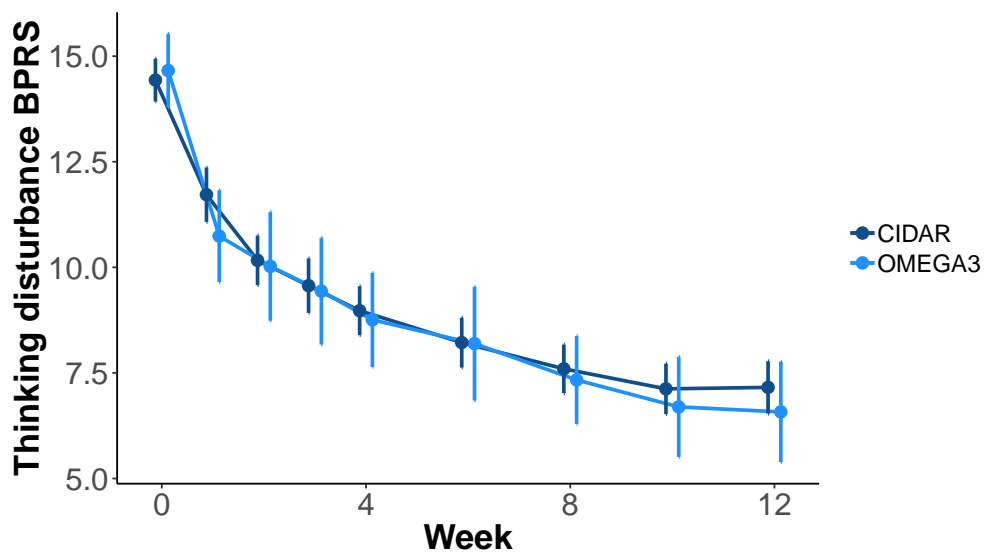
Thus, individual slopes were estimated using mixed models with Restricted Maximum Likelihood (REML) and used as outcome measure in subsequent analyses.

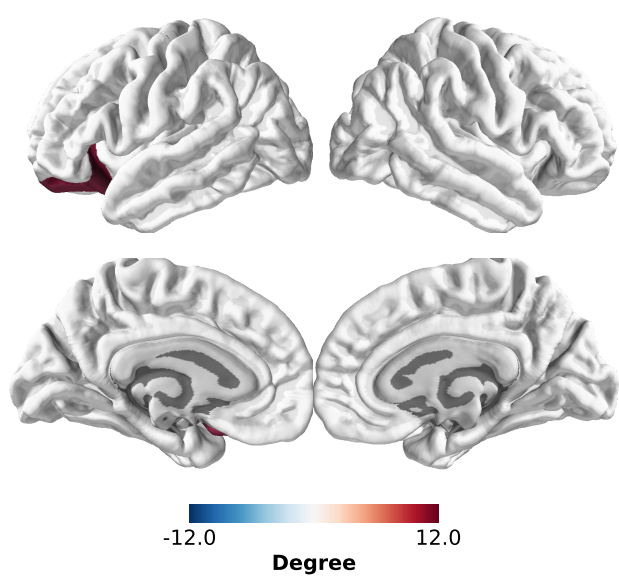
Figure legends

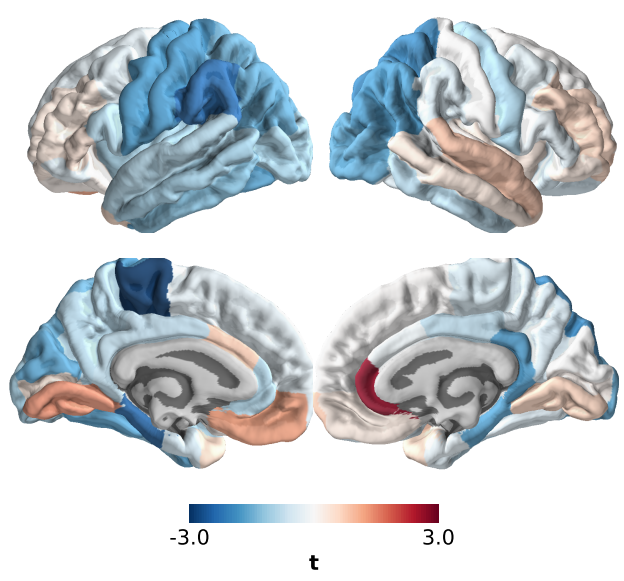
Figure S1: Both schizophrenia cohorts showed a similar average treatment effect. Means with 95% confidence intervals are shown. In both cohorts, symptoms decreased in a log-linear fashion with increasing weeks. To increase statistical power, both cohorts were thus concatenated for the subsequent analysis of treatment response prediction.

Figure S2: Significant group differences in nodal degree between patients with psychosis and healthy controls. Positive values indicate higher nodal degrees in patients compared to controls.

Figure S3: Group differences in cortical thickness. Cortical thickness was reduced in patients compared to controls most prominently in the left paracentral and left parahippocampal gyrus. Note that these reductions did not survive rigid correction for multiple comparisons using false discovery rate (FDR $q < 0.05$).







5.2 Homan et al. 2019b, Neuropsychopharmacology



ARTICLE

Striatal volume and functional connectivity correlate with weight gain in early-phase psychosis

Philipp Homan ^{1,2,3}, Miklos Argyelan ^{1,2,3}, Christina L. Fales ², Anita D. Barber ², Pamela DeRosse ^{1,2,3}, Philip R. Szczekko ⁴, Delbert G. Robinson ^{1,2,3}, Todd Lencz ^{1,2,3} and Anil K. Malhotra ^{1,2,3}

Second-generation antipsychotic drugs (SGAs) are essential in the treatment of psychotic disorders, but are well-known for inducing substantial weight gain and obesity. Critically, weight gain may reduce life expectancy for up to 20–30 years in patients with psychotic disorders, and prognostic biomarkers are generally lacking. Even though other receptors are also implicated, the dorsal striatum, rich in dopamine D2 receptors, which are antagonized by antipsychotic medications, plays a key role in the human reward system and in appetite regulation, suggesting that altered dopamine activity in the striatal reward circuitry may be responsible for increased food craving and weight gain. Here, we measured striatal volume and striatal resting-state functional connectivity at baseline, and weight gain over the course of 12 weeks of antipsychotic treatment in 81 patients with early-phase psychosis. We also included a sample of 58 healthy controls. Weight measurements were completed at baseline, and then weekly for 4 weeks, and every 2 weeks until week 12. We used linear mixed models to compute individual weight gain trajectories. Striatal volume and whole-brain striatal connectivity were then calculated for each subject, and used to assess the relationship between striatal structure and function and individual weight gain in multiple regression models. Patients had similar baseline weights and body mass indices (BMI) compared with healthy controls. There was no evidence that prior drug exposure or duration of untreated psychosis correlated with baseline BMI. Higher left putamen volume and lower sensory motor connectivity correlated with the magnitude of weight gain in patients, and these effects multiplied when the structure–function interaction was considered in an additional exploratory analysis. In conclusion, these results provide evidence for a correlation of striatal structure and function with antipsychotic-induced weight gain. Lower striatal connectivity was associated with more weight gain, and this relationship was stronger for higher compared with lower left putamen volumes.

Neuropsychopharmacology (2019) 0:1–7; <https://doi.org/10.1038/s41386-019-0464-y>

INTRODUCTION

Weight gain is a major side effect of treatment with antipsychotic drugs, but individual weight gain may vary considerably between patients treated with a given antipsychotic agent, especially in the first episode of illness [1].

Although all antipsychotic drugs induce weight gain, some appear to induce more than others [2, 3], and the reasons for the differences between drugs and between patients are unclear [4, 5]. Genetic variability [6–8] and lifestyle likely play a role, but structural and functional differences in the brain's dopaminergic reward system have not been fully understood. In addition to dopamine's function in food reward and in the control of food intake [9], dopamine is also a key factor in schizophrenia and in antipsychotic action, suggesting that one may expect baseline differences in striatal structure and function to account for the variability in antipsychotic-induced weight gain.

Even though other receptors are also strongly implicated in antipsychotic weight gain [10], the dorsal striatum, rich in dopamine D2 receptors, which are antagonized by antipsychotic medications, plays an important role in the human reward

system and in appetite regulation [11–14], suggesting that altered dopamine activity in the striatal reward circuitry may contribute to increased food craving and the resultant weight gain [15]. In line with this notion, previous work has shown that decreased baseline functional activity in the putamen predicted the amount of future antipsychotic weight gain [16], and olanzapine-induced activity in the dorsal striatum was associated with excessive eating behavior [17]. Supporting the hypothesis of altered reward processing in schizophrenia, these results suggest that decreased reward anticipation in the putamen before antipsychotic treatment may predispose to weight gain under antipsychotic treatment. However, we are not aware of studies in weight gain using risperidone and aripiprazole, two widely used second-generation antipsychotic drugs (SGAs) [18].

Furthermore, in addition to altered activation in fMRI tasks, variability in striatal structure and functional connectivity may also contribute to weight gain. Indeed, previous studies have shown higher striatal volumes in addictive behavior [19, 20], as well as weaker fronto-striatal connectivity in obesity [21]. Thus, we

¹Center for Psychiatric Neuroscience, Feinstein Institute for Medical Research, Manhasset, NY, USA; ²Division of Psychiatry Research, Zucker Hillside Hospital, Northwell Health, New York, NY, USA; ³Department of Psychiatry, Donald and Barbara Zucker School of Medicine at Northwell/Hofstra, Hempstead, NY, USA and ⁴James J. Peters Veterans Affairs Medical Center, Bronx, NY, USA

Correspondence: Philipp Homan (phoman1@northwell.edu)

These authors contributed equally: Todd Lencz and Anil K. Malhotra

Received: 20 December 2018 Revised: 14 June 2019 Accepted: 8 July 2019
Published online: 17 July 2019

measured striatal volume and striatal resting-state functional connectivity in patients with early-phase psychosis at baseline, and weight gain over the course of 12 weeks of treatment with risperidone and aripiprazole, and hypothesized that higher striatal volume and lower cortico-striatal connectivity would be associated with more weight gain [21, 22], particularly in brain regions implicated in obesity [21, 23]. We also expected that striatal volume would be higher in patients compared with controls, as found in a previous meta-analysis [24].

MATERIALS AND METHODS

Participants

We used two early-phase psychosis cohorts from two separate 12-week clinical trials, with a similar design and similar treatment effects, resulting in a sample of 81 patients. We defined early-phase psychosis as having taken antipsychotic medications for a cumulative lifetime period of 2 years or less [25, 26]. Details have been published previously [18, 25–27] and are summarized in Table 1. Written informed consent was obtained from adult participants and the legal guardians of participants younger than 18 years. All participants under the age of 18 provided written informed assent. The study was approved by the Institutional Review Board (IRB) of Northwell Health. We also included a sample of 58 age-matched healthy controls (Table 1).

Table 1. Sample characteristics

Characteristic	PSY	Mean	SD	HC	Mean	SD
Males	58		25			
Females	23		33			
Age, years	81	21.5	5.5	58	28.1	11.9
Schizophrenia	57					
Schizophreniform disorder	14					
Psychotic disorder NOS	5					
Schizoaffective disorder	2					
Bipolar I disorder (with psychotic features)	3					
Prior medication exposure (days)	74	8.4	29.6			
Medication naïve	28					
Medication 2 weeks or less	70					
Education, years	76	12.2	2.2	58	13.7	2.9
Weight, lb	81	155.1	35.2	58	156.1	28.6
BMI	81	23.6	4.4	57	24.7	4.1
BPBS total	81	42.7	7.5			
DUP, weeks	76	111.9	177.1			
L caudate, mm ³	81	4061.7	552.4	58	3922.5	590.6
L hippocampus, mm ³	81	4032.7	383	58	4107.4	455.8
L putamen, mm ³	81	6381.8	768.1	58	6316.2	843.6 ^b
R caudate, mm ³	81	4223.4	526.3	58	4103.5	588
R hippocampus, mm ³	81	4086.9	403.9	58	4201	416.2 ^b
R putamen, mm ³	81	6187.1	766.9	58	6042.7	850.4

NOS not otherwise specified, PSY early-phase psychosis patients, HC healthy controls, BPBS Brief Psychiatric Rating Scale, BMI body mass index, DUP duration of untreated psychosis

^aSignificant difference between patients and controls ($P < 0.05$) after adjusting for age, sex, age by sex, body mass index, and total intracranial volume

^bSignificant predictor of weight gain in schizophrenia ($P < 0.05$)

Weight assessments and analysis

Weight measurements were completed at baseline, and then weekly for 4 weeks, and every 2 weeks until week 12. Our analysis included the following two steps: We first estimated individual levels of weight gain with linear mixed models, which allowed us to compute individual weight gain trajectories [28]. Specifically, we used weight as the dependent variable and time (measured in days from baseline) as a continuous predictor, and included a random intercept as well as a random slope for day. The random slopes account for the fact that individuals' trajectories were allowed to vary around the group mean, thereby capturing the phenomenon of primary interest in our study: individual deviances from the average weight gain trajectory. In a second step, we extracted those random slopes, and used them as dependent variable in a linear multivariable regression, with putamen volume as predictor of interest (see below). In other words, in the second step, we tested our primary hypothesis that it was the putamen volume that was correlated with individual weight gain.

Random slopes were estimated using restricted maximum likelihood and used as the dependent variables in our structural and functional imaging analyses (see below). All analyses were conducted in R version 3.6.0. Data and code of the current study are available online at <http://github.com/philiphoman/bmi>.

Structural imaging and analysis

Magnetic resonance imaging exams were conducted on a 3-T scanner (GE Signa HDx). We acquired anatomical scans in the coronal plane using an inversion-recovery prepared 3D fast spoiled gradient (IR-FSPGR) sequence (TR = 7.5 ms, TE = 3 ms, TI = 650 ms, matrix = 256 × 256, FOV = 240 mm), which produced 216 contiguous images (slice thickness = 1 mm) through the whole brain. After image processing and segmentation with FreeSurfer 5.1.0, we measured the volumes of putamen and caudate and also included the hippocampus as control region.

We then computed multivariable regressions for each region of interest, entering the individual weight gain slopes as the dependent variable and a predictor for subcortical volume. To adjust for unspecific confounders, we included additional variables in these models, namely age, sex, the age by sex interaction, baseline body mass index (BMI), duration of untreated psychosis (DUP), and total intracranial volume.

Since our primary hypothesis was based on the previous observation that the putamen is implicated in antipsychotic weight gain [16], we first tested for an association between the average putamen volume and individual weight gain. After demonstrating this association, we used the same model for the left and right putamen separately. In a second step, we also tested for associations between the caudate and the hippocampus with individual weight gain.

Functional imaging and analysis

We performed preprocessing following recommended procedures [29], after excluding patients with motion of more than two standard deviations above the average framewise displacement (FD) [27]. In total, four participants (one female) were excluded due to excessive head motion. Their demographic variables were inspected and were similar to the patients in the included samples. We processed neuroimaging data using SPM12 and Matlab2015b and applied slice time correction, motion correction, co-registration to the T1-weighted image, segmentation, and normalization. For the segmentation and normalization steps, we segmented the T1-weighted image into six tissue types (gray matter, white matter, cerebrospinal fluid (CSF), air, bone, and background), and used the tissue-probability information to register to the ICBM152 MNI template. We then applied a high-pass temporal filter of 0.005 Hz to all voxel time courses and to the motion time courses before nuisance correction. Nuisances were then regressed out of all voxels using CompCor; this

included the 12 motion parameters (absolute and differential motion) and the CompCor components explaining at least 50% of the variance for white matter and CSF voxels [30, 31]. To identify the white matter and CSF voxels that were entered into CompCor, each participant's white matter and CSF tissue-probability maps were thresholded at >99.8% probability to avoid partial voluming. We performed the analyses both with and without global signal regression. After nuisance regression, functional images were spatially smoothed (6-mm FWHM) and temporally filtered (bandpass 0.01–0.1 Hz). To create connectivity maps, the first time points were removed to allow for signal stabilization. Time courses were then extracted for the putamen seeds, which represented functionally distinct anatomical subregions of the striatum [32].

Since our structural analysis revealed a single region to be predictive of weight gain, i.e., the left putamen, we used this as a seed region in our functional connectivity analysis. Adopting the approach by Di Martino et al. [32], $4 \times 4 \times 4$ -mm spheres were defined in the subregions of the left putamen, including the dorsal rostral putamen ($x = -25, y = 8$, and $z = 6$), dorsal caudal putamen ($x = -28, y = 1$, and $z = 3$), and ventral rostral putamen ($x = -20, y = 12$, and $z = -3$). We computed correlation maps for each participant for all three of our seeds by extracting mean activity time courses from each seed region, and by calculating whole-brain voxelwise correlation maps with the extracted waveform as a reference. The resulting correlation maps were z-transformed.

Mean framewise displacement was also included to control for the residual effect of head motion. Given that use of the data scrubbing to eliminate motion-related artifact offers little advantage over group-level corrections and can correct the data incompletely [33], we accounted for head motion at the group level by including mean FD as a nuisance covariate [33, 34]. Group-level analyses were performed independently for each seed with SPM12. For each seed, all maps were entered into a general linear model with age, sex, FD, and baseline BMI as covariates, and the individual weight gain slope as the outcome measure. Significance was defined voxelwise at $P < 0.001$, with familywise error cluster correction at $P < 0.05$. We also included a region of interest analysis for brain areas implicated in obesity, including the dorsal anterior cingulate cortex (dACC; $x = 3, y = -12, z = 36$), right insula (rInsula; $x = 38, y = 18, z = -3$), right orbitofrontal cortex (rOFC; $x = 34, y = 30, z = -3$), and right superior frontal gyrus (rSFG; $x = 22, y = 25, z = 51$). For this analysis, we created

spherical masks with a radius of 4 mm and extracted the mean beta estimates for each region of interest.

Finally, we combined the structural and functional indices of the striatum and their relationship with individual weight gain in an exploratory analysis. We therefore added functional connectivity indices, as well as the functional connectivity by volume interaction to an extended regression model, with individual weight gain slopes as the dependent measure. This model allowed us to test whether striatal volume moderated the association between fronto-striatal connectivity and weight gain. We then performed a leave-one-out cross-validation to derive a measure of predictive performance of this full model, and calculated the percentage of variance explained after cross-validation.

RESULTS

Baseline differences

Patients and controls had similar weights and BMIs at baseline (that were also within the normal range; Table 1). There was no evidence that the duration of untreated psychosis correlated with BMI ($\beta = -0.01, t(62) = -0.14, P = 0.89$) or that prior exposure to antipsychotics (before entering the trial) was correlated with baseline BMI ($\beta = 0.19, t(68) = 1.59, P = 0.117$). Furthermore, non-drug-naïve patients did not have a higher baseline BMI ($M = 23.58, SD = 4.49$) compared with healthy controls ($M = 24.68, SD = 4.08$). The left hippocampal volume was significantly reduced in patients compared with controls (Table 1), but no significant case-control differences were observed for any of the striatal regions.

Striatal volume and weight gain

We found that the average putamen volume was positively correlated with individual weight gain ($\beta = 0.31, t(68) = 2.13, P = 0.036$). Note that this finding did not depend on the selection of covariates we included in our model. To demonstrate this, we also tested for a correlation between putamen volume and individual weight gain, after adjusting for intracranial volume ($\beta = 0.34, t(78) = 2.63, P = 0.01$; Fig. S1a). Although it is good practice to adjust such an analysis for at least intracranial volume, the correlation (while difficult to interpret) is present even without this adjustment ($\beta = 0.36, t(79) = 3.43, P < 0.001$; Fig. S1b).

To explore the contributions of the left and right putamen separately, we then repeated this analysis with the left and right putamen volumes. The left putamen volume correlated with the magnitude of weight gain (Fig. 1a) in patients ($\beta = 0.31$,

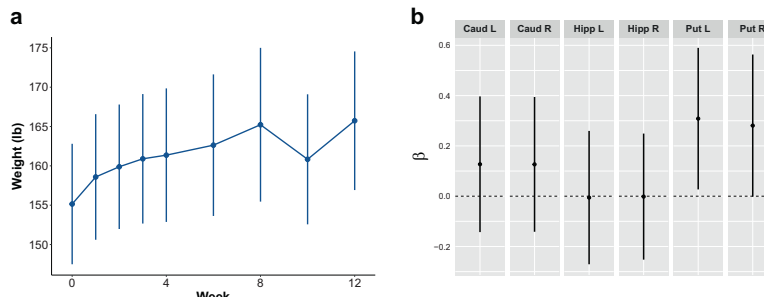


Fig. 1 Striatal volume correlates with weight gain in early-phase psychosis patients ($N = 81$). **a** Weight increased significantly over the course of the trial. Means with 95% confidence intervals are shown. **b** Weight gain in patients correlated with left putamen volume. Standardized beta coefficients with 95% confidence intervals are shown. All models were adjusted for age, sex, age by sex, duration of untreated psychosis, intracranial volume, and body mass index; none of which were significant predictors of weight gain. Error bars not touching the zero line indicate significant effects ($P < 0.05$). Caud, caudate; Hipp, hippocampus; Put, putamen; L, left; R, right

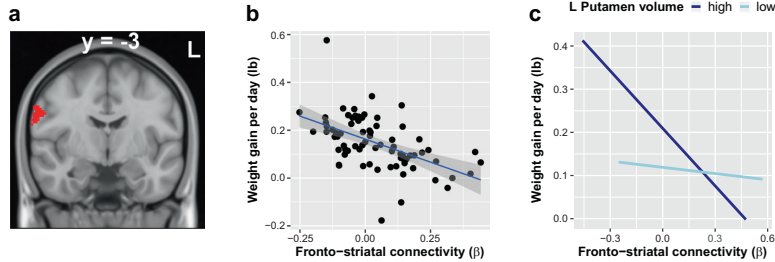


Fig. 2 Fronto-striatal connectivity and the interaction of striatal structure and function correlate with weight gain in early psychosis patients ($N = 75$). **a, b** Lower functional connectivity between the left putamen and the lateral part of the right motor cortex correlated with weight gain. Following up on the left putamen volume finding, we tested for functional connectivity between the left putamen and the whole brain that was associated with weight gain. The left dorsal rostral putamen (red) was used as seed region, and the lateral part of the right sensory motor cortex (red) was the only connected region surviving a voxel level threshold of $P < 0.001$ and a cluster threshold of $P < 0.05$ (corrected for familywise error). **c** Interaction of striatal structure and function correlated with weight gain in exploratory analysis. To illustrate the significant interaction between left putamen volume and connectivity, we plotted regression lines for weight gain and connectivity for the highest quartile (25%) of putamen volume and the lowest quartile (25%) of putamen volume

$t(68) = 2.18$, $P = 0.033$; Fig. 1b), with larger baseline volumes associated with greater weight gain during the subsequent trial.

Striatal connectivity and weight gain

Following up on the left putamen volume finding, we tested for functional resting-state connectivity [27] between the left putamen and the whole brain that was associated with weight gain in 75 patients. Notably, we found similar patterns of functional connectivity (Fig. S2) as previous work in striatal connectivity [32], including our own work on a subsample of the current cohort [35]. For the left dorsal rostral putamen, we found that decreased functional connectivity with the lateral part of the right sensory motor cortex pole also correlated with the amount of weight gain (Fig. 2a, b). Note that the statistical significance of this result did not depend on the inclusion or omission of the covariates we chose. Left putamen volume and fronto-striatal connectivity were not significantly correlated ($\beta = -0.05$, $t(73) = -0.39$, $P = 0.697$).

We did not find evidence that additional striatal connections with predefined regions that have been implicated in obesity (including anterior cingulate cortex, orbitofrontal cortex, and superior frontal gyrus) were associated with antipsychotic weight gain (Fig. S3).

Confirmation of results

Repeating the whole-brain analysis with global signal regressed out during preprocessing yielded essentially the same results (Fig. S4). Specifically, we found the same cluster in the right sensory motor cortex, where resting-state connectivity was negatively correlated with individual weight gain (Fig. S4b). Even though this connection did not survive cluster correction ($P = 0.065$, corrected for familywise error), it did survive correction for false discovery rate ($P = 0.036$).

Notably, the regression models were adjusted for age, sex, intracranial volume, baseline BMI, and duration of untreated psychosis; none of these variables showed a significant association with weight gain. In addition, to verify that the results were robust to the type of medication administered (risperidone vs. aripiprazole), we extended the models by including interactions of medication type and volume as well as medication type and connectivity, respectively, in the two regression models. There was no evidence for an effect of medication type on the weight gain and volume association ($\beta = 0.01$, $t(66) = 0.11$, $P = 0.916$) or the weight gain and connectivity association ($\beta = 0.07$, $t(71) = 0.46$,

$P = 0.648$). In addition, no interactions with volume or connectivity were found for prior exposure to antipsychotics and medication dose during the trial.

Striatal structure and function interaction

These results suggest that patients with higher striatal volume and more negative fronto-striatal connectivity gained more weight during the clinical trial. In an exploratory fashion, we then investigated a potential synergistic effect of striatal structure and function. Therefore, we added functional connectivity indices as well as the functional connectivity by volume interaction to an extended regression model. This model allowed us to test whether striatal volume moderated the association between fronto-striatal connectivity and weight gain. Indeed, we found evidence for an interaction of volume and connectivity ($\beta = -0.29$, $t(65) = -3.74$, $P < 0.001$; Fig. 2c), indicating that the negative relationship between fronto-striatal connectivity and weight gain was weaker with lower compared with higher striatal volumes. Note that this effect remained significant after excluding patients who had bipolar I disorder and a recent manic episode with psychotic features ($N = 3$), and after adjusting the model for type of medication, medication dose during the trial, and prior exposure to antipsychotic drugs. We then assessed how well this full model predicted future weight gain in unseen data. Because we did not have an independent data set available, we addressed this question with leave-one-out cross-validation, and found that the model explained 29% of the variance after cross-validation.

DISCUSSION

Here, we showed that striatal volume and fronto-striatal connectivity correlated with the degree of weight gain associated with antipsychotic treatment. Lower connectivity between the right sensory motor cortex and the left putamen was associated with more weight gain, and this relationship was stronger for higher compared with lower left putamen volume. In accordance with previous studies, we also found lower hippocampal volumes in patients compared with controls [36–38]. Yet, contrary to our expectation, we did not find that other brain areas implicated in obesity showed altered functional connectivity. In addition, we also did not find greater striatal volumes in patients compared with controls, possibly because our patients had only limited exposure to antipsychotic treatment.

We focused our study on the striatum, in line with this region's important role in reward processing and weight gain. Previous studies have shown that treatment with antipsychotics in healthy controls induced an increase in reward activation in the dorsal striatum that was correlated with excessive eating [17] and that attenuated reward anticipation normalizes under treatment with antipsychotics in patients with schizophrenia [39, 40]. However, although altered reward processing is likely to play a role [16], antipsychotic-induced weight gain remains a complex issue [4]. First, one could ask why patients did not gain weight before the antipsychotic treatment if baseline alterations in reward processing are the main cause for weight gain. Indeed, there is evidence suggesting that patients might show metabolic aberrations already before they start treatment, possibly due to unhealthy lifestyle, illness neurobiology, and genetic factors [41–44]. Furthermore, it is important to consider that some patients in the current study were not naïve to antipsychotic drugs but had been exposed to antipsychotic treatment prior to inclusion. Thus, weight gain may have occurred during this time frame. Nevertheless, we did not find evidence that baseline BMI correlated with days of prior drug exposure or that non-drug-naïve patients had a higher baseline BMI compared with controls, speaking against substantial weight gain before the trial. The current trial of 12 weeks, although short, thus appears long enough to induce substantial weight gain with considerable inter-subject variability, especially in subjects with minimal prior antipsychotic exposure [1]. Second, one might ask how antipsychotics and some of their counterparts, dopaminergic agonists, can both induce weight gain, as shown for Parkinson disease [45]. A possible explanation is that weight gain in Parkinson disease is triggered mainly by compulsive eating [45, 46] whereas a decreased reward experience may be the main cause for weight gain induced by antipsychotics. It is also noteworthy that increased dopamine transmission through sympathomimetics, such as amphetamine, typically results in suppressed appetite.

One mechanism that likely contributes to weight gain is thus via altered reward processing in the striatum. The striatum is part of the brain's reward circuitry, which has well-known dopaminergic components as well as neurotransmitters, including opioids, serotonin, and cannabinoids [9, 12, 17, 47, 48]. Accordingly, food consumption increased striatal dopamine in a previous study using positron emission tomography and this increase was positively correlated with meal pleasantness [12]. In addition, food cues elicited dorsal striatum dopamine increase and this increase correlated with hunger perception and food desire [49]. In obesity, dopamine has also been implicated in food reward and the control of eating behavior [50–52]. More specifically, functional magnetic resonance imaging studies in obesity have found altered activation in dopaminergic reward-related areas. Although these studies have described enhanced striatal activation in response to food-related cues [13, 53–55] the actual consumption of food elicited less activation in these areas [53, 54]. As previously suggested [17], these patterns are consistent with an imbalance between (increased) reward expectation and (decreased) reward experience, most likely through dopaminergic disruptions. Overeating could then be seen as a compensation to obtain the anticipated exaggerated reward [17].

Our study extends this model by considering the functional connectivity between the striatum and the sensory motor cortex, which has been implicated in food cue-related activity in obesity [13, 53, 54, 56, 57]. Our study, however, found that the strength of this connectivity was correlated with less weight gain. Furthermore, we found that the association with weight gain was moderated by left putamen volume, with higher volumes together with lower connectivity correlating with more weight gain. The moderating role of the putamen volume suggests a synergistic effect of striatal structure and function, with increased putamen volumes, possibly due to reduced endogenous dopamine

availability in the striatum [19, 20], multiplying the effect of lower cortico-striatal connectivity on weight gain [21, 22].

Some limitations merit comment. First, although the performance of the striatal structure and function model in predicting weight gain was promising (29% of the variance explained after cross validation), the sample size was small and we could not test the model performance in an independent data set. In addition, the functional connectivity measure that entered this model was not an independent measure but likely an overly optimistic estimate of the effect size of the fronto-striatal connectivity [58]. Nevertheless, if replicated in a larger sample, these data may help in the identification of patients at high risk for weight gain upon initiation of antipsychotic treatment. Furthermore, we used two different SGAs in this study, namely risperidone and aripiprazole. Although it is important to underscore that all current antipsychotics share affinity for the dopamine D2 receptors, they may still differ from a pharmacological point of view. For example, risperidone and aripiprazole share D2 receptor antagonism to induce an antipsychotic effect [59] but different receptor systems may be involved in side effects, such as weight gain. Apart from the striatum [16] weight gain has been associated with cortical 5-HT2A receptors in quetiapine monotherapy [60]. In addition, olanzapine exposure in healthy controls indicated negative effects on the peripheral metabolism. These findings suggest that antipsychotic-induced weight gain may involve additional central and peripheral aspects apart from the striatum. However, in the current study we did not find evidence that the type of medication interacted with the effects of striatal volume or fronto-striatal connectivity, suggesting similar effects of both drugs, which is also consistent with our previous finding for a larger trial [18] where no significant differences on weight gain were found between aripiprazole and risperidone. In addition, weight gain differences between aripiprazole and risperidone found in previous studies might reflect a difference in the sedative effect, with risperidone causing more sedation than aripiprazole [2]. Another limitation is that we used three putamen seeds, which we considered separately, thus not correcting for multiple comparisons across seeds. In addition, early-phase psychosis could have been defined differently, for instance, using the duration of untreated psychosis. However, consistent with our previous work, we used a criterion of cumulative exposure to antipsychotic treatment [18, 25, 26, 61]. Finally, future studies with repeated measurements of structural and functional imaging should investigate whether our findings reflect indeed a trait marker in patients prone to weight gain.

In conclusion, the current study showed that striatal structure and function correlated with antipsychotic-induced weight gain. Lower connectivity between the striatum and the sensory motor cortex was associated with more weight gain, and this relationship was stronger for higher compared with lower left putamen volumes in an exploratory analysis. This suggests that an imaging marker at baseline may identify patients who are prone to substantial weight gain during treatment.

FUNDING AND DISCLOSURE

Presented at the 57th Annual Meeting of the American College of Neuropsychopharmacology (ACNP). Supported by NIMH grant P50MH080173 to Dr. Malhotra, grant R01MH060004 to Dr. Robinson, grant R01MH076995 to Dr. Szczek and R21MH101746 to Drs. Robinson and Szczek. Dr Robinson has been a consultant to Costello Medical Consulting, Innovative Science Solutions, Janssen, Lundbeck, Otsuka, and US WorldMeds and has received research support from Otsuka. Dr Malhotra has served as a consultant for Forum Pharmaceuticals and has served on a scientific advisory board for Genomind. Dr Lencz is a consultant for Genomind. The other authors report no financial relationships with commercial interests. The authors declare that they have no conflict of interest.

ACKNOWLEDGEMENTS

The authors thank Dr Lauren Hanna and Dr Juan Gallego for their careful clinical oversight of the study. They acknowledge their patients, their patients' families, and their psychiatry research support staff.

ADDITIONAL INFORMATION

Supplementary Information accompanies this paper at (<https://doi.org/10.1038/s41386-019-0464-y>).

Publisher's note: Springer Nature remains neutral with regard to jurisdictional claims in published maps and institutional affiliations.

REFERENCES

- Correll CU, Manu P, Olshanskiy V, Napolitano B, Kane JM, Malhotra AK. Cardiometabolic risk of second-generation antipsychotic medications during first-time use in children and adolescents. *JAMA*. 2009;302:1765.
- Leucht S, Cipriani A, Spinelli L, Mavridis D, Orrey D, Richter F, et al. Comparative efficacy and tolerability of 15 antipsychotic drugs in schizophrenia: a multiple-treatments meta-analysis. *Lancet*. 2013;382:951–62.
- Musil R, Obermeier M, Russ P, Hamerle M. Weight gain and antipsychotics: a drug safety review. *Exp Opin Drug Saf*. 2015;14:73–96.
- Kapur S, Marques D. Dopamine, striatum, antipsychotics, and questions about weight gain. *JAMA Psychiatry*. 2016;73:107–8.
- Winkelbein S, Leucht S, Kane JM, Homan P. Evaluation of differences in individual treatment response in schizophrenia spectrum disorders: a meta-analysis. *JAMA Psychiatry*. 2019; Jun 3. doi: 10.1001/jamapsychiatry.2019.1530.
- Malhotra AK, Correll CU, Chowdhury NI, Muller DJ, Gregeren PK, Lee AT, et al. Association between common variants near the melanocortin 4 receptor gene and severe antipsychotic drug-induced weight gain. *Arch Gen Psychiatry*. 2012;69:904–12.
- Brandl EJ, Tiwari AK, Zai CC, Nurmi EL, Chowdhury NI, Arenovich T, et al. Genome-wide association study on antipsychotic-induced weight gain in the catie sample. *Pharm J*. 2015;16:352–6.
- Zhang JP, Lenz T, Zhang RX, Niita M, Maayan L, John M, et al. Pharmacogenetic associations of antipsychotic drug-related weight gain: a systematic review and meta-analysis. *Schizophr Bull*. 2016;42:1418–37.
- Volkow ND, Wang G-J, Balster RD. Reward, dopamine and the control of food intake: implications for obesity. *Trends Cogn Sci*. 2011;15:37–46.
- Roerig JL, Steffer KJ, Mitchell JE. Atypical antipsychotic-induced weight gain. *CNS Drugs*. 2011;25:1035–59.
- O'Doherty J, Dayan P, Schultz J, Deichmann R, Friston K, Dolan RJ. Dissociable roles of ventral and dorsal striatum in instrumental conditioning. *Science*. 2004;304:452–4.
- Small DM, Jones-Gotman M, Dagher A. Feeding-induced dopamine release in dorsal striatum correlates with meal pleasantness ratings in healthy human volunteers. *NeuroImage*. 2003;19:1709–15.
- Rothemund Y, Preuschhof C, Bohner G, Baulknecht H-C, Klingebiel R, Flor H, et al. Differential activation of the dorsal striatum by high-calorie visual food stimuli in obese individuals. *NeuroImage*. 2007;37:410–21.
- Nummenmaa L, Hirvonen J, Hannukainen JC, Immonen H, Lindroos MM, Salminen P, et al. Dorsal striatum and its limbic connectivity mediate abnormal anticipatory reward processing in obesity. *PLoS ONE*. 2012;7:e31089.
- Stice E, Youkum S, Blum K, Bonci C. Weight gain is associated with reduced striatal response to palatable food. *J Neurosci*. 2010;30:13105–9.
- Nielsen M, Rostrup E, Wulff S, Glenthøj B, Elbdrup BH. Striatal reward activity and antipsychotic-associated weight change in patients with schizophrenia undergoing initial treatment. *JAMA Psychiatry*. 2016;73:121–8.
- Mathews J, Newcomer JW, Mathews JR, Fales CL, Pierce KK, Akers BK, et al. Neural correlates of weight gain with olanzapine. *Arch Gen Psychiatry*. 2012;69:1226.
- Robinson DG, Gallego JA, John M, Petrides G, Hassoun Y, Zhang JP, et al. A randomized comparison of aripiprazole and risperidone for the acute treatment of first-episode schizophrenia and related disorders: 3-month outcomes. *Schizophr Bull*. 2015;41:1227–36.
- Jacobsen LK, Giedd JN, Gottschalk C, Kosten TR, Krystal JH. Quantitative morphology of the caudate and putamen in patients with cocaine dependence. *Am J Psychiatry*. 2001;158:486–9.
- Ersche KD, Barnes A, Jones PS, Morein-Zamir S, Robbins TW, Bullmore ET. Abnormal structure of frontostriatal brain systems is associated with aspects of impulsivity and compulsivity in cocaine dependence. *Brain*. 2011;134:2013–24.
- Kullmann S, Heni M, Veit R, Ketterer C, Schick F, Haring H-U, et al. The obese brain: association of body mass index and insulin sensitivity with resting state network functional connectivity. *Hum Brain Mapp*. 2012;33:1052–61.
- Mole TB, Mak E, Chien Y, Voon V. Dissociated accumbens and hippocampal structural abnormalities across obesity and alcohol dependence. *Int J Neuropsychopharmacol*. 2016;19:pyw039.
- Devoto F, Zapparoli L, Bonandirini R, Berlingeri M, Ferrulli A, Luzi L, et al. Hungry brains: a meta-analytical review of brain activation imaging studies on food perception and appetite in obese individuals. *Neurosci Biobehav Rev*. 2018;94:271–85.
- Ellison-Wright I, Ghahn DC, Laird AR, Thelen SM, Bullmore E. The anatomy of first-episode and chronic schizophrenia: an anatomical likelihood estimation meta-analysis. *Am J Psychiatry*. 2008;165:1015–23.
- Homan P, Arguelan M, DeRosse P, Szczesko PR, Gallego JA, Hanna L, et al. Structural similarity networks predict clinical outcome in early-phase psychosis. *Neuropsychopharmacology*. 2019;44:915–22.
- Robinson DG, Gallego JA, John M, Hanna LA, Zhang J-P, Birnbaum ML, et al. A potential role for adjunctive omega-3 polyunsaturated fatty acids for depression and anxiety symptoms in recent onset psychosis: results from a 16-week randomized placebo-controlled trial for participants concurrently treated with risperidone. *Schizophr Res*. 2018;204:295–303.
- Sarpal DK, Robinson DG, Fales C, Lenz T, Arguelan M, Karlsgodt KH, et al. Relationship between duration of untreated psychosis and intrinsic corticostriatal connectivity in patients with early phase schizophrenia. *Neuropsychopharmacology*. 2017;42:2214–21.
- Hedeker D, Gibbons RD. Longitudinal data analysis. Volume 451. Hoboken, NJ: John Wiley & Sons; 2006.
- Ciric R, Wolf DH, Power JD, Roalf DR, Baum GL, Ruparel K, et al. Benchmarking of participant-level confound regression strategies for the control of motion artifact in studies of functional connectivity. *NeuroImage*. 2017;154:174–87.
- Behzadi Y, Restom K, Liu J, Liu TT. A component based noise correction method (compcor) for bold and perfusion based fMRI. *NeuroImage*. 2007;37:90–101.
- Muschelli J, Nebel MB, Caffo BS, Barber AD, Pekar JJ, Mostofsky SH. Reduction of motion-related artifacts in resting state fMRI using acompcor. *NeuroImage*. 2014;96:22–35.
- Di Martino A, Scheres A, Margulies DS, Kelly A, Uddin LO, Shehzad Z, et al. Functional connectivity of human striatum: a resting state fMRI study. *Cereb Cortex*. 2008;18:2735–47.
- Yan C-G, Cheung B, Kelly C, Colcombe S, Craddock RC, Di Martino A, et al. A comprehensive assessment of regional variation in the impact of head micromovements on functional connectomics. *NeuroImage*. 2013;76:183–201.
- Power JD, Schlaggar BL, Petersen SE. Recent progress and outstanding issues in motion correction in resting state fMRI. *NeuroImage*. 2015;105:536–51.
- Sarpal DK, Robinson DG, Lenz T, Arguelan M, Ikuta T, Karlsgodt K, et al. Antipsychotic treatment and functional connectivity of the striatum in first-episode schizophrenia. *JAMA Psychiatry*. 2015;72:5.
- Velakoulis D, Pantelis C, McGorry PD, Dodgeon P, Dudgeon P, Brewer W, Cook M, et al. Hippocampal volume in first-episode psychoses and chronic schizophrenia. *Arch Gen Psychiatry*. 1999;56:133.
- Narr KL, Thompson PM, Szeszko P, Robinson D, Jang S, Woods RP, et al. Regional specificity of hippocampal volume reductions in first-episode schizophrenia. *NeuroImage*. 2004;21:1563–75.
- Steen RG, Mull C, McCleure R, Hamer RM, Lieberman JA. Brain volume in first-episode schizophrenia. *Br J Psychiatry*. 2006;188:510–8.
- Nielsen MO, Rostrup E, Wulff S, Bak N, Broberg BV, Lublin H, et al. Improvement of brain reward abnormalities by antipsychotic monotherapy in schizophrenia. *Arch Gen Psychiatry*. 2012;69:1195–9.
- Nielsen MO, Rostrup E, Wulff S, Bak N, Lublin H, Kapur S, et al. Alterations of the brain reward system in antipsychotic naïve schizophrenia patients. *Biol Psychiatry*. 2012;71:898–905.
- Haupt RG, Newcomer JW. Abnormalities in glucose regulation associated with mental illness and treatment. *J Psychosom Res*. 2002;53:925–33.
- Thakore JH, Mann JN, Vlahos I, Martin A, Reznik R. Increased visceral fat distribution in drug-naïve and drug-free patients with schizophrenia. *Int J Obes*. 2002;26:137–41.
- Kohen D. Diabetes mellitus and schizophrenia: historical perspective. *Br J Psychiatry*. 2004;184(547):s64–66.
- Elman I, Borsook D, Lukas SE. Food intake and reward mechanisms in patients with schizophrenia: implications for metabolic disturbances and treatment with second-generation antipsychotic agents. *Neuropsychopharmacology*. 2006;31:2091–120.
- Nierenberg MJ, Waters C. Compulsive eating and weight gain related to dopamine agonist use. *Mov Disord*. 2006;21:524–9.
- Väistö M, Carlsson M, Linder J, Forsgren L, Haglin L. Weight gain and increased central obesity in the early phase of parkinson's disease. *Clin Nutr*. 2014;33:1132–9.

47. Cota D, Barrera JG, Seeley RJ. Leptin in energy balance and reward: two faces of the same coin? *Neuron*. 2006;51:678–80.
48. Wise RA. Role of brain dopamine in food reward and reinforcement. *Philos Trans R Soc B: Biol Sci*. 2006;361:1149–58.
49. Volkow ND, Wang G-J, Fowler JS, Logan J, Jayne M, Franceschi D, et al. Non-hedonic food motivation in humans involves dopamine in the dorsal striatum and methylphenidate amplifies this effect. *Synapse*. 2002;44:175–80.
50. Volkow ND, Wang G-J, Telang F, Fowler JS, Logan J, Jayne M, et al. Profound decreases in dopamine release in striatum in detoxified alcoholics: possible orbitofrontal involvement. *J Neurosci*. 2007;27:12700–6.
51. Volkow ND, Wang G-J, Telang F, Fowler JS, Thanos PK, Logan J, et al. Low dopamine striatal D2 receptors are associated with prefrontal metabolism in obese subjects: possible contributing factors. *NeuroImage*. 2008;42:1537–43.
52. Volkow ND, Wise RA. How can drug addiction help us understand obesity? *Nat Neurosci*. 2005;8:555–60.
53. Stice E, Spoor S, Bohon C, Small DM. Relation between obesity and blunted striatal response to food is moderated by taqia a1 allele. *Science*. 2008;322:449–52.
54. Stice E, Spoor S, Bohon C, Veldhuizen MG, Small DM. Relation of reward from food intake and anticipated food intake to obesity: a functional magnetic resonance imaging study. *J Abnorm Psychol*. 2008;117:924–35.
55. Stoeckel LE, Weller RE, Cook EW, Twieg DB, Knowlton RC, Cox JE. Widespread reward-system activation in obese women in response to pictures of high-calorie foods. *NeuroImage*. 2008;41:636–47.
56. Rapuano KM, Zieselman AL, Kelley WM, Sargent JD, Heatherton TF, Gilbert-Diamond D. Genetic risk for obesity predicts nucleus accumbens size and responsivity to real-world food cues. *Proc Natl Acad Sci USA*. 2016; 114:160–65.
57. Contreras-Rodríguez O, Martín-Pérez C, Vilar-López R, Verdejo-García A. Ventral and dorsal striatum networks in obesity: Link to food craving and weight gain. *Biol Psychiatry*. 2017;81:789–96.
58. Kriegeskorte N, Simmons WK, Bellgowan PS, Baker CI. Circular analysis in systems neuroscience: the dangers of double dipping. *Nat Neurosci*. 2009;12:535–40.
59. Meltzer HY. New trends in the treatment of schizophrenia. *CNS Neurol Disord—Drug Targets*. 2017;16:900–6.
60. Rasmussen H, Ebdrup BH, Oranje B, Pinborg LH, Knudsen GM, Glenthøj B. Neocortical serotonin2a receptor binding predicts quetiapine associated weight gain in antipsychotic-naïve first-episode schizophrenia patients. *Int J Neuropsychopharmacol*. 2014;17:1729–36.
61. Trampush JW, Lencz T, DeRosse P, John M, Gallego JA, Petrides G, et al. Relationship of cognition to clinical response in first-episode schizophrenia spectrum disorders. *Schizophr Bull*. 2015;41:1237–47.

Supplementary Information

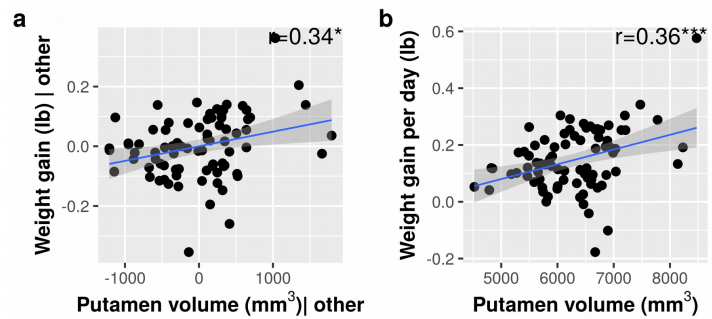


Figure S1: a, b. Positive correlation between putamen volume and individual weight gain. The correlation was present after adjusting for total intracranial volume (a) but also in a correlation without this adjustment (b). Linear regressions with 95% confidence bands are shown.

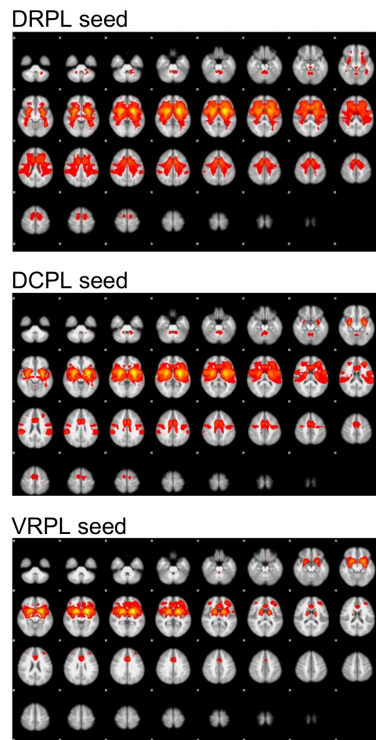


Figure S2: Striatal connectivity between seeds in the left putamen and the whole brain. We used the left dorsal rostral putamen (DRPL), the left dorsal caudal putamen (DCPL), and the left ventral rostral putamen (VRPL) as 4mm-seeds and computed voxel-wise wholebrain connectivity. Images are thresholded at $P < 0.0001$, uncorrected for visualization purposes.

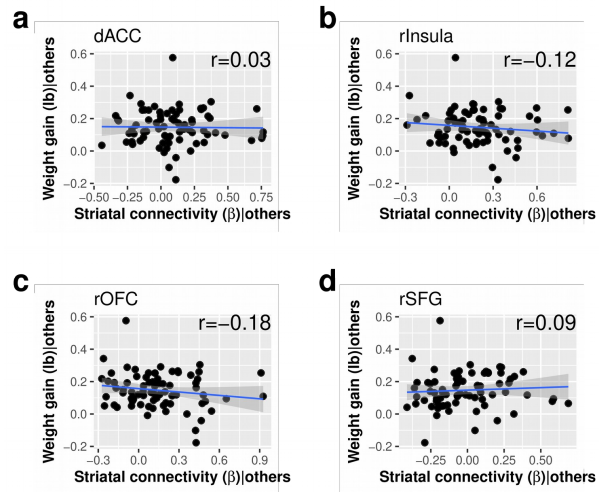


Figure S3: a-d. Striatal connectivity between left putamen and anatomically constrained brain regions implicated in obesity as predictors of weight gain. Partial correlations with 95% confidence bands are shown, after adjustment for age, sex, and BMI. Abbreviations: dACC, dorsal anterior cingulate cortex; rOFC, right orbitofrontal cortex; rSFG, right superior frontal gyrus.

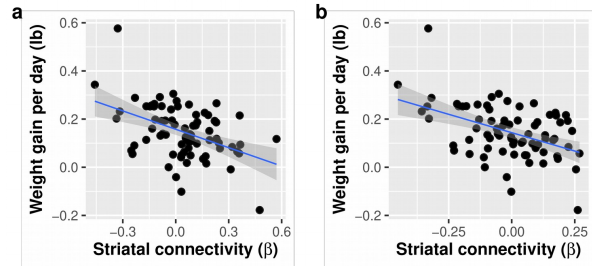


Figure S4: a, b. Similar fronto-striatal connectivity with and without global signal regressed out.
We extracted the beta weights for the connection between the left putamen and the lateral part of the right sensory motor cortex and saw comparable results. a., Without global signal regressed out during preprocessing. b., with global signal regression. Linear regressions with 95% confidence bands are shown.

5.3 Homan et al. 2019c, Nature Neuroscience

Neural computations of threat in the aftermath of combat trauma

Philipp Homan¹, Ifat Levy¹, Eric Feltham^{3,4}, Charles Gordon^{3,4}, Jingchu Hui¹, Jian Li¹, Robert H. Pietrzak^{3,4}, Steven Southwick^{3,4}, John H. Krystal^{3,4}, Ilan Harpaz-Rotem¹^{3,4,7*} and Daniela Schiller^{1,6,7*}

By combining computational, morphological, and functional analyses, this study relates latent markers of associative threat learning to overt post-traumatic stress disorder (PTSD) symptoms in combat veterans. Using reversal learning, we found that symptomatic veterans showed greater physiological adjustment to cues that did not predict what they had expected, indicating greater sensitivity to prediction errors for negative outcomes. This exaggerated weighting of prediction errors shapes the dynamic learning rate (associability) and value of threat predictive cues. The degree to which the striatum tracked the associability partially mediated the positive correlation between prediction-error weights and PTSD symptoms, suggesting that both increased prediction-error weights and decreased striatal tracking of associability independently contribute to PTSD symptoms. Furthermore, decreased neural tracking of value in the amygdala, in addition to smaller amygdala volume, independently corresponded to higher PTSD symptom severity. These results provide evidence for distinct neurocomputational contributions to PTSD symptoms.

On returning from combat, why do some military personnel develop symptoms of PTSD and others do not? PTSD symptoms may develop after exposure to a traumatic event and are characterized by symptoms of re-experiencing, avoidance of trauma reminders, negative alterations in cognitions and mood, and alterations in arousal and reactivity^{1–3}. A prominent learning theory suggests that PTSD symptoms largely reflect maladaptive associative learning during and after a traumatic event⁴. Associative learning of threat⁵ is the process by which benign stimuli such as people, locations, and objects (that is, conditioned stimuli) acquire threatening properties through pairing with an aversive outcome, and have the capacity to trigger and maintain defensive responses well after the aversive event is decoupled from the conditioned stimuli. Although abnormal threat conditioning features prominently in theoretical accounts of PTSD, the manner in which learning becomes dysfunctional is less clear⁵.

Accumulating evidence suggests a variety of impaired learning processes in PTSD, including overgeneralization, heightened contextual anxiety, diminished inhibition in response to safety cues, and failure to retain extinction learning⁶. These findings link PTSD to basic learning processes, but they do not disambiguate specific aspects of learning that may contribute to the disorder, such as the learning rate or the computation of aversive value. It is possible that PTSD-related abnormalities are influenced by learning parameters that we cannot directly observe, but are able to infer from observable behavior. Computational indices, which estimate such latent learning parameters, may be able to detect such differences.

Theories of associative learning, such as the Pearce–Hall learning mechanism⁷, envision that learning cue-outcome associations

involves tracking of several quantities: prediction errors for reinforcement, which occur when the outcome is more or less than expected (that is, surprising), and associability, reflecting the extent to which each cue has been previously accompanied by surprise. The value assigned to cues in the environment is revised in each encounter based on the prediction error. Associability dynamically guides value learning by accelerating it to cues whose predictions are poor (large prediction errors), and decelerating it when predictions become reliable. Here, we used a hybrid version of the Pearce–Hall learning model to estimate the computations performed during associative threat learning^{7–9} and how the behavioral and neural tracking of these computations relate to PTSD symptom severity.

To cover the full spectrum of symptomatology, we recruited 54 combat-exposed veterans with a wide range of PTSD symptoms based on the gold-standard structured clinical interview for PTSD, the Clinician-Administered PTSD Scale (CAPS; Table 1 and Supplementary Fig. 1). Twenty-four participants had a diagnosis of PTSD and 30 participants were combat veteran controls without PTSD diagnosis. We used the threat reversal paradigm—where flexible updating of threat responses is required—together with computational modeling, to uncover latent learning parameters that are relevant for the symptomatology.

We expected that the observed threat learning behavior would be similar across different levels of symptoms (reflecting the unspecific and subtle aberrations found in threat response conditioning in PTSD in general^{10,11}) but that the underlying neural computations might reveal disease-related differences.

The amygdala is a locus of associative learning in the brain^{7,12}, and previous work has linked PTSD symptoms with abnormal

¹Department of Psychiatry, Icahn School of Medicine at Mount Sinai, New York, NY, USA. ²Departments of Comparative Medicine, Neuroscience and Psychology, Yale University, New Haven, CT, USA. ³Department of Psychiatry, Yale University School of Medicine, New Haven, CT, USA. ⁴US Department of Veterans Affairs National Center for PTSD, Clinical Neurosciences Division, VA Connecticut Healthcare System, West Haven, CT, USA. ⁵School of Psychological and Cognitive Sciences and Beijing Key Laboratory of Behavior and Mental Health, Peking University, Beijing, China. ⁶Department of Neuroscience and Friedman Brain Institute, Icahn School of Medicine at Mount Sinai, New York, NY, USA. ⁷These authors contributed equally: Ilan Harpaz-Rotem, Daniela Schiller. *e-mail: ilan.harpaz-rotem@yale.edu; daniela.schiller@mssm.edu

Table 1 | Sample characteristics

Characteristic	N	Mean	s.d.
Males	49		
Females	5		
Age	54	32.8	8
Education	51	3.7	1.2
ASI	52	20.7	13.3
BDI	53	16	13.3
CAPS	54	39.2	32
CES	51	16.8	6.5
STAIS	49	40.8	13.7
Medicated	18		
Comorbidities:			
MDD	17		
Past alcohol abuse	7		
Panic disorder	5		
Past cannabis abuse	4		
Generalized anxiety	3		
Social phobia	3		
Anxiety disorder NOS	2		
Adjustment disorder	1		
Anxiety disorder GMC	1		
Dysthymic disorder	1		
Other DSM-IV Axis I disorder	1		
Past cocaine abuse	1		
Past opiates abuse	1		
Specific phobia	1		

Education was a categorical variable, defined as: 1, 8th grade or less; 2, some high school; 3, high school graduate or General Education Diploma; 4, some college; 5, college graduate; 6, advanced graduate degree. Abbreviations: ASI, Anxiety Sensitivity Index; BDI, Beck Depression Inventory; CES, combat exposure score; STAIS, State Anxiety subscale of the Spielberger State-Trait Anxiety Inventory; MDD, major depressive disorder; NOS, not otherwise specified; GMC, due to general medical condition; s.d., standard deviation; DSM, Diagnostic and Statistical Manual of Mental Disorders.

amygdala structure¹³, as well as heightened amygdala reactivity to stimuli laden with emotionally negative content^{4,14}. Our goal here was thus to examine whether the structural and functional implementations of specific learning computations in the amygdala relate to PTSD symptoms, and whether the threat learning-related function and volume of the amygdala contribute to PTSD symptoms in a complementary manner.

The experiment began with an acquisition phase, in which two visual stimuli (mildly angry faces) were presented consecutively in a pseudorandomized order. One of the stimuli was paired with a mild electric shock on one-third of the trials (face A), while the other was never paired with the shock (face B). The acquisition phase was immediately followed by a reversal phase, in which the contingencies were flipped such that the formerly neutral stimulus (face B) was now paired with a shock and face A became the neutral stimulus (Fig. 1a). Skin conductance response (SCR) served as the index of conditioned defensive responses.

Results

Irrespective of symptoms, veterans show successful reversal learning. Combat-exposed veterans ($N=54$ participants) successfully acquired and reversed threat conditioning, as assessed by the differential SCR (face A versus face B) in the two phases of the task (Fig. 1b). To test for a potential relationship between threat reversal

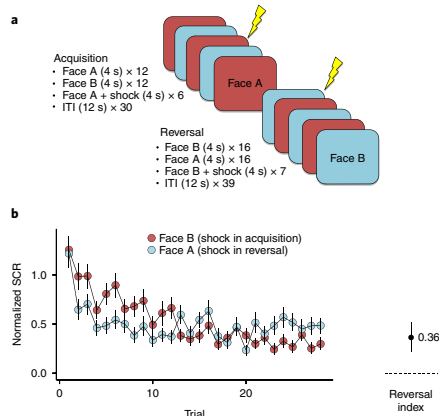


Fig. 1 | Experimental overview. **a**, Experimental design. The experiment consisted of 69 trials and a reinforcement rate of 33%. Stimuli were presented for 4 s in two pseudorandomized orders, followed by an intertrial interval of 12 s. During acquisition, face A was paired with a shock in about one-third of the trials and face B was not paired. Reversal started after 30 trials without previous instructions or warnings. During reversal, face B was now paired with a shock in about one-third of the trials, whereas face A was not paired anymore (ITI, intertrial interval). **b**, Time course of threat reversal learning. Mean normalized SCRs with standard errors ($N=54$ participants). Participants showed successful threat reversal, indicated by a significant interaction of stage by stimulus; that is, a reversal index (subtracting stimulus discrimination (face A–face B) in reversal from stimulus discrimination in acquisition) with 95% confidence intervals that is significantly different from zero in a one-sample t test, two-sided ($t(53)=4.75$, $P<0.001$).

and PTSD symptoms, we used a linear regression with threat reversal index as predictor and CAPS scores as the outcome. Reversal index was calculated by subtracting stimulus discrimination in reversal (that is, face A minus face B) from stimulus discrimination in acquisition (Fig. 1b). Controlling for irrelevant variables (age and gender), the regression revealed no significant relationship between symptoms and reversal learning ($\beta=0.02$, $t(50)=0.13$, two-tailed, $P=0.894$). We also did not find evidence that PTSD symptoms were related to stimulus discrimination during threat acquisition only ($\beta=0.03$, $t(52)=0.22$, two-tailed, $P=0.827$) or during the reversal phase only ($\beta=0.02$, $t(52)=0.12$, two-tailed, $P=0.901$). Additional ways of categorizing veterans as highly and mildly affected did not reveal any significant results (see Methods, ‘Sample characteristics’). These results motivate the use of a computational approach that could potentially reveal latent learning differences across individuals exposed to combat trauma.

Pearce–Hall hybrid model best describes conditioned threat responses. To estimate parameter weights for the specific computations performed during associative threat learning^{15,16} and how they relate to PTSD symptom severity, we used a hybrid Rescorla–Wagner and Pearce–Hall model, which we have previously employed with the same task in healthy participants^{7,8}. The computational model was informed by the Pearce–Hall learning

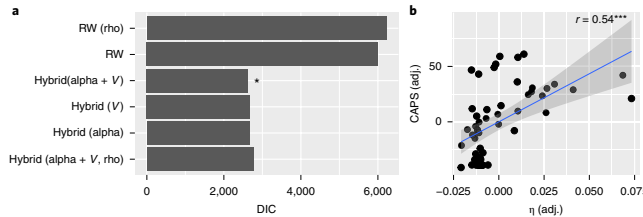


Fig. 2 | Computational model comparison and relationship to PTSD symptoms. **a**, All three versions of the hybrid model informed by the Pearce–Hall learning mechanism outperformed the simpler Rescorla–Wagner (RW) model. In addition, the hybrid model with associability and value outperformed the models with either value only or associability only and was thus the winning model (indicated with an asterisk). An extension of the Rescorla–Wagner or hybrid model with a scaling parameter η for the reversal stage, reflecting the potential change of learning during the reversal stage, did not perform better than the hybrid model with alpha, (associability), and V (value), which we thus kept as the winning model. **b**, Prediction-error weight η predicts symptoms as assessed with the CAPS. Using the best-fit model parameters, we found that a higher prediction-error weight η (which captures the learning rate for associability) predicted more CAPS symptoms. A partial correlation is shown after adjustments for age and gender and a Pearson correlation coefficient with a two-tailed significance test. Error shadings correspond to standard errors. adj., adjusted for all other parameters in the model; *** $P < 0.001$.

mechanism for associability-gated learning⁶. Like the classic Rescorla–Wagner model¹⁶, the hybrid model updates the value of each cue on each presentation of that cue, based on the discrepancy between the expected and obtained outcome, or the prediction error. The hybrid model, however, replaces the constant learning rate of the Rescorla–Wagner model by a dynamic associability parameter⁶. Associability reflects the attention that a cue receives on the basis of how accurately it has predicted outcome in the past. Unreliable cues receive more attention (higher associability) as they are likely to be unreliable in the future; and since they are unreliable, they should be updated preferentially as new information becomes available¹⁷ (see Supplementary Material for details and for simulated parameter recovery as well as model fits and Supplementary Figs. 2 and 3).

First, to verify the suitability of the model, we conducted model comparison between several versions of reinforcement learning models. Using hierarchical Bayesian modeling we fitted three different versions of this hybrid model to the SCR data; all three outperformed the simpler Rescorla–Wagner model (deviance information criterion, DIC: 6003.91). In addition, the hybrid model with associability (α) and an additional predictor for value (V) updating (DIC: 2630.37) outperformed the models with either value alone (DIC: 2678.75) or associability alone (DIC: 2661.6) and was thus the winning model (Fig. 2a). There was no evidence that an additional scaling parameter for the reversal stage (reflecting a different prediction-error weight for the reversal stage) improved the model fit (DIC: 2772.27). Notably, similar results were obtained when using maximum likelihood estimation (MLE) as in a previous study (ref.); see Supplementary Material for details and Supplementary Fig. 4). These findings indicate that the recorded SCRs during reversal learning reflect value expectations modulated by cue-specific attention. Next, we used this winning hybrid ($\alpha + V$) model to examine whether learning parameters that describe behavior and neural activity relate to PTSD symptom severity.

Symptomatic veterans assign higher weights to prediction errors. To understand how the model computations relate to overt PTSD symptoms, we used the best-fit model parameters. In the winning hybrid model, the prediction-error weight η , which can be seen as a learning rate for associability, is a quantity estimated for each participant from the SCR. The prediction-error weight quantifies how much weight is assigned to wrong predictions when updating trial-by-trial associability. It is possible that more symptomatic combat

veterans would be more sensitive to prediction errors, and will assign higher weights to them. Indeed, we found that higher prediction-error weight was associated with higher CAPS symptoms ($\beta = 0.55$, $t(50) = 4.57$, two-tailed, $P < 0.001$; Fig. 2b; note that this association held up when using a non-parametric rank correlation test that is more robust to outliers, see Supplementary Material). This finding suggests that highly symptomatic combat veterans were more influenced by prediction errors, weighing them more strongly as they adjusted trial-by-trial attention to cues.

Symptomatic veterans show altered amygdala value computation. During the reversal task, the value assigned to each cue is continuously updated on the basis of associability-gated prediction error. Mathematically, a value in a current trial reflects the value in the previous trial plus prediction error multiplied by associability. Associability in each trial is updated by the weighted prediction error in the previous trial (see Supplementary Material for details). As reported above, the prediction error weight was positively associated with PTSD symptoms. As the weighted prediction error shapes value, we next examined whether the neural tracking of value related to PTSD symptoms.

We focused our neural investigation on the amygdala, given its role in associative learning¹², value encoding^{18–21}, and evidence linking PTSD symptoms with heightened amygdala reactivity to emotionally negative stimuli^{4,13}. Given that amygdala morphology has also been linked with stress-related psychopathology^{13,22}, we examined whether amygdala neural computations and morphology are different manifestations of the same source problem (that is, redundant) or whether they incrementally explain variance in PTSD symptoms.

To address this, we calculated linear regression models including functional (value encoding based on the winning hybrid model) and structural indices for amygdala as predictors of the PTSD symptoms (for a similar analysis using the classic Rescorla–Wagner model, see Supplementary Figs. 5–7). To account for unspecific intersubject variability, these models were adjusted for age, gender, head movement and total intracranial volume (see also Supplementary Material). We found a structure-function relationship with CAPS in the right amygdala (Fig. 3a), where both volume ($\beta = -0.52$, $t(47) = -2.02$, two-tailed, $P = 0.01$; Fig. 3b) and neural activity ($\beta = -0.29$, $t(47) = -2.02$, two-tailed, $P = 0.049$; Fig. 3c) independently predicted the total CAPS score. In the left amygdala, the effect of value-dependent activity remained significant

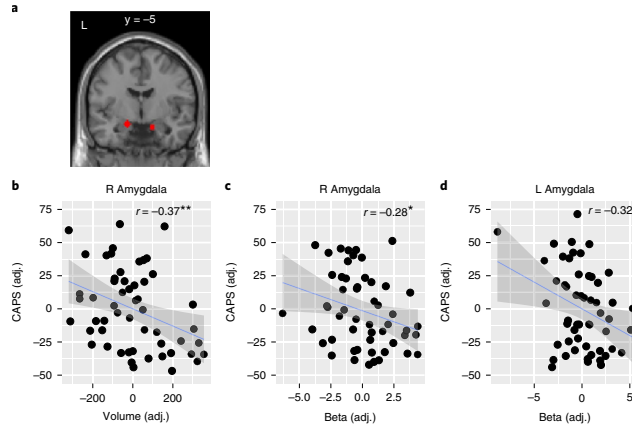


Fig. 3 | Amygdala structure and value computation contribute to PTSD symptoms using a hybrid computational model of associability and value encoding. **a**, Region of interest (ROI) used in the computational imaging analysis. The amygdala (red) was defined functionally, using the contrast of conditioned stimuli (both CS+ and CS-) versus baseline. **b-d**, Amygdala volume and value-dependent neural activity independently contribute to PTSD symptoms. Partial correlations are shown ($N=54$ participants) with Pearson correlation coefficients and two-tailed significance tests. Right amygdala volume and activity as well as left amygdala activity correlated negatively with PTSD symptoms as measured with CAPS. Thus, lower value tracking in the amygdala and smaller amygdala volume correspond to higher symptom severity. Regressions were adjusted for age, gender, head movement, and total intracranial volume. Error shadings correspond to standard errors. adj., adjusted; ** $P < 0.01$; * $P < 0.05$.

when including amygdala volume in the same model ($\beta=-0.34$, $t(47)=-2.34$, two-tailed, $P=0.024$; Fig. 3d), but no independent effect for volume emerged ($\beta=-0.25$, $t(47)=-1.27$, two-tailed, $P=0.211$).

We verified that the findings were comparable when restricting the study sample to the male participants and when using non-parametric rank correlations (see Supplementary Material). We also confirmed that individual differences in right amygdala volumes did not affect the effect of neural activity on CAPS symptoms (see Supplementary Material and Supplementary Fig. 8).

To further characterize the relationship between structure and function we added the interaction term to the model and found that there was no evidence for a synergistic effect between these independent variables (right amygdala: $\beta=-0.95$, $t(46)=-0.88$, two-tailed, $P=0.385$; left amygdala: $\beta=-0.91$, $t(46)=-0.78$, two-tailed, $P=0.437$). However, the correlation between structure and function (adjusting for total head volume) was significant and negative (right amygdala: $\beta=-0.39$, $t(49)=-2.11$, two-tailed, $P=0.04$; left amygdala: $\beta=-0.39$, $t(49)=-2.13$, two-tailed, $P=0.038$). A possible explanation is a compensatory recruitment of amygdala neurons in veterans with smaller amygdala volumes, probably due to a stress-related gray matter reduction.²³

To fully characterize the brain-behavior relationship with respect to symptoms, we tested whether individual differences in prediction-error weights were associated with differences in amygdala volume. We entered the prediction-error weight (η) as an outcome measure into a linear regression and used amygdala volume as predictor, including additional regressors for age, gender and total intracranial volume. We did not find evidence that right amygdala volume ($\beta=-0.22$, $t(49)=-1.14$, two-tailed, $P=0.26$) or left amygdala volume ($\beta=-0.19$, $t(49)=-1$, two-tailed, $P=0.321$) were associated with prediction-error weight.

In addition to value computation, the winning hybrid model also captures prediction error and associability, both of which are associated with amygdala neural activity^{8,9,17}. Since they are not strongly correlated in the hybrid model²³, they can be assessed separately (see also Supplementary Material and Supplementary Fig. 9). We therefore computed a second general linear model (GLM) with trial-by-trial regressors for associability, shock occurrence, and prediction error, all of which were parametric modulators of cue offset, as this is the time point when prediction error and associability are computed. We expected that tracking of associability in the amygdala¹⁷, reflecting the proposed attention-gating role of this brain region, would be attenuated by PTSD symptoms. However, we did not find evidence for a relationship between amygdala neural activity and PTSD symptoms for either associability (left: $\beta=-0.14$, $t(47)=-1.01$, two-tailed, $P=0.316$; right: $\beta=-0.06$, $t(47)=-0.43$, two-tailed, $P=0.667$) or prediction error (left: $\beta=-0.03$, $t(47)=-0.2$, two-tailed, $P=0.839$; right: $\beta=0.04$, $t(47)=0.28$, two-tailed, $P=0.781$), suggesting that amygdala value encoding contributes to the symptoms of PTSD, whereas associability and prediction error were less influential.

All together, these findings show that lower neural tracking of value in the amygdala, in addition to smaller amygdala volumes, corresponded to higher PTSD symptom severity.

Additional brain regions tracking threat computations. The striatum, the hippocampus and the dorsal anterior cingulate cortex (dACC) have also been implicated in the computations related to threat learning^{24,25}. We extended our analysis to these brain regions and tested whether neural tracking of value, associability and prediction error in these regions correlated with PTSD symptoms. Using a linear mixed model with brain region and CAPS as factors and neural value computations as an outcome, we found a main

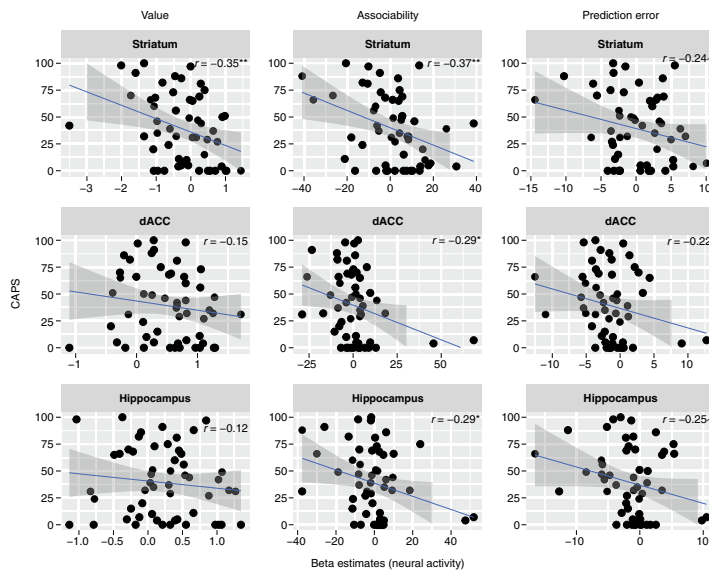


Fig. 4 | Neural computations of value, associability and prediction error and their relationship to CAPS symptoms for different ROIs. We found negative correlations for value encoding as well as associability that were attenuated for prediction error ($N=54$ participants). Pearson correlation coefficients are shown with two-tailed significance tests. Error shadings correspond to standard errors. $^{**}P<0.01$; $^{*}P<0.05$; $^{*}P<0.1$.

effect of CAPS ($F(1, 52)=5.49, P=0.023$) as well as an interaction of brain region and CAPS ($F(2, 104)=3.14, P=0.047$), driven by significant negative correlations between value tracking in the striatum (Fig. 4). These results suggest that, similar to amygdala, lower value tracking in the striatum (but not hippocampus or dACC) relates to higher symptom severity.

To test for a relationship between PTSD symptoms and neural tracking of associability and prediction error in these regions, all of which have been implicated in prediction error^{30,31} and associability^{25,38,39} encoding, we computed a linear mixed model with brain region, learning component and CAPS as factors, and neural activity as the dependent variable. We found an interaction of learning component and CAPS ($F(1, 208)=20.43, P<0.001$), driven by negative correlations between neural tracking of associability and CAPS that were attenuated for prediction error in all three regions (Fig. 4). We confirmed that these findings for value, associability and prediction-error computation were robust to the gender imbalance, clinical heterogeneity and medication status (see Supplementary Material). We also verified that the correlations were present when testing for non-parametric rank correlations. These results indicate that the lower tracking of associability (and less so of prediction error) in the striatum, hippocampus and dACC relate to higher symptom severity.

Finally, to investigate a dissociation of associability and prediction error in amygdala and striatum as reported in a previous study⁴, we tested for an interaction of region (amygdala, striatum) and learning component (associability, prediction error). To improve

comparability between the current and the previous study, we ran this analysis only in veterans without a diagnosis of PTSD, and found no evidence for dissociation ($F(3, 203)=0.58, P=0.629$). We also did not find evidence that the amygdala tracked associability in the current study in veterans without PTSD.

The absence of a dissociation that was found in a previous study⁴ merits an explanation. First, it is noteworthy that the current study does replicate the computational results of the previous study⁴, namely the superiority of the hybrid model over the Rescorla-Wagner model. On the neural level, the previous study found an interaction of region (amygdala, striatum) and learning component (associability, prediction error) that had a medium to large effect size (Cohen's $d=0.66$, 95% confidence interval (CI): 0.12; 1.17, $t(16)=2.71$, one-sample t -test, two-tailed, $P=0.02$). In the current study, we found that this interaction was not significant (Cohen's $d=-0.13$, 95% CI: -0.49; 0.23, $t(29)=-0.7$, one-sample t test, two-tailed, $P=0.49$). Rather, the striatum, but not amygdala, tracked associability in addition to tracking prediction error.

Several factors could explain this result. First and foremost, the current study's population was exposed to combat trauma, therefore meeting criterion A (exposure to a traumatic event) in the clinical assessment of PTSD symptoms and, in addition, was exposed to chronic stress associated with a deployment to combat zone. One may speculate that this traumatic stress (which has been shown to affect amygdala functioning^{13,22,30}) may be the root cause for a shift in tracking from the amygdala to the striatum as part of brain plasticity. Second, the current sample differed significantly from the

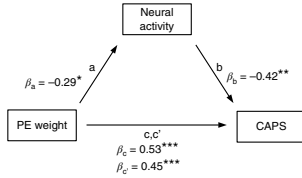


Fig. 5 | Associability-related neural activity in the right striatum partially mediates the relationship between prediction-error weights and CAPS. Standardized regression coefficients are shown ($N=54$ participants) and their statistical significance tested with one-sample t tests, two-tailed. Both prediction-error weights and striatal neural tracking of associability independently predicted PTSD symptoms as measured with CAPS when included as predictors in the same model. PE, prediction error; *** $P<0.001$; ** $P<0.01$; * $P<0.05$.

previous sample in terms of gender ratio (M/F=49/5 in the current study versus 9/8 in Li and colleagues; $P=0.001$) and age range (20–52 in the current study versus 18–31 in Li and colleagues). Alternatively, given that we ran this analysis only in veterans without a diagnosis of PTSD ($N=30$), a lack of statistical power might have contributed to the non-replication.

Brain-behavior relationship. Prediction-error weights shape the computations of value and associability. The neural underpinnings of higher prediction-error weights, observed in the behavior of individuals with more PTSD symptoms, may therefore relate to computations of value in the amygdala and the striatum, as well as to computations of associability in the striatum, dACC and hippocampus. While PTSD symptoms correlated positively with prediction-error weights, however, they correlated negatively with the neural tracking of value and associability. To better understand these inverse relationships we conducted a mediation analysis. This analysis revealed that the correlation between prediction-error weight and CAPS was partially mediated by the tracking of associability (but not prediction error) in the right striatum, as shown in the four steps of a mediation analysis (Fig. 5). We found that: (1) prediction-error weight positively correlated with CAPS ($\beta=0.54$, $t(52)=4.62$, two-tailed, $P<0.001$); (2) prediction-error weight negatively correlated with neural activity ($\beta=-0.29$, $t(52)=-2.22$, two-tailed, $P=0.03$); (3) neural activity negatively correlated with CAPS ($\beta=-0.43$, $t(52)=-3.43$, two-tailed, $P=0.001$); and (4) prediction-error weight (eta) and neural activity independently predicted CAPS ($\text{eta}: \beta=0.45$, $t(51)=3.89$, two-tailed, $P<0.001$; neural activity: $\beta=-0.3$, two-tailed, $t(51)=-2.55$, $P=0.014$). Finally, we tested whether the difference between path c and c' was significantly different from zero. To maximize statistical power, we used non-parametric bootstrapping with 5,000 draws to derive an empirical null distribution. We found that the difference between the effect with the mediator present and the effect without it (paths c and c' ; Fig. 5) was indeed significant ($\beta=0.09$, 95% CI: 0.02; 0.2; $P=0.01$). This result indicates that our mediation model supports a significant partial mediation.

This suggests that—at least for the right striatum and associability—both higher prediction-error weights and decreased neural tracking of associability are independently related to higher CAPS symptoms. Speculatively then, the higher weight assigned to prediction errors might be a compensatory adjustment for the decreased neural tracking of associability. We did not find evidence that the neural tracking in any other region fully or partially mediated the relationship between prediction-error weights and CAPS.

Together, these findings indicate that the effect of higher prediction-error weights in individuals with higher CAPS scores was complemented by decreased striatal activity during associability computation.

Discussion

The current study found that even highly affected combat veterans were able to perform reversal learning when the SCRs were analyzed using conventional summary statistics. A more fine-grained computational analysis, however, revealed that subtle differences in latent learning components are at play: symptomatic veterans assigned more weight to prediction errors. An intuitive way of interpreting this result is in terms of attention. Highly affected individuals were more sensitive when their predictions about outcomes were wrong, and they exaggerated their adjustment to the cues that did not predict what they had expected. This behavior may be associated with the increased aversion to ambiguous losses, which was recently observed in PTSD in the context of economic decision-making. Future research will need to determine the exact relationships between decision making under uncertainty, reinforcement learning, and post-trauma symptomatology^{1,2,3}.

On the neural level, we found that the neural computations that were shaped by these altered prediction-error weights contributed to the symptoms of PTSD: aversive value encoding in the amygdala and striatum, and associability computations in the striatum, dACC, and hippocampus. Our study further indicates that the right amygdala computations contribute to the symptomatology above and beyond the effects of smaller amygdala volumes¹³, suggesting additive effects of right amygdala volume and function. A model-based functional magnetic resonance imaging (fMRI) analysis such as the one used in this study can therefore not only indicate where in the brain a certain task-related activity emerges, but also which computations are probably performed.

The implication of these findings for PTSD becomes clear when the absence of behavioral differences (as indexed by reversal learning) is considered: as is well known from the behavioral (and, to a lesser extent, from the fMRI) literature, no consistent and clinically relevant differences have emerged in threat conditioning paradigms³⁴, which is surprising given the proposed central role of threat conditioning in the pathophysiology of PTSD. A possible explanation is that behavioral measures, for example, SCR, are noisy and can indeed be interpreted as noisy realizations of deterministic learning models³⁵. This suggests that the differences that are relevant for the disease may in fact be reflected by the latent parameters of the generative model rather than the noisy behavioral data.

Although all veterans were combat-exposed, only some of them developed symptoms strong enough to warrant a classical (DSM based) PTSD diagnosis. While our results do not allow us to draw causal inferences, our data do support the notion that veterans may develop more severe PTSD symptoms in response to altered neural computation of value and associability in several brain regions. Interestingly, the enhanced sensitivity to prediction errors was partially mediated by the striatal associability computations, suggesting that both increased prediction-error weight and decreased striatal tracking of associability independently contribute to PTSD symptoms. It is possible that the enhanced sensitivity to prediction errors might be the product of the decreased neural associability tracking.

All in all, these results suggest that exploiting the combined power of computational, morphological, and functional analyses enable us to relate latent markers of learning and morphological indices to overt symptoms, as specific targets for investigating trauma-related psychopathology and its potential treatment.

ARTICLES

NATURE NEUROSCIENCE

Online content

Any methods, additional references, Nature Research reporting summaries, source data, statements of data availability and associated accession codes are available at <https://doi.org/10.1038/s41593-018-0315-x>.

Received: 10 July 2018; Accepted: 4 December 2018;
Published online: 21 January 2019

References

1. American Psychiatric Association. *Diagnostic and Statistical Manual of Mental Disorders*, 4th edn (American Psychiatric Publishing, Arlington, 2013).
2. Pietrzak, R. H., Tsai, J., Harpz-Rotem, I., Whealin, J. M. & Southwick, S. M. Support for a novel five-factor model of posttraumatic stress symptoms in three independent samples of Iraq/Afghanistan veterans: a confirmatory factor analytic study. *J. Psychiatr. Res.* **46**, 317–322 (2012).
3. Harpz-Rotem, I., Tsai, J., Pietrzak, R. H. & Hoff, R. The dimensional structure of posttraumatic stress symptomatology in 323,903 U.S. veterans. *J. Psychiatr. Res.* **49**, 31–36 (2014).
4. Lissek, S. & van Meurs, B. Learning models of PTSD: theoretical accounts and psychobiological evidence. *Int. J. Psychophysiol.* **98**, 594–605 (2015).
5. Pavlov, I. *Conditioned Reflexes* (Oxford Univ. Press, Oxford, 1927).
6. Pearce, J. M. & Hall, G. A model for Pavlovian learning: variations in the effectiveness of conditioned but not of unconditioned stimuli. *Psychol. Rev.* **87**, 532–552 (1980).
7. Schiller, D., Levy, I., Niv, Y., LeDoux, J. E. & Phelps, E. A. From fear to safety and back: reversal of fear in the human brain. *J. Neurosci.* **28**, 11517–11525 (2008).
8. Li, J., Schiller, D., Schoenbaum, G., Phelps, E. A. & Daw, N. D. Differential roles of human striatum and amygdala in associative learning. *Nat. Neurosci.* **14**, 1250–1252 (2011).
9. Atlas, L. Y., Doll, B. B., Li, J., Daw, N. D. & Phelps, E. A. Instructed knowledge shapes feedback-driven aversive learning in striatum and orbitofrontal cortex, but not the amygdala. *eLife* **5**, e15192 (2016).
10. Duits, P. et al. Updated meta-analysis of classical fear conditioning in the anxiety disorders. *Depress. Anxiety* **32**, 239–253 (2015).
11. Browning, M., Behrens, T. E., Jocham, G., O'Reilly, J. X. & Bishop, S. J. Anxious individuals have difficulty learning the causal statistics of aversive environments. *Nat. Neurosci.* **18**, 590–596 (2015).
12. LeDoux, J. E. Emotion circuits in the brain. *Annu. Rev. Neurosci.* **23**, 155–184 (2000).
13. Pietrzak, R. H. et al. Amygdala-hippocampal volume and the phenotypic heterogeneity of posttraumatic stress disorder: a cross-sectional study. *JAMA Psychiatry* **72**, 396–398 (2015).
14. Admon, R. et al. Human vulnerability to stress depends on amygdala's predisposition and hippocampal plasticity. *Proc. Natl. Acad. Sci. USA* **106**, 14120–14125 (2009).
15. Neumeister, P. et al. Specific amygdala response to masked fearful faces in post-traumatic stress relative to other anxiety disorders. *Psychol. Med.* **48**, 1209–1217 (2018).
16. Rescorla, R. & Wagner, A. in *Classical Conditioning II: Current Research and Theory* (eds Black A. H. & Prokasy, W. F.) (Appleton-Century-Crofts, New York, 1972).
17. Roessch, M. R., Esber, G. R., Li, J., Daw, N. D. & Schoenbaum, G. Surprise! Neural correlates of Pearce-Hall and Rescorla-Wagner coexist within the brain. *Eur. J. Neurosci.* **35**, 1190–1200 (2012).
18. Jin, J., Zelano, C., Gottfried, J. A. & Mohanty, A. Human amygdala represents the complete spectrum of subjective valence. *J. Neurosci.* **35**, 15145–15156 (2015).
19. Belova, M. A., Paton, J. J., Morrison, S. E. & Salzman, C. D. Expectation modulates neural responses to pleasant and aversive stimuli in primate amygdala. *Neuron* **55**, 970–984 (2007).
20. Klavir, O., Genud-Gabai, R. & Paz, R. Functional connectivity between amygdala and cingulate cortex for adaptive aversive learning. *Neuron* **80**, 1290–1300 (2013).
21. Genud-Gabai, R., Klavir, O. & Paz, R. Safety signals in the primate amygdala. *J. Neurosci.* **33**, 17986–17994 (2013).
22. Morey, R. A. et al. Mid-Atlantic MIRECC Workgroup. Amygdala volume changes in posttraumatic stress disorder in a large case-controlled veterans group. *Arch. Gen. Psychiatry* **69**, 1169–1178 (2012).
23. Wroocklage, K. M. et al. Cortical thickness reduction in combat exposed U.S. veterans with and without PTSD. *Eur. Neuropsychopharmacol.* **27**, 515–525 (2017).
24. Raio, C. M., Hartley, C. A., Orederra, T. A., Li, J. & Phelps, E. A. Stress attenuates the flexible updating of aversive value. *Proc. Natl. Acad. Sci. USA* **114**, 11241–11246 (2017).
25. Roessch, M. R., Calhoun, D. J., Esber, G. R. & Schoenbaum, G. Neural correlates of variations in event processing during learning in basolateral amygdala. *J. Neurosci.* **30**, 2464–2471 (2010).
26. Schultz, W. Dopamine neurons and their role in reward mechanisms. *Curr. Opin. Neurobiol.* **7**, 191–197 (1997).
27. O'Doherty, J. P., Dayan, P., Friston, K., Critchley, H. & Dolan, R. J. Temporal difference models and reward-related learning in the human brain. *Neuron* **38**, 329–337 (2003).
28. Preuschoff, K. & Bossaerts, P. Adding prediction risk to the theory of reward learning. *Ann. N.Y. Acad. Sci.* **1104**, 135–146 (2007).
29. Behrens, T. E., Woolrich, M. W., Walton, M. E. & Rushworth, M. F. Learning the value of information in an uncertain world. *Nat. Neurosci.* **10**, 1214–1221 (2007).
30. Etikin, A. & Wager, T. D. Functional neuroimaging of anxiety: a meta-analysis of emotional processing in PTSD, social anxiety disorder, and specific phobia. *Am. J. Psychiatry* **164**, 1476–1488 (2007).
31. Rudereman, L. et al. Posttraumatic symptoms and aversion to ambiguous losses in combat veterans. *Depress. Anxiety* **33**, 606–613 (2016).
32. Brown, V. M. et al. Associability-modulated loss learning is increased in post-traumatic stress disorder. *eLife* **7**, e30150 (2018).
33. Daw, N. D. in *Decision Making, Affect, and Learning: Attention and Performance XXIII* (eds Delgado, M. R., Phelps, E. A. & Robbins, T. W.) (Oxford Univ. Press, New York, 2011).

Acknowledgements

The main source of funding for this work was provided by NIMH 105535 R01 grant awarded to J. Harpz-Rotem and D. Schiller (MPI) and funding provided by the Clinical Neurosciences Division of the National Center for PTSD. Additional support was provided by Klingenstein-Sims Fellowship Award in the Neurosciences to D. Schiller, The Brain and Behavior Research Foundation 23260 to J. Harpz-Rotem, Chinese NSF grant 31421003 to J. Li, and the Swiss National Science Foundation grant SNF 161077 to P. Homan. The analytic work was supported in part through the computational resources and staff expertise provided by Scientific Computing at the Icahn School of Medicine at Mount Sinai.

Author contributions

JL., IHR, and DS designed the study. E.F., C.G., I.L., and I.H.R. collected the data. J.H. scored the data. P.H. analyzed the data. JL., JL., I.H.R., and D.S. contributed to data analysis. J.H.K., R.H.P., and S.S. contributed to the interpretation of the results. P.H., JL., I.H.R., and D.S. wrote the first draft of the manuscript. All authors contributed to the final version of the manuscript.

Competing interests

The authors report no competing interests.

Additional information

Supplementary information is available for this paper at <https://doi.org/10.1038/s41593-018-0315-x>.

Reprints and permissions information is available at www.nature.com/reprints.

Correspondence and requests for materials should be addressed to I.H. or D.S.

Publisher's note: Springer Nature remains neutral with regard to jurisdictional claims in published maps and institutional affiliations.

© The Author(s), under exclusive licence to Springer Nature America, Inc. 2019

Methods

Sample characteristics. General description and excluded participants. A total of 77 participants took part in the experiment. Due to problems with the SCR equipment or measurement problems during the functional scan, we did not obtain complete skin conductance and/or functional imaging data of 23 participants. These participants were similar compared to the included participants (see Supplementary Table 1). This was confirmed by comparing age, CAPS, BDI, STAI-S, ASI, CES and education between excluded and included participants in a linear mixed model with the within subject factor metric (with the aforementioned variables as levels) and the between subject factor sample (levels: included, excluded) as well as a random intercept. Importantly, the effects of sample ($F(1, 75.05) = 0.05, P = 0.832$) and the metric by sample interaction ($F(6, 434.7) = 0.13, P = 0.993$) were both not significant.

Thus, the full analysis was conducted on 54 combat veterans (see Table 1 for complete demographic and psychopathology details). The sample partially overlaps ($N=30$) with the sample in a previous report¹. The main reason to consider the partially overlapping structural data in the current study is that it increased the predictive validity of the right amygdala neural computations effect. In addition, since volume had already been shown to be predictive of CAPS symptoms¹, the current study aimed to explicitly test whether the effect of neural computation goes beyond this effect of volume.

The study was approved by the Yale University Human Investigating Committee and the Human Subjects Subcommittee of the VA Connecticut Healthcare System and compliance with all relevant ethical regulations was ensured throughout the study. All participants gave informed consent and were paid for their participation. Sample size was determined based on the assumption of a medium to large ($\eta^2 = 0.4$) brain-behavior relationship between PTSD symptoms and blood-oxygenation-level-dependent (BOLD) activation. The necessary sample size was thus calculated as $N = 46$ with 80% power and $N = 61$ with 90% power.

Addressing the gender imbalance in the study sample. Since there was a considerable gender imbalance in our study sample (49 of the 54 participants were male), we verified that all of the main results of the current study hold up when restricting the study sample to only male participants. Specifically, the effect of higher prediction-error weight predicting more CAPS symptoms remained significant ($\beta = 0.51, t(46) = 4.03$, two-tailed, $P < 0.001$). In addition, the effect of value computation for the right amygdala changed only minimally ($\beta = -0.27, t(43) = -1.78$, two-tailed, $P = 0.083$) and remained significant for the left amygdala ($\beta = -0.36, t(43) = -2.38$, two-tailed, $P = 0.022$); and the volume effect for the right amygdala remained significant ($\beta = -0.5, t(43) = -2.54$, two-tailed, $P = 0.015$).

In addition, the interaction of region and CAPS remained significant for value computation ($F(2, 94) = 3.12, P = 0.049$), and the interaction of learning component by CAPS remained significant for associability and prediction-error computation ($F(1, 188) = 21.94, P < 0.001$).

Thus, the heterogeneity introduced by gender seems to be negligible in this study, which is why we decided to keep the female participants in the sample to maximize statistical power of the otherwise relatively small study and precision of the estimated effects.

Addressing the clinical heterogeneity of the study sample. We recruited veterans with a wide range of psychopathology, from completely healthy to pronounced PTSD, which can be seen from the distributions of PTSD (CAPS), depression (BDI), and anxiety symptoms (STAI-S; ASI; Supplementary Fig. 1). Nevertheless, the reversal learning index did not differ significantly between combat veterans with and without PTSD ($t(48.46) = 0.17$, two-tailed, $P = 0.868$), between combatants with high versus low PTSD (median split; $t(36.15) = -0.51$, two-tailed, $P = 0.611$), or between combat veterans with CAPS values at the extreme lower (CAPS ≤ 20 ; $N = 19$) or extreme high end (CAPS ≥ 65 ; $N = 10$; $t(10.73) = 0.48$, two-tailed, $P = 0.638$).

To confirm that our main results were not significantly influenced by the clinical heterogeneity in our sample, we adjusted our models testing for neural computations of value, associability and prediction error for comorbidities and medication status. For value computation, the region by CAPS interaction remained significant when the model was adjusted for the number of comorbidities and medication status ($F(3, 153) = 3.51, P = 0.017$). In addition, the effect was also robust to the adjustment for depression (BDI; $F(3, 153) = 3.73, P = 0.013$), state anxiety (STAI-S; $F(3, 141) = 3.57, P = 0.016$) and anxiety sensitivity (ASI; $F(3, 150) = 3, P = 0.032$).

Similarly, for associability and prediction-error computation, the learning component by CAPS interaction remained significant when the model was held up when using non-parametric rank correlation tests. Specifically, we confirmed this for the correlation between prediction-error weight and CAPS ($\rho = 0.52$, two-tailed, $P < 0.001$), for the correlation between left amygdala neural value tracking and CAPS ($\rho = -0.3$, two-tailed, $P = 0.03$), the correlation between right amygdala volume and CAPS ($\rho = -0.37$, two-tailed, $P = 0.005$), the correlation

between right amygdala neural value tracking and CAPS ($\rho = -0.27$, two-tailed, $P = 0.046$), the correlation between striatum neural value tracking and CAPS ($\rho = -0.35$, two-tailed, $P = 0.009$), the correlation between striatum neural associability tracking and CAPS ($\rho = -0.37$, two-tailed, $P = 0.006$), the correlation between dACC neural associability tracking and CAPS ($\rho = -0.29$, two-tailed, $P = 0.031$), and the correlation between hippocampus neural associability tracking and CAPS ($\rho = -0.29$, two-tailed, $P = 0.033$).

Together, these results suggest that the findings of this study were robust to the clinical heterogeneity of the study sample, and that the correlations we report were robust to outliers.

Study design. The study consisted of a threat reversal learning experiment during fMRI on a single day. Threat learning was measured with SCR; structural magnetic resonance images were acquired in the same MRI session, immediately before the task. Participants were randomly assigned to one of two trial orders (see below). Due to the study design, data collection and analysis were not performed blind to the conditions of the experiments.

Screening procedures. Psychopathology was assessed using the Structural Clinical Interview for DSM-IV, the gold-standard CAPS for PTSD diagnosis. Exclusion criteria were mental retardation, psychosis, bipolar disorder, substance dependency (life time), drug abuse in the past year, alcohol abuse in the past 60 days, neurological disorders, learning disabilities, attention deficit hyperactivity disorder, use of antipsychotic, hypnotic or sedative medications and less than 30 days' stable dose of antidepressants. Participants currently below PTSD clinical cutoff (that is, presence of at least one criterion B symptom, at least three criterion C symptoms, at least two criterion D symptoms, as well as criteria A, E and F met) with a history of PTSD diagnosis were also excluded (remitting PTSD). We additionally measured the combat exposure score (CES), depression with the BDI, anxiety sensitivity with the ASI and state anxiety with the STAI-S. Participants underwent breathalyzer and urine tests before the experiment to further validate substance use beyond the Structured Clinical Interview for DSM-IV.

Experimental task. We used the same task as in a previous study on threat reversal in healthy participants; that is, a threat discrimination and reversal task, with delay conditioning and partial reinforcement of about 33% (Fig. 1a). Participants were told that they would see visual images on a screen while receiving shocks. The level of the shocks was determined by participants before the experiment. Participants inside the MRI were instructed to pay attention to the screen and try to figure out the relationship between the stimuli and the shocks. Importantly, we did not mention the two stages or the reversal of contingencies. The conditioned stimuli were two mildly angry male faces from the Ekman series.

Stimuli and apparatus. The unconditioned stimulus was a mild electric shock to the foot (200ms duration, 50 pulses s⁻¹). The stimuli were presented for 4s, with a 12 s intertrial interval in which a fixation point was presented (Fig. 1a). During acquisition, one face (face A) was paired with the unconditioned stimulus on one-third of the trials, while the other (face B) was never paired with the unconditioned stimulus. During reversal, these contingencies switched, and face B was now paired with the unconditioned stimulus on approximately one-third of the trials and face A was not paired with the unconditioned stimulus. The order of the different trial types was pseudorandomized (no consecutive reinforced trials and no more than two consecutive trials of each kind), and the designation of faces into 'face A' and 'face B' was counterbalanced across participants. During acquisition, there were 12 presentations of each of the faces, intermixed with an additional six presentations of face A that co-terminated with the unconditioned stimulus. Reversal immediately followed acquisition, and the transition between the stages was unsignaled. This stage consisted of 16 presentations of each of the faces, intermixed with seven additional presentations of face B that co-terminated with the unconditioned stimulus. We considered the first trial in which face B co-terminated with the unconditioned stimulus as the beginning of the reversal stage (Fig. 1a).

Physiological data acquisition and analysis. Mild shocks were delivered through a stimulating bar electrode attached to the participant's right ankle. A BIOPAC stimulator charged by a stabilized current was used, with cable leads that were magnetically shielded and grounded through a radio frequency filter. The participants were asked to set the level of the shock themselves using a work-up procedure before scanning. In this procedure, a participant was first given a very mild shock (20V, 200ms, 50 pulses/s), which was gradually increased to a level the participant indicated as uncomfortable, but not painful (with a maximum level of 70V). Skin conductance was assessed with shielded Ag-AgCl electrodes, filled with standard NaCl electrolyte gel and attached to the middle phalanges of the second and third fingers of the left hand. The electrode cables were grounded through an radio frequency filter panel. The skin conductance signal was amplified and recorded with a BIOPAC Systems skin conductance module connected to a computer.

Data were continuously recorded at a rate of 200 samples per second. An off-line analysis of the analog skin conductance waveforms was conducted with

ARTICLES

NATURE NEUROSCIENCE

AcqKnowledge software (BIOPAC Systems). The level of SCR was assessed for each trial as the base-to-peak amplitude difference in skin conductance of the largest deflection (in microsiemens; μs) in the 0.5–4.5-s latency window after stimulus onset. The minimal response criterion was 0.02 μs . Responses below this criterion were encoded as zero. The raw skin conductance scores were square-root transformed to normalize the distributions, and scaled according to each participant's average response to the unconditioned stimulus.

Statistical analysis. We averaged the learning effects (face A minus face B) across trials by stage (acquisition, reversal) for each participant and calculated a threat reversal index by subtracting the learning effect of reversal from the learning effect of acquisition. To assess whether participants showed successful threat reversal, we tested whether the reversal index was significantly different from zero with a one-sample t -test. The threshold for this analysis was set at $P < 0.05$, two-tailed. The relationship between latent learning parameters (see below) and PTSD symptomatology was estimated with a linear regression model. Data distribution was assumed to be normal but this was not formally tested. However, individual data points are shown in scatter plots throughout the manuscript.

Computational modeling. Following classic computational learning theory¹, we assumed a deterministic learning model and a probabilistic observation model to describe the generation of our data. The deterministic learning model describes the dynamics of how internal variables gate learning, while the observation model describes how the internal variables are realized in observed data.

Pearce–Hall learning model. Unlike the Rescorla–Wagner model (see below) that treats the learning rate as constant, the Pearce–Hall model for associability-gated learning substitutes associability for the constant learning rate. Thus, such a model incorporates prediction-error-driven value updating into an associability model resulting in the hybrid model:

$$\begin{aligned}\delta_n &= r_n - V_n(x_n) \\ V_{n+1}(x_n) &= V_n(x_n) + \kappa\alpha_n(x_n)\delta_n \\ \alpha_{n+1}(x_n) &= \eta[\delta_n] + (1-\eta)\alpha_n(x_n).\end{aligned}\quad (1)$$

Here, x_n is the conditioned stimulus on trial n (conditioned stimulus: CS+ or CS-) and r_n as the unconditioned stimulus delivered (1 for unconditioned stimulus, 0 for no unconditioned stimulus). The punishment prediction error δ_n measures the difference between the expected and predicted shock on trial n . The associability α for the value update is a variable. The value for the conditioned stimulus not observed on trial n remains unchanged. Since associability of trial n depends on absolute prediction errors from past but not current trials, associability $\alpha_n(x_n)$ and prediction error δ_n are relatively uncorrelated.

To derive the best fits for this model, we assumed that $V_0 = 0.5$, reflecting the assumption that getting a shock or not was equally likely for the first trial. We compared the fit of different versions of the hybrid model to the SCR data by optimizing the free parameters of each model. We assumed the likelihood of each trial's SCR S_n to be an independent and identically distributed Gaussian distribution around a mean determined by value, associability or the combination of both value and associability as predicted by the model on that trial (plus a constant term):

$$\begin{aligned}S_n &\sim \text{Normal}(\beta_0 + \beta_1 V_n(x_n), \sigma) \\ S_n &\sim \text{Normal}(\beta_0 + \beta_1 \alpha_n(x_n), \sigma) \\ S_n &\sim \text{Normal}(\beta_0 + \beta_1 V_n(x_n) + \beta_2 \alpha_n(x_n), \sigma).\end{aligned}\quad (2)$$

As can be seen, these correspond to linear regressions of value or associability, or the combination of both, to the SCR. We tested all three possible combinations (equations 1–3; Hybrid (V); Hybrid (α); Hybrid ($\alpha + V$)), all in separate fits of all free parameters.

Using Hierarchical Bayesian modeling, we first verified that we could recover simulated parameters of initial associability (α_0), κ and the associability learning rate, η (Supplementary Fig. 2). We also ruled out that an extended model with an additional scaling parameter that captured a change of the prediction-error weight for the reversal stage would fit the data better (Fig. 2a).

Rescorla–Wagner learning model. Although we found that a hybrid model of associability and value computation outperformed a simpler Rescorla–Wagner model, we were also interested in how a basic Rescorla–Wagner model could explain value computation in the amygdala. The Rescorla–Wagner model is the standard model of error-driven predictive learning. It assumes that the expected value (V) for each trial is updated according to the learning rate and the prediction error:

$$\begin{aligned}V_{n+1}(x_n) &= V_n(x_n) + \alpha\delta_n \\ \delta_n &= r_n - V_n(x_n).\end{aligned}\quad (3)$$

Here, x_n is the conditioned stimulus on trial n (face A or face B) and r_n as the unconditioned stimulus delivered (1 for unconditioned stimulus, 0 for no

unconditioned stimulus). The punishment prediction error δ_n measures the difference between the expected and predicted shock on trial n . The learning rate α for the value update is a constant free parameter. The expected value for the conditioned stimulus absent on trial n remains unchanged. To derive the best fits from the Rescorla–Wagner model, we assumed that $V_0 = 0.5$, reflecting the assumption that getting a shock or not was equally likely for the first trial. We considered that model-based value computation would be correlated with amygdala activity, and that this correlation would be more negative for individuals with higher levels of PTSD symptoms. After verifying that simulated parameters could be recovered with the hierarchical Bayesian approach used in this study (Supplementary Fig. 5) and that the model indeed fitted the recorded SCRs (Supplementary Fig. 6), we calculated linear regression models including functional (value encoding) and structural indices for amygdala as predictors of the PTSD symptoms. To account for unspecific intersubject variability, these models were adjusted for learning rate, age, gender, head movement and total intracranial volume. For the right amygdala (Supplementary Fig. 7a), we found that volume predicted CAPS symptoms ($\beta = -0.49$, $t(46) = -2.59$, two-tailed, $P = 0.013$ and Supplementary Fig. 7b) while neural activity as a predictor did not reach statistical significance ($\beta = -0.28$, $t(46) = -2$, two-tailed, $P = 0.052$ and Supplementary Fig. 7c). In the left amygdala, the effect of value-dependent activity remained significant when including amygdala volume in the same model ($\beta = -0.35$, $t(46) = -2.42$, two-tailed, $P = 0.02$ and Supplementary Fig. 7d), but no independent effect for volume emerged ($\beta = -0.2$, $t(46) = -1.04$, two-tailed, $P = 0.303$).

We also confirmed that the results were robust to the specific ROI definition of the amygdala and that individual differences in right amygdala volumes did not affect the effect of neural activity on CAPS symptoms. We repeated our analysis of right amygdala value computation using the winning hybrid ($\alpha + V$) model. We used the individual amygdala segmentations as computed by FreeSurfer as masks for the ROI analysis of the right amygdala in SPM. After running the recon-all pipeline in FreeSurfer, we converted and binarized the subcortical segmentation of each individual to NIfTI format. We then applied the individual normalization parameters calculated by SPM during the SPM preprocessing pipeline to warp the FreeSurfer segmentation to the Montreal Neurological Institute space. A figure (Supplementary Fig. 8) shows two illustrative participants with individual amygdala masks (estimated in FreeSurfer and indicated in red) projected on to their T1-weighted brain anatomy in SPM.

Given that we found an effect of volume for the right amygdala, we thus extracted the mean beta estimates of these individual right amygdala masks and entered the estimates in a multivariable regression model, using CAPS as the dependent measure and the beta estimates together with amygdala volume as predictors, adjusting for age, gender and intracranial volume. We found a similar effect for the neural activity compared to the original findings in the right amygdala ($\beta = -0.3$, $t(48) = -2.07$, two-tailed, $P = 0.044$), suggesting that the BOLD effects were correctly estimated.

To further characterize the relationship between structure and function we added the interaction term to the model and found that there was no evidence for a synergistic effect between these independent variables (right amygdala: $\beta = -0.7$, $t(45) = -0.71$, two-tailed, $P = 0.48$; left amygdala: $\beta = -0.02$, $t(45) = -0.02$, two-tailed, $P = 0.988$). Moreover, the correlation between structure and function was not significant (right amygdala: $r(52) = 0.05$, two-tailed, $P = 0.742$; left amygdala: $r(52) = 0.04$, two-tailed, $P = 0.797$). Further, a mediation analysis with amygdala volume as a mediator of the association between value activity and CAPS symptoms did not show evidence for full or partial mediation; instead, inclusion of amygdala volume did in fact improve the predictive validity of neural activity. A possible explanation is a compensatory recruitment of amygdala neurons in veterans with smaller amygdala volumes, probably due to a stress-related gray matter reduction³¹.

We also tested a potential difference in learning rates between acquisition and reversal and additionally tested an extended version of the Rescorla–Wagner model. We added an additional scaling parameter ρ , which captures the change in the learning rate during the reversal stage. For acquisition, we thus used the classical Rescorla–Wagner model:

$$\begin{aligned}V_{n+1}(x_n) &= V_n(x_n) + \alpha\delta_n \\ \delta_n &= r_n - V_n(x_n),\end{aligned}\quad (4)$$

and the extended model for reversal:

$$\begin{aligned}V_{n+1}(x_n) &= V_n(x_n) + \rho\alpha\delta_n \\ \delta_n &= r_n - V_n(x_n),\end{aligned}\quad (5)$$

where ρ is the scaling parameter. We performed a model comparison between the two models, computing the DIC that captures the goodness of fit of a Bayesian hierarchical model with lower values meaning better fits³². Notably, we found that the simpler model provides a better fit to the data (extended model: DIC = 6223.11; simpler model: DIC = 6003.91).

Finally, we investigated whether fitting V_0 , the initial value, as an additional free parameter would improve the model fit and found that the resulting DIC was higher than the one from the original simpler model; we thus kept the simpler model with V_0 fixed at 0.5.

Hierarchical Bayesian model fitting. *Bayesian modeling versus MLE.* We used Hierarchical Bayesian analysis (HBA) to obtain estimates of the free parameters in our computational models. The advantage of HBA compared to MLE is that individual differences are accounted for but information across individuals is pooled so that individual estimates are pulled toward the population mean (an effect sometimes referred to as shrinkage¹).

In MLE, on the other hand, point estimates are obtained that maximize the likelihood of the data for each individual separately¹. Individual ML estimates, however, may suffer from noise and may be unreliable when faced with an insufficient amount of data¹. In addition, there is no guarantee that non-linear optimization algorithms commonly used (such as fmincon in MATLAB) will provide a set of parameter values that uniquely maximize the log-likelihood; indeed, premature stops of the algorithm are common, which provide a local (and thus sub-optimal) instead of a global maximum of the likelihood function¹. Group-level analysis of MLE, which treats a group as a single subject and estimates a single set of parameters for a whole group of individuals, is commonly used to generate fMRI regressors for model-based analyses as it is supposed to generate more reliable estimates needed for fMRI¹, but it inevitably ignores individual differences and does not allow for group comparisons.

Hybrid model comparison using MLE. Nevertheless, to replicate the model comparison reported in Li and colleagues more directly¹, we also performed a model comparison of the hybrid models using MLE as in the aforementioned study, and ranked all three hybrid models as well as the Rescorla–Wagner model according to their Bayesian Information Criterion (BIC). Consistent with the results in Li and colleagues¹, the model with the lowest BIC was the hybrid ($\alpha + V$) model, outperforming the other hybrid models as well as the Rescorla–Wagner model (Supplementary Fig. 4a). More specifically, direct comparisons using likelihood ratio tests revealed that the Hybrid (V) model outperformed the Rescorla–Wagner analysis model ($\chi^2 = 408.11$, d.f. = 108, $P < 0.001$), and the Hybrid ($\alpha + V$) outperformed the Rescorla–Wagner model ($\chi^2 = 877.61$, d.f. = 162, $P < 0.001$), the Hybrid (V) model ($\chi^2 = 469.5$, d.f. = 54, $P < 0.001$) and the Hybrid (α) model ($\chi^2 = 348.54$, d.f. = 54, $P < 0.001$).

We did not find evidence that the individual MLE model fits interacted with the PTSD symptomatology; the correlation between model parameters and symptoms was essentially flat for each of the four models (Supplementary Fig. 4b).

Details on the Bayesian modeling procedure. To perform HBA, we used the probabilistic programming language Stan v2.15.1 (Stan Development Team, 2014), which makes use of Markov chain Monte Carlo (MCMC) sampling algorithms termed Hamiltonian Monte Carlo. Hamiltonian Monte Carlo provides an efficient sampling algorithm even for multilevel models and highly correlated parameters³.

For the Rescorla–Wagner model, individual parameters were assumed to be drawn from group-level normal distributions. Normal and half-Cauchy distributions were used for the priors of the group-level means and standard deviations, respectively^{39,40}. We used weakly informative priors³ to minimize the influence of those priors on the posterior distributions with our relatively small sample size. As the learning rate α is bounded between 0 and 1, we used the inverse probit transformation (the cumulative distribution function of a unit normal distribution) to convert unconstrained values into this range. The mathematical relationship between the probability density function and the cumulative density function of the unit normal distribution guarantees that this transformation that the converted prior will be uniformly distributed between 0 and 1. Stan provides a fast approximation of the inverse probit transformation (the `Phi_approx` function) to achieve this. The learning rate was thus declared as follows:

$$\begin{aligned}\mu_{\alpha'} &\sim \text{Normal}(0, 1) \\ \sigma_{\alpha'} &\sim \text{half-Cauchy}(0, 5) \\ \alpha' &\sim \text{Normal}(\mu_{\alpha'}, \sigma_{\alpha'}) \\ \alpha &= \text{Probit}^{-1}(\alpha')\end{aligned}$$

where $\mu_{\alpha'}$ and $\sigma_{\alpha'}$ are hyper-parameters that dictate the distribution of α' and sequentially α .

A total of 2,000 samples were drawn after 1,000 burn-in samples for each of four chains (resulting in a total of 8,000 samples). To assess the convergence of the chains for each parameter, we used the Gelman–Rubin test⁴¹ that calculates an \bar{R} statistic, with \bar{R} values close to 1.00 indicating that the MCMC chains have converged to the target distributions.

Notably, the \bar{R} values obtained for all model parameters were 1.00, and visual inspection of MCMC chains confirmed the mixing of MCMC samples. In addition, effective sample sizes (ESS) of model parameters, which are associated with autocorrelation and mixing of MCMC chains (with a smaller ESS indicating higher autocorrelation), were typically greater than 1,000 (out of 8,000 total samples). The minimum ESS of hyper-parameters was 592. Visual inspection of the parameters with smaller ESS confirmed their convergence to the target distributions.

For the hybrid models, priors of individual parameters were again assumed to be drawn from group-level normal distributions, but normal and half-normal

distributions were used for the priors of the group-level means and standard deviations, respectively.

Parameter recovery tests. To further verify the plausibility of our model, we used simulated data to test whether simulated parameters could be recovered (recovery tests). We generated true parameter values, simulated synthetic behavioral data based on the parameters and recovered their parameter values using the HBA described in the previous section. Results confirmed that the model was successful at recovering the simulated parameters (Supplementary Figs. 2 and 5).

Statistical analysis. For the Rescorla–Wagner model, we used the individual posterior means of the learning rate to calculate the trial-wise expected value for each participant. These values were used as parametric modulators in the model-based fMRI analysis. For the hybrid model, trial-wise expected value, associability and prediction error were used as parametric modulators in the model-based fMRI analysis (see below).

Structural magnetic resonance imaging and analysis. A Siemens Trio TIM 3T and 12-channel receiver array head coil were used for data acquisition. High-resolution T1-weighted anatomical images ($1 \times 1 \times 1 \text{ mm}^3$) were acquired with an MPAGE pulse sequence (voxel size $1 \times 1 \times 1 \text{ mm}^3$; repetition time = 2.5 s; echo time = 2.77 ms; flip angle = 7°; 256×256 matrix, 176 sagittal slices of 1 mm).

Blinded to the clinical status, image processing and segmentation were conducted using the automated FreeSurfer recon-all pipeline (<http://surfer.nmr.mgh.harvard.edu>). FreeSurfer transforms brains from native space to standard space to perform subcortical segmentation, and then transforms them back to native space to extract individual amygdala volumes. We thus used those extracted measures of amygdala volume for each participant and restricted the analysis to this a priori ROI. Amygdala volume measures were then used as predictors in multivariable linear regressions (see below).

Notably, excessive head motion was found to be associated with reduced estimates of gray matter thickness and volume compared to age- and gender-matched samples and consequently with inflated effect sizes⁴². Following a recent suggestion that participants' head movement during functional imaging sequence may provide a proxy for head movement during the structural sequence (where no head movement is recorded), we calculated the total head movement in mm during fMRI for each participant and included this scalar as a covariate in the statistical analysis⁴². Importantly, this covariate was used as a proxy measure for head movement during the anatomical session. The movement during the fMRI session was regressed out in the fMRI design matrix. Note that the exclusion of this additional regressor in the multivariable regression did not alter the main results of our analysis.

fMRI and analysis. Functional images were acquired using a single-shot gradient echo planar imaging sequence (repetition time = 2,000 ms; echo time = 25 ms; field of view = 192 cm; flip angle = 75°; bandwidth = 4,340 Hz per pixel; echo spacing = 0.29 ms). Forty contiguous oblique axial slices ($3 \times 3 \times 3 \text{ mm}^3$ voxels) parallel to the anterior–commissure–posterior–commissure line were obtained.

Analysis of the imaging data were conducted using SPM 12 (<http://filion.ac.uk/spm12>). After discarding the first eight volumes, native-space images were realigned, slice-time corrected and co-registered to each subject's structural scan. Structural image preprocessing included segmentation, bias correction and spatial normalization; these normalization parameters were also used to normalize the functional images. Finally, functional images were smoothed with a Gaussian kernel (4 mm full-width at half-maximum).

Model-based fMRI analysis. We conducted a computational analysis using the hybrid Pearce–Hall learning model, with the fMRI regressors derived from the fits to the SCR data. Cue onset and offset were modeled as two discrete events, and each expected value (V) regressor was included as a parametric modulator of the stimulus onset event. In addition, the occurrence of a shock (0 for trials with no shock, 1 for trials with a shock) and prediction error were modeled as parametric modulators of cue offset.

Six regressors modeling affine head-motion parameters were also included in the GLM. All events were convolved with a canonical gamma-variate hemodynamic response function. The contrast of interest was the correlation of expected value V , corresponding to the expectation of a shock on each trial, with the BOLD response in the brain. We thus computed images of this contrast for each participant and used the contrast images as input for the ROI-based analyses. Our ROI-based analysis focused on the amygdala. We defined the amygdala ROIs functionally, using an independent contrast of conditioned stimuli (both face A and face B) versus baseline and a relatively loose contrast of $P < 0.001$. For each ROI, we extracted the mean beta estimates obtained from the GLM for the correlation of expected value V with the BOLD response. The beta estimates were then entered as predictors in multivariable linear regressions.

To assess the independent contributions of structural and functional indices on PTSD symptoms, we then calculated multivariable linear regressions including both the structural and functional indices as predictors, and the symptoms as measured with the CAPS as outcome measures. For each ROI, the structural index was the volume, the functional indices were the extracted mean beta estimates

ARTICLES

NATURE NEUROSCIENCE

obtained from the computational GLM for the correlation of expected value V with the BOLD response. These models were adjusted for learning rate, age, gender, head movement and total intracranial volume to adjust for unspecific intersubject variability.

In addition to the amygdala, we extended our analysis to the dACC, the striatum and hippocampus. The dACC was defined with an independent functional contrast (face A versus face B in acquisition, corresponding to conditioned stimulus: CS+ versus CS-); since Li and colleagues¹ found the strongest activation in the caudate nucleus, we used a contrast of shock occurrence versus baseline in a sample of healthy control participants who underwent the same task to ensure reliable activation^{10,11}. Like the functional contrast for the dACC, this contrast for the striatum was also independent of the computational contrasts. The hippocampal ROI was defined anatomically using the WFU Pickatlas¹². We then used two separate GLMs to examine neural activity related to value encoding (GLM 1) as well as associability and prediction error (GLM 2). Replicating the design of a previous study in reversal learning and value encoding for GLM 1, we included value encoding as parametric modulator of stimulus onset and included shock occurrence and prediction error as additional regressors of stimulus offset. For GLM 2, we followed the design of the previous study by Li and colleagues¹ and included associability, shock occurrence and prediction error as parametric modulators of stimulus offset.

We then extracted the beta estimates of the ROIs and computed separate linear mixed models for value computation as well as associability and prediction error, respectively. Neural activity was used as the dependent variable in these models, and predictors for region and CAPS (model 1, predicting value computation) as well as learning component (model 2; predicting associability and prediction error) were entered as predictors. In addition, we included a random intercept and a random slope for region to account for the within-subject correlations.

We also performed a computational analysis using the simpler Rescorla-Wagner learning model, with the fMRI regressors derived from the fit to the SCR data. Cue onset and offset were modeled as two discrete events, and each expected value (V) regressor was included as a parametric modulator of the stimulus onset event. In addition, the occurrence of a shock (0 for trials with no shock, 1 for trials with a shock) and prediction error were modeled as parametric modulators of cue offset, but are not considered in this study due to algebraic collinearity with the V regressor. This means that the parametric regressor of interest was expected value, which modulated cue onset, while the regressors for shock outcome and prediction error were included in the design matrix (modulating cue offset) but are not considered in this study.

While this setup is in line with previous studies using the same reversal paradigm together with computational modeling^{1,2}, we manually confirmed that the amount of collinearity in the fMRI design matrix was acceptable. We calculated the variance inflation factor (VIF) for the value regressor. The VIF reflects how much the variance of the estimated regression coefficient is increased by the correlation among the model regressors. Its square root quantifies how larger the standard error is compared with what it would be if the regressor were uncorrelated with the model regressors. While it is common practice to consider a VIF > 10 as problematic, it is important to note that even in the presence of collinearity the regression coefficients will be unbiased. As the term VIF suggests, what is affected is the variance of the estimates, resulting in increased noise and reduced statistical power. However, we verified that the VIF of the value regressor was below five for each participant, with a mean VIF across participants of 1.5

(s.d. 0.13) suggesting that collinearity was not an issue for this design. Supporting this conclusion, the effects for amygdala value computation on CAPS symptoms remained significant when including the amygdala activation during shocks in the same model (left: $\beta = -0.34$, $t(46) = -2.32$, two-tailed, $P = 0.025$; right: $\beta = -0.31$, $t(46) = -2.14$, two-tailed, $P = 0.038$).

Reporting Summary: Further information on research design is available in the Nature Research Reporting Summary linked to this article.

Code availability

The code used for the analyses is available online at: <http://osf.io/rxsw2/>.

Data availability

Data used to support the conclusions of this study is available online at: <http://osf.io/rxsw2/>.

References

34. Spiegelhalter, D., Best, N., Carlin, B. & Van der Linde, A. Bayesian measures of model complexity and fit (with discussion). *J. R. Stat. Soc. B* **64**, 583–639 (2002).
35. Gelman, A. et al. *Bayesian Data Analysis* 3rd edn (CRC Press, Boca Raton, 2013).
36. Myung, I. J. Tutorial on maximum likelihood estimation. *J. Math. Psychol.* **47**, 90–100 (2003).
37. Ahn, W.-Y., Haines, N. & Zhang, L. Revealing neurocomputational mechanisms of reinforcement learning and decision-making with the hbayesdm package. *Comput. Psychiatr.* **1**, 24–57 (2017).
38. Gelman, A., Lee, D. & Guo, J. Stan: A probabilistic programming language for Bayesian inference and optimization. *J. Educ. Behav. Stat.* **40**, 530–543 (2015).
39. Ahn, W.-Y. et al. Decision-making in stimulant and opiate addicts in protracted abstinence: evidence from computational modeling with pure users. *Front. Psychol.* **5**, 849 (2014).
40. Gelman, A. Prior distributions for variance parameters in hierarchical models (comment on article by Browne and Draper). *Bayesian Anal.* **1**, 515–534 (2006).
41. Gelman, A. & Rubin, D. B. Inference from iterative simulation using multiple sequences. *Stat. Sci.* **7**, 457–472 (1992).
42. Savalia, N. K. et al. Motion-related artifacts in structural brain images revealed with independent estimates of in-scanner head motion. *Hum. Brain. Mapp.* **38**, 472–492 (2017).
43. Cools, R., Clark, L., Owen, A. M. & Robbins, T. W. Defining the neural mechanisms of probabilistic reversal learning using event-related functional magnetic resonance imaging. *J. Neurosci.* **22**, 4563–4567 (2002).
44. Dodds, C. M. et al. Methylphenidate has differential effects on blood oxygenation level-dependent signal related to cognitive subprocesses of reversal learning. *J. Neurosci.* **28**, 5976–5982 (2008).
45. Maldjian, J. A., Laurienti, P. J., Kraft, R. A. & Burdette, J. H. An automated method for neuroanatomic and cytoarchitectonic atlas-based interrogation of fMRI data sets. *Neuroimage* **19**, 1233–1239 (2003).

Reporting Summary

Nature Research wishes to improve the reproducibility of the work that we publish. This form provides structure for consistency and transparency in reporting. For further information on Nature Research policies, see [Authors & Referees](#) and the [Editorial Policy Checklist](#).

Statistical parameters

When statistical analyses are reported, confirm that the following items are present in the relevant location (e.g. figure legend, table legend, main text, or Methods section).

n/a Confirmed

- The [exact sample size \(n\)](#) for each experimental group/condition, given as a discrete number and unit of measurement
- An indication of whether measurements were taken from distinct samples or whether the same sample was measured repeatedly
- The statistical test(s) used AND whether they are one- or two-sided
Only common tests should be described solely by name; describe more complex techniques in the Methods section.
- A description of all covariates tested
- A description of any assumptions or corrections, such as tests of normality and adjustment for multiple comparisons
- A full description of the statistics including [central tendency](#) (e.g. means) or other basic estimates (e.g. regression coefficient) AND [variation](#) (e.g. standard deviation) or associated [estimates of uncertainty](#) (e.g. confidence intervals)
- For null hypothesis testing, the test statistic (e.g. F, t, r) with confidence intervals, effect sizes, degrees of freedom and P value noted
Give P values as exact values whenever suitable.
- For Bayesian analysis, information on the choice of priors and Markov chain Monte Carlo settings
- For hierarchical and complex designs, identification of the appropriate level for tests and full reporting of outcomes
- Estimates of effect sizes (e.g. Cohen's d, Pearson's r), indicating how they were calculated
- Clearly defined error bars
State explicitly what error bars represent (e.g. SD, SE, CI)

Our web collection on [statistics for biologists](#) may be useful.

Software and code

Policy information about [availability of computer code](#)

Data collection

AcqKnowledge software (version 4, BIOPAC Systems)

Data analysis

Stan 2.15.1, R version 3.3.2, Matlab Version 8.6.0.267246 (R2015b), SPM 12

For manuscripts utilizing custom algorithms or software that are central to the research but not yet described in published literature, software must be made available to editors/reviewers upon request. We strongly encourage code deposition in a community repository (e.g. GitHub). See the Nature Research [guidelines for submitting code & software](#) for further information.

Data

Policy information about [availability of data](#)

All manuscripts must include a [data availability statement](#). This statement should provide the following information, where applicable:

- Accession codes, unique identifiers, or web links for publicly available datasets
- A list of figures that have associated raw data
- A description of any restrictions on data availability

The data that support the findings of this study as well as the code used for the analyses are available from the corresponding authors upon reasonable request.

Field-specific reporting

Please select the best fit for your research. If you are not sure, read the appropriate sections before making your selection.

Life sciences Behavioural & social sciences Ecological, evolutionary & environmental sciences

For a reference copy of the document with all sections, see nature.com/authors/policies/ReportingSummary-flat.pdf

Life sciences study design

All studies must disclose on these points even when the disclosure is negative.

Sample size	Sample size was determined based on the assumption of a medium to large ($r = 0.4$) brain-behavior relationship between PTSD symptoms and BOLD activation. The necessary sample size was thus calculated as N=46 with 80% power and N=61 with 90% power.
Data exclusions	A total of 77 participants took part in the experiment. Due to problems with the SCR equipment or measurement problems during the functional scan, we did not obtain complete skin conductance and/or functional imaging data of 23 participants.
Replication	We did not replicate our findings in an independent sample. To ensure reproducibility of our findings we structured the analyses with a 'Makefile' which documents the dependencies between different analysis modules and allows to run the analyses using the 'make' command at the Unix command line. All the code used is organized in a git repository and is available from the authors upon request.
Randomization	In this study, combat veterans with varying degrees of psychopathology were recruited. Thus, due to the study design, group-membership (combats with PTSD versus combats without PTSD) was not randomized but predetermined. We did, however, randomize participants to two experimental orders in the reversal learning experiment.
Blinding	Since participants did not receive a treatment but were tested in an experiment, blinding was not applicable in this study.

Reporting for specific materials, systems and methods

Materials & experimental systems

n/a	Involved in the study
<input checked="" type="checkbox"/>	<input type="checkbox"/> Unique biological materials
<input checked="" type="checkbox"/>	<input type="checkbox"/> Antibodies
<input checked="" type="checkbox"/>	<input type="checkbox"/> Eukaryotic cell lines
<input checked="" type="checkbox"/>	<input type="checkbox"/> Palaeontology
<input checked="" type="checkbox"/>	<input type="checkbox"/> Animals and other organisms
<input type="checkbox"/>	<input checked="" type="checkbox"/> Human research participants

Methods

n/a	Involved in the study
<input checked="" type="checkbox"/>	<input type="checkbox"/> ChIP-seq
<input checked="" type="checkbox"/>	<input type="checkbox"/> Flow cytometry
<input type="checkbox"/>	<input checked="" type="checkbox"/> MRI-based neuroimaging

Human research participants

Policy information about [studies involving human research participants](#)

Population characteristics 54 participants, mean age: 32.81 (7.97), 49 males, 5 females; mean CAPS score 39.22 (32.01).

Recruitment Participants were recruited from the community by posting research flyers at several VA hospital in the region, VA community-based clinics, Veterans Centers, universities bulletin boards, and at universities veterans' organization offices.

Magnetic resonance imaging

Experimental design

Design type	Task; event-related
Design specifications	69 trials, 4 s each, intertrial interval 12s.
Behavioral performance measures	The behavioral performance was measured with skin conductance response. Skin conductance was assessed with shielded Ag-AgCl electrodes, filled with standard NaCl electrolyte gel, and attached to the middle phalanges of the second and third fingers of the left hand. The electrode cables were grounded through an RF filter panel. The skin conductance signal was amplified and recorded with a BIOPAC Systems skin conductance module connected to a

computer. Data were continuously recorded at a rate of 200 samples per second. An off-line analysis of the analog skin conductance waveforms was conducted with AcqKnowledge software (BIOPAC Systems). The level of skin conductance response was assessed for each trial as the base-to-peak amplitude difference in skin conductance of the largest deflection (in microsiemens) in the 0.5–4.5 s latency window after stimulus onset. The minimal response criterion was 0.02 microsiemens. Responses below this criterion were encoded as zero. The raw skin conductance scores were square root transformed to normalize the distributions, and scaled according to each participant's average response to the US. We averaged the learning effects (face A minus face B) across trials by stage (acquisition, reversal) for each participant and calculated a threat reversal index by subtracting the learning effect of reversal from the learning effect of acquisition. To assess whether participants showed successful threat reversal, we tested whether the reversal index was significantly different from zero with a one sample t-test.

Acquisition

Imaging type(s)	Structural and functional.
Field strength	3 Tesla.
Sequence & imaging parameters	Structural: MPRAGE pulse sequence (voxel size 1x1x1 mm; repetition time =2.5 s; echo time =2.77 ms; flip 363 angle =7°; 256×256 matrix, 176 sagittal slices of 1 mm). Functional: single-shot gradient echo EPI sequence (TR =2000 ms; 380 TE =25 ms; FOV =192 cm; flip angle =75°; bandwidth =4340 Hz/px; echo spacing =0.29 ms). Forty contiguous oblique-axial slices (3×3×3 mm voxels) parallel to the AC-PC line.
Area of acquisition	Whole brain scan.
Diffusion MRI	<input type="checkbox"/> Used <input checked="" type="checkbox"/> Not used

Preprocessing

Preprocessing software	Analysis of the imaging data were conducted using SPM 12 (http://fil.ion.ac.uk/spm12). After discarding the first eight volumes, native-space images were realigned, slice-time corrected, and coregistered to each subject's structural scan. Structural image preprocessing included segmentation, bias correction, and spatial normalization; these normalization parameters were also used to normalize the functional images. Finally, functional images were smoothed with a Gaussian kernel (4 mm FWHM).
Normalization	Structural image preprocessing included spatial normalization, these normalization parameters were also used to normalize the functional images.
Normalization template	MNI.
Noise and artifact removal	Motion parameters.
Volume censoring	No volumes were censored.

Statistical modeling & inference

Model type and settings	We performed a computational analysis using the Rescorla-Wagner learning model, with the fMRI regressors derived from the fits to the skin conductance data. Cue onset and offset were modeled as two discrete events, and each computational regressor was included as a parametric modulator of the stimulus onset or offset event. In addition, the occurrence of a shock (0 for trials with no shock, 1 for trials with a shock) was modeled as parametric modulators of cue offset. Six regressors modeling affine head-motion parameters were also included in the GLM. All events were convolved with a canonical gamma-variate hemodynamic response function (HRF). The contrast of interest was the correlation of expected value V, corresponding to the expectation of a shock on each trial, with the BOLD response in the brain. We thus computed images of this contrast for each participant and used the contrast images as input for ROI-based analysis.
Effect(s) tested	For each ROI, we extracted the mean beta estimates obtained from the GLM for the correlation of expected value V with the BOLD response for each participant. These beta estimates were then entered as predictors in multivariable linear regressions, with the psychopathology symptoms as outcome measure.
Specify type of analysis:	<input type="checkbox"/> Whole brain <input checked="" type="checkbox"/> ROI-based <input type="checkbox"/> Both
Anatomical location(s)	Amygdala, dACC, and striatum were defined functionally; the hippocampus was defined using the WFU Pickatlas.
Statistic type for inference (See Eklund et al. 2016)	Mean beta estimates extracted from the ROI.
Correction	ROI-based analysis.

Models & analysis

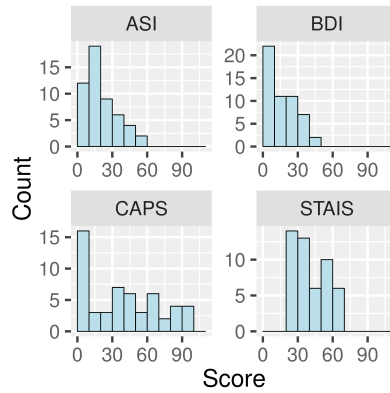
n/a	Involved in the study
<input checked="" type="checkbox"/>	Functional and/or effective connectivity
<input checked="" type="checkbox"/>	Graph analysis
<input checked="" type="checkbox"/>	Multivariate modeling or predictive analysis

In the format provided by the authors and unedited.

Neural computations of threat in the aftermath of combat trauma

Philipp Homan¹, Ifat Levy^{1,2}, Eric Feltham^{3,4}, Charles Gordon^{3,4}, Jingchu Hu¹, Jian Li^{1,5}, Robert H. Pietrzak^{3,4}, Steven Southwick^{3,4}, John H. Krystal^{3,4}, Ilan Harpaz-Rotem^{1,6,7*} and Daniela Schiller^{1,6,7*}

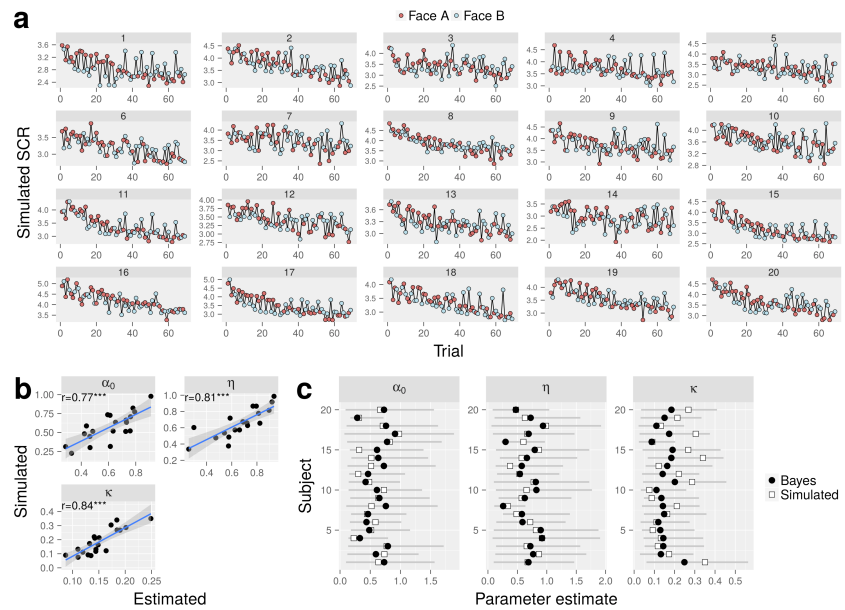
¹Department of Psychiatry, Icahn School of Medicine at Mount Sinai, New York, NY, USA. ²Departments of Comparative Medicine, Neuroscience and Psychology, Yale University, New Haven, CT, USA. ³Department of Psychiatry, Yale University School of Medicine, New Haven, CT, USA. ⁴US Department of Veterans Affairs National Center for PTSD, Clinical Neurosciences Division, VA Connecticut Healthcare System, West Haven, CT, USA. ⁵School of Psychological and Cognitive Sciences and Beijing Key Laboratory of Behavior and Mental Health, Peking University, Beijing, China. ⁶Department of Neuroscience and Friedman Brain Institute, Icahn School of Medicine at Mount Sinai, New York, NY, USA. ⁷These authors contributed equally: Ilan Harpaz-Rotem, Daniela Schiller. *e-mail: ilan.harpaz-rotem@yale.edu; daniela.schiller@mssm.edu



Supplementary Figure 1

Distributions of psychopathology in the study sample show the wide range of symptoms in participants, from completely healthy to highly affected by PTSD.

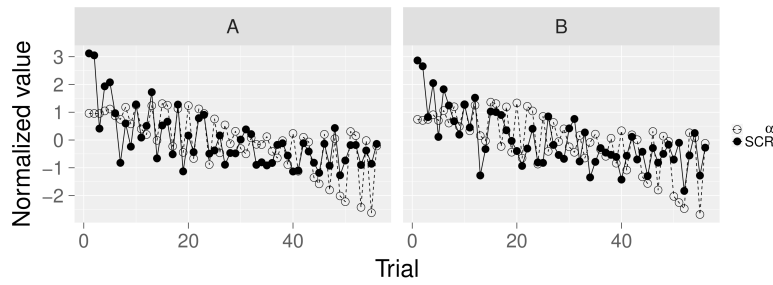
ASI, Anxiety Sensitivity Index; BDI, Beck Depression Inventory; CAPS, Clinician-Administered PTSD Scale; CES, combat exposure score; STAIS, State Anxiety subscale of the Spielberger State-Trait Anxiety Inventory.



Supplementary Figure 2

Hierarchical Bayesian model recovers simulated learning parameters.

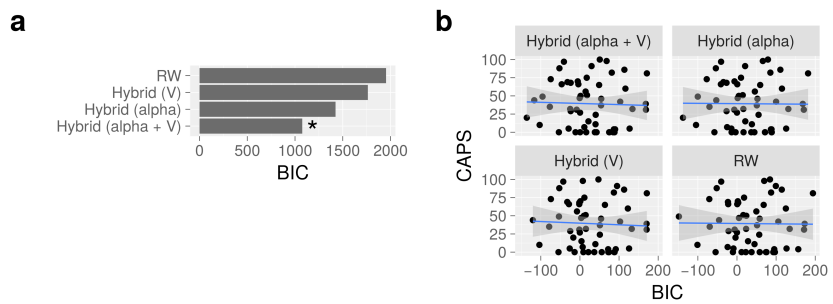
To validate our Hierarchical Bayesian hybrid model before testing it in the clinical dataset, we simulated skin conductance data in 20 participants. We estimated the initial associability α_0 , K , the normalization factor, and η , the prediction error weight. **a. Simulated data in 20 subjects.** **b. Correlations between estimated and simulated values.** The Bayesian model successfully recovered the simulated values. Pearson correlation coefficients with two-tailed significance tests are shown. Error shadings correspond to standard errors. **c. Estimated parameters with 90% credible intervals and simulated parameters.** All simulated parameters were within the 90% credible intervals of the estimated parameters, indicating successful parameter recovery. $^{***}, P < 0.001$.



Supplementary Figure 3

Average skin conductance response across subjects and the best-fit associability trace for all trials without a shock.

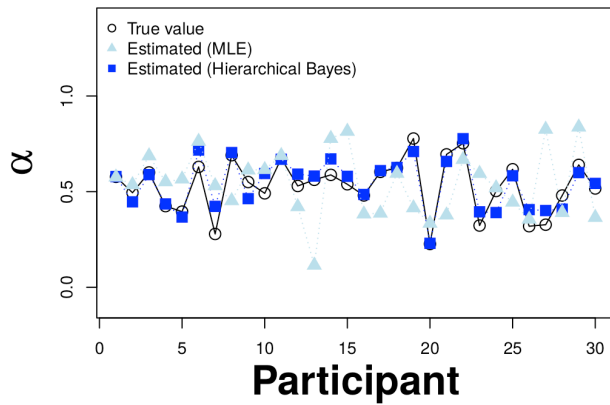
As there were two experimental orders, time courses are displayed for each order separately ($N = 54$ participants). All traces were z-transformed and mean-centered for displaying purpose.



Supplementary Figure 4

Model comparison using maximum likelihood estimation (MLE) and the relationship of model fits to PTSD symptoms.

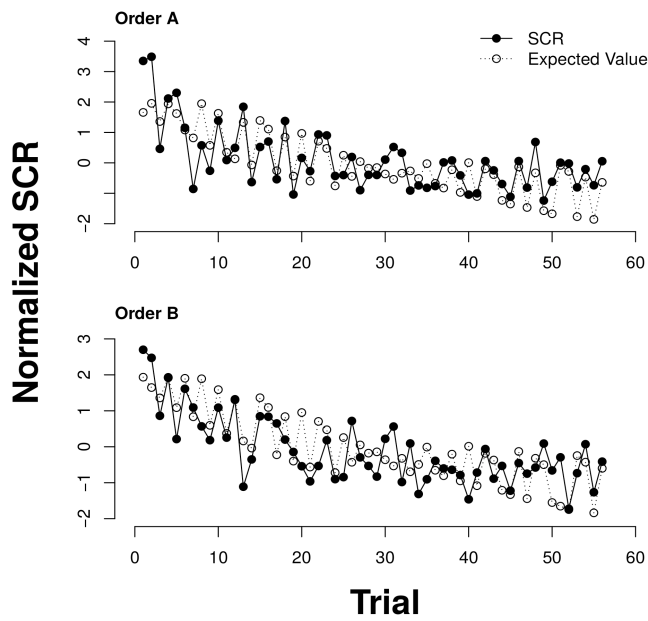
a. MLE analysis is consistent with the Bayesian analysis and a previous study. In line with a previous study,⁸ the hybrid model with the lowest Bayesian Information Criterion (BIC) was the hybrid ($\alpha + V$) model, outperforming the other hybrid models as well as the Rescorla-Wagner (RW) model. The asterisk indicates the winning model. **b. No evidence that model fits interacted with the symptom levels of PTSD.** The correlation between model fits and symptoms was essentially flat for each of the 4 models. Error shadings correspond to standard errors. PTSD, posttraumatic stress disorder. CAPS, Clinician-Administered PTSD Scale; RW, Rescorla-Wagner model.



Supplementary Figure 5

Hierarchical Bayesian model recovers simulated learning parameters of a Rescorla–Wagner model.

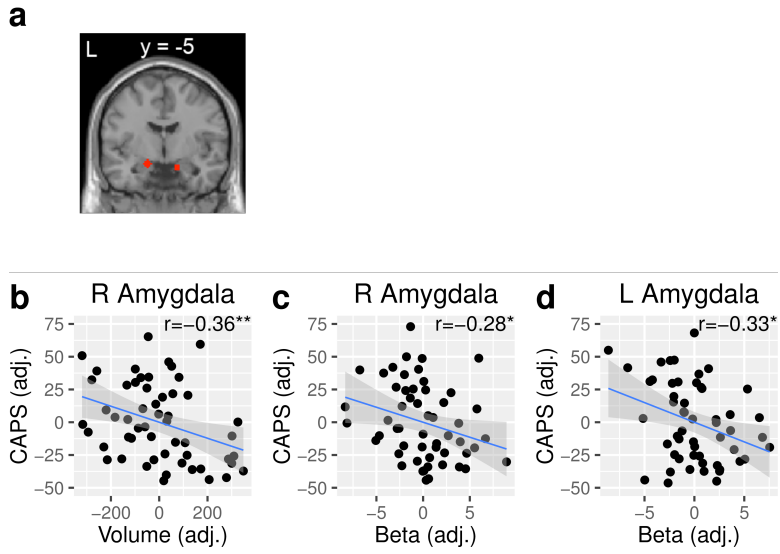
To validate our Hierarchical Bayesian model before testing it in the clinical dataset, we simulated skin conductance data in 30 participants. We estimated the learning rate α (the free parameter in the Rescorla–Wagner model) using our Hierarchical Bayesian model coded in Stan and also compared it to a Maximum Likelihood Estimation (MLE) using the non-linear optimizer fmincon in MATLAB. The Bayesian model successfully recovered the simulated values.



Supplementary Figure 6

Average skin conductance response across subjects and the best-fit expected value trace for all trials without a shock using a Rescorla-Wagner model.

As there were two experimental orders, time courses are displayed for each order separately ($N = 54$ participants). All traces were z-transformed and mean-centered for displaying purpose.

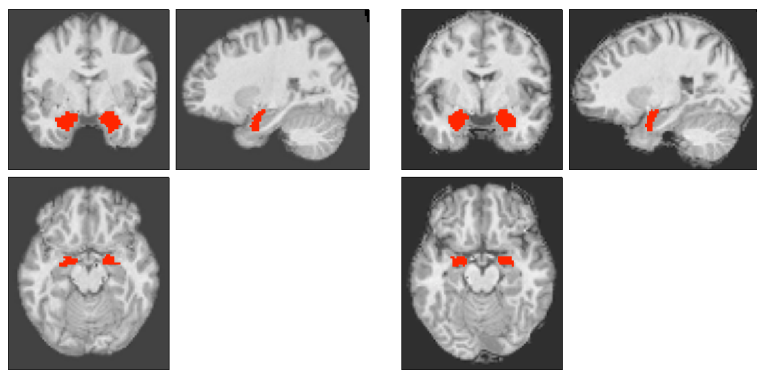


Supplementary Figure 7

Amygdala structure and value computation contribute to PTSD symptoms using a Rescorla-Wagner model.

a. Regions of interest used in the computational imaging analysis. The amygdala (red) was defined functionally, using the contrast of conditioned stimulus vs. baseline. **b-d. Amygdala volume and value-dependent neural activity independently contribute to PTSD symptoms.** Partial correlations are shown ($N = 54$ participants) with Pearson correlation coefficients and two-tailed significance tests. Right amygdala volume and activity as well as left amygdala activity correlated negatively with the PTSD symptoms as measured with the CAPS. Regressions were adjusted for learning rate, age, gender, head movement, and total intracranial volume.

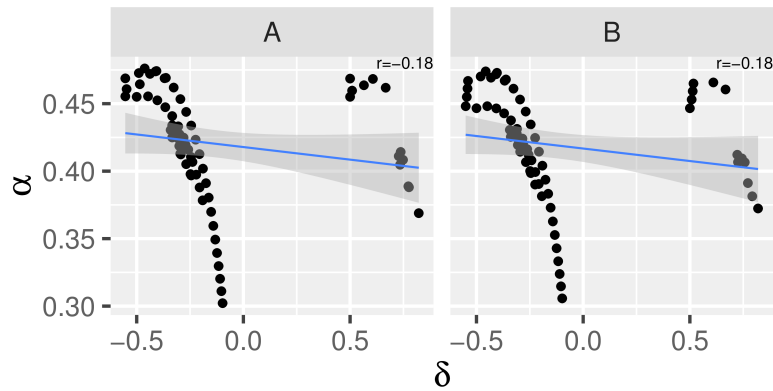
Error shadings correspond to standard errors. CAPS, Clinician-Administered PTSD Scale; adj., adjusted; **, $P < 0.01$; *, $P < 0.05$.



Supplementary Figure 8

Individual amygdala regions of interest for two illustrative participants.

To ensure accurate appearance in the published version, please use the Symbol font for all symbols and Greek letters. Brain slices are shown at $x = 24$, $y = -4$, $z = -16$ in the Montreal Neurological Institute (MNI) coordinate system, using the neurological convention (i.e., left is left).



Supplementary Figure 9

Regression of prediction error (δ) and associability (α) shows that the two learning components were not significantly correlated.

Data for both experimental orders (A and B) is shown ($N = 69$ trials) together with Pearson correlation coefficients and two-tailed significance tests. Error shadings correspond to standard errors.

Supplementary Tables and Figures

Characteristic	N	Mean	SD
Males	23		
Females	0		
VCC	11		
VPTSD	12		
Age	23	33.61	8.02
Education	23	3.57	1.12
ASI	21	19.67	11.74
BDI	23	15.83	11.51
CAPS	23	36.35	31.31
CES	23	16.96	5.92
STAIS	22	40.73	11.97

Table S1: Characteristics of excluded participants due to missing skin conductance and/or functional imaging data. Abbreviations: ASI, Anxiety Sensitivity Index; BDI, Beck Depression Inventory; CAPS, Clinician-Administered PTSD Scale; CES, combat exposure score; STAIS, subscale of the Spielberger State-Trait Anxiety Inventory; SD, Standard deviation; VCC, veteran combat controls; VPTSD, veterans with posttraumatic stress disorder.

5.4 Winkelbeiner et al. 2019, JAMA Psychiatry

Evaluation of Differences in Individual Treatment Response in Schizophrenia Spectrum Disorders A Meta-analysis

Stephanie Winkelbeiner, PhD; Stefan Leucht, MD; John M. Kane, MD; Philipp Homan, MD, PhD

+ Supplemental content

IMPORTANCE An assumption among clinicians and researchers is that patients with schizophrenia vary considerably in their response to antipsychotic drugs in randomized clinical trials (RCTs).

OBJECTIVE To evaluate the overall variation in individual treatment response from random variation by comparing the variability between treatment and control groups.

DATA SOURCES Cochrane Schizophrenia, MEDLINE/PubMed, Embase, PsycINFO, Cochrane CENTRAL, BIOSIS Previews, ClinicalTrials.gov, and World Health Organization International Clinical Trials Registry Platform from January 1, 1955, to December 31, 2016.

STUDY SELECTION Double-blind, placebo-controlled, RCTs of adults with a diagnosis of schizophrenia spectrum disorders and prescription for licensed antipsychotic drugs.

DATA EXTRACTION AND SYNTHESIS Means and SDs of the Positive and Negative Syndrome Scale pretreatment and posttreatment outcome difference scores were extracted. Data quality and validity were ensured by following the PRISMA guidelines.

MAIN OUTCOMES AND MEASURES The outcome measure was the overall variability ratio of treatment to control in a meta-analysis across RCTs. Individual variability ratios were weighted by the inverse-variance method and entered into a random-effects model. A personal element of response was hypothesized to be reflected by a substantial overall increase in variability in the treatment group compared with the control group.

RESULTS An RCT was simulated, comprising 30 patients with schizophrenia randomized to either the treatment or the control group. The different components of variation in RCTs were illustrated with simulated data. In addition, we assessed the variability ratio in 52 RCTs involving 15 360 patients with a schizophrenia or schizoaffective diagnosis. The variability was slightly lower in the treatment compared with the control group (variability ratio = 0.97; 95% CI, 0.95–0.99; $P = .01$).

CONCLUSIONS AND RELEVANCE In this study, no evidence was found in RCTs that antipsychotic drugs increased the outcome variance, suggesting no personal element of response to treatment but instead indicating that the variance was slightly lower in the treatment group than in the control group; although the study cannot rule out that subsets of patients respond differently to treatment, it suggests that the average treatment effect is a reasonable assumption for the individual patient.

Author Affiliations: Author affiliations are listed at the end of this article.

Corresponding Authors: Stephanie Winkelbeiner, PhD, Center for Psychiatric Neuroscience, Feinstein Institute for Medical Research, 75-59 263rd St, New York, NY 11004 (swinkelbe@northwell.edu); Philipp Homan, MD, PhD, Center for Psychiatric Neuroscience, Feinstein Institute for Medical Research, 75-59 263rd St, New York, NY 11004 (phoman@northwell.edu).

JAMA Psychiatry. doi:10.1001/jamapsychiatry.2019.1530
Published online June 3, 2019.

© 2019 American Medical Association. All rights reserved.

Personalized medicine is based on a widely held assumption that patients differ substantially in their response to treatments. The goal of personalized medicine is to find the right treatment for the right patient. Psychiatry is no exception. An assumption among clinicians and researchers alike is that the response to antipsychotic drugs by patients with psychosis differs considerably between individuals.¹

We report that this assumption may be unfounded. Although variation in the observed treatment responses obviously exists, it is crucial to distinguish between observed and true treatment response: observed response consists of true response plus regression to the mean, some placebo effects, and random terms such as (but not restricted to) measurement error. First, we exemplify why confusing observed with true treatment response is so common, and we use simulated data to show how variation that is purely random and unrelated to permanent differences in treatment response may suggest the need for personalized treatment. Next, we review the evidence of the differences in treatment response by conducting a meta-analysis of the variation in antipsychotic treatment trials. Although this issue is brought up by statisticians regularly,² it deserves more attention from a general psychiatric audience.

Where does the assumption of individual differences in treatment response come from? In general, antipsychotic drugs are assessed in randomized clinical trials (RCTs), the criterion standard for identifying the efficacy of a treatment. In RCTs, patients are assessed at baseline (eg, with the Positive and Negative Syndrome Scale [PANSS]) and randomized to either a treatment or a control group. What RCTs can ultimately provide is an answer to whether a treatment works in general. This average treatment effect is derived from the direct comparison of the response between the treatment and the control groups, which is imperative in an RCT.³ Understandably, this answer may leave clinicians unsatisfied; after all, they are treating individual, and not typical, patients. From a clinical perspective, patients vary considerably in their response to antipsychotic drugs, and the general response may seem almost like an uninformed guess for the individual patient. Furthermore, clinicians seem to prefer categories such as normal or abnormal and responders or nonresponders to inform diagnostic and therapeutic decisions. A consequence is that many investigators now try to personalize medicine by aiming to tailor treatments to individual patients. They agree that response to treatment varies from patient to patient.

However, estimating individual response to treatment, known as the treatment-by-patient interaction, is more complex than often appreciated and depends on laborious study designs, such as repeated crossover trials.² However, as we illustrate with simulated data, such study designs are needed to distinguish individual response to treatment from other components of variation that are unrelated to permanent differences in treatment response.⁴⁻⁷

By design, RCTs cannot estimate the treatment-by-patient interaction, the index of individual response. Although RCTs do not tell anything about individual response, they might indicate something about the presence of individual response. As recognized early by Fisher,⁸ an increase in variance in the treatment group compared with the control group could indicate the presence of variation in response to treatment.² The strength of this increase

Key Points

Question Is there evidence from randomized clinical trials that patients respond differently to antipsychotic drugs?

Findings In this meta-analysis of 52 randomized clinical trials involving 15 360 patients with a schizophrenia or schizoaffective diagnosis, the outcome variability in the antipsychotic drug treatment group was not higher but slightly lower than that in the placebo control group.

Meaning This study cannot rule out that individual differences in drug response might still exist, but it does question the assumption of a personal element of response to antipsychotic treatment.

would then quantify the size of the personal element of response and provide evidence for the presence of a treatment-by-patient interaction.⁹ A method has been developed to compare variances between groups across studies¹⁰ and has been adopted by a meta-analysis package.¹¹ In psychiatry, this method has been applied to compare variances in brain structure¹² and inflammatory parameters in psychosis.¹³ This method compares the variance of treatment and control by computing their ratio: a ratio of 1 means equal variances, a ratio greater than 1 means more variability in the treatment group, and a ratio smaller than 1 means less variability in the treatment group compared with the control group.^{10,12,13}

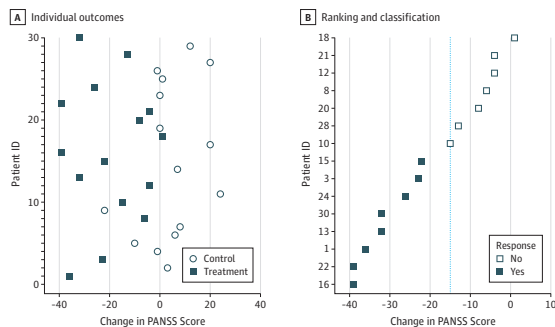
This study is organized in 2 parts. The first part illustrates the different components of variation in RCTs with simulated data, showing the importance of recognizing the treatment-by-patient interaction (which reflects individual treatment response) as the component of interest. The second part shows the results of a meta-analysis, which tested for the presence of treatment-by-patient interaction in empirical data from antipsychotic drug RCTs. We compared the overall variability in the treatment group with the overall variability in the control group, using data from a recently published meta-analysis,¹⁴ summarizing 24 years of placebo-controlled, antipsychotic RCTs in schizophrenia. We hypothesized that compared with control, the often-highlighted heterogeneity in patients with schizophrenia would be reflected by a clinically relevant increase in overall variance of treatment, outcome, which is compatible with a personal element of response that deviates from the estimated average treatment effects.

Methods

Trial Simulation

To illustrate the different components of variation in RCTs, we simulated data from patients with schizophrenia who were randomized to either the antipsychotic treatment or control group and assessed with the PANSS and a positive effect of treatment (Cohen $d = 1.32$; $t_{2,75} = 3.46$; $P = .002$). First, we added a single crossover condition with either a constant or a varying treatment effect, and then we added a double crossover to this simulated trial. With these additions, we show how the variability between and within patients has to be distinguished from the treatment-by-patient interaction, the component reflecting the individual differences in treatment response.

Figure 1. Observed Response Suggests Heterogeneity in Treatment Response



A. Thirty patients with schizophrenia were randomized to either the antipsychotic treatment or the control group. Despite the trial being simulated, with a main effect of treatment (Cohen $d = 1.32$; $t_{22.5} = 3.46$; $P = .002$), it may be tempting to infer from the Positive and Negative Syndrome Scale (PANSS) pretreatment and posttreatment outcome difference scores that some patients in the treatment group responded better than others. This observed pretreatment and posttreatment outcome difference can be misleading given

that individual differences might be merely some unexplained components of variance. B. The treatment group patients are ranked according to the observed pretreatment and posttreatment outcome differences and classified as responders or nonresponders based on an arbitrary threshold (dashed light blue line). Although the ranking is not necessary for the classification, it increases the perception of individual differences in response to treatment.

Meta-analysis

To ensure data quality and validity, this meta-analysis was conducted in accordance with the PRISMA guidelines. We searched Cochrane Schizophrenia, MEDLINE/PubMed, Embase, PsycINFO, Cochrane CENTRAL, BIOSIS Previews, ClinicalTrials.gov, and World Health Organization International Clinical Trials Registry Platform from January 1, 1955, to December 31, 2016.

Using the meta-analysis of Leucht et al¹⁵ as a basis, we included published and unpublished double-blind, placebo-controlled RCTs of at least 3 weeks' duration. These studies investigated adults with a diagnosis of schizophrenia spectrum disorders and prescription for licensed antipsychotic medications, except clozapine. Studies were excluded if they investigated relapse prevention, patients with predominant negative symptoms, patients with major concomitant somatic or psychiatric illness, or intramuscular formulations of antipsychotic treatment, or if they were Chinese research. We included only studies that reported the necessary information (mean, SD, and sample size) of the PANSS pretreatment and posttreatment outcome difference scores.

In studies that combined comparisons of multiple antipsychotic drugs with placebo, we calculated an aggregated SD across all comparisons, leaving only 1 SD per study. We extracted the PANSS means and SDs of the pretreatment and posttreatment outcome difference scores as well as the sample sizes for the treatment and the control groups. Further information on the search strategy is published elsewhere.¹⁵

Statistical Analysis

The SDs of the pretreatment and posttreatment outcome difference scores in the treatment and control groups consist of

the same variance components, including the within-patient variation. The treatment group, however, may also include the additional treatment-by-patient interaction, which could indicate the presence of individual response differences. Thus, in the case of a variable treatment effect, an increase of the variance in the treatment group, compared with the control group, should be observable. To assess this variation, we calculated for each comparison between antipsychotic and placebo drugs the relative variability of treatment and control as the log variability ratio ($\log VR$)¹⁶ with

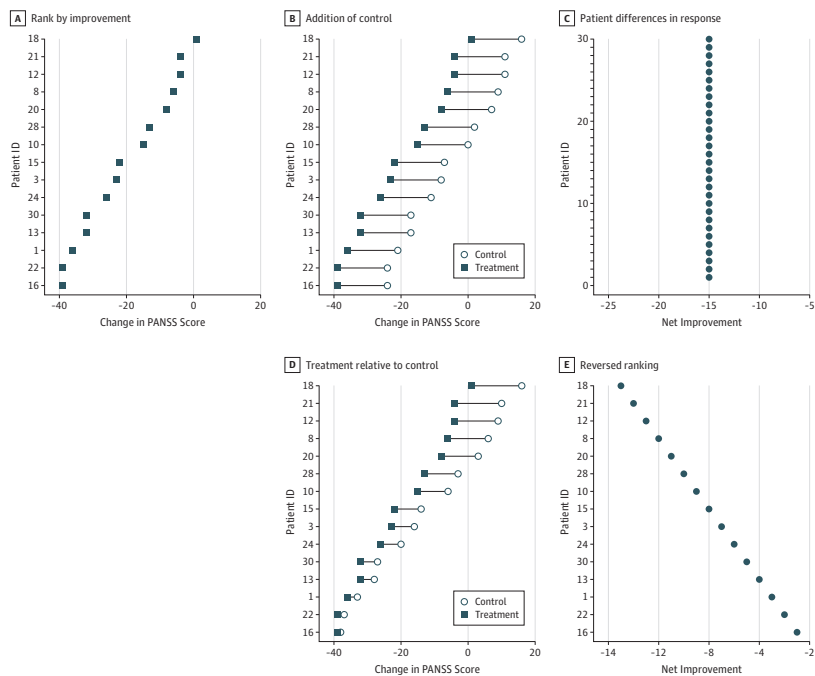
$$\log VR = \log \left(\frac{SD_{Tx}}{SD_{Cx}} \right) + \frac{1}{2(n_{Tx} - 1)} - \frac{1}{2(n_{Cx} - 1)}$$

in which SD_{Tx} was the reported sample SD for treatment, SD_{Cx} was the reported sample SD for control, n_{Tx} was the treatment sample size, and n_{Cx} the control sample size.¹⁰ The corresponding sampling variance ($SD_{\log VR}^2$) for each comparison between antipsychotic and placebo drugs can be expressed as follows:

$$SD_{\log VR}^2 = \frac{1}{2(n_{Tx} - 1)} + \frac{1}{2(n_{Cx} - 1)}$$

We did not find an association between the pretreatment and posttreatment outcome difference scores and their respective SDs in the data for the control group ($\beta = 0.16$; $P = .15$; eFigure 1A in the Supplement) or the treatment group ($\beta = -0.05$; $P = .63$; eFigure 1B in the Supplement). For this reason, we did not consider the log coefficient of variation ratio ($\log CVR$) as an additional index for comparing variabilities.¹⁰

Figure 2. Consequences of Between-Patient Variation



Two simulated scenarios are shown: one with a constant treatment effect across patients (A-C), and one with a reversed ranking after a control condition is taken into account (D, E). A, Using the same ranking from the simulated parallel trial, we show that ranking is a flawed approach to quantifying symptom improvement. B, When adding a control condition to the initial parallel trial, the seeming differences in improvement from patients in the treatment group vanish. C, The crossover trial simulation eliminates spurious differences in the outcome

and reveals no between-patient differences in response. Although seemingly unlikely, such a scenario cannot be ruled out from the results of a parallel group trial. In another scenario, a variable treatment effect is added to a parallel trial (A). D, Differences in improvement may reverse the ranking if patients varied in their response to the treatment compared with controls. E, The patient who appeared to have improved the most in D had actually the smallest net improvement. PANSS indicates Positive and Negative Syndrome Scale.

We weighted each log VR with the inverse of this sampling variance¹¹ and entered it into a random-effects model. This approach allows for the quantification of the true individual response, after adjusting for within-patient variability and regression to the mean.^{5,9} Results were back-transformed from the log scale for better interpretability, with a variability ratio higher than 1, indicating greater variability under treatment compared with control, and a ratio lower than 1, indicating less variability under treatment compared with control.

The analysis was performed from October 31, 2018, to March 29, 2019, with the R package metafor, version 2.0.0,¹¹ and the manuscript was produced with the R package knitr, version 1.20, in RStudio (R Foundation for Statistical Comput-

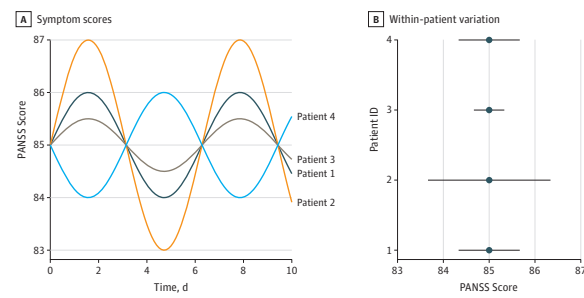
ing). All the data and code we used are freely available online to ensure reproducibility (<https://doi.org/10.17605/OSF.IO/QARVS>).

Results

Simulation

We simulated an RCT of 30 patients with schizophrenia randomized to either the treatment or the control group. The individual pretreatment and posttreatment outcome differences (Figure 1A) might tempt us to infer that some patients in the treatment group responded better than others. We might then rank these patients according to their outcome and clas-

Figure 3. Random Within-Patient Fluctuations



Four patients from the simulated trial were measured repeatedly over time using the Positive and Negative Syndrome Scale (PANSS). A, The differences in a patient's symptom severity scores from time point to time point are independent of any intervention. B, Measuring repeatedly and calculating the means over all time points account for random within-patient fluctuations and reveal that patients had the same mean PANSS score. What differed was the amount of random fluctuation, which might be a highly unlikely scenario but, until tested, cannot be assumed is not true.

sify them as either responders or nonresponders. However, such ranking and classification can be misleading.

Although seemingly different (Figure 2A), adding a simulated crossover condition to the initial parallel trial may reveal that the apparent differences in improvement among patients in the treatment group vanish (Figure 2B) and the treatment effect may actually be constant across patients (Figure 2C). Such a scenario cannot be ruled out from the results of a parallel group trial. In addition, the same ranking (Figure 2A) may reflect yet another scenario, in which differences in improvement as calculated from a crossover condition may reverse the ranking (Figure 2D), such that patients who appeared to have improved the most had actually the smallest net improvement (Figure 2E). Apparent outcome differences among patients in an RCT may still be compatible with a constant treatment effect.

Next, outcome differences may also be found within patients. Assessing patients repeatedly over time might reveal that symptoms fluctuate randomly around the same mean score (Figure 3). This fluctuation shows that within-patient variability alone may suggest differences in treatment response that are a mere reflection of random fluctuation.

Again, we can add a simple crossover condition to the simulated parallel group trial (Figure 4A), in which each patient received both the treatment (antipsychotic drug) and control (placebo). Only by running the crossover trial once again (Figure 4B) can we determine whether the differences observed in the first crossover trial are indeed stable features of the patients. The net improvement from crossover trial 1 may not replicate in crossover trial 2, which indicates that the response differences are still not stable features of the patients (Figure 4C). For that stability to be the case, we would have to see a similar outcome in crossover trial 1 (Figure 4A) as in crossover trial 2 (Figure 4D), in which case we have identified a substantial treatment-by-patient interaction (Figure 4E).

A careful distinction of the sources of variation in a simulated RCT has shown that it is not trivial to distinguish the source of primary interest (treatment-by-patient interaction) from components that tell nothing about individual re-

sponse. In the meta-analysis, we assessed whether evidence exists for such treatment-by-patient interaction across antipsychotic drug trials.

Meta-analysis

We investigated 75 comparisons of antipsychotic drug with placebo in 52 RCTs.¹⁷⁻⁶⁸ None of these studies used a design such as repeated crossovers that would have allowed for a direct estimate of individual responses. Overall, a total of 15 360 patients with a schizophrenia or schizoaffective diagnosis were included, of whom 8550 (55.7%) had been randomized to the treatment group and 6810 (44.3%) to the control group (more details can be found in the eResults in the Supplement).

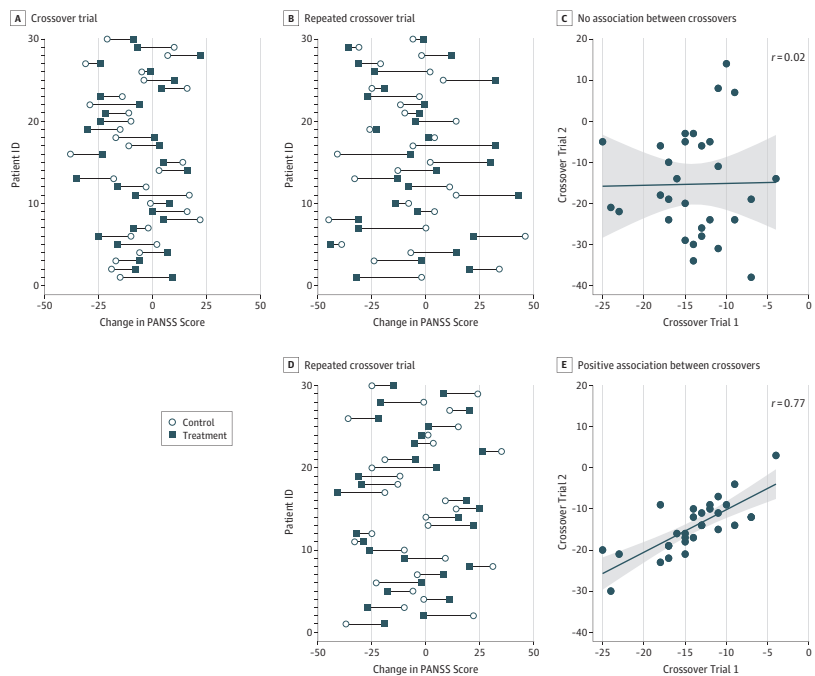
We found an overall lower variability in treatment compared with control (variability ratio = 0.97; 95% CI, 0.95-0.99; $P = .01$; Figure 5¹⁷⁻⁶⁸). This finding indicates that the overall variability across treatment groups was 3% lower compared with that in the control groups. Furthermore, we compared the variances in individual antipsychotic drug outcome and found the same pattern, with lower variability across treatment compared with control (variability ratio = 0.97; 95% CI, 0.95-1.00; $P = .02$; eFigure 2 in the Supplement).

No evidence was found that antipsychotic treatment increased the outcome variance compared with the control. Instead, the outcome variance was slightly lower in the treatment than in the control group.

Discussion

A widespread belief among clinicians and researchers is that patients differ substantially in their antipsychotic treatment response, but finding evidence for this assumption is complex. A likely explanation, supported by the simulations conducted for this study, is that taking an observed treatment response as the true treatment response is tempting, compelling us to ignore the components of variation most likely encountered: random variation within patients and differences between patients. The existing empirical evidence for such in-

Figure 4. Estimating Treatment-by-Patient Interaction With Repeated Crossover Trials



The same simulation is shown of 30 patients with schizophrenia in a parallel trial assessed with the Positive and Negative Syndrome Scale (PANSS). A, Patients received both the antipsychotic and placebo drugs in a crossover trial. B, Only by running a crossover trial more than once can we identify whether individual response is a trait or a permanent feature of the patient. C, Associating the net improvement from crossover trials 1 and 2 (solid dots) shows that advantages from the first trial do not replicate in the second ($r = 0.02$; 95% CI). In this scenario, response to treatment is not a permanent feature of the patient.

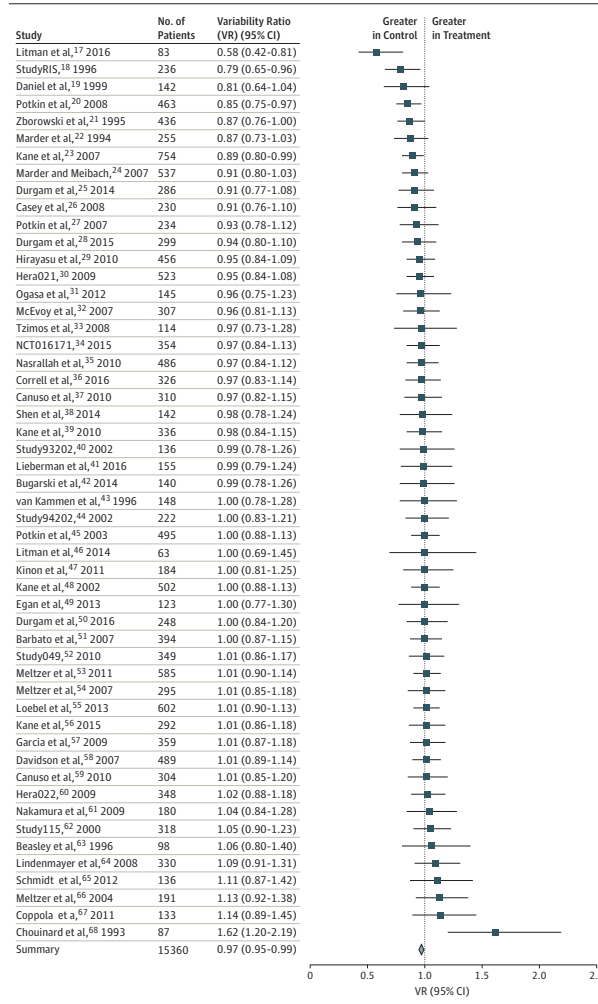
D, Another scenario using the same crossover trial 1 (A) and repeating it, we might observe that the response was almost identical to the response in crossover trial 1. E, Patients responded similarly in both trials ($r = 0.77$; 95% CI). In this scenario, we can consider response to treatment as a trait in these patients. Repeatability of the association from one crossover trial to the next in the same sample is the only way to separate treatment-by-patient interaction from random within-patient variation and to determine whether response is a trait or a state.

dividual differences is weaker than expected: No evidence was found that the antipsychotic drug increased the outcome variance compared with the placebo. Instead, the outcome variance was slightly lower in the treatment group. With this finding, we still cannot rule out that subsets of patients responded differently to treatment, but the overall small difference in variances suggests that the average treatment effect is a reasonable assumption for the individual patient. By assuming heterogeneity in treatment outcomes, we might ultimately introduce noise into clinical practice by refusing to go with the best available evidence, the average treatment effect derived from RCTs.²

Although RCTs are questioned regularly, sometimes using questionable arguments,⁶⁹ they remain the criterion stan-

dard in clinical research. They provide unbiased estimates of the relative efficacy of an intervention, which even the largest observational studies cannot provide.⁷⁰ In addition, appreciating the role of randomization in RCTs is important. Randomization is not compatible with the notion that specific features, such as placebo response, increase in one but not the other group in an RCT. If evidence existed of an enhanced placebo response over time, as has been suggested repeatedly in the past years,¹⁴ this response would have been apparent in both the control and the treatment groups because of randomization and thus would have canceled out. Furthermore, the concept of placebo response, although regularly investigated,⁷¹ cannot be studied by looking at the observed responses in con-

Figure 5. Lower Variability in the Treatment Group Compared With the Control Group Across Antipsychotic Drug Parallel Trials



The forest plot shows the VR together with its 95% CI for treatment vs control across 52 studies. Each study is listed with its respective citation number. The overall VR was lower for treatment compared with control group.

trol groups,⁷² for the same reasons that this approach does not work for the treatment groups, as this study has shown.

Comparing the variabilities between treatment and control groups may provide valuable insight into the presence of indi-

vidual response and the scope of personalized medicine. Recently, other groups have taken a similar approach to assess the presence of individual differences in brain structure¹² and immunological parameters in psychosis.¹³ We assumed that, in the presence of

a personal element of response to treatment, the variance in the treatment group should be higher compared with the control group, which in turn would require further investigation (eg, with n-of-1 trials).⁷³⁻⁷⁵ However, our results indicate that overall variability in the treatment groups was slightly lower, if only by a modest amount (1% to 5%). One explanation might be that the treatment had a stabilizing quality⁹ that reduced the variability in the treatment group. An example for such variance stabilization might be the floor effect, in which the assessment instrument is too coarse to capture patient improvements over a certain level.

Nevertheless, given the slightly lower variability under treatment compared with control found in this study, we cannot rule out that individual differences in response to antipsychotic drugs might still exist. A subset of ill patients may have responded well to treatment, whereas less affected patients may not have improved, resulting in an overall decreased variance under treatment than under control.⁹ Yet, the finding of a narrow CI around an overall only slightly lower variability suggests that substantial differences in drug response are rather unlikely. Thus, analyses aimed at estimating individual response might be premature until these differences have been shown to exist and to be clinically relevant.

As the simulations have shown, labeling patients as responders might be misleading. The label suggests that true response has been established as a permanent feature of the patient, even though the label is a mere reflection of the observed response, which includes true response plus regression to the mean, some placebo effect, and random terms such as measurement error. Thus, response rates that are calculated in RCTs reflect observed but not true response. We suggest that biomarker research aimed at identifying response to treatment of individuals or subgroups should consider the possibility that

treatment outcome is less heterogeneous than anticipated and might even be close to constant across individuals.

Limitations

This meta-analysis has some limitations. First, the calculation of the pretreatment and posttreatment outcome difference scores varied between studies. Although some RCTs calculated the differences between outcome and baseline PANSS scores, others used analysis of covariances with the baseline PANSS scores and additional variables as covariates. Thus, some of the included SDs of change were adjusted for covariates but others were not. Second, the use of pretreatment and posttreatment outcome difference scores might lead to a loss of information and might not be sensitive enough to capture differences in response to treatment.⁷⁶ Third, we assumed that individual responses to treatment were reflected by increased variance in the treatment group. Yet, this increased variance could have also indicated the presence of subgroups who responded differently to the treatment.⁹ Such a case would argue for stratified medicine rather than personalized medicine, in which subgroups of patients receive varying treatments. As any interaction, a treatment-by-patient interaction is ultimately scale dependent, which means it can be removed by transformation of the scale.⁷⁷

Conclusions

Until the differences in individual response to treatment have been demonstrated with careful designs, the overall small differences in outcome variance suggest that the average treatment effect is a reasonable assumption for the individual patient.

ARTICLE INFORMATION

Accepted for Publication: April 27, 2019.

Published Online: June 3, 2019.

doi:10.1001/jamapsychiatry.2019.1530

Author Affiliations: Center for Psychiatric Neuroscience, Feinstein Institute for Medical Research, Manhasset, New York (Winkelbeiner, Kane, Homan); Division of Psychiatry Research, Zucker Hillside Hospital, Northwell Health, New York, New York (Winkelbeiner, Kane, Homan); Department of Psychiatry, Zucker School of Medicine at Northwell/Hofstra, Hempstead, New York (Winkelbeiner, Kane, Homan); University Hospital of Psychiatry and Psychotherapy, University of Bern, Bern, Switzerland (Winkelbeiner); Department of Psychiatry and Psychotherapy, Technische Universität München, Munich, Germany (Leucht).

Author Contributions: Drs Homan and Winkelbeiner had full access to all of the data in the study and take responsibility for the integrity of the data and the accuracy of the data analysis.

Concept and design: Winkelbeiner, Leucht, Homan. **Acquisition, analysis, or interpretation of data:**

All authors.

Drafting of the manuscript: Winkelbeiner, Homan. **Critical revision of the manuscript for important intellectual content:** All authors.

Statistical analysis: Winkelbeiner, Homan.

Obtained funding: Winkelbeiner. **Administrative, technical, or material support:**

All authors.

Supervision: Homan.

Conflict of Interest Disclosures: Dr Winkelbeiner reported grants from Swiss National Science Foundation during the conduct of the study. Dr Leucht reported personal fees from LB Pharma International, H Lundbeck A/S, Otsuka Pharmaceutical, Teva Pharmaceutical Industries Ltd, LTS Lohmann Therapy Systems, Gedeon Richter, Recordati SpA, MSD, Boehringer Ingelheim and Sandoz, Janssen Pharmaceutical, Eli Lilly & Company, SanofiAventis, and Servier Laboratories outside of the submitted work; reanalysis of a clinical trial together with Geodon Richter and the publication of its results; and honoraria from Johnson & Johnson, MSD, Angelini, and Sunovion. Dr Kane reported grants from Otsuka, Lundbeck, and Janssen, as well as other from Allergan, Allergan, Forum, Genentech, Lundbeck, Intracellular Therapies, Janssen, Johnson & Johnson, Merck, Neurocrine, Otsuka, Pierre Fabre, Reviva, Roche, Sunovion, Takeda, Teva, Vanguard Research Group, and LB Pharmaceuticals outside of the submitted work. No other disclosures were reported.

Meeting Presentation: The results of this study were presented at the World Congress of Biological

Psychiatry, June 3, 2019, Vancouver, British Columbia, Canada.

Additional Contributions: The authors thank Majnu John, PhD, Department of Mathematics, Zucker School of Medicine at Northwell/Hofstra, for advice on the analysis of the current study, as well as Stephen Senn, PhD, Methodology and Statistics, Luxembourg Institute of Health, and Daniel Guinart, MD, Department of Psychiatry, Zucker School of Medicine at Northwell/Hofstra, for helpful comments on the manuscript. These individuals received no additional compensation, outside of their usual salary, for their contributions.

Additional Information: All data and code are freely available online to ensure reproducibility (<https://doi.org/10.17605/OSF.IO/QARVS>).

REFERENCES

- Garver DL, Holcomb JA, Christensen JD. Heterogeneity of response to antipsychotics from multiple disorders in the schizophrenia spectrum. *J Clin Psychiatry*. 2000;61(12):964-972. doi:10.4088/JCP.v61i123
- Senn S. Mastering variation: variance components and personalised medicine. *Stat Med*. 2016;35(7):966-977. doi:10.1002/sim.6739
- Senn S. Trying to be precise about vagueness. *Stat Med*. 2007;26(7):1417-1430. doi:10.1002/sim.2639

- 4.** Homan P, Kane JM. Clozapine as an early-stage treatment. *Acta Psychiatr Scand*. 2018;138(4):279-280. doi:10.1111/acps.12965
- 5.** Hecksteden A, Kraushaar J, Schraag-Rosenberger F, Theisen D, Senn S, Meyer T. Individual response to exercise training - a statistical perspective. *J Appl Physiol* (1985). 2015;118(12):1450-1459. doi:10.1152/japplphysiol.00714.2014
- 6.** Hecksteden A, Pitsch W, Rosenberger F, Meyer T. Repeated testing for the assessment of individual response to exercise training. *J Appl Physiol* (1985). 2018;124(6):1567-1579. doi:10.1152/japplphysiol.00896.2017
- 7.** Dworkin RH, McDermott MP, Farrar JT, O'Connor AB, Senn S. Interpreting patient treatment response in analgesic clinical trials: implications for genotyping, phenotyping, and personalized pain treatment. *Pain*. 2014;155(3):457-460. doi:10.1002/pain.00714.019
- 8.** Bennett JH, ed. *Statistical Inference and Analysis: Selected Correspondence of RA Fisher*. Oxford, UK: Clarendon Press; 1990. Cited by: Senn S. Seven myths of randomisation in clinical trials: implications for genotyping, phenotyping, and personalized pain treatment. *Pain*. 2014;155(3):457-460. doi:10.1002/pain.00714.019
- 9.** Cortés J, González JA, Medina MN, et al. Does evidence support the high expectations placed in precision medicine? A bibliographic review. *F1000 Res*. 2019;7:30. doi:10.12688/f1000research.13490.4
- 10.** Nakagawa S, Poulin R, Mengersen K, et al. Meta-analysis of variation: ecological and evolutionary applications and beyond. *Methods Ecol Evol*. 2015;6(2):143-152. doi:10.1111/2041-210X.12309
- 11.** Viechtbauer W. Conducting meta-analyses in R with the metafor package. *J Stat Softw*. 2010;36(3):1-48. doi:10.18637/jss.v036.i03
- 12.** Brugge SP, Howes OD. Heterogeneity and homogeneity of regional brain structure in schizophrenia: a meta-analysis. *JAMA Psychiatry*. 2017;74(11):1104-1111. doi:10.1001/jamapsychiatry.2017.2663
- 13.** Pillinger T, Osimo EF, Brugge S, Mondelli V, McCutcheon RA, Howes OD. A meta-analysis of immune parameters, variability, and assessment of modal distribution in psychosis and test of the immune subgroup hypothesis [published November 8, 2018]. *Schizophr Bull*. 2018. doi:10.1093/schbul/sby160
- 14.** Leucht S, Leucht C, Huhn M, et al. Sixty years of placebo-controlled antipsychotic drug trials in acute schizophrenia: systematic review, bayesian meta-analysis, and meta-regression of efficacy predictors. *Br J Psychiatry*. 2017;211(3):127-129. doi:10.1192/bj.psy.2017.20103
- 15.** Hedges LV, Nowell A. Sex differences in mental test scores, variability, and numbers of high-scoring individuals. *Science*. 1995;269(5220):41-45. doi:10.1126/science.7604277
- 16.** Litman RE, Smith MA, Doherty JJ, et al. AZD8529, a positive allosteric modulator at the mGluR2 receptor, does not improve symptoms in schizophrenia: a proof of principle study. *Schizophr Res*. 2016;172(1-3):152-157. doi:10.1016/j.schres.2016.02.001
- 17.** StudyRIS. Office of Clinical Pharmacology and Biopharmacy Review. NDA number: 20272. Janssen-Cilag, data on file 1996. Cited by: Leucht S, Leucht C, Huhn M, et al. Sixty years of placebo-controlled antipsychotic drug trials in acute schizophrenia: systematic review, bayesian meta-analysis, and meta-regression of efficacy predictors. *Am J Psychiatry*. 2017;174(10):927-942. doi:10.1176/ajp.2017.16121358
- 18.** Hecksteden A, Kraushaar J, Schraag-Rosenberger F, Theisen D, Senn S, Meyer T. Individual response to exercise training - a statistical perspective. *J Appl Physiol* (1985). 2015;118(12):1450-1459. doi:10.1152/japplphysiol.00714.2014
- 19.** Daniel DG, Zimbroff DL, Potkin SG, Reeves KR, Harrigan EP, Lakshminarayanan M, Ziprasidone Study Group. Ziprasidone 80 mg/day and 160 mg/day in the acute exacerbation of schizophrenia and schizoaffective disorder: a 6-week placebo-controlled trial. *Neuropsychopharmacology*. 1999;20(5):491-505. doi:10.1016/S0893-133X(98)00090-6
- 20.** Potkin SG, Litman RE, Torres R, Wolfgang CD. Efficacy of loperamide in the treatment of schizophrenia: initial phase 3 studies. *J Clin Psychopharmacol*. 2008;28(2)(suppl 1):S4-S11. doi:10.1073/jcp.0603181692787
- 21.** Zborowski J, Schmitz P, Staser J, et al. Efficacy and safety of sertrindole in a trial of schizophrenia patients. *Biol Psychiatry*. 1995;38(3):661-662. doi:10.1016/0006-3229(95)94656-H
- 22.** Marder SR, Meibach RC. Risperidone in the treatment of schizophrenia. *Am J Psychiatry*. 1994;151(6):825-835. doi:10.1176/jcp.151.6.825
- 23.** Kane J, Canas F, Kramer M, et al. Treatment of schizophrenia with paliperidone extended-release tablets: a 6-week placebo-controlled trial. *Schizophr Res*. 2007;90(1-3):147-161. doi:10.1016/j.schres.2006.09.012
- 24.** Marder SR, Kramer M, Ford L, et al. Efficacy and safety of paliperidone extended-release tablets: results of a 6-week, randomized, placebo-controlled study. *Biol Psychiatry*. 2007;62(12):1363-1370. doi:10.1016/j.biopsych.2007.10.017
- 25.** Durgam S, Starace A, Li D, et al. An evaluation of the safety and efficacy of cariprazine in patients with acute exacerbation of schizophrenia: a phase II, randomized clinical trial. *Schizophr Res*. 2014;152(2-3):450-457. doi:10.1016/j.schres.2013.11.041
- 26.** Casey DE, Sands EE, Heisterberg J, Yang H-M. Efficacy and safety of bifeprunox in patients with an acute exacerbation of schizophrenia: results from a randomized, double-blind, placebo-controlled, multicenter, dose-finding study. *Psychopharmacol (Ber)*. 2008;200(3):317-331. doi:10.1007/s00213-008-1207-7
- 27.** Potkin SG, Cohen M, Panagides J. Efficacy and tolerability of asenapine in acute schizophrenia: a placebo- and risperidone-controlled trial. *J Clin Psychopharmacol*. 2007;68(10):1492-1500. doi:10.1088/JCP.68n1004
- 28.** Durgam S, Cutler AJ, Lu K, et al. Cariprazine in acute exacerbation of schizophrenia: a fixed-dose, phase 3, randomized, double-blind, placebo- and active-controlled trial. *J Psychopharmacol*. 2015;29(12):e1574-e1582. doi:10.1088/1464-0748.2015.09997
- 29.** Hirayasu Y, Tomioka M, Iizumi M, Kikuchi H. A double-blind, placebo-controlled, comparative study of paliperidone extended release (ER) tablets in patients with schizophrenia. *Jpn J Clin Psychopharmacol*. 2010;15:2077-2103.
- 30.** HeraO21, 041-0215H. A multicenter, randomized, double-blind, fixed-dose, 6-week trial of the efficacy and safety of asenapine compared with placebo using olanzapine positive control in subjects with an acute exacerbation of schizophrenia. Center for Drug Evaluation and Research. Medical review(s); 2009. Cited by: Leucht S, Leucht C, Huhn M, et al. Sixty years of placebo-controlled antipsychotic drug trials in acute schizophrenia: systematic review, bayesian meta-analysis, and meta-regression of efficacy predictors. *Am J Psychiatry*. 2017;174(10):927-942. doi:10.1176/ajp.2017.16121358
- 31.** Ogasa M, Kimura T, Nakamura M, Guarino J. Lurasidone in the treatment of schizophrenia: a 6-week, placebo-controlled study. *Psychopharmacology (Berl)*. 2013;225(3):519-530. doi:10.1007/s00213-012-2838-2
- 32.** McEvoy JP, Daniel DG, Carson WH Jr, McQuade RD, Marcus RN. A randomized, double-blind, placebo-controlled, study of the efficacy and safety of aripiprazole 10, 15 or 20 mg/day for the treatment of patients with acute exacerbations of schizophrenia. *J Psychiatr Res*. 2007;41(10):895-905. doi:10.1016/j.jpsychires.2007.05.002
- 33.** Tsimios A, Samokhvalov V, Kramer M, et al. Safety and tolerability of oral paliperidone extended-release tablets in elderly patients with schizophrenia: a double-blind, placebo-controlled study with six-month open-label extension. *Am J Geriatr Psychiatry*. 2008;16(1):31-43. doi:10.1097/JGP.0b013e1815a3e7a
- 34.** ClinicalTrials.gov. A study of the efficacy and safety of asenapine in participants with an acute exacerbation of schizophrenia. Identifier: NCT01617187. <https://clinicaltrials.gov/ct2/show/NCT01617187?cond=A+study+of+the+efficacy+and+safety+of+asenapine+in+participants+with+an+acute+exacerbation+of+schizophrenia&rank=1>. Accessed October 31, 2016.
- 35.** Nasralah HA, Silva R, Phillips D, et al. Lurasidone for the treatment of acutely psychotic patients with schizophrenia: a 6-week, randomized, placebo-controlled study. *J Psychiatr Res*. 2013;47(5):670-677. doi:10.1016/j.jpsychires.2013.01.020
- 36.** Correll CU, Skuban A, Hobart M, et al. Efficacy of brexpiprazole in patients with acute schizophrenia: review of three randomized, double-blind, placebo-controlled studies. *Schizophr Res*. 2016;174(1-3):82-92. doi:10.1016/j.schres.2016.04.012
- 37.** Canuso CM, Schoeler N, Cardthers J, et al. Paliperidone extended-release in schizoaffective disorder: a randomized, controlled study comparing a flexible dose with placebo in patients treated with and without antidepressants and/or mood stabilizers. *J Clin Psychopharmacol*. 2010;30(5):487-495. doi:10.1097/JCP.0b013e181eeb600
- 38.** Shen JH, Zhao Y, Rosenzweig-Lipson S, et al. A 6-week randomized, double-blind, placebo-controlled, comparative trial of vabicaserin in acute schizophrenia. *J Psychiatr Res*. 2014;53:14-22. doi:10.1016/j.jpsychires.2014.02.012
- 39.** Kane JM, Cohen M, Zhao J, Alphs L, Panagides J. Efficacy and safety of asenapine in a placebo- and haloperidol-controlled trial in patients with acute exacerbation of schizophrenia. *J Clin Psychopharmacol*. 2010;30(2):106-115. doi:10.1097/JCP.0b01318135d6f
- 40.** Study93202. Center for Drug Evaluation and Research. Application number 21-436. Medical review(s); 2002. Cited by: Leucht S, Leucht C, Huhn M, et al. Sixty years of placebo-controlled antipsychotic drug trials in acute schizophrenia: systematic review, bayesian meta-analysis, and meta-regression of efficacy predictors. *Am J Psychiatry*. 2017;174(10):927-942. doi:10.1176/ajp.2017.16121358
- 41.** Lieberman JA, Davis RE, Correll CU, et al. ITI-007 for the treatment of schizophrenia: A 4-week randomized, double-blind, controlled trial. *Biol Psychiatry*. 2016;79(9):952-961. doi:10.1016/j.biopsych.2015.08.026
- 42.** Bugarski-Kirila D, Wang A, Abi-Saab D, Blättler T. A phase II/III trial of bitoperin monotherapy compared with placebo in patients with an acute exacerbation of schizophrenia: results from the

- CandleLyte study. *Eur Neuropsychopharmacol.* 2014; 24(7):1024-1036. doi:[10.1016/j.euroneuro.2014.03.007](https://doi.org/10.1016/j.euroneuro.2014.03.007)
43. van Kammen DP, McEvoy JP, Targum SD, Kardatzke D, Sebree TB. A randomized, controlled, dose-ranging trial of sertraline in patients with schizophrenia. *Psychopharmacology (Berl).* 1996; 124(1-2):168-175. doi:[10.1007/BF02245618](https://doi.org/10.1007/BF02245618)
44. Study94203. Center for Drug Evaluation and Research. Application number 21-436. Medical review(s). 2002. Cited by: Leucht S, Leucht C, Huhn M, et al. Sixty years of placebo-controlled antipsychotic drug trials in acute schizophrenia: systematic review, bayesian meta-analysis, and meta-regression of efficacy predictors. *Am J Psychiatry.* 2017;174(10):927-942. doi:[10.1176/appi.ajp.2017.17121358](https://doi.org/10.1176/appi.ajp.2017.17121358)
45. Potkin SG, Saha AR, Kujawa MJ, et al. Aripiprazole as an antipsychotic with a novel mechanism of action, and risperidone vs placebo in patients with schizophrenia and schizoaffective disorder. *Arch Gen Psychiatry.* 2003;60(7):681-690. doi:[10.1001/archpsyc.60.7.681](https://doi.org/10.1001/archpsyc.60.7.681)
46. Litman RE, Smith MA, Desai DG, Simpson T, Swett D, Kanes SJ. The selective neurokinin 3 antagonist AZD2624 does not improve symptoms or cognition in schizophrenia: a proof-of-principle study. *J Clin Psychopharmacol.* 2014;38(2):199-204. doi:[10.1097/JCP.0000000000000001](https://doi.org/10.1097/JCP.0000000000000001)
47. Kinon BJ, Zhang L, Millen BA, et al; HBII Study Group. A multicenter, inpatient, phase 2, double-blind, placebo-controlled dose-ranging study of LY2140023 monohydrate in patients with DSM-IV schizophrenia. *J Clin Psychopharmacol.* 2011;31(3):349-355. doi:[10.1097/JCP.0b013e318218cd5](https://doi.org/10.1097/JCP.0b013e318218cd5)
48. Kane JM, Carson WH, Saha AR, et al. Efficacy and safety of aripiprazole and haloperidol versus placebo in patients with schizophrenia and schizoaffective disorder. *J Clin Psychiatry.* 2002;63(9):763-771. doi:[10.4088/JCP09m0903](https://doi.org/10.4088/JCP09m0903)
49. Egan MF, Zhao X, Smith A, et al. Randomized controlled study of the T-type calcium channel antagonist MK-8998 for the treatment of acute psychosis in patients with schizophrenia. *Hum Psychopharmacol.* 2013;28(2):124-133. doi:[10.1002/hup.2289](https://doi.org/10.1002/hup.2289)
50. Durgam S, Litman RE, Papadakis K, Li D, Németh G, Laszlovszky I. Cariprazine in the treatment of schizophrenia: a proof-of-concept trial. *J Clin Psychopharmacol.* 2016;31(2):61-68. doi:[10.1097/JCP.0000000000000010](https://doi.org/10.1097/JCP.0000000000000010)
51. Barbato L, Newcomer J, Heisterberg J, Yeung P, Shapiro N. Efficacy and metabolic profile of bifeprunox in patients with schizophrenia. Paper presented at: 11th International Congress on Schizophrenia Research; March 28 to April 1, 2007; Colorado Springs, CO.
52. Study049. A 6-week, double-blind, randomized, fixed dose, parallel-group study of the efficacy and safety of three dose levels of SM-13496 (lurasidone) compared to placebo and haloperidol in patients with schizophrenia who are experiencing an acute exacerbation of symptoms. Center for Drug Evaluation and Research; Medical review(s). 2010. Cited by: Leucht S, Leucht C, Huhn M, et al. Sixty years of placebo-controlled antipsychotic drug trials in acute schizophrenia: systematic review, bayesian meta-analysis, and meta-regression of efficacy predictors. *Am J Psychiatry.* 2017;174(10):927-942. doi:[10.1176/appi.ajp.2017.16121358](https://doi.org/10.1176/appi.ajp.2017.16121358)
53. Meltzer HY, Cuccia J, Silva R, et al. Lurasidone in the treatment of schizophrenia: a randomized, double-blind, placebo-and olanzapine-controlled study. *Am J Psychiatry.* 2011;168(9):957-967. doi:[10.1176/appi.ajp.2011.10060907](https://doi.org/10.1176/appi.ajp.2011.10060907)
54. Meltzer HY, Barbato L, Heisterberg J, Yeung P, Shapiro N. A randomized, double-blind, placebo-controlled efficacy and safety study of bifeprunox as treatment for patients with early-exacerbated schizophrenia. *Schizophr Bull.* 2007;33(2):446.
55. Loebel A, Cuccia J, Sarma K, et al. Efficacy and safety of lurasidone 80 mg/day and 160 mg/day in the treatment of schizophrenia: a randomized, double-blind, placebo- and active-controlled trial. *Schizophr Res.* 2013;145(1-3):101-109. doi:[10.1016/j.schres.2013.01.009](https://doi.org/10.1016/j.schres.2013.01.009)
56. Kane JM, Zulon S, Wang Y, et al. Efficacy and safety of cariprazine in acute exacerbation of schizophrenia: results from an international, phase III clinical trial. *J Clin Psychopharmacol.* 2015;35(4):367-373.
57. Garcia E, Robert M, Peris F, Nakamura H, Sato N, Terazawa Y. The efficacy and safety of olanseratane compared with haloperidol in acute-phase schizophrenia: a randomized, double-blind, placebo-controlled multicentre study. *CNS Drugs.* 2009;23(7):615-625. doi:[10.2165/00023210-200923070-00006](https://doi.org/10.2165/00023210-200923070-00006)
58. Davidson M, Emrley R, Kramer M, et al. Efficacy, safety and early response of paliperidone extended-release tablets (paliperidone ER): results of a 6-week, randomized, placebo-controlled study. *Schizophr Res.* 2007;93(1-3):117-130. doi:[10.1016/j.schres.2007.03.003](https://doi.org/10.1016/j.schres.2007.03.003)
59. Canuso CM, Lindenmayer J-P, Kosik-Gonzalez C, et al. A randomized, double-blind, placebo-controlled study of 2 dose ranges of paliperidone extended-release in the treatment of subjects with schizoaffective disorder. *J Clin Psychiatry.* 2010;71(5):587-598. doi:[10.4088/JCP09m05564.y010](https://doi.org/10.4088/JCP09m05564.y010)
60. Hera022. SHH 04-022. A multicenter, randomized, double-blind, fixed-dose, 6-week trial of the efficacy and safety of asenapine compared with placebo using olanzapine positive control in subjects with an acute exacerbation of schizophrenia. Center for Drug Evaluation and Research; Medical review(s). 2009. Cited by: Leucht S, Leucht C, Huhn M, et al. Sixty years of placebo-controlled antipsychotic drug trials in acute schizophrenia: systematic review, bayesian meta-analysis, and meta-regression of efficacy predictors. *Am J Psychiatry.* 2017;174(10):927-942. doi:[10.1176/appi.ajp.2017.16121358](https://doi.org/10.1176/appi.ajp.2017.16121358)
61. Nakamura M, Ogasa M, Guarino J, et al. Lurasidone in the treatment of acute schizophrenia: a double-blind, placebo-controlled trial. *J Clin Psychiatry.* 2009;70(6):829-836. doi:[10.4088/JCP08m04905](https://doi.org/10.4088/JCP08m04905)
62. Study115. Center for Drug Evaluation and Research. Approval package for application number 20-822. Medical review(s). 2009. Cited by: Leucht S, Leucht C, Huhn M, et al. Sixty years of placebo-controlled antipsychotic drug trials in acute schizophrenia: systematic review, bayesian meta-analysis, and meta-regression of efficacy predictors. *Am J Psychiatry.* 2017;174(10):927-942. doi:[10.1176/appi.ajp.2017.16121358](https://doi.org/10.1176/appi.ajp.2017.16121358)
63. Beasley CM Jr, Sanger T, Satterlee W, Tolleson G, Tran P, Hamilton S. Olanzapine versus placebo: results of a double-blind, fixed-dose olanzapine trial. *Psychopharmacology (Berl).* 1996;124(1-2):159-167. doi:[10.1007/BF02245618](https://doi.org/10.1007/BF02245618)
64. Lindenmayer J-P, Brown D, Liu S, Brecher M, Meulen J. The efficacy and tolerability of once-daily extended release quetiapine fumarate in hospitalized patients with acute schizophrenia: a 6-week randomized, double-blind, placebo-controlled study. *Psychopharmacol Bull.* 2008;44(3):11-35.
65. Schmidt ME, Kent JM, Daly E, et al. A double-blind, randomized, placebo-controlled study with JNJ-37822681, a novel, highly selective, fast dissociating D₂ receptor antagonist in the treatment of acute exacerbation of schizophrenia. *Eur Neuropsychopharmacol.* 2012;22(10):721-733. doi:[10.1016/j.euroneuro.2012.02.007](https://doi.org/10.1016/j.euroneuro.2012.02.007)
66. Meltzer HY, Arvanitis L, Bauer D, Rein W. Meta-Trial Study Group. Placebo-controlled evaluation of four novel compounds for the treatment of schizophrenia and schizoaffective disorder. *Am J Psychiatry.* 2004;161(6):975-984. doi:[10.1176/appi.ajp.161.6.975](https://doi.org/10.1176/appi.ajp.161.6.975)
67. Coppola D, Melkote R, Lannie C, et al. Efficacy and safety of paliperidone extended release 1.5 mg/day-a double-blind, placebo- and active-controlled, study in the treatment of patients with schizophrenia. *Psychopharmacol Bull.* 2011;44(2):54-72.
68. Chouinard G, Jones B, Remington G, et al. A Canadian multicenter placebo-controlled study of fixed doses of risperidone and haloperidol in the treatment of chronic schizophrenic patients. *J Clin Psychopharmacol.* 1993;13(1):25-40. doi:[10.1097/00004714-199302000-00004](https://doi.org/10.1097/00004714-199302000-00004)
69. Senn S. Seven myths of randomisation in clinical trials. *Stat Med.* 2013;32(9):1439-1450. doi:[10.1002/sim.5713](https://doi.org/10.1002/sim.5713)
70. Leucht S, Davis J, Mithani S, et al. Efficacy and skepticism about using national registers to analyze psychotropic drug outcomes. *JAMA Psychiatry.* 2018;75(4):314-315. doi:[10.1001/jamapsychiatry.2017.4704](https://doi.org/10.1001/jamapsychiatry.2017.4704)
71. Kubo K, Fleischhacker WW, Suzuki T, Yasu-Furukori N, Mimura M, Uchida H. Placebo effects in adult and adolescent patients with schizophrenia: combined analysis of nine RCTs. *Acta Psychiatr Scand.* 2019;139(2):108-116. doi:[10.1111/aps.12960](https://doi.org/10.1111/aps.12960)
72. Hróbjartsson A, Gotzsche PC. Is the placebo powerless? an analysis of clinical trials comparing placebo with no treatment. *N Engl J Med.* 2001;344(21):1594-1602. doi:[10.1056/NEJM200105243442106](https://doi.org/10.1056/NEJM200105243442106)
73. Senn S. Applying results of randomised trials to patients: N of 1 trials are needed. *BMJ.* 1998;317(7157):537-538. doi:[10.1136/bmj.317.7157.537](https://doi.org/10.1136/bmj.317.7157.537)
74. Wang R, Lagakos SW, Ware JH, Hunter DJ, Drazen JM. Statistics in medicine-reporting of subgroup analyses in clinical trials. *N Engl J Med.* 2007;357(21):2189-2194. doi:[10.1056/NEJMrs0707003](https://doi.org/10.1056/NEJMrs0707003)
75. Araújo A, Julious S, Senn S. Understanding variation in sets of N-of-1 trials. *PLoS One.* 2016;11(12):e0167167. doi:[10.1371/journal.pone.0167167](https://doi.org/10.1371/journal.pone.0167167)
76. Joyce DW, Tracy DK, Shergill SS. Are we failing clinical trials? a case for strong aggregate outcomes. *Psychol Med.* 2018;48(2):177-186. doi:[10.1017/S003329171700124](https://doi.org/10.1017/S003329171700124)
77. González AB, Cox DR. Interpretation of interaction: a review. *Ann Appl Stat.* 2007;1(2):371-385. doi:[10.1214/07-AOAS124](https://doi.org/10.1214/07-AOAS124)

Supplementary Online Content

Winkelbeiner S, Leucht S, Kane JM, Homan P. Evaluation of differences in individual treatment response in schizophrenia spectrum disorders: a meta-analysis. *JAMA Psychiatry*. Published online June 3, 2019. doi:10.1001/jamapsychiatry.2019.1530

eResults

eFigure 1. No Associations Between Means and SDs

eFigure 2. Variability for Treatment vs Control Across All Investigated Antipsychotic Drugs

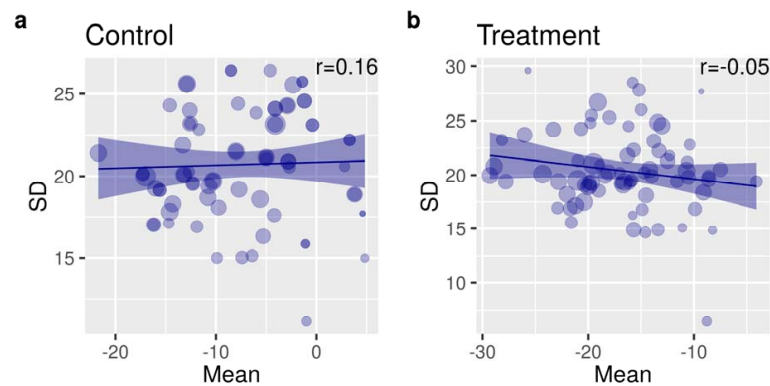
This supplementary material has been provided by the authors to give readers additional information about their work.

eResults

For the studies we had access to, 26 (35%) used an analysis of covariance model, 1 (1%) a mixed model for repeated measures, 25 (33%) an analysis of variance, and 8 (11%) a constrained longitudinal data analysis, whereas information was not available from 15 (20%) studies.

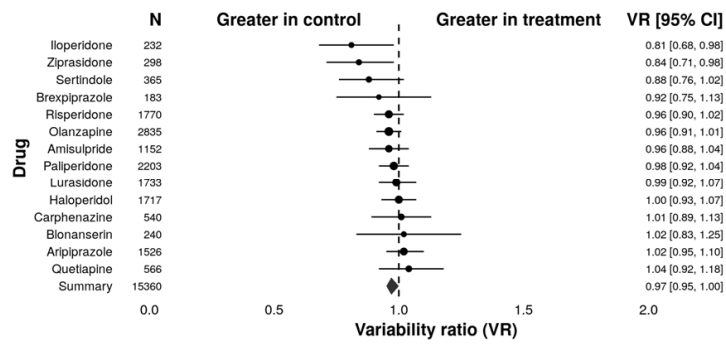
The models included covariates of which ‘baseline’ was the most frequent in 43 (57%) comparisons followed by ‘center’ in 25 (33%), ‘baseline-by-visit’ in 25 (33%), ‘body weight’ in 25 (33%), ‘age’ in 25 (33%), ‘height’ in 25 (33%), ‘duration of hospitalization’ in 25 (33%), ‘number of hospitalization’ in 25 (33%), and ‘age at onset’ in 25 (33%).

eFigure 1. No Associations Between Means and SDs



a, b. The mean pretreatment and posttreatment difference scores were not significantly associated with the SDs across studies for control ($\beta = 0.16$; $P = .15$) or for treatment ($\beta = -0.05$; $P = .62$).

eFigure 2. Variability for Treatment vs Control Across All Investigated Antipsychotic Drugs



The forest plot shows the result of a random-effects model of the variability ratio (VR) of treatment versus control across all investigated antipsychotic drugs ($VR = 0.97$; 95% CI, 0.95; 1.00; $P = .02$). The size of the dots reflects the sample size of the respective study. N, number of patients.

5.5 Winkelbeiner et al. 2018, Schizophrenia Research



Letter to the Editor

Decreased blood flow in the right insula and middle temporal gyrus predicts negative formal thought disorder in schizophrenia



Dear Editors,

Formal thought disorder (FTD) causes severe disturbances of language and communication, and affects 50%–80% of people with schizophrenia (Roche et al., 2015). It is part of the disorganization syndrome that has been found to distinguish patients with schizophrenia from patients with psychotic bipolar disorder, and may, thus, inform differential diagnosis (Palaniyappan et al., 2018). The breakdown of effective communication in FTD is associated with structural and functional alterations of the fronto-temporal language network (Cavelti et al., 2018; Horn et al., 2009; Kircher et al., 2008; Palaniyappan et al., 2015; Strik et al., 2017; Sumner et al., 2017) but might extend to areas outside this network including the amygdala (Cavelti et al., 2018; Spalletta et al., 2010; Sumner et al., 2017), hippocampus (Cavelti et al., 2018; Kircher et al., 2008; Spalletta et al., 2010; Sumner et al., 2017), and insula (Cavelti et al., 2018; Horn et al., 2009; Palaniyappan et al., 2015; Sumner et al., 2017). This range of FTD-associated brain areas might be partly due to the variety of symptoms subsumed under "FTD". Thus, a differentiation into potential subtypes such as positive FTD (i.e., unanticipated, bizarre, or inappropriately expressed speech) and negative FTD (i.e., speech reduced in quantity, content, or fluency) as suggested by factor analytical studies might be more accurate (Roche et al., 2015). Positive FTD has been associated with decreased cortical thickness of the superior temporal gyrus (STG) (Horn et al., 2009), increased activity in the middle temporal gyrus (MTG) (Kuperberg et al., 2007), and decreased volume of the amygdala (Spalletta et al., 2010) and hippocampus (Kircher et al., 2008; Spalletta et al., 2010), whereas negative FTD has been associated with decreased gray matter volume in areas including the MTG and insula (Palaniyappan et al., 2015). However, no study to date has investigated both structural and functional measures to determine if positive and negative FTD reflect two neurophysiologically distinct entities. Therefore, we examined cortical thickness, subcortical volume, and blood perfusion of language (MTG and STG) and language-associated brain areas (amygdala, hippocampus, and insula) as predictors of positive and negative FTD in schizophrenia.

We included twenty-four right-handed and German-speaking patients with a schizophrenia spectrum disorder according to the DSM-IV-TR between 18 and 65 years of age. Severity of FTD was assessed using the Thought, Language, and Communication (TLC) scale, with the subscales Disorganization and Emptiness providing measures of positive and negative FTD. All subjects gave written informed consent. The study was approved by the ethics committee of the Kanton Bern, Switzerland (see the Supplementary Material for details on the study sample and comparisons with healthy controls).

A 3 T Magnetom Verio system (Siemens Erlangen, Germany) was used to create the high-resolution 3D T1-weighted images with a gradient echo and the absolute cerebral blood flow (CBF) images with pseudo continuous arterial spin labeling. Structural images were processed using FreeSurfer 5.1.0, perfusion images were analyzed using FSL 5.0. Mean regional CBF (rCBF), cortical thickness, and subcortical volume values were extracted for every region of interest (see Supplementary Fig. 1). We used multivariable linear regression analyses in R 3.1.3 with the TLC Total score ($n = 24$), Emptiness score ($n = 16$), and Disorganization score ($n = 16$) as dependent variables, the normalized rCBF, cortical thickness, and subcortical volume as independent variables, and age and whole brain global cortical thickness or subcortical volume, respectively, as covariates. The missing values for the TLC subscales were due to missing single items, while the total scores were obtained for all participants. Results were corrected to adjust for false discovery rate (FDR) and considered significant for $p < 0.05$ (see the Supplementary Material for more details).

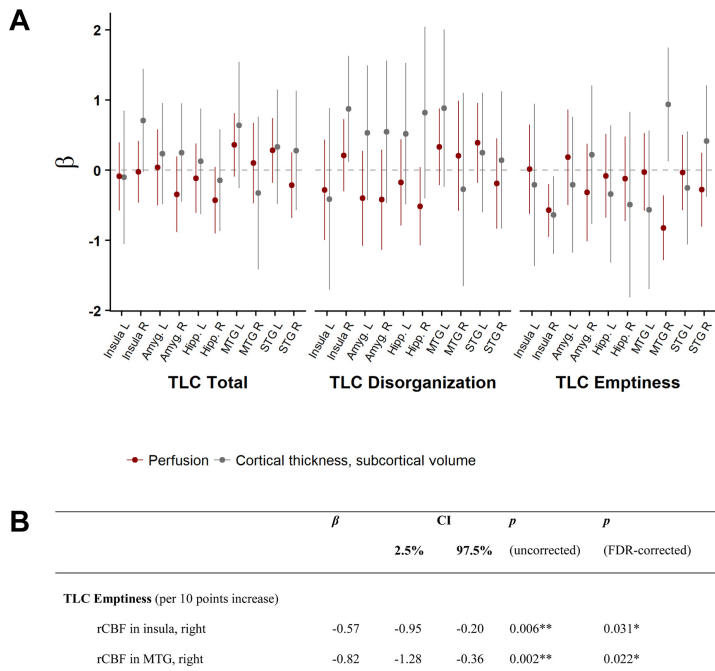
Negative FTD (TLC Emptiness) was significantly correlated with decreased rCBF in the right insula (FDR-corrected $p = 0.031$; Fig. 1) and in the right MTG (FDR-corrected $p = 0.022$; Fig. 1). Positive FTD (TLC Disorganization) did not significantly correlate with structural or metabolic measures ($p > 0.050$; Fig. 1).

This study provided evidence that metabolic changes in the right insula and MTG contribute to negative FTD in schizophrenia. This finding might be best understood in the light of the disconnection hypothesis which suggests that a perturbed lateralization of usually left-sided language areas leads to more diffuse language processing (Kircher et al., 2008). As the insula is also involved in the integration and sequencing of information into a stringent stream of consciousness (Strik et al., 2017), the decreased rCBF found in this region could explain deficient planning of utterances of speech underlying FTD. Yet, we did not find evidence for structural correlates of negative FTD, as well as structural or metabolic correlates of positive FTD. While this is in contrast to previous studies (Horn et al., 2009; Kircher et al., 2008; Kuperberg et al., 2007; Palaniyappan et al., 2015; Spalletta et al., 2010), it is in line, nonetheless, with frequently reported null findings (for a review see Sumner et al., 2017). The most likely explanation is the small sample size of the current study that limits a conclusive decision whether the non-significant findings actually reflect the absence of effects altogether or whether the effects were present but too small to be detected.

While this study provided preliminary evidence that abnormal blood perfusion contributes to negative FTD, studies investigating larger samples are needed to elucidate whether positive and negative FTD effectively reflect distinct entities of FTD with different neurophysiological characteristics.

Funding

This research has been supported by grants from the Swiss National Science Foundation (#320030_146789, #152619, #127359).



Abbreviations. CI, confidence interval; rCBF, regional cerebral blood flow; FDR, false discovery rate; MTG, middle temporal gyrus; TLC, Thought, Language, and Communication scale.

Multivariate linear regression; Significance at: *, $p < 0.05$; **, $p < 0.01$.

Fig. 1. A priori defined regions of interest (ROI) with cortical thickness or subcortical volume and regional cerebral blood flow (rCBF). A. Standardized regression coefficients with 95% confidence intervals are shown. Mean beta values (dots) represent the partial correlations (positive > 0 ; negative < 0) of regional cerebral blood flow (perfusion; red), cortical thickness, and subcortical volume (gray) in the ROIs (amygdala (Amyg.), hippocampus (Hipp.), insula, middle temporal gyrus (MTG), and superior temporal gyrus (STG)) with formal thought disorder (FTD). Confidence intervals not touching the zero line indicate an uncorrected significant effect at $p < 0.05$. B. Significant results of multivariable linear regression analyses. Partial correlations of the Thought, Language, and Communication (TLC) scores for negative FTD (TLC Emptiness) with metabolic measures before and after false discovery rate (FDR)-correction.

Contributors

AF, WS, HH, and PH designed the study. MC collected the data. SW, AF, and PH analyzed the data. SW and MC wrote the first draft of the manuscript. All authors contributed to and approved the final manuscript versions.

Conflicts of interest

None.

Acknowledgement

The authors thank Karin Laimböck for helping with the data collection.

Appendix A. Supplementary material

Supplementary data to this article can be found online at <https://doi.org/10.1016/j.schres.2018.06.009>.

References

- Cavelti, M., Kircher, T., Nagels, A., Strik, W., Homan, P., 2018. Is formal thought disorder in schizophrenia related to structural and functional aberrations in the language network? A systematic review of neuroimaging findings. *Schizophr. Res.* <https://doi.org/10.1016/j.schres.2018.02.051>.
- Horn, H., Federspiel, A., Wirth, M., Mueller, T.J., Wiest, R., Wang, J.J., Strik, W., 2009. Structural and metabolic changes in language areas linked to formal thought disorder. *Br. J. Psychiatry* 194, 130–138.
- Kircher, T., Whitney, C., Krings, T., Huber, W., Weis, S., 2008. Hippocampal dysfunction during free word association in male patients with schizophrenia. *Schizophr. Res.* 101 (1), 242–255.
- Kuperberg, G.R., Decker, T., Holt, D.J., Goff, D., West, W., 2007. Increased temporal and prefrontal activity in response to semantic associations in schizophrenia. *Arch. Gen. Psychiatry* 64 (2), 138–151.
- Palaniappan, L., Mahmood, J., Balain, V., Mougham, O., Gowland, P.A., Liddle, P.F., 2015. Structural correlates of formal thought disorder in schizophrenia: an ultra-high field multivariate morphometry study. *Schizophr. Res.* 168 (1–2), 305–312.
- Palaniappan, L., Deshpande, G., Lanka, P., Rangaprakash, D., Iwabuchi, S., Francis, S., Liddle, P.F., 2018. Effective connectivity within a triple network brain system

- discriminates schizophrenia spectrum disorders from psychotic bipolar disorder at the single-subject level. *Schizophr. Res.* <https://doi.org/10.1016/j.schres.2018.01.006>.
- Roche, E., Creed, L., Macmahon, D., Brennan, D., Clarke, M., 2015. The epidemiology and associated phenomenology of formal thought disorder: a systematic review. *Schizophr. Bull.* 41 (4), 951–962.
- Spalletta, G., Spolezini, I., Cherubini, A., Rubino, I.A., Siracusano, A., Piras, F., Caltagirone, C., Marini, A., 2010. Cortico-subcortical underpinnings of narrative processing impairment in schizophrenia. *Psychiatry Res. Neuroimaging* 182 (1), 77–80.
- Strik, W., Stegmayer, K., Walther, S., Dierks, T., 2017. Systems Neuroscience of Psychosis: mapping schizophrenia symptoms onto brain systems. *Neuropsychobiology* 75 (3), 100–116.
- Sumner, P.J., Bell, I.H., Rossell, S.L., 2017. A systematic review of the structural neuroimaging correlates of thought disorder. *Neurosci. Biobehav. Rev.* 84, 299–315.

Stephanie Winkelbeiner¹

*Translational Research Center, University Hospital of Psychiatry and Psychotherapy, University of Bern, 3000 Bern 60, Switzerland
Center for Psychiatric Neuroscience, The Feinstein Institute for Medical Research, Zucker School of Medicine at Northwell/Hofstra, New York, NY, USA*

Corresponding author at: Translational Research Center, University Hospital of Psychiatry and Psychotherapy, University of Bern, 3000 Bern 60, Switzerland.
E-mail address: stephanie.winkelbeiner@upd.unibe.ch.

Maria Luisa Cavelti¹

*Translational Research Center, University Hospital of Psychiatry and Psychotherapy, University of Bern, 3000 Bern 60, Switzerland
Orygen, The National Centre of Excellence in Youth Mental Health & Centre for Youth Mental Health, University of Melbourne, Parkville, VIC 3052, Australia*

Andrea Federspiel
Katharina Kunzelmann

Thomas Dierks
Werner Strik

Translational Research Center, University Hospital of Psychiatry and Psychotherapy, University of Bern, 3000 Bern 60, Switzerland

Helge Horn
*Translational Research Center, University Hospital of Psychiatry and Psychotherapy, University of Bern, 3000 Bern 60, Switzerland
Institute for Psychiatry and Psychotherapy Bern, Waisenhausplatz 25, 3011 Bern, Switzerland*

Philipp Homan
*Translational Research Center, University Hospital of Psychiatry and Psychotherapy, University of Bern, 3000 Bern 60, Switzerland
Center for Psychiatric Neuroscience, The Feinstein Institute for Medical Research, Zucker School of Medicine at Northwell/Hofstra, New York, NY, USA*

5 March 2018
Available online xxxx

¹ Shared first authorship: The authors contributed equally to this work.

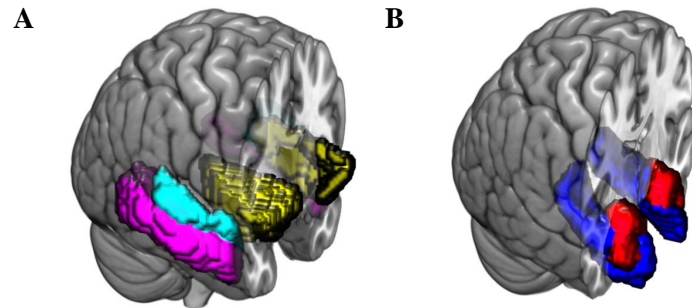
Supplementary Material for
“Decreased blood flow in the right insula and MTG predict negative formal thought disorder in schizophrenia”

This file includes:

Supplementary Figure 1

Supplementary Tables 1 - 3

Figure



Supplementary Figure 1. Regions of interest (ROIs). ROI masks were created using the Harvard-Oxford atlas (Desikan et al., 2006) and the Jülich histological atlas (Eickhoff et al., 2007). ROIs were chosen bilaterally based on previous findings of reduced laterality of the language system (Kircher et al., 2002; Palaniyappan and Liddle, 2012). **A.** Cortical ROIs including the insula (yellow), the middle temporal gyrus (cyan), and the superior temporal gyrus (violet). **B.** Subcortical ROIs including the amygdala (red) and the hippocampus (blue).

Materials and methods

Subjects

This study was conducted at the University Hospital of Psychiatry in Bern, Switzerland, between 2011 and 2014. Our sample of 37 subjects included 24 patients with a schizophrenia spectrum disorder according to the DSM-IV-TR (Association, 2000) and 13 healthy controls, recruited among the employees of the hospital and through personal contacts. Inclusion criteria for patients were a diagnosis of a schizophrenia spectrum disorder confirmed by an experienced clinician, age between 18 and 65 years, sufficient fluency in German, and right-handedness according to the Edinburgh Inventory (Oldfield, 1971). Inclusion criteria for healthy controls further comprised no current major psychiatric DSM-IV Axis I diagnoses. Exclusion criteria for both patients and controls were left-handedness, pregnancy, any contraindications for MRI (e.g., metal-containing implants such as a pacemaker or cochlear implant, claustrophobia), history of serious neurological issues, or current abuse of alcohol and/or psychoactive substances (apart from nicotine). General psychopathology was assessed using the Positive and Negative Syndrome Scale (PANSS) (Kay et al., 1987). Severity of FTD was assessed using the Thought, Language, and Communication (TLC) (Andreasen, 1986) scale. The TLC subscales TLC Disorganization and TLC Emptiness provided measures of positive and negative FTD, respectively (Nagels et al., 2013).

All subjects gave written informed consent. Assessment of psychopathology as well as magnetic resonance imaging (MRI) were conducted on the same day by a trained clinician. The study was approved by the ethics committee of the Kanton Bern, Switzerland.

Data acquisition

Magnetic resonance imaging (MRI) was performed on a 3T Magnetom Verio system (Siemens Erlangen, Germany) with a 12-channel array head coil. Structural images were acquired using high-resolution 3D T1-weighted imaging with a gradient echo (MP-RAGE). The 160 sagittal slices of 1.0 mm thickness, 256 x 256 mm² field of view (FOV), and a matrix size 256 x 256 had a voxel size of 1 x 1 x 1 mm³. Further scan parameters were 2.30 ms repetition time (TR), 2.98 ms echo time (TE), and 900 ms inversion time (TI). Absolute cerebral blood perfusion was measured using pseudo continuous arterial spin labeling (pCASL) (Dai et al., 2008; Wu et al., 2007). The following parameters were used: TR/TE = 4000/30 ms, FOV= 230 x 230 mm², matrix size 64 x 64; six slices at a distance of 1.5 mm; slice thickness 6.0 mm; bandwidth 1446 kHz per pixel; echo spacing 0.78 ms; number of measurements n = 100. Labeling was performed at 90 mm below the isocenter of the imaging region and a post-labeling delay of 1.25 s was set (to allow the labeled water protons to perfuse into the imaging slices), with a label time of 1.6 s.

Data analysis

Cortical thickness and subcortical volume were calculated using the T1-weighted MR images and Freesurfer 5.1.0 (<http://www.surfer.nmr.mgh.harvard.edu/>). The technical details of these procedures have been described in prior publications (Dale et al., 1999; Fischl et al., 1999). For further analyses, we used the cortical thickness and subcortical volume estimates of the ROIs that Freesurfer calculated based on the Desikan-Killiany atlas' parcellation (Desikan et al., 2006) and segmentation of the whole brain.

Perfusion images were analyzed with the Functional MRI of the Brain (FMRIB) Software Library (FSL 5.0) (Smith et al., 2004). First, the raw pCASL data was motion-

corrected with the FMRIB Linear Registration Tool (MCFLIRT) (Jenkinson et al., 2002) and outliers were detected and removed. Second, in order to create a mean difference map for each subject, control-tag pairwise differences were computed. These maps were normalized by the equilibrium magnetization (M_0) of arterial blood estimated via the magnetization of cerebral spinal fluid (CSF). Third, Bayesian Inference for Arterial Spin Labeling MRI (BASIL) (Chappell et al., 2009) was employed to calculate resting state perfusion, which provides blood flow in absolute units ([ml/100g/min]), with the following parameters: BAT = 1.25, TR = 4.0, TE = 3.0, T1 (blood) = 1.65 s, and alpha = 0.85. The application of a gray matter (GM) mask and partial volume correction (Chappell et al., 2011) ensured that only GM voxels were included in the CBF calculation. Fourth, after spatial normalization and transformation into MNI space with FLIRT (Jenkinson et al., 2002) and FNIRT, the FMRIB Non-Linear Registration Tool (Andersson et al., 2007), perfusion data was spatially smoothed with a 6 mm FWHM Gaussian kernel. Lastly, anatomical perfusion masks were created for the ROIs (amygdala, hippocampus, insula, MTG, and STG) based on the Harvard-Oxford atlas (Desikan et al., 2006) and the Jülich histological atlas (Eickhoff et al., 2007) in MNI space (see Supplementary Figure 1). The mean regional CBF (rCBF) for every ROI was extracted by masking the whole brain with the ROI-specific mask, and normalized by dividing the regional by the global CBF. The normalized rCBF for each ROI was then used for further analyses.

Statistical analysis

In order to examine the relationship of cortical thickness, subcortical volume, and rCBF measures in the ROIs with severity of FTD, a series of multivariable linear regression analyses was performed, using the statistical software package R 3.1.3. The TLC Sum score ($n = 24$), TLC Emptiness score ($n = 16$), and TLC Disorganization score ($n = 16$) for all schizophrenia patients were entered as dependent variables, the normalized rCBF values, cortical thickness,

and subcortical volume values of the ROIs as independent variables, and age and whole brain global cortical thickness or subcortical volume, depending on the ROI being cortical or subcortical, as covariates. The missing values for the TLC Emptiness and TLC Disorganization scales are due to missing single TLC items that are needed for the calculation of these subscales. To account for multiple comparisons, the false discovery rate (FDR) method was employed. Results below $p < 0.05$ (FDR corrected) were considered significant.

Tables

Supplementary Table 1. Patient's demographic and clinical characteristics.

Characteristic	Controls	Patients	Group comparison		
	M ± SD (n = 13)	M ± SD (n = 24)	Statistic	Value	p
Gender no. F/Ma	8/5	7/17	<i>Fisher's exact</i>	NA	0.083
Age (years)	29.31 ± 3.99	34.21 ± 10.91	<i>Wilcoxon</i> -test	133	0.473
Education (years)	17.50 ± 1.08	12.75 ± 2.91	<i>Wilcoxon</i> -test	220	0.001***
Diagnosis DSM-IV-TR 295.9/295.7/295.4	NA	16/2/6	NA		
Age of onset	NA	24.77 ± 7.48	NA		
Duration of illness (years)	NA	9.51 ± 7.84	NA		
CPZE (mg)	NA	957.71 ± 1681.33	NA		
PANSS					
Positive Syndrome	NA	16.38 ± 5.36	NA		
Negative Syndrome	NA	12.75 ± 4.99	NA		
General Psychopathology	NA	28.83 ± 6.92	NA		
Total Score	NA	57.96 ± 12.05	NA		
TLC (median [range])					
Emptiness	NA	2.00 [0.00 - 26.00]	NA		
Disorganization	NA	2.00 [0.00 - 8.00]	NA		
Total Score	NA	8.00 [1.00 - 30.00]	NA		

Abbreviations: F, female; Ma, male; M, mean; NA, not applicable; DSM-IV-TR, Diagnostic and Statistical Manual of Mental Disorders; CPZE, chlorpromazine equivalents; PANSS, Positive and Negative Syndrome Scale; SD, standard deviation; TLC, Thought, Language, and Communication scale.

Significant at: *, p < 0.05; **, p < 0.01; ***, p < 0.001.

Supplementary Table 2. Mean (\pm SD) cortical thickness and subcortical volume values.

Regions of interest	Controls	Patients	Group differences		
	$M \pm SD$	$M \pm SD$	t	df	p
	[range]	[range]			
Amygdala ($\times 10^3$ mm 3)					
Left	1.65 \pm 0.21 [1.27 - 2.00]	1.52 \pm 0.30 [0.51 - 1.94]	-1.45	35	0.157
Right	1.68 \pm 0.24 [1.21 - 2.05]	1.62 \pm 0.23 [1.06 - 2.02]	-0.81	35	0.424
Hippocampus ($\times 10^3$ mm 3)					
Left	4.01 \pm 0.31 [3.54 - 4.50]	3.77 \pm 0.57 [2.23 - 4.81]	-1.40	35	0.172
Right	4.14 \pm 0.36 [3.57 - 4.61]	3.93 \pm 0.48 [3.01 - 4.79]	-1.38	35	0.178
Insula (mm)					
Left	3.02 \pm 0.11 [2.83 - 3.23]	2.94 \pm 0.17 [2.60 - 3.39]	-1.52	35	0.137
Right	2.98 \pm 0.15 [2.65 - 3.13]	2.95 \pm 0.20 [2.63 - 3.46]	-0.54	35	0.595
MTG (mm)					
Left	2.88 \pm 0.11 [2.72 - 3.05]	2.84 \pm 0.18 [2.47 - 3.29]	-0.67	35	0.504
Right	2.85 \pm 0.13 [2.59 - 3.02]	2.80 \pm 0.16 [2.55 - 3.19]	-0.86	35	0.395
STG (mm)					
Left	2.85 \pm 0.10 [2.74 - 3.01]	2.81 \pm 0.18 [2.47 - 3.17]	-0.74	35	0.462
Right	2.86 \pm 0.14 [2.64 - 3.18]	2.79 \pm 0.15 [2.57 - 3.15]	-1.46	35	0.154
Whole brain					
Volume ($\times 10^6$ mm 3)	505.86 \pm 51.31 [427.58 - 562.06]	482.38 \pm 65.16 [346.26 - 607.20]	-0.71	35	0.485
Thickness (mm)	2.46 \pm 0.09 [2.27 - 2.61]	2.44 \pm 0.11 [2.15 - 2.69]	-1.12	35	0.270

Abbreviations. M, mean; MTG, middle temporal gyrus; SD, standard deviation; STG, superior temporal gyrus.

Significant at: * $p < 0.05$.

Supplementary Table 3. Mean (\pm SD) normalized regional and absolute global CBF.

Regions of interest	Controls		Patients		Group differences		
	$M \pm SD$		$M \pm SD$		t	df	p
	[range]	[range]	[range]	[range]			
(n = 13)	(n = 24)						
rCBF in amygdala							
Left	0.70 \pm 0.10 [0.54 – 0.86]		0.81 \pm 0.11 [0.62 – 1.04]		2.86	35	0.007**
Right	0.67 \pm 0.11 [0.52 – 0.88]		0.75 \pm 0.12 [0.52 – 1.03]		2.09	35	0.044*
rCBF in hippocampus							
Left	0.89 \pm 0.15 [0.67 – 1.12]		0.93 \pm 0.11 [0.76 – 1.11]		0.95	35	0.347
Right	0.80 \pm 0.17 [0.62 – 1.14]		0.80 \pm 0.09 [0.63 – 0.95]		-0.03	35	0.978
rCBF in insula							
Left	1.21 \pm 0.14 [1.01 – 1.51]		1.15 \pm 0.19 [0.83 – 1.51]		0.93	35	0.361
Right	0.93 \pm 0.21 [0.77 – 1.42]		0.81 \pm 0.15 [0.59 – 1.30]		-1.95	35	0.059
rCBF in MTG							
Left	1.34 \pm 0.27 [0.98 – 1.79]		1.38 \pm 0.20 [0.87 – 1.68]		0.55	35	0.583
Right	1.20 \pm 0.15 [1.01 – 1.57]		1.22 \pm 0.14 [0.99 – 1.56]		0.53	35	0.598
rCBF in STG							
Left	1.27 \pm 0.30 [0.86 – 1.91]		1.30 \pm 0.18 [0.88 – 1.52]		0.393	35	0.697
Right	1.05 \pm 0.21 [0.84 – 1.57]		1.13 \pm 0.17 [0.93 – 1.56]		1.32	35	0.233
Global CBF [ml/100g/min]							
	47.55 \pm 12.95 [30.79 – 82.73]		40.67 \pm 9.27 [24.10 – 63.35]		-1.87	35	0.070

Abbreviations. rCBF, regional cerebral blood flow; M, mean; MTG, middle temporal gyrus; SD, standard deviation; STG, superior temporal gyrus.

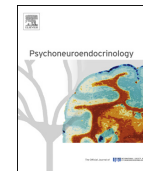
Significant at: *, $p < 0.05$; **, $p < 0.01$.

References

- Andersson, J.L., Jenkinson, M., Smith, S., 2007. Non-linear optimisation. FMRIB technical report TR07JA1. University of Oxford FMRIB Centre: Oxford, UK.
- Andreasen, N.C., 1986. Scale for the assessment of thought, language, and communication (TLC). *Schizophrenia Bulletin* 12(3), 473.
- Association, A.P., 2000. Diagnostic and statistical manual of mental disorders (4th ed., text rev.). American Psychiatric Association, Washington, D. C.
- Chappell, M., Groves, A., MacIntosh, B., Donahue, M., Jezzard, P., Woolrich, M., 2011. Partial volume correction of multiple inversion time arterial spin labeling MRI data. *Magnetic resonance in medicine* 65(4), 1173-1183.
- Chappell, M.A., Groves, A.R., Whitcher, B., Woolrich, M.W., 2009. Variational Bayesian inference for a nonlinear forward model. *IEEE Transactions on Signal Processing* 57(1), 223-236.
- Dai, W., Garcia, D., de Bazelaire, C., Alsop, D.C., 2008. Continuous flow-driven inversion for arterial spin labeling using pulsed radio frequency and gradient fields. *Magn Reson Med* 60(6), 1488-1497.
- Dale, A.M., Fischl, B., Sereno, M.I., 1999. Cortical surface-based analysis: I. Segmentation and surface reconstruction. *NeuroImage* 9(2), 179-194.
- Desikan, R.S., Ségonne, F., Fischl, B., Quinn, B.T., Dickerson, B.C., Blacker, D., Buckner, R.L., Dale, A.M., Maguire, R.P., Hyman, B.T., 2006. An automated labeling system for subdividing the human cerebral cortex on MRI scans into gyral based regions of interest. *NeuroImage* 31(3), 968-980.
- Eickhoff, S.B., Paus, T., Caspers, S., Grosbras, M.-H., Evans, A.C., Zilles, K., Amunts, K., 2007. Assignment of functional activations to probabilistic cytoarchitectonic areas revisited. *NeuroImage* 36(3), 511-521.

- Fischl, B., Sereno, M.I., Dale, A.M., 1999. Cortical surface-based analysis: II: inflation, flattening, and a surface-based coordinate system. *NeuroImage* 9(2), 195-207.
- Jenkinson, M., Bannister, P., Brady, M., Smith, S., 2002. Improved optimization for the robust and accurate linear registration and motion correction of brain images. *NeuroImage* 17(2), 825-841.
- Kay, S.R., Flszbein, A., Opfer, L.A., 1987. The positive and negative syndrome scale (PANSS) for schizophrenia. *Schizophrenia bulletin* 13(2), 261.
- Kircher, T.T., Liddle, P., Brammer, M., Williams, S., Murray, R., McGuire, P., 2002. Reversed lateralization of temporal activation during speech production in thought disordered patients with schizophrenia. *Psychological medicine* 32(3), 439-449.
- Nagels, A., Stratmann, M., Ghazi, S., Schales, C., Frauenheim, M., Turner, L., Fährmann, P., Hornig, T., Katzev, M., Müller-Isberner, R., 2013. The German translation and validation of the scale for the assessment of thought, language and communication: a factor analytic study. *Psychopathology* 46(6), 390-395.
- Oldfield, R.C., 1971. The assessment and analysis of handedness: The Edinburgh inventory. *Neuropsychologia* 9(1), 97-113.
- Palaniyappan, L., Liddle, P.F., 2012. Dissociable morphometric differences of the inferior parietal lobule in schizophrenia. *European Archives of Psychiatry and Clinical Neuroscience* 262(7), 579-587.
- Smith, S.M., Jenkinson, M., Woolrich, M.W., Beckmann, C.F., Behrens, T.E., Johansen-Berg, H., Bannister, P.R., De Luca, M., Drobniak, I., Flitney, D.E., Niazy, R.K., Saunders, J., Vickers, J., Zhang, Y., De Stefano, N., Brady, J.M., Matthews, P.M., 2004. Advances in functional and structural MR image analysis and implementation as FSL. *NeuroImage* 23 Suppl 1, S208-219.

Wu, W.C., Fernandez-Seara, M., Detre, J.A., Wehrli, F.W., Wang, J., 2007. A theoretical and experimental investigation of the tagging efficiency of pseudocontinuous arterial spin labeling. Magn Reson Med 58(5), 1020-1027.



Reduction in total plasma ghrelin levels following catecholamine depletion: Relation to bulimic and depressive symptoms

Philipp Homan ^a, Simona Grob ^b, Gabriella Milos ^b, Ulrich Schnyder ^b,
Gregor Hasler ^{c,*}

^a Department of Endocrinology, Diabetology & Clinical Nutrition, Inselspital, University of Bern, Switzerland

^b Department of Psychiatry and Psychotherapy, University Hospital, Zurich, Switzerland

^c University Hospital of Psychiatry, University of Bern, Switzerland

Received 29 October 2012; received in revised form 13 December 2012; accepted 27 December 2012

KEY WORDS

Ghrelin;
Depression;
Catecholamines;
Bulimia nervosa;
PYY remission;
Dopamine;
Norepinephrine

Summary There is increasing preclinical and clinical evidence of the important role played by the gastric peptide hormone ghrelin in the pathogenesis of symptoms of depression and eating disorders. To investigate the role of ghrelin and its considered counterpart, peptide tyrosine tyrosine (PYY), in the development of bulimic and depressive symptoms induced by catecholamine depletion, we administered the tyrosine hydroxylase inhibitor alpha-methyl-paratyrosine (AMPT) in a randomized, double-blind, placebo-controlled crossover, single-site experimental trial to 29 healthy controls and 20 subjects with fully recovered bulimia nervosa (rBN). We found a decrease between preprandial and postprandial plasma ghrelin levels ($p < 0.0001$) and a post-prandial rise in plasma PYY levels ($p < 0.0001$) in both conditions in the entire study population. Plasma ghrelin levels decreased in the entire study population after treatment with AMPT compared to placebo ($p < 0.006$). AMPT-induced changes in plasma ghrelin levels were negatively correlated with AMPT-induced depressive symptoms ($p < 0.004$). Plasma ghrelin and plasma PYY levels were also negatively correlated ($p < 0.05$). We did not observe a difference in ghrelin or PYY response to catecholamine depletion between rBN subjects and healthy controls, and there was no correlation between plasma ghrelin and PYY levels and bulimic symptoms induced by catecholamine depletion. These findings suggest a relationship between catecholamines and ghrelin with depressive symptoms.

© 2013 Elsevier Ltd. All rights reserved.

Introduction

There is increasing evidence suggesting an association between ghrelin and mood. It has been shown in preclinical experiments that ghrelin might be part of the defense against stress-induced depression and anxiety (Lutter et al., 2008).

* Corresponding author at: University Hospital of Psychiatry, University of Bern, Bolligenstrasse 111, 3000 Bern, Switzerland.
Tel.: +41 31 930 9543; fax: +41 31 930 9921.

E-mail addresses: g.hasler@bluewin.ch, gregor.hasler@puk.unibe.ch (G. Hasler).

Specifically, ghrelin levels were increased in a chronic social defeat stress model of depression, and ghrelin receptor knockout mice showed an increase in depression-like behaviors such as social avoidance (Lutter et al., 2008). In addition, ghrelin involvement is reported in the dopaminergic mesolimbic circuitry, a system that communicates hedonic and reinforcing aspects of natural rewards. High concentrations of ghrelin receptor have been reported in the ventral tegmental area (VTA) (Guan et al., 1997; Zigman et al., 2006), which supports a role for ghrelin in VTA-mediated reward signaling, which is typically impaired in patients suffering from anhedonia (Nestler and Carlezon, 2006; Sullivan and Dufresne, 2006). Additional evidence for ghrelin involvement in the regulation of mood is that ghrelin infusion into the lateral ventricle in rats produced an anxiolytic-like effect (Isogawa et al., 2005) and inhibition of ghrelin induced an increase in depression-like and anxiety-like behaviors (Kanehisa et al., 2006). In clinical studies, patients suffering from major depression (MDD) had lower plasma ghrelin levels (Barim et al., 2009) and antidepressant effects were reported following ghrelin administration (Kluge et al., 2011). Together, these findings suggest that ghrelin plays a role in the pathogenesis of depressive symptoms.

The eating disorder bulimia nervosa (BN) is frequently associated with depressive symptoms. In BN, patients may eat large amounts of food (binge eating) and feel a lack of control over the eating. The binge eating is then followed by a compensatory behavior, such as purging (e.g., vomiting, use of laxatives, excessive exercise). In line with the increased food intake in BN, patients with the disorder have been reported to have elevated ghrelin concentrations at baseline (Kojima et al., 2005; Prince et al., 2009; Tanaka et al., 2002, 2003). However, some studies are in disagreement with these findings, showing normal (Devlin et al., 2012; Monteleone et al., 2005, 2008; Troisi et al., 2005) or decreased (Monteleone et al., 2003) ghrelin levels in BN.

Although the pathways underlying plasma ghrelin level changes in the pathogenesis of depressive symptoms are still largely unknown, it has been hypothesized that they are mediated by activation of the sympathetic nervous system and catecholamine release (Mundinger et al., 2006; Zhao et al., 2010). In fact, there is increasing *in vitro* and *in vivo* evidence for a stimulatory effect of catecholamines on ghrelin (Gagnon and Anini, 2012; Iwakura et al., 2011; Schulpis et al., 2004; Zhao et al., 2010). An instructive paradigm to further evaluate the influence of catecholamines on ghrelin is to transiently deplete catecholamine stores by oral administration of alpha-methyl-paratyrosine (AMPT) (Berman et al., 1999; Hasler et al., 2008). AMPT is a competitive inhibitor of tyrosine hydroxylase, the rate-limiting enzyme in catecholamine synthesis (Nagatsu et al., 1964). Transient decreases in catecholamine transmission by depletion of central dopamine and norepinephrine stores are evidenced by reduced plasma, urine, and cerebrospinal fluid concentrations of catecholamines and their metabolites (Stine et al., 1997) and by decreased occupancy of striatal dopamine receptors (Verhoeff et al., 2003). As catecholamine depletion is also a reliable way to induce transient depressive symptoms (Berman et al., 1999), the association of mood and ghrelin can also be evaluated by catecholamine depletion. Thus, the aim of the current study was to test the role of catecholaminergic ghrelin secretion in humans. In addition,

we assessed the effects of catecholamine depletion on peptide tyrosine tyrosine (PYY) plasma levels, because by modulating satiety, PYY has been considered a counterpart of ghrelin (Batterham et al., 2006; Karra and Batterham, 2010; Murphy and Bloom, 2006). We hypothesized that plasma ghrelin levels would decrease upon catecholamine depletion, and that alterations in ghrelin levels would be negatively correlated to catecholamine-induced depressive symptoms (Carlini et al., 2012). As altered ghrelin and PYY levels have previously been reported in bulimia nervosa (Kojima et al., 2005), an additional hypothesis was that catecholamine depletion would be associated with different alterations in hormone secretion in subjects with remitted bulimia nervosa (rBN) compared to healthy controls, which is why we included a patient-group with rBN and a healthy control group. We chose remitted patients because AMPT effects in symptomatic patients were shown to be considerably smaller than AMPT effects in fully remitted subjects, possibly due to a ceiling effect (Miller et al., 1996).

Methods and materials

Participants

We used the data from the study sample described in (Grob et al., 2012) and recruited females aged 19–39 years who had previously met DSM-IV criteria for BN and had been in remission from BN for at least six months (index subjects; $n = 23$) or who had no history of any psychiatric disorder and no major psychiatric condition in first-degree relatives (control subjects; $n = 30$). The screening visit included a diagnostic Structured Clinical Interview for DSM-IV with a psychiatrist and a physical examination. In order to obtain comparable samples, participants for both study groups were recruited by advertisements in local newspapers and announcements at the University of Zurich and the Swiss Federal Institute of Technology Zurich (ETH). Exclusion criteria included current Axis I psychiatric disorders, a lifetime diagnosis of psychosis, major medical or neurological illness, psychoactive medication exposure within six months, pregnancy, lifetime history of substance dependence, and suicidal ideation or a history of suicide attempts. All subjects gave written, informed consent before participation. The study protocol was approved by the ethics committee of the Canton Zurich (Kantonale Ethikkommission Zürich).

Experimental design

This was a randomized, double-blind, placebo-controlled, crossover study during which all subjects underwent two identical sessions separated by at least seven days wherein they received either AMPT or placebo. Each session included a two-day stay at the Department of Psychiatry and Psychotherapy of the University Hospital of Zurich. One-bed rooms with a separate lavatory were available on a separated floor for all participants, and they had no contact with other hospitalized subjects. None of the rBN subjects had been previously hospitalized at this Department of Psychiatry and Psychotherapy. Participants received regular standardized meals during the hospital sessions. Each subject was contacted daily by telephone for three subsequent days after

each trial for follow-up interviews. In order to avoid any risk of adverse reaction, body weight-adjusted oral doses of AMPT of 40 mg/kg, to a maximum of 4 g over 22 h (at 0900 h, 1200 h, and 1900 h on day one and 0700 h on day two), were administered. During sham depletion, subjects received inactive placebo on day one at 0900 h and 1200 h and 25 mg oral diphenhydramine on day one at 1900 h and on day two at 0700 h, because AMPT frequently induces mild sedation and this effect can be imitated by diphenhydramine (Miller et al., 1996). To prevent formation of crystalluria during AMPT administration, the subjects were instructed to drink at least 2 L of water daily. Possible adverse reactions were assessed regularly (26, 30, 54, 78, and 102 h after the first AMPT/placebo administration) during hospitalization by medical examination including blood pressure measurement, and for three subsequent days after each trial session as part of the daily telephone follow-up interview.

Blood samples

During each session, blood samples were drawn before and at 26 h after the first AMPT dose in order to measure plasma ghrelin and PYY levels using Total Radioimmunoassay (RIA) (Millipore, Millipore Corporation, Billerica, MA, USA). The sensitivity of the RIA used to measure plasma ghrelin levels was 93 pg/mL, the intra-assay coefficient of variation (CV) was 6.1%, the inter-assay CV was 16.5%. The RIA measured total (acylated plus desacylated) ghrelin. The sensitivity of the RIA used to measure plasma PYY levels was 10 pg/mL, the intra-assay CV was 8.4%, the inter-assay CV was 7.1%. The RIA measured total plasma PYY levels. The first sample was drawn immediately before, the second one within 1 h after eating a regular standardized breakfast. Previous research suggested that these two measurements might serve as

surrogates for 24-h profiles to estimate overall ghrelin levels (Cummings et al., 2001).

Behavioral assessment

Behavioral ratings were conducted immediately before the first AMPT/placebo dose (pre-challenge) and at 26, 30, 54, 78, and 102 h after the first dose. Depressive symptoms were assessed with the Montgomery–Åsberg Depression Rating Scale (MADRS). In addition, participants completed various self-report ratings, including the German version of the Eating Disorder Examination-Questionnaire (EDE-Q) (Hilbert and Tuschen-Caffier, 2006).

Statistical analysis

Full factorial linear mixed models with restricted maximum likelihood estimation were applied to determine the effects of treatment, diagnosis, and treatment-by-diagnosis on each hormone. Baseline plasma levels of hormones were included as fixed effects. In all models a heterogeneous compound symmetry covariance structure, chosen considering the lowest Akaike's Information Criterion (AIC), was appropriate for the repeated measures. Subject number and treatment sequence were included as random effects in all models. To evaluate the relationship between alterations induced by catecholamine depletion in hormone levels and clinical scales (MADRS, EDE-Q), additional Pearson correlation coefficients were calculated. Therefore, the differences in plasma ghrelin and PYY levels between the second and first (*i.e.*, baseline) measurement were calculated for each subject and each condition. The difference obtained from the AMPT condition was then subtracted from the difference obtained from the placebo condition, reflecting the

Table 1 Demographic and clinical characteristics of unmedicated subjects with remitted bulimia nervosa (rBN) and healthy controls.

Characteristic	rBN (n = 20)	Controls (n = 29)	p-Value
Sex, No. f/m	20/0	29/0	n.a.
Age, mean (SD), y	29.1 (4.7)	28.7 (3.9)	0.7
BMI, mean (SD), kg/m ²	21.7 (3.1)	22.4 (2.3)	0.3
BMI min, mean (SD), kg/m ²	17.2 (2.2)	20.2 (1.7)	<0.0001
BMI max, mean (SD), kg/m ²	24.0 (3.5)	23.8 (3.0)	0.8
Age at onset, mean (SD), y	15.5 (4.7)	n.a.	n.a.
Educational level (SD), y	16.5 (3.1)	17.3 (3.0)	0.4
Time in remission, months			
Mean (SD)	31.9 (28.1)	n.a.	n.a.
Range	4–84	n.a.	n.a.
First degree relative(s) with a history of bulimia nervosa, No.	2	0	0.2
First degree relative(s) with a history of anorexia nervosa, No.	2	0	0.2
Remote (>1 year ago) history of alcohol abuse, No.	2	0	0.2
History of drug abuse, No.	2	1	0.6
Ghrelin plasma concentration at first measurement, mean (SD), pg/mL	1064 (311.7)	1190.9 (380.8)	0.2
PYY plasma concentration at first measurement, mean (SD), pg/mL	122.5 (41.7)	116.8 (29.6)	0.6
MADRS score at first measurement, mean (SD)	3.3 (3.2)	0.4 (0.9)	<0.0001
EDE-Q score at first measurement, mean (SD)	8.0 (10.0)	1.7 (2.0)	<0.002

BMI, Body Mass Index; BMI min, minimal Body Mass Index during disease; BMI max, maximal Body Mass Index during disease; MADRS, Montgomery–Åsberg Depression Rating Scale; n.a., not applicable.

AMPT-induced change in plasma levels. In the same manner, the differences between the MADRS and EDE-Q scores obtained for each subject in the AMPT session versus the placebo session were calculated to reflect the magnitude of AMPT-induced depressive and bulimic symptoms. The significance threshold for these contrasts was set at alpha = 0.05, two-tailed. SAS 9.2 (SAS Institute, Cary, North Carolina, USA, <http://www.sas.com>) was used for all analyses. Means are reported with their associated standard deviations.

Results

Three rBN subjects and one healthy control subject had to be excluded from the study because of inadequate or missing (e.g., insufficient quantity or hemolysis) blood samples, leaving 20 rBN subjects and 29 healthy controls. The clinical and demographic characteristics of study participants, including baseline parameters, are detailed in Table 1. The rBN subjects had significantly more depressive symptoms at baseline versus the healthy controls ($t [1, 47] = 4.4, p < 0.0001$) and they had histories of significantly lower minimal body mass indexes (BMI) ($t [1, 47] = -5.32, p < 0.0001$). The rBN subjects retained a significantly greater number of bulimic symptoms at study entry compared to the healthy controls ($t [1, 47] = 3.32, p < 0.002$). AMPT induced depressive symptoms in the entire sample ($F [1, 167] = 8.83, p = 0.003$), but to a greater extent in rBN (diagnosis-effect; $F [1, 47] = 31.77, p < 0.0001$). There was no drug-by-diagnosis interaction evident ($p = 0.12$). There was a negative correlation between plasma ghrelin levels and plasma PYY levels in the placebo condition in the entire sample ($r = -0.2, p < 0.05$).

Ghrelin concentrations in plasma

There were no sequence ($F [1, 47] = 0.08, p = 0.8$) or sequence-by-treatment ($F [1, 46] = 2.31, p = 0.1$) effects on ghrelin plasma concentration, confirming that no carry-over effects were present. Consequently, ghrelin data of both sessions were further examined. Mean plasma levels of ghrelin before and after catecholamine depletion are shown in Fig. 1. The mean ghrelin plasma levels at baseline did not differ between rBN subjects and healthy controls ($t [1, 47] = -1.23, p = 0.2$, Table 1). Catecholamine depletion with AMPT led to significant reductions in plasma ghrelin levels ($F [1, 46] = 8.53, p < 0.006$, Fig. 1) and there was a significant reduction in plasma ghrelin levels in both conditions ($F [1, 46] = 48.81, p < 0.0001$, Fig. 1). There was no effect of diagnosis ($F [1, 47] = 0.18, p = 0.7$) or plasma ghrelin levels and no treatment-by-diagnosis interaction ($F [1, 46] = 0.28, p = 0.6$).

PYY concentrations in plasma

There were no sequence ($F [1, 47] = 0.99, p = 0.3$) or sequence-by-treatment ($F [1, 46] = 0.04, p = 0.8$) effects on PYY plasma concentration, confirming that no carryover effects were present. Consequently, PYY data of both sessions were further examined. Mean plasma levels before and after catecholamine depletion are shown in Fig. 1. Mean PYY plasma levels at baseline did not differ between rBN subjects

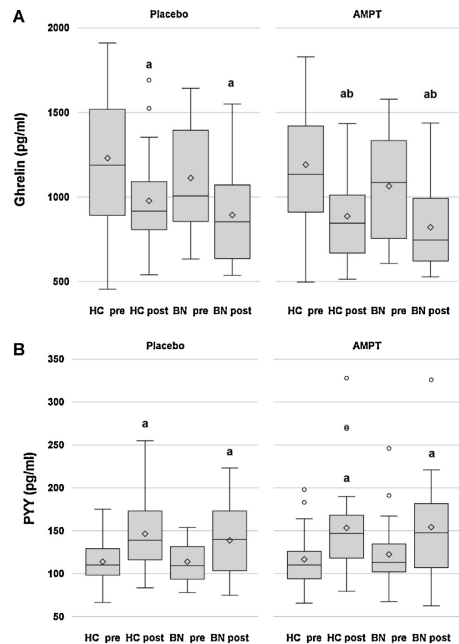


Figure 1 (A) Boxplots of plasma ghrelin concentrations before and after catecholamine depletion in subjects with remitted bulimia nervosa ($n = 20$) and healthy controls ($n = 29$). The first sample was drawn immediately before, the second one within 1 h after eating a regular standardized breakfast. HC pre, healthy controls before treatment; HC post, healthy controls after treatment; BN pre, remitted bulimia nervosa patients before treatment; BN post, remitted bulimia nervosa patients after treatment. a = significant time-effect ($p < 0.0001$). b = significant treatment effect ($p < 0.006$). (B) Boxplots of plasma PYY concentrations before and after catecholamine depletion in subjects with remitted bulimia nervosa ($n = 20$) and healthy controls ($n = 29$). The first sample was drawn immediately before, the second one within 1 h after eating a regular standardized breakfast. HC pre, healthy controls before treatment; HC post, healthy controls after treatment; BN pre, remitted bulimia nervosa patients before treatment; BN post, remitted bulimia nervosa patients after treatment. a = significant time-effect ($p < 0.0001$).

and healthy controls ($t [1, 47] = 0.57, p = 0.6$, Table 1). The plasma PYY levels were not significantly different after catecholamine depletion following AMPT administration ($F [1, 46] = 0.59, p = 0.4$), but there was a significant increase in plasma PYY levels in the second measurement compared to baseline in both conditions ($F [1, 46] = 62.81, p < 0.0001$, Fig. 1). No diagnosis effect ($F [1, 47] = 0.52, p = 0.5$) or treatment-by-diagnosis interaction ($F [1, 46] = 0.02, p = 0.9$) was evident.

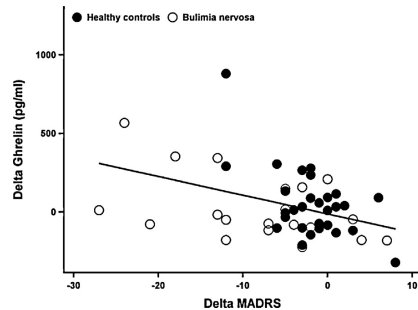


Figure 2 Correlation between the α -methyl-para-tyrosine (AMPT)-induced change in depressive symptoms (MADRS) and the AMPT-induced change in plasma ghrelin concentrations in subjects with remitted bulimia nervosa ($n = 20$) and healthy controls ($n = 29$). The AMPT-induced changes in ghrelin concentrations correlated with the corresponding changes in depressive symptoms rated by the MADRS ($r = -0.41$, $p < 0.004$). The change in ghrelin levels for each subject reflects the difference in the level obtained with AMPT versus that obtained with placebo. The difference between the MADRS score obtained for each subject in the AMPT session and that obtained in the placebo session was calculated to reflect the magnitude of the AMPT-induced effect on depression ratings. MADRS, Montgomery–Åsberg Depression Rating Scale.

Association between AMPT-induced changes in plasma ghrelin and PYY concentrations and behavioral ratings

There was a significant correlation between AMPT-induced changes in plasma ghrelin levels and AMPT-induced changes in depressive symptoms measured with the MADRS ($r = -0.41$, $p < 0.004$, Fig. 2), but there was no correlation between the AMPT-induced change in bulimic symptoms measured using the EDE-Q and the AMPT-induced change in the plasma ghrelin concentrations ($p = 0.4$) or between the AMPT-induced change in the plasma PYY concentrations and the AMPT-induced change in MADRS ($p = 0.2$) and EDE-Q ($p = 0.71$) scores.

Discussion

This is the first study to investigate the effects of catecholamine depletion on plasma ghrelin concentration in individuals with remitted BN and healthy controls. The ghrelin levels decreased in the entire study population after treatment with AMPT compared to placebo. This decrease in ghrelin plasma levels was negatively correlated with the depressive symptoms induced by catecholamine depletion. Plasma ghrelin levels and plasma PYY levels were also negatively correlated. We also observed a significant decrease between preprandial and postprandial plasma ghrelin levels and a significant increase between preprandial and postprandial plasma PYY levels. We did not find a difference

between rBN subjects and healthy controls with regard to ghrelin or PYY response to catecholamine depletion.

The role of ghrelin in depression and anxiety in humans remains to be further clarified (Schellekens et al., 2012). Communication between gut and central nervous system is mediated by a system known as the brain–gut axis, which regulates appetite and satiety and maintains the body's energy homeostasis (Stanley et al., 2005; Suzuki et al., 2010). Dysregulation of the brain–gut axis is associated with metabolic imbalances found in eating disorders as well as in association with stress, anxiety, and depression (Goldbacher and Matthews, 2007; Pallister and Waller, 2008; Swinbourne and Touyz, 2007). Our results confirmed decreased plasma ghrelin levels following catecholamine depletion. This is in line with previous findings suggesting that ghrelin secretion is mediated via catecholaminergic neurotransmission (Mundinger et al., 2006; Zhao et al., 2010). An effect of catecholamines on ghrelin secretion has been shown both *in vitro* (Gagnon and Anini, 2012; Iwakura et al., 2011; Zhao et al., 2010) and *in vivo* (Hosoda and Kangawa, 2008; Zhao et al., 2010). Specifically, depletion of catecholamines with reserpine in the sympathetic nervous system in mice completely blocked plasma ghrelin after a 24-h fast, but did not affect mice that were fed beforehand (Zhao et al., 2010). The aforementioned study also examined the effect of catecholamines on ghrelin-secreting cells *in vitro* and found that addition of norepinephrine or epinephrine to culture medium stimulated ghrelin secretion. This effect was blocked by the selective β -1-adrenergic antagonist atenolol. Thus, it appears possible that elevations in plasma ghrelin induced by fasting are caused by locally released norepinephrine that stimulates ghrelin-secreting cells directly through β 1 receptors (Zhao et al., 2010). Our finding is partly in contrast to a previous study in humans in which morning preprandial ghrelin levels in patients with phenylketonuria, a condition known for decreased catecholamine production, were not different from those of healthy controls (Schulpis et al., 2004). However, that study also found a positive correlation between ghrelin and catecholamine levels across both groups, which is in line with a catecholaminergic influence on ghrelin secretion (Schulpis et al., 2004).

In our study, decreases in plasma ghrelin levels and depressive symptoms after catecholamine depletion were inversely correlated. Altered ghrelin levels and depression have been linked by an increasing amount of evidence. Augmented plasma ghrelin levels were found in mice following chronic defeat stress, and it was suggested that ghrelin might be involved in the defense against stress-induced depression and anxiety (Lutter et al., 2008). Additional findings in rodents have shown that mice spent more time in the open arm of an elevated plus maze and less time immobile during forced swim test following caloric restriction or subcutaneous ghrelin injection, suggesting anxiolytic-like and antidepressant-like effects of elevated plasma ghrelin (Cabral et al., 2012). Furthermore, it has been proposed that ghrelin reduces stress-induced anxiety by stimulating the HPA axis at the anterior pituitary (Spencer et al., 2012). In line with this is the activation of CRH-producing neurons and increased corticotropin-releasing hormone gene expression in the paraventricular nucleus of the hypothalamus following ghrelin administration (Cabral et al., 2012). In addition, administration of ghrelin has previously been

suggested to reverse depressive-like behavior induced by bilateral olfactory bulbectomy in mice (Carlini et al., 2012). Ghrelin infusion into the lateral ventricle in rats produced an anxiolytic-like effect (Isogawa et al., 2005), and inhibition of ghrelin induced an increase in depression-like and anxiety-like behaviors in rats (Kanehisa et al., 2006). In humans, ghrelin involvement in the etiology of depressive disorders has been suggested by a study that demonstrated lower plasma ghrelin levels in depressed patients (Barim et al., 2009). While the correlation between ghrelin and depression has been absent from other studies (Kluge et al., 2009; Schanze et al., 2008), a polymorphism in the ghrelin gene has nevertheless been correlated with depression symptomatology (Nakashima et al., 2008), and antidepressant effects following ghrelin administration have been reported in patients with major depression (Kluge et al., 2011).

The decrease between preprandial and postprandial plasma ghrelin levels in our study is consistent with the literature (Cummings et al., 2001; LeSauter et al., 2009; Nass et al., 2008; Small and Bloom, 2004). The preprandial rise and postprandial fall in plasma ghrelin levels gives further evidence for the suggested role that ghrelin plays in meal initiation (Cummings et al., 2001). In addition, previous research showed that ghrelin samples drawn before and after breakfast correlated strongly with 24-h integrated area under the curve values, suggesting that two measurements might serve as surrogates for 24-h profiles to estimate overall ghrelin levels (Cummings et al., 2001).

Contrary to our hypothesis, there was no difference in plasma ghrelin levels between study participants with BN and healthy controls. However, previous studies that have reported elevated baseline ghrelin concentrations in BN have been highly heterogeneous with respect to the study design and did not include findings for subjects in remission from BN (Prince et al., 2009).

In addition, in the present study, there was no measured effect of AMPT on plasma PYY levels. The effects of catecholamines and of adrenergic agonists on PYY secretion have been well documented (Plaisancie et al., 1995; Walsh, 1994), so the lack of an AMPT effect on PYY in the current study was somewhat surprising. However, we did find a postprandial rise of plasma PYY levels which is consistent with previous research. Plasma PYY concentrations increase following a meal (Hellstrom et al., 2004), and PYY has therefore been considered as a meal terminator opposed to ghrelin in the digestive behavior (Zwirska-Korczala et al., 2007). In line with this, we also found that plasma PYY levels were inversely correlated with plasma ghrelin levels. However, this correlation was evident in the placebo condition only, which might be explained by the fact that AMPT had an effect on plasma ghrelin levels but not on plasma PYY levels. Ghrelin concentrations are generally negatively correlated with levels of leptin, which, like PYY, is a peptide hormone connected with the signaling of satiety (Camina et al., 2003). In addition, a negative interaction between PYY and ghrelin has been suggested at the level of vagal afferents of the hypothalamus (Konturek et al., 2004). In support of this possibility, PYY infusion significantly decreased plasma ghrelin levels (Batterham et al., 2003) and a negative correlation of PYY with ghrelin has been reported by Kojima et al. (2005).

Some limitations of the present study should be noted. We did not reliably assess the phase of the menstrual cycle in our participants, and subjects were tested in both the follicular and luteal phases, which may represent a potentially confounding factor. However, previous research has not documented effects of the menstrual cycle on AMPT-induced symptoms (Hasler et al., 2008). Next, it is important to be careful about attributing causality when interpreting correlations between AMPT-induced depression and AMPT-induced changes in plasma ghrelin levels. In particular, there was no indication as to whether depression caused changes in ghrelin levels, changes in ghrelin levels caused depression, or whether they were associated, because both were induced by catecholamine depletion. Finally, the specificity of our results was limited by the AMPT effects of reducing synthesis of norepinephrine as well as dopamine.

In conclusion, the present study has demonstrated an AMPT-induced decrease in plasma ghrelin levels that was negatively correlated with depressive symptoms. These findings give further evidence for a catecholamine-related involvement of ghrelin in the modulation of mood. Future studies should be aimed at continuing investigation of the neuronal substrates of mood modulation through ghrelin.

Role of funding source

This research was supported by the Swiss National Science Foundation Nr. 32003B-117763.

Conflict of interest

None declared.

Acknowledgment

We are grateful to Kurt Laederach for valuable comments on the manuscript.

References

- Barim, A.O., Aydin, S., Colak, R., Dag, E., Deniz, O., Sahin, I., 2009. Ghrelin, paraoxonase and arylesterase levels in depressive patients before and after citalopram treatment. *Clin. Biochem.* 42, 1076–1081.
- Batterham, R.L., Cohen, M.A., Ellis, S.M., Le Roux, C.W., Withers, D.J., Frost, G.S., Ghatei, M.A., Bloom, S.R., 2003. Inhibition of food intake in obese subjects by peptide YY3-36. *N. Engl. J. Med.* 349, 941–948.
- Batterham, R.L., Heffron, H., Kapoor, S., Chivers, J.E., Chandarana, K., Herzog, H., Le Roux, C.W., Thomas, E.L., Bell, J.D., Withers, D.J., 2006. Critical role for peptide YY in protein-mediated satiation and body-weight regulation. *Cell Metab.* 4, 223–233.
- Berman, R.M., Narasimhan, M., Miller, H.L., Anand, A., Cappiello, A., Oren, D.A., Heninger, G.R., Charney, D.S., 1999. Transient depressive relapse induced by catecholamine depletion: potential phenotypic vulnerability marker? *Arch. Gen. Psychiatry* 56, 395–403.
- Cabral, A., Suescun, O., Zigman, J.M., Perello, M., 2012. Ghrelin indirectly activates hypophysiotropic CRF neurons in rodents. *PLoS One* 7, e31462.
- Camina, J.P., Carreira, M.C., Micic, D., Pombo, M., Kelestimur, F., Dieguez, C., Casanueva, F.F., 2003. Regulation of ghrelin secretion and action. *Endocrine* 22, 5–12.

- Carlini, V.P., Machado, D.G., Buteler, F., Ghersi, M., Ponzio, M.F., Martini, A.C., Schiotti, H.B., de Cuneo, M.F., Rodrigues, A.L., de Bariglio, S.R., 2012. Acute ghrelin administration reverses depressive-like behavior induced by bilateral olfactory bulbectomy in mice. *Peptides* 35, 160–165.
- Cummings, D.E., Purnell, J.Q., Frayo, R.S., Schmidova, K., Wisse, B.E., Weigle, D.S., 2001. A preprandial rise in plasma ghrelin levels suggests a role in meal initiation in humans. *Diabetes* 50, 1714–1719.
- Devlin, M.J., Kissileff, H.R., Zimmerli, E.J., Samuels, F., Chen, B.E., Brown, A.J., Geliebter, A., Walsh, B.T., 2012. Gastric emptying and symptoms of bulimia nervosa: effect of a prokinetic agent. *Physiol. Behav.* 106, 238–242.
- Gagnon, J., Anini, Y., 2012. Insulin and norepinephrine regulate ghrelin secretion from a rat primary stomach cell culture. *Endocrinology* 153, 3646–3656.
- Goldbacher, E.M., Matthews, K.A., 2007. Are psychological characteristics related to risk of the metabolic syndrome? A review of the literature. *Ann. Behav. Med.* 34, 240–252.
- Grob, S., Pizzagalli, D.A., Dutra, S.J., Stern, J., Morgeli, H., Milos, G., Schnyder, U., Hasler, G., 2012. Dopamine-related deficit in reward learning after catecholamine depletion in unmedicated, remitted subjects with bulimia nervosa. *Neuropsychopharmacology* 37, 1945–1952.
- Guan, X.M., Yu, H., Palyha, O.C., McKee, K.K., Feighner, S.D., Sirinathsinghji, D.J., Smith, R.G., Van der Ploeg, L.H., Howard, A.D., 1997. Distribution of mRNA encoding the growth hormone secretagogue receptor in brain and peripheral tissues. *Brain Res. Mol. Brain Res.* 48, 23–29.
- Hasler, G., Fromm, S., Carlson, P.J., Luckenbaugh, D.A., Waldeck, T., Geraci, M., Roiser, J.P., Neumeister, A., Meyers, N., Charney, D.S., Drevets, W.C., 2008. Neural response to catecholamine depletion in unmedicated subjects with major depressive disorder in remission and healthy subjects. *Arch. Gen. Psychiatry* 65, 521–531.
- Hellstrom, P.M., Geliebter, A., Naslund, E., Schmidt, P.T., Yahav, E.K., Hashim, S.A., Yeomans, M.R., 2004. Peripheral and central signals in the control of eating in normal, obese and binge-eating human subjects. *Br. J. Nutr.* 92 (Suppl 1), S47–S57.
- Hilbert, A., Tuschen-Caffier, B., 2006. Eating Disorder Examination. Verlag für Psychotherapie, Münster.
- Hosoda, H., Kangawa, K., 2008. The autonomic nervous system regulates gastric ghrelin secretion in rats. *Regul. Pept.* 146, 12–18.
- Isogawa, K., Fujiki, M., Akiyoshi, J., Tsutsumi, T., Kodama, K., Matsushita, H., Tanaka, Y., Kobayashi, H., 2005. Anxiolytic suppression of repetitive transcranial magnetic stimulation-induced anxiety in the rats. *Prog. Neuropsychopharmacol. Biol. Psychiatry* 29, 664–668.
- Iwakura, H., Ariyasu, H., Hosoda, H., Yamada, G., Hosoda, K., Nakao, K., Kangawa, K., Akamizu, T., 2011. Oxytocin and dopamine stimulate ghrelin secretion by the ghrelin-producing cell line, MGN3-1 in vitro. *Endocrinology* 152, 2619–2625.
- Kanehisa, M., Akiyoshi, J., Kitaiuchi, T., Matsushita, H., Tanaka, E., Kodama, K., Hanada, H., Isogawa, K., 2006. Administration of antisense DNA for ghrelin causes an antidepressant and anxiolytic response in rats. *Prog. Neuropsychopharmacol. Biol. Psychiatry* 30, 1403–1407.
- Karra, E., Batterham, R.L., 2010. The role of gut hormones in the regulation of body weight and energy homeostasis. *Mol. Cell. Endocrinol.* 316, 120–128.
- Kluge, M., Schüssler, P., Dresler, M., Schmidt, D., Yassouridis, A., Uhr, M., Steiger, A., 2011. Effects of ghrelin on psychopathology, sleep and secretion of cortisol and growth hormone in patients with major depression. *J. Psychiatr. Res.* 45, 421–426.
- Kluge, M., Schüssler, P., Schmid, D., Uhr, M., Kleyer, S., Yassouridis, A., Steiger, A., 2009. Ghrelin plasma levels are not altered in major depression. *Neuropsychobiology* 59, 199–204.
- Kojima, S., Nakahara, T., Nagai, N., Muranaga, T., Tanaka, M., Yasuhara, D., Masuda, A., Date, Y., Ueno, H., Nakazato, M., Naruo, T., 2005. Altered ghrelin and peptide YY responses to meals in bulimia nervosa. *Clin. Endocrinol. (Oxf.)* 62, 74–78.
- Konturek, S.J., Konturek, J.W., Pawlik, T., Brzozowski, T., 2004. Brain-gut axis and its role in the control of food intake. *J. Physiol. Pharmacol.* 55, 137–154.
- LeSauter, J., Hoque, N., Weintraub, M., Pfaff, D.W., Silver, R., 2009. Stomach ghrelin-secreting cells as food-entrainable circadian clocks. *Proc. Natl. Acad. Sci. U. S. A.* 106, 13582–13587.
- Lutter, M., Sakata, I., Osborne-Lawrence, S., Rovinsky, S.A., Anderson, J.G., Jung, S., Birnbaum, S., Yanagisawa, M., Elmquist, J.K., Nestler, E.J., Zigman, J.M., 2008. The orexigenic hormone ghrelin defends against depressive symptoms of chronic stress. *Nat. Neurosci.* 11, 752–753.
- Miller, H.L., Delgado, P.L., Salomon, R.M., Heninger, G.R., Charney, D.S., 1996. Effects of alpha-methyl-para-tyrosine (AMPT) in drug-free depressed patients. *Neuropsychopharmacology* 14, 151–157.
- Monteleone, P., Martiadis, V., Fabrazzo, M., Serritella, C., Maj, M., 2003. Ghrelin and leptin responses to food ingestion in bulimia nervosa: implications for binge-eating and compensatory behaviours. *Psychol. Med.* 33, 1387–1394.
- Monteleone, P., Martiadis, V., Rigamonti, A.E., Fabrazzo, M., Giordani, C., Muller, E.E., Maj, M., 2005. Investigation of peptide YY and ghrelin responses to a test meal in bulimia nervosa. *Biol. Psychiatry* 57, 926–931.
- Monteleone, P., Serritella, C., Martiadis, V., Scognamiglio, P., Maj, M., 2008. Plasma obestatin, ghrelin, and ghrelin/obestatin ratio are increased in underweight patients with anorexia nervosa but not in symptomatic patients with bulimia nervosa. *J. Clin. Endocrinol. Metab.* 93, 4418–4421.
- Mundinger, T.O., Cummings, D.E., Taborsky Jr., G.J., 2006. Direct stimulation of ghrelin secretion by sympathetic nerves. *Endocrinology* 147, 2893–2901.
- Murphy, K.G., Bloom, S.R., 2006. Gut hormones and the regulation of energy homeostasis. *Nature* 444, 854–859.
- Nagatsu, T., Levitt, M., Udenfriend, S., 1964. Tyrosine hydroxylase. The initial step in norepinephrine biosynthesis. *J. Biol. Chem.* 239, 2910–2917.
- Nakashima, K., Akiyoshi, J., Hatano, K., Hanada, H., Tanaka, Y., Tsuru, J., Matsushita, H., Kodama, K., Isogawa, K., 2008. Ghrelin gene polymorphism is associated with depression, but not panic disorder. *Psychiatr. Genet.* 18, 257.
- Nass, R., Farhy, L.S., Liu, J., Prudom, C.E., Johnson, M.L., Veldhuis, P., Pezzoli, S.S., Oliveri, M.C., Gaylinn, B.D., Geysen, H.M., Thorner, M.O., 2008. Evidence for acyl-ghrelin modulation of growth hormone release in the fed state. *J. Clin. Endocrinol. Metab.* 93, 1988–1994.
- Nestler, E.J., Carlezon Jr., W.A., 2006. The mesolimbic dopamine reward circuit in depression. *Biol. Psychiatry* 59, 1151–1159.
- Pallister, E., Waller, G., 2008. Anxiety in the eating disorders: understanding the overlap. *Clin. Psychol. Rev.* 28, 366–386.
- Plaisancie, P., Bernard, C., Chayvialle, J.A., Cuber, J.C., 1995. Release of peptide YY by neurotransmitters and gut hormones in the isolated, vascularly perfused rat colon. *Scand. J. Gastroenterol.* 30, 568–574.
- Prince, A.C., Brooks, S.J., Stahl, D., Treasure, J., 2009. Systematic review and meta-analysis of the baseline concentrations and physiologic responses of gut hormones to food in eating disorders. *Am. J. Clin. Nutr.* 89, 755–765.
- Schanze, A., Reulbach, U., Scheuchenzuber, M., Groschl, M., Kornhuber, J., Kraus, T., 2008. Ghrelin and eating disturbances in psychiatric disorders. *Neuropsychobiology* 57, 126–130.
- Schellekens, H., Finger, B.C., Dinan, T.G., Cryan, J.F., 2012. Ghrelin signalling and obesity: at the interface of stress, mood and food reward. *Pharmacol. Ther.* 135, 316–326.

- Schulpis, K.H., Papassotiriou, I., Vounatsou, M., Karikas, G.A., Tsakiris, S., Chrousos, G.P., 2004. Morning preprandial plasma ghrelin and catecholamine concentrations in patients with phenylketonuria and normal controls: evidence for catecholamine-mediated ghrelin regulation. *J. Clin. Endocrinol. Metab.* **89**, 3983–3987.
- Small, C.J., Bloom, S.R., 2004. Gut hormones and the control of appetite. *Trends Endocrinol. Metab.* **15**, 259–263.
- Spencer, S.J., Xu, L., Clarke, M.A., Lemus, M., Reichenbach, A., Geenen, B., Kozicic, T., Andrews, Z.B., 2012. Ghrelin regulates the hypothalamic-pituitary-adrenal axis and restricts anxiety after acute stress. *Biol. Psychiatry* **72**, 457–465.
- Stanley, S., Wynne, K., McGowan, B., Bloom, S., 2005. Hormonal regulation of food intake. *Physiol. Rev.* **85**, 1131–1158.
- Stine, S.M., Krystal, J.H., Petrakis, I.L., Jatlow, P.I., Heninger, G.R., Kosten, T.R., Charney, D.S., 1997. Effect of alpha-methyl-para-tyrosine on response to cocaine challenge. *Biol. Psychiatry* **42**, 181–190.
- Sullivan, R.M., Dufresne, M.M., 2006. Mesocortical dopamine and HPA axis regulation: role of laterality and early environment. *Brain Res.* **1076**, 49–59.
- Suzuki, K., Simpson, K.A., Minnion, J.S., Shillito, J.C., Bloom, S.R., 2010. The role of gut hormones and the hypothalamus in appetite regulation. *Endocr. J.* **57**, 359–372.
- Swinbourne, J.M., Touyz, S.W., 2007. The co-morbidity of eating disorders and anxiety disorders: a review. *Eur. Eat. Disord. Rev.* **15**, 253–274.
- Tanaka, M., Naruo, T., Muranaga, T., Yasuhara, D., Shiiya, T., Nakazato, M., Matsukura, S., Nozoe, S., 2002. Increased fasting plasma ghrelin levels in patients with bulimia nervosa. *Eur. J. Endocrinol.* **146**, R1–R3.
- Tanaka, M., Naruo, T., Nagai, N., Kuroki, N., Shiiya, T., Nakazato, M., Matsukura, S., Nozoe, S., 2003. Habitual binge/purge behavior influences circulating ghrelin levels in eating disorders. *J. Psychiatr. Res.* **37**, 17–22.
- Troisi, A., Di Lorenzo, G., Lega, I., Tesauro, M., Bertoli, A., Leo, R., Iantorno, M., Pecchioli, C., Rizza, S., Turriziani, M., Lauro, R., Siracusano, A., 2005. Plasma ghrelin in anorexia, bulimia, and binge-eating disorder: relations with eating patterns and circulating concentrations of cortisol and thyroid hormones. *Neuroendocrinology* **81**, 259–266.
- Verhoeff, N.P., Christensen, B.K., Hussey, D., Lee, M., Papatheodorou, G., Kopala, L., Rui, Q., Zipursky, R.B., Kapur, S., 2003. Effects of catecholamine depletion on D2 receptor binding, mood, and attentiveness in humans: a replication study. *Pharmacol. Biochem. Behav.* **74**, 425–432.
- Walsh, J.H., 1994. *Physiology of the Gastrointestinal Tract*. Raven Press, New York.
- Zhao, T.J., Sakata, I., Li, R.L., Liang, G., Richardson, J.A., Brown, M.S., Goldstein, J.L., Zigman, J.M., 2010. Ghrelin secretion stimulated by β 1-adrenergic receptors in cultured ghrelinoma cells and in fasted mice. *Proc. Natl. Acad. Sci. U. S. A.* **107**, 15868–15873.
- Zigman, J.M., Jones, J.E., Lee, C.E., Saper, C.B., Elmquist, J.K., 2006. Expression of ghrelin receptor mRNA in the rat and the mouse brain. *J. Comp. Neurol.* **494**, 528–548.
- Zwirska-Korczala, K., Konturek, S.J., Sodowski, M., Wylezol, M., Kuka, D., Sowa, P., Adamczyk-Sowa, M., Kukla, M., Berdowska, A., Rehfeld, J.F., Bielanski, W., Brzozowski, T., 2007. Basal and postprandial plasma levels of PYY, ghrelin, cholecystokinin, gastrin and insulin in women with moderate and morbid obesity and metabolic syndrome. *J. Physiol. Pharmacol.* **58** (Suppl. 1), 13–35.



Magnetic resonance spectroscopy investigations of functionally defined language areas in schizophrenia patients with and without auditory hallucinations



Philipp Homan ^{a,1}, Peter Vermathen ^{b,1}, Claudia Van Swam ^a, Andrea Federspiel ^a, Chris Boesch ^b, Werner Strik ^c, Thomas Dierks ^{a,*}, Daniela Hubl ^a, Roland Kreis ^b

^a Department of Psychiatric Neurophysiology, University Hospital of Psychiatry, University of Bern, Switzerland

^b Unit for Magnetic Resonance Spectroscopy and Methodology, Department of Clinical Research and Institute of Diagnostic, Interventional and Pediatric Radiology, University of Bern, Switzerland

^c University Hospital of Psychiatry, University of Bern, Switzerland

ARTICLE INFO

Article history:

Accepted 8 March 2014

Available online 17 March 2014

Keywords:

Magnetic resonance spectroscopy

N-acetyl-aspartate

Myo-inositol

Schizophrenia

Auditory hallucinations

Language

ABSTRACT

Background: Cerebral dysfunction occurring in mental disorders can show metabolic disturbances which are limited to circumscribed brain areas. Auditory hallucinations have been shown to be related to defined cortical areas linked to specific language functions. Here, we investigated if the study of metabolic changes in auditory hallucinations requires a functional rather than an anatomical definition of their location and size to allow a reliable investigation by magnetic resonance spectroscopy (MRS).

Methods: Schizophrenia patients with (AH; n = 12) and without hallucinations (NH; n = 8) and healthy controls (HC; n = 11) underwent a verbal fluency task in functional MRI (fMRI) to functionally define Broca's and Wernicke's areas. Left and right Heschl's gyri were defined anatomically.

Results: The mean distances in native space between the fMRI-defined regions and a corresponding anatomically defined area were 12.4 ± 6.1 mm (range: 2.7–36.1 mm) for Broca's area and 16.8 ± 6.2 mm (range: 4.5–26.4 mm) for Wernicke's area, respectively. Hence, the spatial variance was of similar extent as the size of the investigated regions. Splitting the investigations into a single voxel examination in the frontal brain and a spectroscopic imaging part for the more homogeneous field areas led to good spectral quality for almost all spectra. In Broca's area, there was a significant group effect ($p = 0.03$) with lower levels of N-acetyl-aspartate (NAA) in NH compared to HC ($p = 0.02$). There were positive associations of NAA levels in the left Heschl's gyrus with total ($p = 0.03$) and negative ($p = 0.006$) PANSS scores. In Broca's area, there was a negative association of myo-inositol levels with total PANSS scores ($p = 0.008$).

Conclusion: This study supports the neurodegenerative hypothesis of schizophrenia only in a frontal region whereas the results obtained from temporal regions are in contrast to the majority of previous studies. Future research should test the hypothesis raised by this study that a functional definition of language regions is needed if neurochemical imbalances are expected to be restricted to functional foci.

© 2014 Elsevier Inc. All rights reserved.

Introduction

¹H Magnetic Resonance Spectroscopy (MRS) has been used in clinical and research investigations of human brain physiology and pathology for over two decades (Barker et al., 2009). Since it is currently not possible to acquire whole brain MRS measurements with high spatial resolution in a timeframe that is endurable for (living) subjects, regions of interest (ROIs) are commonly defined. Most often, the region

to be examined is chosen based on pathological structural abnormalities or in extended brain areas presumed to be involved in the targeted patho-physiologic processes. In both cases, the region of interest (ROI) is chosen using anatomic landmarks. However, from functional brain studies it is well known that besides substantial individuality of cortical morphology (Ono et al., 1990; Uylings et al., 2005), there is considerable interindividual variability in terms of the exact location of cortical activation for specific brain functions (E.A. Allen et al., 2012; Burton et al., 2001; Fedorenko et al., 2010; Xiong et al., 2000). Hence, if metabolic disturbances are hypothesized to be restricted to or most expressed in limited areas representing specific brain function, the ROIs for MRS investigations have to be defined functionally in each subject. Furthermore, because most MRS studies use either single voxel (SV) localization techniques or spectroscopic imaging (SI) of single

* Corresponding author at: Department of Psychiatric Neurophysiology, University Hospital of Psychiatry, Bolligenstrasse 111, CH-3000 Bern 60, Switzerland. Fax: +41 31 9308961.

E-mail address: dierks@puk.unibe.ch (T. Dierks).

¹ These two authors contributed equally to this work.

slices where the ROIs must be known and defined at the time of data acquisition, the functional definition of the ROI must usually precede MRS. Alternatively, spectroscopic whole brain analyses by multislice or 3D techniques (Maudsley et al., 2006), where ROIs can be chosen during data analysis, could be performed without knowledge of the exact region to be targeted, but these techniques are usually not considered to be as reliable and not as time-efficient for small focused ROIs, in particular when using short echo times. Since previous studies have shown dysfunctions in circumscribed cerebral areas related to the language system we investigated auditory verbal hallucinations (AVH) as a potential case of local limited metabolic imbalance.

It is well known that AVH comprise a critical domain in schizophrenia, including a low quality of life since about 30% of patients do not sufficiently respond to medication (Copolov et al., 2004; Shergill et al., 1998). Notably, 25% of patients with AVH had made serious suicide attempts driven by their voices (Hor and Taylor, 2010). Thus, a better understanding of the neural underpinnings of AVH might contribute to a better treatment regime (Homan et al., 2011; Kindler et al., 2013). However, an obstacle of a more sophisticated understanding of AVH lies in the complexity of the process possibly including anatomical, functional and neurochemical aspects and the corresponding complexity of investigation approaches. Several imaging studies found an association of speech- and language related cerebral regions and AVH. In an early functional magnetic resonance imaging (fMRI) study we showed that the cerebral activity in the primary auditory cortex during the experience of internal voices is comparable to the activation caused by external auditory stimuli (Dierks et al., 1999). We propose that this dysfunctional activity may account for the belief of externality of the voices the patients hear, which may be further supported by the measurement of auditory evoked potentials in EEG, where we found higher EEG activity in left temporal regions and lower AEP amplitudes during AVH compared to phases without AVH (Hubl et al., 2007). Thus, we suggested that pre-activation of the primary auditory cortex competes for processing resources with the external stimuli (Hubl et al., 2007) and that these alterations might be the microstructural basis responsible for the dysfunctional primary auditory cortex activity. A processing failure in Wernicke's area may promote a disturbed feedback loop reflected in altered connectivity of Broca's and Wernicke's areas (Hubl et al., 2004) and a pathological activation of Heschl's gyrus.

However, EEG and MRI cannot assess the molecular basis of schizophrenia and psychotic symptoms, and our understanding of the molecular changes in schizophrenia is essentially based on the observed effects of psychoactive drugs. MRS offers a tool to measure neurochemical alterations, here with respect to AVH.

With MRS, the chemical composition of cerebral tissue is determined non-invasively by measuring the magnetic resonance signal of hydrogen in specific metabolites (Barker et al., 2009; Jansen et al., 2006). The metabolite N-acetyl-aspartate (NAA) is considered a marker of neuronal viability and/or integrity. NAA concentrations are reduced in affected areas in neurodegenerative diseases (Adalsteinsson et al., 2000) and correlate with cognitive performance (Jung et al., 1999). With respect to schizophrenia, MRS may allow to disentangle the meaning of white matter and gray matter volume reductions which may stand for neuronal loss or dysfunction (Abbott and Bustillo, 2006). Although there are inconsistencies in the literature (Steen et al., 2005), most previous research found that in schizophrenia NAA is decreased in frontal and temporal regions and in the thalamus (Brugge et al., 2011). NAA concentrations in the thalamus and the duration of positive symptoms were negatively correlated in schizophrenia patients (Theberge et al., 2003). Martinez-Granados et al. (2008) found a decreased ratio of NAA to choline ratio in the thalamus of schizophrenia patients compared to healthy controls and in the right thalamus of hallucinating patients compared to not hallucinating patients and controls. In addition, hippocampal NAA levels have been reported to be decreased in hallucinating patients (Heckers, 2001).

The metabolite myo-inositol (ml) has been shown to be present in glial but not neuronal cells in vitro (Brand et al., 1993) and since gliosis may lead to increased ml concentrations, ml has been found to be increased in neurodegenerative diseases such as Alzheimer's disease (Miller et al., 1993). With respect to schizophrenia, an increase in ml concentrations compared to healthy controls would be compatible with the neurodegenerative hypothesis but has not been found as of yet (Delamilleure et al., 2002). Instead, most studies have shown that ml levels in schizophrenia are largely unaltered (as reviewed in Schwerk et al., 2014). In addition, there do not seem to be any published investigations into potential relations of ml content and presence of AVH, so investigations of this metabolite in AVH can be done only in an exploratory fashion.

In the current study, we used a verbal fluency (VF) task in fMRI to functionally define speech related ROIs (Broca's and Wernicke's areas) in each subject for a subsequent neurochemical analysis with MRS in two patient groups (AH: schizophrenia patients with AVH; NH: schizophrenia patients without AVH for the last 12 months) and a healthy control group (HC). In addition, left and right Heschl's gyri (HG) were defined anatomically. Thus, the four target ROIs for MRS were Broca's and Wernicke's areas (both on the left side) and left and right HG. Since Broca's area lies in the frontal part of the brain, where optimizing the magnetic field homogeneity is challenging, but the other 3 areas are in relative proximity with less stringent difficulties for field homogenization, the MRS signal acquisition was split into two parts. First, Broca's area was investigated by single voxel MRS, then the other 3 ROIs were examined by SI of a single slice, the position and orientation of which were defined by these 3 ROIs.

In accordance with previous findings of NAA being decreased in schizophrenia in frontal and temporal regions and in the thalamus (Brugge et al., 2011; Martinez-Granados et al., 2008), we hypothesized to find a relative reduction of NAA in the functionally defined Wernicke's area in hallucinating schizophrenia patients compared to patients without hallucinations and controls. In an additional exploratory analysis, we tested for metabolic changes in further metabolites, like ml, choline (Cho) and glutamate (Glu) or glutamate plus glutamine (Glx).

Methods and materials

Participants

The investigation was conducted in accordance with the Declaration of Helsinki and approved by the local ethics committee (Kantonale Ethikkommission Bern). To ensure informed consent, the investigator explained the aims and procedure of the study to the potential subject verbally, providing all important information. Then the potential subject was given written instructions as well as time to ask any questions. Only then the decision whether or not to participate in the study was made, and subjects provided written consent to participate in the study.

Three groups were investigated in the current study: AH ($n = 12$), NH ($n = 8$), and HC ($n = 11$). General inclusion criteria for patients were: aged between 25 and 50 years, right handedness, ICD-10 diagnostic criteria for schizophrenia or schizo-affective disorder, a history for schizophrenia of more than 5 years, no substance use other than nicotine, and the ability to give written informed consent. AH could but did not have to perceive AVH at the time of the measurement. According to their anamnesis (patients' files and clinical interview) these patients perceived AVH in most of their acute exacerbations (90%). NH did not experience AVH at the time of investigation nor in the previous 12 months and did not perceive AVH in most of their exacerbations (less than 10%). Individual psychopathology was assessed in a clinical interview involving the assessment of the Positive and Negative Syndrome Scale (PANSS) (Kay et al., 1987). All 3 groups were age- and gender-matched. Inclusion criteria for HC were: no current or previous neurological or psychiatric disorder, no severe somatic-medical disorder, no substance use other than nicotine, the ability to give written

informed consent, and – valid for all subjects – no contraindications for MRI.

Statistical analysis of behavioral data

PANSS scores were compared between AH and NH using two-sample t-tests. In addition, positive symptoms within the PANSS scores were compared using two-sample t-tests. The statistical threshold for these contrasts was set at $p < 0.05$, two-tailed. SAS 9.2 (SAS Institute Inc., Cary, NC, USA) was used for all analyses. The means of the data are reported with their standard deviations.

MRI examinations

All examinations were performed at 3 T on a Siemens Trio scanner using a 12-channel receive head coil. MRI included multiple quick localizer images to check for gross patient motion, and the manufacturer's auto-align procedure (referencing the individual brain to a prescription in an atlas brain) was used to ensure consistency in scan prescription (used primarily for slice orientations in MRI). For blood oxygen level dependent (BOLD)-sensitive functional MRI (fMRI), thirty-five axial slices (slice thickness = 3 mm, interslice distance = 0.75 mm), parallel to the plane crossing the anterior and posterior commissures (AC/PC) and covering the whole supratentorial brain, were acquired with a 2D echo planar imaging sequence (repetition time/echo time [TR/TE] = 2.66 s/30 ms, flip angle [FA] = 90°, field of view [FOV] = 192 × 192 mm², matrix = 64 × 64, voxel size = 3 × 3 × 3 mm³, with 0.75 mm gap between slices). 80 scans were measured. For morphologic evaluation and brain segmentation, a 3-D gradient echo sequence (mdeft (Kay et al., 1987), TR/TE/TI 7.92 ms/2.48 ms/910 ms, FA 16°) was measured initially providing 176 sagittal slices with a nominal 1 mm³ voxel size, 256 mm × 224 mm field of view (FoV) and a matrix size of 256 × 192 pixel resolution.

fMRI task and analysis

Prior to MRS, but in the same session all subjects performed a VF language task that has been shown to reliably activate Wernicke's and Broca's areas (Fig. 1). During the scan, subjects were exposed to visual stimuli on an LCD-Monitor eyeglass (Resonance Technology, Inc., Northridge, USA). Conditions alternated between a rest (R) and a VF condition, each lasting 30 s. The task started with the R-condition (gray screen with a fixation cross). In the VF condition, a letter was displayed and subjects were instructed to silently produce as many verbs starting with the shown letter.

At the scanner console, a one-sample t-test was computed after motion correction to reveal brain regions that were significantly activated during the VF-blocks compared to the R-blocks. The resulting statistical parametric maps were used to identify Broca's area (left side) and Wernicke's area (left side) for the MRS scan in each subject individually. Left and right HG were anatomically identified in each subject. We used the stringent criterion of $p < 0.001$ (uncorrected) for the threshold value. However, we decreased the threshold to $p < 0.01$ in subjects where not enough activity was present near the expected ROI.

Offline MRI and fMRI data analysis was realized using Matlab (Matlab version 7, release 2010b; The MathWorks, Inc., Natick, MA, USA), SPM8 (Wellcome Trust Centre for Imaging, London, England; www.fil.ion.ucl.ac.uk/spm8), and the toolbox aslm (Homan et al., 2012).

Post-hoc preprocessing of the images included slice-scan time correction, removing low-frequency drifts, 3-D motion detection, and spatial smoothing with a Gaussian Kernel (8-mm full width at half maximum, FWHM). Co-registration of the 2-D functional to the 3-D structural images was performed. The anatomical and functional data sets were then transformed into normalized MNI space. Each subject's individual stimulation condition was modeled by a boxcar function that was convolved with a double gamma hemodynamic response

function to create the design matrix for the general linear model (GLM). The design matrix included motion parameters as covariates. A contrast was computed by calculating a one-sample t-test on the difference between VF-predictors and R-predictors. The statistical threshold for these analyses was set at a cluster-level threshold of $p < 0.05$, whole-brain corrected for familywise error.

ROI placement: interindividual differences in location of activation

To document interindividual variation of the activation areas and to test whether a functional definition of Broca's and Wernicke's areas had indeed been necessary, activation foci were determined in each subject in postprocessing and compared to the coordinates of a likely anatomically prescribed ROI (pars opercularis and pars triangularis of the left inferior frontal gyrus for Broca's area and the posterior section of the left superior temporal gyrus for Wernicke's area) in native space. However from these areas no MRS data were acquired except if these overlapped with the functional definition.

MRS data acquisition

SV MRS using an optimized implementation of short TE Point-RESolved Spectroscopy (PRESS) (Bottomley, 1984) was performed in the frontal lobe centered in the functionally defined Broca's area (TE 22 ms, TR 3 s, 16 step phase rotation, single slice outer volume suppression, 128 scans, 14 × 14 × 14 mm³, 2000 Hz bandwidth, 2048 time points, water presaturation; a minimum TE of 22 ms realized by using a shorter excitation pulse and shorter but stronger gradient pulses compared with the product PRESS sequence that allowed a minimum TE of 30 ms). If the functionally defined ROI happened to lie very close to the skull, the ROI for SV MRS was rotated and moved slightly away from the skull such as to best avoid subcutaneous lipids, but to still include the fMRI-proven active area. In addition, to optimize spectral quality for this ROI close to the skull, it was important to set the transmit frequency at the center of the spectrum (2.5 ppm, preventing unnecessarily large relative chemical shift induced shifts of the excited ROI), to use a B1 map in order to use proper flip angles with best ROI profiles and to verify that the gradient polarity of the slice-selective pulses was such that the effective ROI for lipid resonances was shifted away from the skull.

2D short TE PRESS SI (TE 30 ms, TR 1.7 s, 12 outer volume suppression slices, 4 averages, weighted acquisition, matrix 20 × 20 with circular k-space sampling, FOV 160 mm, thickness 15 mm, individually adjusted volume, 1200 Hz bandwidth, 1024 time points, water presaturation) was used to obtain spectra from Wernicke's area, and the left and right HG. The plane prescription parameters were calculated from the coordinates of these three ROIs obtained from the anatomic and functional maps. Fast spin echo MRIs were obtained coplanar and orthogonal to the SI slice to individually define the size of the localization area, including the ROIs with extra space to prevent edge effects in excitation, and to place four outer volume saturation slices to prevent fold in of lipid signals from subcutaneous fat.

MRS data processing

SV data was processed using jMRUI (Stefan et al., 2009) version 5.0. Individually stored acquisitions were averaged and the residual water signal was removed by Henkel Lankos Singular Value Decomposition (HSVD) before modeling with QUEST (Ratiney et al., 2004). The following metabolites were included as basis spectra obtained from spectral simulation also using jMRUI (NMRscopeA, pulse sequence with ideal RF pulses assumed): NAA, Ch (as 1:2 mixture of phosphocholine:glycerophosphocholine), Cr (as 1:1 mixture of creatine and phosphocreatine), mI, Glu, glutamine, aspartate, glutathione, and taurine. In addition, an experimental macromolecule baseline, obtained with metabolite nulling in GM, was included to model the baseline. Details



Fig. 1. Functional activity from a verbal fluency task overlaid on axial and coronal views of structural images as determined in 2 schizophrenia patients with AVH. The spatial variability of the activation in the left inferior frontal region demonstrates the individual location of Broca's area. The images are plotted in native space.

on the acquisition parameters for the macromolecular baseline using metabolite nulling can be found in Chong et al. (2011) (HLSVD was used to eliminate the residual water from the metabolite nulled spectrum and HLSVD was also used to parameterize the baseline to be used as noiseless basis spectrum, which in addition had been narrowed by the expected Lorentzian linewidth in order to be compatible with the QUEST algorithm that enforced identical linewidths for all base spectra, including the macromolecular baseline). The QUEST algorithm with inbase background handling and 6 truncated points was used to model further baseline features. Area estimates with fitting errors above 50% were excluded from further analysis.

SI measurements yielded multiple spectra within the PRESS localization volume and processing included spatial apodization and spatial zerofilling to 32×32 . The spectra were assigned to brain structures using co-registered MRIs for anatomical guidance.

In order to relate metabolite values to WM, GM and CSF voxel contributions, tissue segmentation was used. GM, WM, and CSF composition of all examined ROIs was approximated from the segmented mdefit images neglecting the exact ROI shape (given that the exact cuboid profile and SI ROI size are unknown, it was approximated by a sphere).

Spectra from a single SI voxel of the SI data set were selected at the activated Wernicke's area, and the left and right HG. For Wernicke's area, the voxel closest to the center of activation was selected. Only in very few cases, when the center of activation was located at the border between ROIs, a half-voxel shift was performed. The spectra were processed separately, also using JMRUI. The data were analyzed using AQSES as quantitation method (Poulet et al., 2007). The same metabolites as for the SV spectra were included as basis spectra (NAA, Ch, Cr, ml, Glu, glutamine, aspartate, glutathione, and taurine) and also the macromolecule baseline was included. In contrast to the SV spectra analysis, the

residual water was not removed, but the fit restricted to a frequency region upfield from water. While SV spectra were fitted assuming common damping for all metabolites (i.e. same line broadening), linewidths of resonances were fitted individually for SI spectra.

Results for both, SV and SI spectra were expressed as ratios with regard to creatine without any relaxation corrections. Linewidth and SNR values were obtained to control for potential systematic differences between subject groups.

Statistical analysis of MRS data

MRS data of each metabolite of interest was pooled to comprise data for each region of interest (ROI) measured with SI. Wernicke's area, left and right HG were defined as ROI, as well as Broca's area, which, however, had been separately assessed in SV MRS. Metabolites of prime interest were NAA and mI. To account for the repeated measurements in the same subjects, full factorial linear mixed models with restricted maximum likelihood estimations were used to examine the effects of various outcome measures. Schwarz's Bayesian criteria were used to determine the best fitting covariance structure for each set of measures because the typical compound symmetry approach used by ANOVA did not provide the appropriate structure for the data. The effects of group (3 levels; AH, NH, HC), region (3 levels; Wernicke's area, left and right HG) and their interaction on the NAA levels and mI levels were assessed with linear mixed models with an autoregressive covariance structure. The effect of group on Broca's area was assessed in a separate model because of the different method of measurement. Additional computations included the effect of psychopathology (PANSS total, positive, negative scores) for each ROI to assess the association of NAA and mI levels and psychopathology. All models included the percentage of GM as covariate of no interest. Subject numbers were included as additional effects to account for the repeated measurements in the SI models. Post hoc t-tests involved a Tukey-correction for multiple comparisons. The significance thresholds for these contrasts were set at $\alpha = 0.05$, two-tailed. SAS 9.2 (SAS Institute Inc., Cary, NC, USA) was used for all analyses. The means of the data are reported with their associated standard deviations.

Results

Behavioral data

Sample characteristics with mean values and standard deviations are detailed in Table 1. The mean levels of psychopathology as measured with the PANSS total score in AH and NH were 67.4 ± 19.0 and 53.4 ± 8.5 , respectively ($t[1, 18] = 1.95, p = 0.07$). The mean levels of positive symptoms within the PANSS in AH and NH were 22.3 ± 6.0 and 13.5 ± 3.2 , respectively ($t[1, 18] = 3.83, p = 0.001$). There was no significant difference in medication levels in terms of chlorpromazine equivalents (CPZE) between AH and NH. AH were medicated with 638 ± 541 mg CPZE, NH with 2389 ± 4111 mg CPZE ($p = 0.16$).

Table 1

Subject characteristics of schizophrenia patients with persistent auditory hallucinations (AH; $n = 12$), schizophrenia patients without persistent auditory hallucinations (NH; $n = 8$), and healthy controls (HC; $n = 11$). Mean values and standard deviations are reported. Abbreviations: f = female, m = male; PANSS = Positive and Negative Syndrome Scale; y = years; mo = months; CPZE = chlorpromazine equivalent.

	AH (n = 12)	NH (n = 8)	HC (n = 11)	p-Value
Gender, m/f	7/5	7/1	6/5	0.35
Age, y	42.3 (9.7)	41.2 (14.7)	43.1 (10.4)	0.94
Age of onset, y	25.9 (7.8)	26.2 (7.0)	n.a.	0.92
Duration of illness, mo	161.0 (80.3)	157.5 (127.2)	n.a.	0.94
PANSS total	67.4 (19.0)	53.4 (8.5)	n.a.	0.07
PANSS positive	22.3 (6.0)	13.5 (3.2)	n.a.	0.001
PANSS negative	16.2 (8.0)	16.7 (4.5)	n.a.	0.87
CPZE, mg	638 (541)	2389 (4111)	n.a.	0.16

fMRI data: group analysis and ROI placement

Typical activation maps from 2 AH subjects are presented in Fig. 1 illustrating the interindividual spatial variance in activated Broca's area in native space.

Group analysis

In 3 subjects (2 AH, 1 NH), the ROIs had to be defined anatomically because of a lack of activation near the expected areas of Broca's or Wernicke's area. In the remaining 28 subjects, the mean distances in native space between the individually defined ROIs using fMRI and a corresponding anatomical definition were 12.4 ± 6.1 mm (range: 2.7–36.1 mm) for Broca's area and 16.8 ± 6.2 mm (range: 4.5–26.4 mm) for Wernicke's area, respectively.

MRS data: general results

Data quality was acceptable in almost all subjects (one SV spectrum from Broca was excluded because of strong motion effects along with 6 SI spectra (4 spectra from Wernicke's area (2 from AH and 2 from NH) and 2 spectra from the right HG of AH)). Typical SI spectra for the HG and Wernicke's ROIs are reproduced in Fig. 2, while group averaged spectra are given for Broca's area in Fig. 3. Mean linewidths and SNR values did not differ significantly between groups in any of the ROIs. Overall, mean (± 1 SD) linewidths for Broca, Wernicke's, HG left and HG right were 6.9 ± 2.2 Hz, 9.6 ± 1.9 Hz, 9.1 ± 1.8 Hz, and 9.3 ± 1.8 Hz, respectively. Individual linewidths were different for NAA in HG left and in HG right between HC and NH (HG left: 8.2 ± 2.1 Hz vs. 10.2 ± 1.4 Hz, $p = 0.03$; HG right: 8.8 ± 2.2 Hz vs. 10.8 ± 1.6 Hz, $p = 0.03$, both without corrections for multiple comparisons), and for Cr in HG right between AH and NH (10.3 ± 1.7 Hz vs. 11.9 ± 1.2 Hz, $p = 0.03$). None of these differences were significant after correcting for multiple comparisons.

ROI composition in terms of WM and GM percentage was not different between groups for any ROI. Mean GM percentages as determined by segmentation ranged between $54 \pm 9\%$ in HG and $61 \pm 9\%$ in Wernicke's area.

MRS data: NAA/Cr

The mean NAA ratios with standard errors for each region and each group are shown in Fig. 4A. In Broca's area, there was a significant group effect ($F[2, 26] = 3.94, p = 0.03$) that was attributable to lower levels in NH compared to HC ($t[1, 26] = 2.8, p = 0.02$). For the NAA levels measured with SI, there was an effect of region at trend level ($F[2, 49] = 2.83, p = 0.07$). Post-hoc tests revealed that NAA/Cr was higher at a trend level in left HG compared to Wernicke's area ($t[1, 49] = 2.27, p = 0.07$). In the SI data, there was neither a significant group-effect ($F[2, 49] = 1.21, p = 0.31$), nor a significant group-by-region interaction ($F[4, 49] = 1.81, p = 0.14$).

Correlation analysis showed that there was a positive association of the NAA levels in the left HG with the total PANSS scores ($F[1, 15] = 5.92, p = 0.03$; Fig. 4C) and the negative PANSS scores ($F[1, 15] = 10.36, p = 0.006$; Fig. 4C), but no significant relation with the positive PANSS scores.

MRS data: mI/Cr

The mean mI levels with standard errors for each region and group are shown in Fig. 4B. mI levels measured with SI did not show a significant effect of region ($F[2, 49] = 0.39, p = 0.68$), group ($F[2, 49] = 1.2, p = 0.31$) nor group-by-region interaction ($F[4, 49] = 0.74, p = 0.57$).

In Broca's area, there was no group-effect ($F[2, 26] = 0.03, p = 0.97$) either, but a negative association of the mI levels with the total PANSS scores ($F[1, 15] = 9.35, p = 0.008$; Fig. 4D) and a trend towards

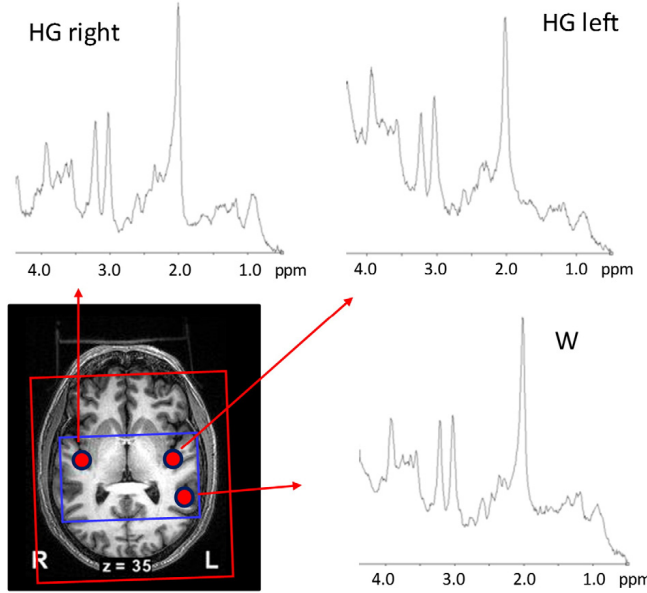


Fig. 2. Sample spectra from SI shown as obtained from a AH patient to demonstrate the setup for data acquisition and to show data quality in a single subject. The anatomical MR image shows and was prescribed to contain the targeted ROIs, Heschl's gyri (HG left, HG right) and Wernicke's area (W). The image also shows the position and size of the localized SI PRESS-box (in blue) and the field of view of the SI data set. MR signal visible in the anatomic images outside the head originates from the goggles used to display the functional task.

significance in a negative association of ml levels and the negative PANSS scores ($F[1, 15] = 3.54, p = 0.08$; Fig. 4D).

MRS data: further metabolites

In an exploratory fashion, metabolites beyond those involved in our original hypotheses (NAA and ml) were evaluated. The analysis was

restricted to those metabolites that had Cramer Rao uncertainties in individual spectra from Broca's below 50% for the large majority of subjects. These included total choline (all ROIs), glutamate (SV), glutamate plus glutamine (Glx, SI), and taurine (SV). None of these metabolites (as ratios vs. Cr) showed any significant group effects.

Discussion

This study assessed possible neurochemical and functional differences between patients with AVH, patients that had not had AVH for the last 12 months, and healthy control subjects. Four regions within the cerebral language system were chosen for a neurochemical analysis. However, it is well established that there are crucial neuroanatomical variations across subjects in terms of location and function (Ono et al., 1990; Uylings et al., 2005) that persist to a substantial degree after normalization into a common anatomical space (Amunts et al., 2000; Aronson et al., 1996; Bottomley, 1984; Derrfuss et al., 2009) and that are particularly relevant with respect to the functional specification of cerebral language regions (Bauer and Whybrow, 2001). A possible reason for inconsistencies between functional imaging studies of the language system is the application of group analyses in most of the investigations, which might have resulted in an underestimation of individual differences (Bauer and Whybrow, 2001). In addition, it has been shown that only sensory processes of a rather low-level can be linked reliably to macroanatomy, and functional variability increases systematically if cognitive processes of higher order are involved (Yamada and Wilber, 1990). Thus, the current study used fMRI to functionally define two ROIs of the cerebral language system for subsequent MRS analysis. This approach allowed taking interindividual variability of functional areas within the language system into account. It is well known that two of the assessed ROIs, Broca's area and Wernicke's

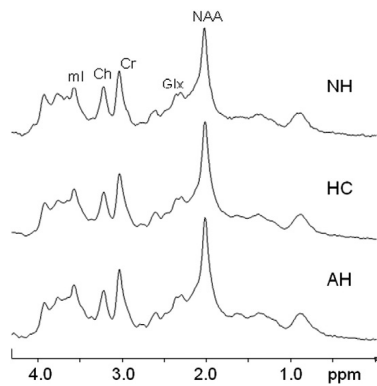


Fig. 3. Group-averaged single voxel spectra from Broca's area, which had been defined by a preceding fMRI scan. To ease visual comparison, the spectra have been matched in linewidth and in intensity to reach equal width and peak intensity for the creatine methyl peak.

area, show a considerable amount of variation among healthy subjects. We therefore compared the functional loci with the most likely anatomically defined loci in each subject and found that the mean distance of the functional and the corresponding anatomical loci for Broca's area (12 mm) and Wernicke's area (17 mm) was in the same range as in previous studies and larger or of the same size as the individual activation areas. If these ROIs had been prescribed anatomically for the MRS investigation the investigated volume ($14 \times 14 \times 14$ mm) would only rarely have covered most of the functional activation area. Inversely, to guarantee the functional activity focus to be within the MRS ROI, one would have to increase the voxel size considerably, which would come with an enormous dilution effect with areas of different function and also with more white matter. However, the current study could not statistically test the difference between neurochemical results in functionally defined language regions (Broca's area and Wernicke's area) versus those that could have been obtained in the corresponding regions defined by anatomical landmarks since this would have substantially prolonged the study procedure in a population of particularly vulnerable patients with limited resilience and compliance. The spectral quality was quite good for all spectra and ROIs, even though one ROI (Broca's) was in a frontal location that is known to show significant field inhomogeneities. Hence, the strategy to split the investigations into a single voxel examination in the 'difficult' frontal brain and a spectroscopic imaging examination for those brain areas with a more homogeneous field distribution paid off leading to a very limited number of rejected spectra. In addition to reduced field homogeneity and broader lines, a multi-slice or volumetric SI investigation would have been longer and probably subject to more motion-related artifacts.

In spite of the functional definition of two of the MRS ROIs, no neurochemical imbalances were found to support the hypotheses of a relative reduction of NAA in Wernicke's area in hallucinating schizophrenia patients compared to patients without hallucinations and controls. Instead, NAA ratios as measured with SV in Broca's area revealed a group-difference between NH and HC that was attributable to lower NAA ratios in NH. In addition, a regional difference was found for NAA ratios as measured by SI, with higher levels in the left HG compared to Wernicke's area across the whole sample, but no group-differences. In terms of correlations between neurochemical levels and patients' symptom scores, there were positive associations between the total as well as the negative PANSS scores and the NAA levels in the left HG for all patients (AH, NH). Both patient groups also showed negative associations of psychopathological symptoms as measured with the total and the negative PANSS scores and ml levels in Broca's area.

The current study used a combined approach to measure functional and neurochemical parameters in the same subjects. A verbal fluency task was used to functionally define ROIs in each subject individually that were then assessed with MRS. This approach tries to overcome some of the inherent limitations that have been discussed with respect to an anatomical definition of ROIs. In addition, the combination allows testing conflicting hypotheses in the same subjects (P. Allen et al., 2012). However, our neurochemical results are largely conflicting with what we had hypothesized a priori. The assessment of neurochemistry within functionally and anatomically defined ROIs revealed a group-difference in NAA concentrations in Broca's area only, where NH showed lower concentrations compared to HC. This finding is in

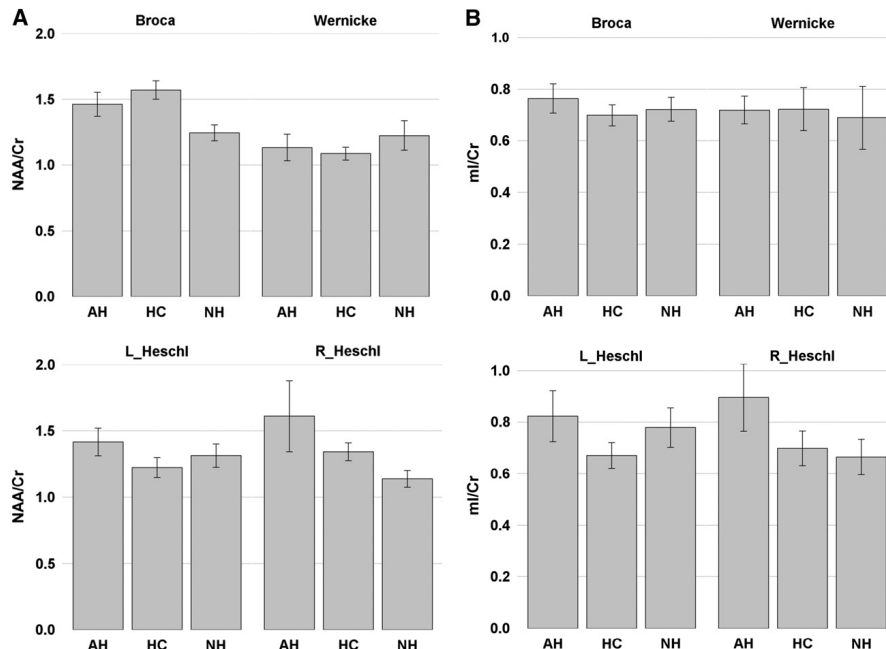


Fig. 4. A. The mean NAA levels with standard errors for each region and group (AH, NH, HC). B. The mean ml levels with standard errors for each region and group. C. A positive association of the NAA ratio in the left Heschl and the total PANSS score ($r = 0.59$, $p = 0.007$) and the negative PANSS score ($r = 0.6$, $p = 0.006$). D. A negative association of the ml ratios in Broca's area and the total PANSS score ($r = -0.52$, $p = 0.02$) and a trend towards significance in the negative association of ml levels and the negative PANSS score ($r = -0.44$, $p = 0.06$).

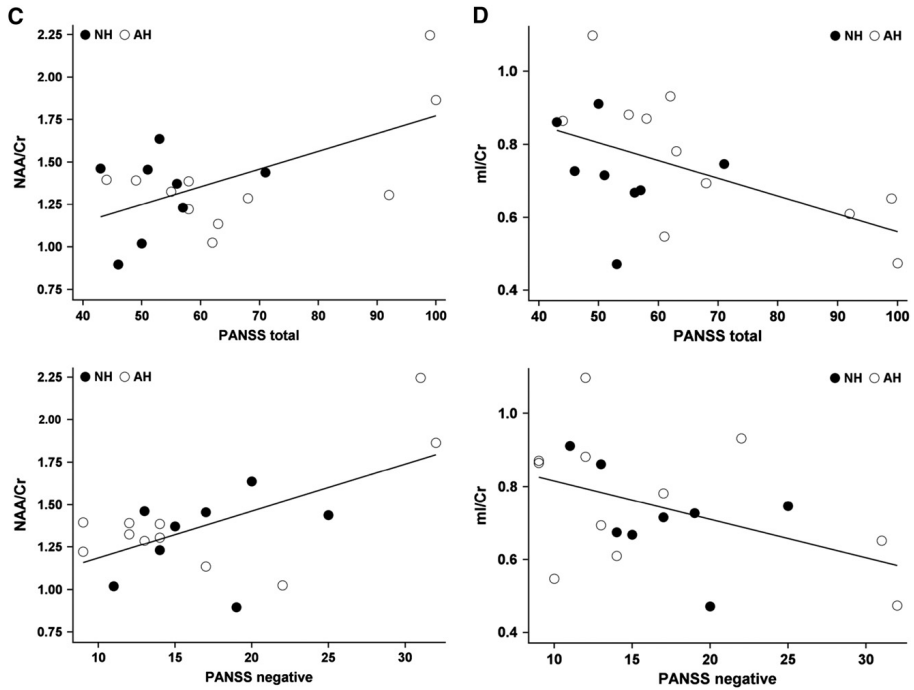


Fig. 4 (continued).

contrast to our a-priori hypothesis that there would be a reduction in NAA concentrations in Wernicke's area of AH compared to NH and HC. Overall, we found decreased NAA only in Broca's area in our patient population, which is also in contrast to most of the current literature where generally it is found (though more at long echo time, see below) that NAA in schizophrenia is decreased in frontal and temporal regions and in the thalamus (Brugge et al., 2011; Heckers, 2001; Martinez-Granados et al., 2008), although there are a number of conflicting results as summed up in a meta-analysis by Steen et al. (2005). Specifically, there is some evidence that the effects on NAA levels in schizophrenia patients are dependent on antipsychotic medications in that typical antipsychotic medication is associated with lower NAA levels and atypical neuroleptics are possibly associated with less of a reduction (Braus et al., 2001, 2002; Ende et al., 2000) (reviewed in Steen et al., 2005) or even elevated NAA concentrations (Bertolino et al., 2001). Furthermore, Bracken et al. (2013) recently concluded that the apparent NAA deficit in schizophrenia might mainly be caused by changes in the transverse relaxation time of NAA, rather than the NAA content, which would explain why NAA deficits are primarily reported for studies using long echo times. In addition, the detected positive correlation between NAA in the left HG and psychopathology in all patients is also in contrast with the hypothesis that schizophrenia might be a progressive neurodegenerative disease involving left temporal regions. However, we have recently suggested that a gray matter deficit found in language and primary auditory areas in AH compared to NH may reflect a loss of neuropil (compatible with experience-dependent modeling of the cortical column architecture) rather than neuronal cell degeneration (van Swam et al., 2012). In addition, all of

the above interpretations of NAA levels solely base on the putative role of NAA as a marker for the density of healthy neurons, but NAA levels may also reflect mitochondrial activity, osmolytic balance and has other putative roles, which led K.K. Bhakoo recently to conclude in his review on NAA metabolism that "... its function/s remains an enigma" (Bhakoo, 2012).

With respect to mI, the values in the collapsed patients group showed a negative association with the psychopathology in Broca's area. This result is incompatible with a neurodegenerative hypothesis of schizophrenia (Delamilleure et al., 2002) but may indicate either decreased glial content or more dysfunctional glia in more severe disease (Chang et al., 2007).

Several limitations should be noted. Our sample size was small, particularly with respect to the NH group. Remarkably, it has been noted that this confound of a small sample size is particularly evident in previous studies using the categorical distinction between AH and NH (P. Allen et al., 2012) (though we did not even find a trend to support the original hypothesis of a relative reduction of NAA in Wernicke's area in hallucinating schizophrenia patients). To evaluate the designed and actual power of the study, we calculated the minimal detectable difference for the sample sizes of AH and NH in the NAA levels of Wernicke's area for two cases; first for the ideal case with the variability as found in the healthy control group and full group size, and second for the actual situation as found post hoc with the larger variability found in the patient groups. At 80% probability and two-sided 0.05 significance level the study would have detected a difference in NAA levels in Wernicke's area between AH and NH of 0.23 units (i.e., about 21% of the normal level) for the ideal case and 0.48 units (about 44% of the

normal level) for the actual situation. However, the actually measured difference in the mean NAA levels in AH and NH was 0.09 units only. In addition, we studied patients on medication, which means that medication confounds of antipsychotics have to be taken into account. However, we tried to take this possible variable into account by matching as well as possible AH and NH by their CPZE, so there was no significant difference in CPZE in AH and NH. Furthermore, the VF-task during fMRI did not include any behavioral measure, so we do not have a control for the subjects' compliance. We also had to weaken our initial threshold defining a NH patient as someone who had not had experienced hallucinations in the past 5 years to a more lenient criterion of 12 months without AVH. In addition, we did not assess the psychopathology (i.e. AVH) during the MRI scan which means that patients may have experienced AVH during the MRI procedure. Instead, AVH and other psychopathological symptoms were assessed before the MRI procedure. In terms of methodology, it should be noted that creatine levels were taken for concentration estimation, as used by a large fraction of the published studies on schizophrenia. The use of CSF-corrected water signal would be a better suited reference, but is not available for this and most SI studies in general because of time reasons. However, given the information from both large meta-analyses (Brugge et al., 2011; Steen et al., 2005), there is only very limited reason to suspect relevant alterations of creatine content in schizophrenia patients, though there is some speculation of increased metabolism with associated increased creatine levels in temporal areas (Brugge et al., 2011).

In conclusion, the present study supports the neurodegenerative hypothesis of schizophrenia only in a frontal region whereas the results obtained from temporal regions do not support this hypothesis and are in contrast to the majority of previous studies that have found NAA reductions in temporal and frontal regions. In addition, the difference we documented between a functional and an anatomical definition of regions to be studied by MRS suggests that future research should test the hypothesis that a functional definition of language regions is needed if neurochemical imbalances are expected to be restricted to functional foci.

Acknowledgments

Support from the "Stiftung für klinische neuro-psychiatrische Forschung, Bern, Switzerland" and the Swiss National Science Foundation (3100A0-103938) is gratefully acknowledged.

References

- Abbott, C., Bustillo, J., 2006. What have we learned from proton magnetic resonance spectroscopy about schizophrenia? A critical update. *Curr. Opin. Psychiatry* 19, 125–139.
- Adalsteinsson, E., Sullivan, E.V., Kleinhans, N., Spielman, D.M., Pfefferbaum, A., 2000. Longitudinal decline of the neuronal marker N-acetyl aspartate in Alzheimer's disease. *Lancet* 355, 1696–1697.
- Allen, E.A., Erhardt, E.B., Wei, Y., Eichele, T., Calhoun, V.D., 2012a. Capturing inter-subject variability with group independent component analysis of fMRI data: a simulation study. *Neuroimage* 59, 4141–4159.
- Allen, P., Modinos, G., Hubl, D., Shields, G., Cachia, A., et al., 2012b. Neuroimaging beyond hallucinations in schizophrenia: from neuroanatomy to neurochemistry and beyond. *Schizophr. Bull.* 38, 695–703.
- Amunts, K., Malikovic, A., Mohlberg, H., Schormann, T., Zilles, K., 2000. Brodmann's areas 17 and 18 brought into stereotaxic space—where and how variable? *Neuroimage* 11, 66–84.
- Aronson, R., Offman, H.J., Joffe, R.T., Taylor, C.D., 1996. Triiodothyronine augmentation in the treatment of refractory depression. A meta-analysis. *Arch. Gen. Psychiatry* 53, 842–848.
- Barker, P.B., Bizzzi, A., De Stefano, N., Gullapalli, R.P., Lin, D.D.M., 2009. *Clinical MR Spectroscopy. Techniques and Applications*. Cambridge University Press.
- Bauer, M., Whybrow, P.C., 2001. Thyroid hormone, neural tissue and mood modulation. *World J. Biol. Psychiatry* 2, 59–69.
- Bertolino, A., Callicott, J.H., Mattay, V.S., Weidenhamer, K.M., Rakow, R., et al., 2001. The effect of treatment with antipsychotic drugs on brain N-acetylaspartate measures in patients with schizophrenia. *Biol. Psychiatry* 49, 39–46.
- Blakow, K.K., 2012. N-acetyl-aspartate (NAA) metabolism. In: Lathia, A. (Ed.), *Advances in Neurobiology*. Springer, New York, pp. 1075–1093.
- Bottomley, P.A., 1984. Selective volume method for performing localized NMR spectroscopy, US Patent 4 480 228. USA.
- Bracken, B.K., Rouse, E.D., Renshaw, P.F., Olson, D.P., 2013. T₂ relaxation effects on apparent N-acetylaspartate concentration in proton magnetic resonance studies of schizophrenia. *Psychiatry Res.* 213, 142–153.
- Brand, A., Richter-Landsberg, C., Leibfritz, D., 1993. Multinuclear NMR studies on the energy metabolism of glial and neuronal cells. *Dev. Neurosci.* 15, 289–298.
- Braus, D.F., Ende, G., Weber-Fahr, W., Demirakca, T., Henn, F.A., 2001. Favorable effect on neuronal viability in the anterior cingulate gyrus due to long-term treatment with atypical antipsychotics: an MRSI study. *Pharmacopsychiatry* 34, 251–253.
- Braus, D.F., Ende, G., Weber-Fahr, W., Demirakca, T., Tost, H., et al., 2002. Functioning and neuronal viability of the anterior cingulate neurons following antipsychotic treatment: MR-spectroscopic imaging in chronic schizophrenia. *Eur. Neuropsychopharmacol.* 12, 145–152.
- Brugge, S., Davis, J.M., Leucht, S., Stone, J.M., 2011. Proton magnetic resonance spectroscopy and illness stage in schizophrenia—a systematic review and meta-analysis. *Biol. Psychiatry* 69, 495–503.
- Burton, M.W., Noll, D.C., Small, S.I., 2001. The anatomy of auditory word processing: individual variability. *Brain Lang.* 77, 119–131.
- Chang, L., Friedman, J., Ernst, T., Zhong, K., Tsopelas, N.D., et al., 2007. Brain metabolite abnormalities in the white matter of elderly schizophrenic subjects: implication for glial dysfunction. *Biol. Psychiatry* 62, 1396–1404.
- Chong, D.G., Kreis, R., Bölliger, C.S., Boesch, C., Slotboom, J., 2011. Two-dimensional linear-combination model fitting of magnetic resonance spectra to define the macromolecule baseline using FITAID, a Fitting Tool for Arrays of Interrelated Datasets. *MAGMA* 24, 147–164.
- Copolov, D., Trauer, T., Mackinnon, A., 2004. On the non-significance of internal versus external auditory hallucinations. *Schizophr. Res.* 69, 1–6.
- Delamilleil, P., Constans, J.M., Fernandez, J., Brazo, P., Benali, K., et al., 2002. Proton magnetic resonance spectroscopy (1H MRS) in schizophrenia: investigation of the right and left hippocampus, thalamus, and prefrontal cortex. *Schizophr. Bull.* 28, 329–339.
- Derrfuss, J., Brass, M., von Cramon, D.Y., Lohmann, G., Amunts, K., 2009. Neural activations at the junction of the inferior frontal sulcus and the inferior precentral sulcus: inter-individual variability, reliability, and association with sulcal morphology. *Hum. Brain Mapp.* 30, 299–311.
- Dierks, T., Linden, D.E., Jandl, M., Formisano, E., Goebel, R., et al., 1999. Activation of Heschl's gyrus during auditory hallucinations. *Neuron* 22, 615–621.
- Ende, G., Braus, D.F., Walter, S., Weber-Fahr, W., Soher, B., et al., 2000. Effects of age, medication, and illness duration on the N-acetyl aspartate signal of the anterior cingulate region in schizophrenia. *Schizophr. Res.* 41, 389–395.
- Fedorenko, E., Hsieh, P.J., Nieto-Castanon, A., Whitfield-Gabrieli, S., Kanwisher, N., 2010. New method for fMRI investigations of language: defining ROIs functionally in individual subjects. *J. Neurophysiol.* 104, 1177–1194.
- Heckers, S., 2001. Neuroimaging studies of the hippocampus in schizophrenia. *Hippocampus* 11, 520–528.
- Homan, P., Kindler, J., Federspiel, A., Flury, R., Hubl, D., et al., 2011. Muting the voice: a case of arterial spin labeling-monitored transcranial direct current stimulation treatment of auditory verbal hallucinations. *Am. J. Psychiatry* 168, 853–854.
- Homan, P., Kindler, J., Hubl, D., Dierks, T., 2012. Auditory verbal hallucinations: imaging, analysis, and intervention. *Eur. Arch. Psychiatry Clin. Neurosci.* 262 (Suppl. 2), 91–95.
- Hor, K., Taylor, M., 2010. Suicide and schizophrenia: a systematic review of rates and risk factors. *J. Psychopharmacol.* 24, 81–90.
- Hubl, D., Koenig, T., Strik, W., Federspiel, A., Kreis, R., et al., 2004. Pathways that make voices: how verbal changes in auditory hallucinations. *Arch. Gen. Psychiatry* 61, 658–668.
- Hubl, D., Koenig, T., Strik, W.K., Garcia, L.M., Dierks, T., 2007. Competition for neuronal resources: how hallucinations make themselves heard. *Br. J. Psychiatry* 190, 57–62.
- Jansen, J.F., Backes, W.H., Nicolay, K., Kooi, M.E., 2006. 1H MR spectroscopy of the brain: absolute quantification of metabolites. *Radiology* 240, 318–332.
- Jung, R.E., Yeo, R.A., Chiulli, S.J., Sibbitt Jr., W.L., Weers, D.C., et al., 1999. Biochemical markers of cognition: a proton MR spectroscopy study of normal human brain. *Neuroreport* 10, 3327–3331.
- Kay, S.R., Fiszbein, A., Opler, L.A., 1987. The positive and negative syndrome scale (PANSS) for schizophrenia. *Schizophr. Bull.* 13, 261–276.
- Kindler, J., Homan, P., Jann, K., Federspiel, A., Flury, R., et al., 2013. Reduced neuronal activity in language-related regions after transcranial magnetic stimulation therapy for auditory verbal hallucinations. *Biol. Psychiatry* 73, 518–524.
- Martinez-Granados, B., Brontos, O., Martinez-Bisbal, M.C., Celda, B., Martí-Bonmatí, L., et al., 2008. Spectroscopic metabolomic abnormalities in the thalamus related to auditory hallucinations in patients with schizophrenia. *Schizophr. Res.* 104, 13–22.
- Maudsley, A.A., Darkazani, A., Alger, J.R., Hall, L.O., Schuff, N., et al., 2006. Comprehensive processing, display and analysis for *in vivo* MR spectroscopic imaging. *NMR Biomed.* 19, 492–503.
- Miller, B.L., Moats, R.A., Shonk, T., Ernst, T., Woolley, S., et al., 1993. Alzheimer disease: depiction of increased cerebral myo-inositol with proton MR spectroscopy. *Radiology* 187, 433–437.
- Ono, M., Kubik, S., Abernathy, C., 1990. *Atlas of the Cerebral Sulci*. Georg Thieme Verlag.
- Pouillet, J.B., Sima, D.M., Simonetti, A.W., De Neuter, B., Vanhamme, L., et al., 2007. An automated quantitation of short echo time MRS spectra in an open source software environment: AQES. *NMR Biomed.* 20, 493–504.
- Ratiney, H., Coenradie, Y., Cavassila, S., van Ormondt, D., Graveron-Demilly, D., 2004. Time-domain quantitation of 1H short echo-time signals: background accommodation. *MAGMA* 16, 284–296.
- Schwerk, A., Alves, F.D., Pouwels, P.J., van Amelsvoort, T., 2014. Metabolic alterations associated with schizophrenia: a critical evaluation of proton magnetic resonance spectroscopy studies. *J. Neurochem.* 128, 1–87.

- Shergill, S.S., Murray, R.M., McGuire, P.K., 1998. Auditory hallucinations: a review of psychological treatments. *Schizophr. Res.* 32, 137–150.
- Steen, R.G., Hamer, R.M., Lieberman, J.A., 2005. Measurement of brain metabolites by ^1H magnetic resonance spectroscopy in patients with schizophrenia: a systematic review and meta-analysis. *Neuropsychopharmacology* 30, 1949–1962.
- Stefan, D., Di Cesare, F., Andrasescu, A., Popa, E., Lazariev, A., Vescovo, E., Strbak, O., Williams, S., Starcuk, Z., Cabanas, M., van Ormondt, D., Graveron-Demilly, D., 2009. Quantitation of magnetic resonance spectroscopy signals: the JMRUI software package. *Meas. Sci. Technol.* 20.
- Theberge, J., Al-Semaan, Y., Williamson, P.C., Menon, R.S., Neufeld, R.W., et al., 2003. Glutamate and glutamine in the anterior cingulate and thalamus of medicated patients with chronic schizophrenia and healthy comparison subjects measured with 4.0-T proton MRS. *Am. J. Psychiatry* 160, 2231–2233.
- Uylings, H.B., Rajkowska, G., Sanz-Arigita, E., Amunts, K., Zilles, K., 2005. Consequences of large interindividual variability for human brain atlases: converging macroscopical imaging and microscopical neuroanatomy. *Anat. Embryol. (Berl.)* 210, 423–431.
- van Swam, C., Federspiel, A., Hubl, D., Wiest, R., Boesch, C., et al., 2012. Possible dysregulation of cortical plasticity in auditory verbal hallucinations—a cortical thickness study in schizophrenia. *J. Psychiatr. Res.* 46, 1015–1023.
- Xiong, J., Rao, S., Jerabek, P., Zamarripa, F., Woldorff, M., et al., 2000. Intersubject variability in cortical activations during a complex language task. *Neuroimage* 12, 326–339.
- Yamada, M., Wilber, J.F., 1999. Reciprocal regulation of prothyrotropin-releasing hormone (TRH) mRNA in the rat anterior hypothalamus by thyroid hormone: dissociation from TRH concentrations during hypothyroidism. *Neuropeptides* 15, 49–53.



Formal thought disorder is related to aberrations in language-related white matter tracts in patients with schizophrenia

Marialuisa Cavelti^{a,b,1,*}, Stephanie Winkelbeiner^{a,1}, Andrea Federspiel^a, Sebastian Walther^a, Katharina Stegmayer^a, Stéphanie Giezendanner^c, Karin Laimböck^a, Thomas Dierks^a, Werner Strik^a, Helge Horn^{a,d}, Philipp Homan^{a,e}

^a Translational Research Center, University Hospital of Psychiatry and Psychotherapy, University of Bern, Bern 60 3000 Switzerland

^b Orygen, The National Centre of Excellence in Youth Mental Health & Centre for Youth Mental Health, University of Melbourne, Parkville, VIC 3052, Australia

^c Centre for Primary Health Care, University of Basel, Liestal 4410, Switzerland

^d Institute for Psychiatry and Psychotherapy Bern, Waisenhausplatz 25, Bern 3011, Switzerland

^e Center for Psychiatric Neuroscience, The Feinstein Institute for Medical Research, Hofstra Northwell School of Medicine, New York, NY, USA

ARTICLE INFO

Keywords:

Diffusion tensor imaging (DTI)
Fractional anisotropy (FA)
psychosis
Arcuate fasciculus (AF)
inferior fronto-occipital fasciculus (IFOF)
inferior longitudinal fasciculus (ILF)
superior longitudinal fasciculus (SLF)
uncinate fasciculus (UF)

ABSTRACT

This study examined the hypothesis that a fronto-temporal disconnection in the language network underpins formal thought disorder (FTD) in schizophrenia. Forty-nine patients with a schizophrenia spectrum disorder (27 with mild FTD, 22 with severe FTD) and 26 healthy controls (HC) were included. Overall psychopathology and FTD were assessed by the Positive and Negative Syndrome Scale and the Thought, Language, and Communication scale, respectively. White matter (WM) microstructure was analysed using Tract-Based Spatial Statistics. In patients, severity of overall FTD (TLC Sum Score) was predicted by decreased fractional anisotropy (FA) in the right superior longitudinal fasciculus (SLF), and severity of negative FTD (TLC Emptiness subscale) was predicted by increased FA in the left SLF and arcuate fasciculus (AF). Notably, these results were no longer significant after correction for multiple comparisons. Compared with HC, patients showed lower FA in all the investigated language-related WM tracts as well as across the whole WM skeleton. No difference in FA was found between patients with severe and patients with mild FTD. Our results are compatible with earlier studies reporting impairments in widely spread WM tracts including those related to language processing in patients with schizophrenia.

1. Introduction

Formal thought disorder (FTD) is a severe language disturbance and a core syndrome of schizophrenia (Bleuler, 1958). This syndrome, however, is not only found in schizophrenia or schizoaffective disorders, but also in the general population, in people at high risk of developing psychosis, and in people with non-psychotic disorders (Roche et al., 2015). Therefore, FTD should be considered as both a dimensional entity of speech pathology and a categorical entity in terms of a trait marker for psychosis (Roche et al., 2015). Rather than being a single entity, FTD spans various abnormalities of speech, including organization, rate, impoverishment, and degree of idiosyncrasy. FTD can be distinguished into objective positive (e.g. derailment) and subjective positive (e.g. pressure/rush of thought) forms as well as objective negative (e.g. poverty of speech) and subjective negative (e.g. thought blocking) forms (Nagels et al., 2013), which have different

neuropsychological correlates. For instance, positive FTD has been related to executive dysfunctions, and negative FTD to deficits in lexico-semantic retrieval (Nagels et al., 2016; Silverstein et al., 1991). Overall, FTD is as disabling as other symptoms of schizophrenia, limiting therapeutic relationship and psychological recovery (Cavelti et al., 2016), social and occupation functioning, wellbeing and life satisfaction (Sigaudo et al., 2014; Tan et al., 2014).

FTD in schizophrenia has been linked to structural and functional abnormalities in language-related brain regions. Structural studies found grey matter (GM) volume reductions in the left temporo-parietal junction (TPJ), including Wernicke's area (Horn et al., 2010, 2009; Rajarethnam et al., 2000), and both volume decrease (Horn et al., 2009; Sans-Sansa et al., 2013) and increase (Palaniyappan et al., 2015) in the left inferior frontal gyrus (IFG), overlapping with Broca's area, to be associated with FTD. Functional studies reported increased resting blood flow (Horn et al., 2009; Stegmayer et al., 2017) and increased

* Corresponding author at: Translational Research Center, University Hospital of Psychiatry and Psychotherapy, University of Bern, Bern 60 3000 Switzerland.

E-mail address: marieluisa.cavelti@upd.unibe.ch (M. Cavelti).

¹ Shared first authorship: The authors contributed equally to this work.

neural activity (Kircher et al., 2003, 2001a,b; McGuire et al., 1998) in the TPJ and the IFG to be associated with FTD. Interestingly, recent findings indicate that positive and negative FTD may be differently associated with structural and functional abnormalities in the language network (Palaniyappan et al., 2015; Sans-Sansa et al., 2013; Stegmayer et al., 2017; Viher et al., 2018). For instance, Sans-Sansa et al. (2013) found ‘fluent disorganization’ (a positive FTD symptom) to be correlated with volume reductions in both Broca’s and Wernicke’s areas, whereas ‘poverty of content of speech’ (a negative FTD symptom) was correlated with reductions in the medial frontal/orbitofrontal cortex. This research has led to the hypothesis that a fronto-temporal disconnection in the language network may underlie FTD in schizophrenia (Cavelti et al., 2018; Horn et al., 2012; Kircher, 2008; Strik et al., 2017, 2008).

By examining white matter (WM) fibre bundles we can study the structural foundations of information transmission between distant brain regions of the language network. Yet, only few studies have examined WM abnormalities in relation to FTD in schizophrenia so far. These studies found an inverse relation between FTD and FA in the right cingulum bundle (Bopp et al., 2017), the splenium of the corpus callosum along with the retroentorhinal limb and the posterior limb of the internal capsule (Arnedo et al., 2015), the left cerebellum (Rigucci et al., 2013), and language-related tracts including the left middle longitudinal fascicle (MdLF) (Asami et al., 2013), inferior fronto-occipital fasciculi (IFOF) (Rigucci et al., 2013; Viher et al., 2018), inferior longitudinal fasciculi (ILF) (Rigucci et al., 2013; Viher et al., 2018), superior longitudinal fasciculi (SLF) (Viher et al., 2018), and uncinate fascicle (UF) (Viher et al., 2018). Zhou et al. (2017) reported a positive association between FA in the right SLF II, belonging to the MdLF, and FTD in patients with first episode psychosis. However, also non-significant correlations between disorganized speech and FA have been reported (Viher et al., 2016). The SLF, which includes the arcuate fasciculus (AF), represents the dorsal language pathway and is involved in sound-to-motor mapping. The IFOF, ILF, and UF are components of the ventral language pathway that is accountable for sound-to-meaning integration (Friederici, 2015). The MdLF has only recently been detected in humans (Makris et al., 2017), and its location and function for language processing remain a subject of debate (e.g., Kellmeyer et al., 2013; Wang et al., 2013).

In order to test the hypothesis of a fronto-temporal disconnection of the language network as neural correlate of FTD in schizophrenia (Kircher, 2008; Strik et al., 2008), the current study examined aberrations in language-related WM tracts in relation to FTD in patients with schizophrenia and healthy controls (HC). Thereby, we intended to overcome some of the methodological limitations of recent studies, such as the usage of a general psychopathology measure rather than a measure specifically developed to assess FTD, the lack of differentiating between subtypes of FTD such as positive and negative forms (Cavelti et al., 2018), the lack of specific hypotheses with regard to FTD (Sumner et al., 2017), and the usage of whole brain approaches that prevent drawing conclusions regarding the specificity of a region for a certain symptom/syndrome (Gelman and Stern, 2006). We employed tract-based spatial statistics (TBSS), which is currently considered one of the leading methods for diffusion tensor imaging (DTI) analysis. It is superior to traditional voxel-based morphometry (VBM) in terms of alignment and smoothing issues (Smith et al., 2006), and to tractography, because it provides a quantitative and objective measure of diffusion parameters for group comparisons (Jbabdi and Johansen-Berg, 2011; Smith et al., 2006). We investigated the SLF, AF, IFOF, ILF, and UF as regions of interest (ROIs), all major structures of the dorsal and ventral language pathways (Friederici, 2015). We assessed FTD by the Thought, Language and Communication (TLC) scale that allows to distinguish positive (Disorganization subscale) and negative (Emptiness subscale) FTD (Nagels et al., 2013). In accordance with recent studies (Asami et al., 2013; Rigucci et al., 2013; Viher et al., 2018; Zhou et al., 2017), we hypothesized that in patients with schizophrenia severity of

FTD is predicted by lower FA in the ROIs. In addition, we conducted a subsequent whole-brain analysis in order to explore whether other brain areas than the *a-priori* ROIs were affected by FTD, too. We hypothesized that patients with schizophrenia show lower FA in the ROIs and in the whole brain than HC, with patients with severe FTD showing even lower FA than patients with mild FTD.

2. Methods

2.1. Subjects

The study was conducted at the University Hospital of Psychiatry in Bern, Switzerland, between 2011 and 2014. For the advantage of a bigger sample size, data from two studies with similar methods were combined. The final sample consisted of 75 subjects, including 49 patients with a schizophrenia spectrum disorder according to DSM-IV-TR (American Psychiatric Association, 2000) and 26 HC recruited among the employees of the University Hospital of Psychiatry and through personal contacts. For all participants, inclusion criteria were age between 18 and 65 years, good German language skills that allowed to understand the consent procedure and to undergo the clinical assessment, and right-handedness according to the Edinburgh Inventory (Oldfield, 1971). Participants were excluded if they were left-handed, pregnant, showed any contraindications for MRI (e.g. metal-containing implants such as pacemaker or cochlear implants, claustrophobia), had a history of serious neurological issues, or reported current abuse of alcohol and/or psychoactive substances (apart from nicotine). Diagnoses were confirmed by an experienced clinician (first sample) or the Mini-International Neuropsychiatric Interview (MINI) (Lecrubier et al., 1997) (second sample). Additionally, HC had no current major psychiatric DSM-IV Axis I diagnoses, as assessed with the screening questionnaire of the Structured Clinical Interview for DSM-IV Axis I Disorders (First et al., 1996) (first sample) or the MINI (second sample). Positive symptoms (Positive Syndrome subscale), negative symptoms (Negative Syndrome subscale), general psychopathology (General Psychopathology subscale), and overall psychopathology (Total Score) were assessed using the Positive and Negative Syndrome Scale (PANSS) (Kay et al., 1987). Severity of overall FTD was assessed using the TLC Sum Score, severity of positive FTD using the TLC subscale Disorganization, and severity of negative FTD using the TLC subscale Emptiness (Nagels et al., 2013). Patients were stratified according to their TLC Sum Score (which ranges between 0 and 63) into a mild (mFTD; TLC < 10; N = 27) and a severe (sFTD; TLC ≥ 10; N = 22) FTD group (see Table 1). A cut-off of 10 was chosen predefined in the initial study proposal. For comparison, we also stratified patients based on a median split of the TLC Sum Score (mFTD: TLC < 8, N = 24; sFTD: TLC ≥ 8, N = 25; see Supplementary Fig. 1). Overall, the results did not differ depending on the cut-off used to stratify the patients. Thus, in the following, we are going to report the group comparisons based on the original cut-off of 10 only.

All subjects gave written informed consent. Assessments of psychopathology as well as magnetic resonance imaging (MRI) were conducted on the same day by a trained clinician. Both studies were approved by the ethics committee of the Kanton Bern, Switzerland.

2.2. DTI data acquisition

Diffusion tensor images were acquired from two different magnet resonance scanners at the Department of Neuroradiology of the University Hospital Bern, Switzerland. Both scanners used spin echo planar imaging with two 180° pulses at a minimum b-value of 0 s/mm² and a maximum b-value of 1300 s/mm² along 42 non-collinear directions. Thirty-nine subjects were scanned with a 3T Magnetom Verio SYNGO system (Siemens Erlangen, Germany) and a 12-channel array head coil. Following parameters were used: TR/TE = 9100/88 ms, matrix = 128*128, field of view (FOV) = 256*256 mm², slices = 55

Table 1
Participants' demographics.

	Controls	Patients		Group differences			
		Mild FTD M (SD) [range] (n = 26)	Severe FTD M (SD) [range] (n = 27)	Test	Value	df	p
Gender no. F/Ma	12/14	11/16	6/16	χ^2	1.87	2	0.393
Age (years)	38.73 (11.76) [25.00–60.00]	35.59 (11.80) [19.00–62.00]	37.36 (11.07) [20.00–56.00]	F test	0.49	2	0.615
Education (years)	(n = 22) 15.95 (2.61) [12.00–20.00]	13.98 (3.27) [9.00–21.00]	12.66 (3.17) [9.00–19.00]	F test	6.53	2	0.003*
Diagnosis DSM-IV. 295.9/295.7/295.4	NA	17/8/2	17/4/1	χ^2	1.17	2	0.558
Age of onset	NA	25.52 (8.60) [0.00–43.00]	23.00 (7.44) [16.00–49.00]	t test	1.62	45	0.300
Duration of illness (years)	NA	940 (9.83) [0.08–38.75]	14.64 (11.82) [0.08–38.00]	t test	-1.68	46	0.100
CPZE (mg)	NA	686.96 (1561.06) [100.00–8333.00]	614.32 (619.32) [0.00–3000.00]	t test	0.21	47	0.838
PANSS							
Positive Syndrome	NA	14.30 (5.38) [7.00–27.00]	21.27 (6.16) [13.00–33.00]	t test	-4.23	47	0.001***
Negative Syndrome	NA	14.74 (5.60) [7.00–25.00]	15.68 (6.68) [7.00–35.00]	t test	-0.56	47	0.577
General Psychopathology	NA	29.59 (7.55) [17.00–48.00]	35.09 (11.14) [17.00–63.00]	t test	-2.05	47	0.046*
Total Score	NA	58.63 (14.84) [36.00–97.00]	72.05 (19.88) [37.00–112.00]	t test	-2.70	47	0.010**
TLC							
Disorganization	NA	(n = 24) 0.88 (2.03) [0.00–8.00]	(n = 17) 12.59 (7.72) [0.00–26.00]	Mann–Whitney-U	33.00	NA	0.001***
Emptiness	NA	(n = 24) 1.25 (2.19) [0.00–8.00]	(n = 17) 1.12 (2.29) [0.00–9.00]	Mann–Whitney-U	206.00	NA	0.963
Sum Score	NA	2.30 (2.73) [0.00–8.00]	17.86 (7.00) [10.00–31.00]	Mann–Whitney-U	0.00	NA	0.001***

Notes: M, mean; Ma, male; F, female; NA, not applicable; DSM-V, Diagnostic and Statistical Manual of Mental Disorders; CPZE, chlorpromazine equivalents; PANSS, Positive and Negative Syndrome Scale; SD, standard deviation; TLC, Thought, Language and Communication scale.

Significant at: *, p < 0.05; **, p < 0.01; ***, p < 0.001.

with a slice thickness of 2.2 mm, a gap thickness of 0 mm, voxel size = 2*2*2.2 mm³, and a pixel bandwidth of 1336 Hz/pixel. All other subjects (n = 36) were scanned with a 3T Magnetom Trio TIM system (Siemens Erlangen, Germany) also using a 12-channel array head coil. Following parameters were used: TR/TE = 8000/92 ms, matrix = 128 × 128, FOV = 256*256 mm², slices = 59 with a slice thickness of 2 mm, a gap thickness of 0 mm, voxel size = 2*2*2 mm³, and a pixel bandwidth of 1346 Hz/pixel. All images were positioned in the axial plane parallel to the commissure line. Scanners differed significantly in their signal-to-noise ratio ($t(73) = 2.12$, $p = 0.038$) (see Supplementary Fig. 2). However, linear regression analysis revealed no significant group-by-scanner interaction ($F(2, 69) = 0.35$, $p = 0.704$). To account for the difference in signal-to-noise ratio between scanners, groups were matched according to the scanner type, and scanner type was considered as a covariate in the analyses.

2.3. DTI data analyses

We used the Functional MRI of the Brain (FMRIB) TBSS software tools (Smith et al., 2006), part of the FMRIB Software Library (FSL 5.0) (Jenkinson et al., 2012). First, images were corrected for the effects of head movement and eddy currents. Second, FA images were created by fitting a tensor model to each voxel of the diffusion data and BET was used for brain extraction to exclude all non-brain voxels (Smith, 2002). Third, FA images of all subjects were aligned to the 1*1*1 mm³ Montreal Neurological Institute (MNI) standard space using FNIRT (Andersson et al., 2007a, b). The target image used in the registrations was the FMRIB58_FA standard-space image. As proof of robustness of the results, FA images of all subjects were also aligned to a study specific template to account for individual structural differences and its results are presented in Supplementary Fig. 3. Fourth, each subject's FA image was averaged to create the mean FA skeleton representing all

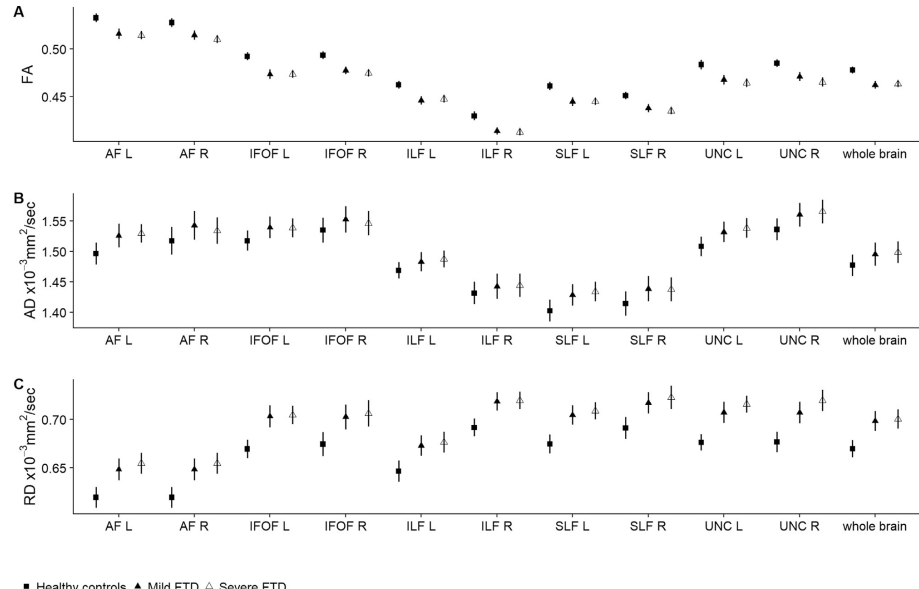


Fig. 1. (A) Fractional anisotropy (FA), (B) axial diffusivity (AD), and (C) radial diffusivity (RD) for all investigated white matter tracts. The scatterplots show the distribution of mean (\pm standard deviation) for healthy controls (squares), patients with mild (filled rectangles) and with severe formal thought disorder (outline rectangles) in all regions of interest and the whole brain skeleton.

major WM tracts common to the sample. The skeleton was thresholded at an FA value of 0.2 to prevent inclusion of non-skeletal voxels (Smith et al., 2006). Fifth, each subject's aligned FA data was projected onto the skeleton to be used in the voxel-wise cross-subject statistics. After every pre-processing step, data quality was checked visually using *fsview* and *fsleyes*. Sixth, ROI anatomical masks for the IFOF, ILF, SLF, and UF (Supplementary Fig. 4) were created based on the Johns Hopkins University (JHU) ICBM-DTI-81 WM labels atlas and the JHU-WM tractography atlas in MNI space (Hua et al., 2009; Wakana et al., 2004). In order to create the AF mask, the temporal branch of the SLF (JHU-WM tractography atlas) was selected. Lastly, mean FA values per subject were extracted from the ROIs by masking the FA skeleton with the created JHU-masks and from the whole brain by extracting the mean across the whole FA skeleton and used in further statistical analyses. Additionally, axial diffusivity (AD) and radial diffusivity (RD) were calculated using the FA images to achieve nonlinear registration as well as skeletonisation stages and to estimate the projection vectors from each subject onto the mean FA skeleton (see Supplementary Fig. 5). AD is thought to represent the movement in the direction of maximum diffusion, and RD to represent the movement perpendicular to this axis (Jones et al., 2013).

2.4. Statistical analyses

In order to examine the relationship between WM aberrations in the ROIs and severity of FTD, a series of multivariate linear regression analyses was performed, using the statistical program R 3.1.3 (Team, 2017). The TLC subscale scores were only available for a subsample of patients ($N = 41$). The regression analyses were based on this subsample. We

divided the test scores (TLC subscales, PANSS subscales) by the factor 10 to get a larger, and thus easier to read beta value. The TLC Sum, Disorganization Score (as an index of positive FTD), and Emptiness Score (as an index of negative FTD) were entered as dependent variables, mean FA values from the different ROIs as independent variables, and age, gender, scanner type, and whole brain FA as covariates. A second series of multivariate linear regression analyses was conducted in order to explore if WM aberrations in the ROIs are also related to overall psychopathology, using the PANSS Total Score, Positive Syndrome Scale, and Negative Syndrome Scale as dependent variables and the same independent variables and covariates as before. To account for possible biases due to multiple comparisons, false discovery rate (FDR) method was employed. Additionally, in order to examine if further WM tracts are affected by FTD in addition to the *a-priori* defined ROIs, voxel-wise cross-subject statistical analyses based on the whole WM skeleton were performed with randomize, using the data of all 49 participants. This non-parametric, permutation testing procedure of FSL uses a general linear model (GLM) (Smith et al., 2006), which we set up with age, gender, and scanner type as covariates. Exploratory pair-wise comparisons between groups (sFTD < HC, mFTD < HC, HC < sFTD, HC < mFTD, sFTD < mFTD, mFTD < sFTD) were conducted for the FA extracted from the whole brain skeleton. All contrasts were tested with 10'000 Monte Carlo random permutations. A threshold-free cluster enhancement (TFCE) was employed (Smith and Nichols, 2009) to enhance cluster-like structures in images. Results were corrected for multiple comparison (TFCE corrected) and labelled using the JHU-WM tractography atlas and the JHU ICBM-DTI-81 WM labels atlas to identify the impacted WM tracts (clusters > 100 voxels). To correct for the number of contrasts, the significance level was set to a $p < 0.01$ in order to protect from false positives.

3. Results

3.1. Descriptive statistics

The study sample ($N = 75$) consisted of 27 (36.0%) patients with mFTD, 22 (29.3%) patients with sFTD, and 26 (34.7%) HC. Patients did not differ from HC in age and gender, but in years of education. Post hoc Tukey test showed that patients with sFTD had significantly fewer years of education compared to HC ($p = 0.002$; see Supplementary Fig. 5). No significant group differences in years of education were found between patients with sFTD and patients with mFTD, as well as between patients with mFTD and HC. Patient groups did not differ in diagnosis, age of onset, duration of illness, and medication dosage (chlorpromazine equivalents) (Woods, 2003). However, significant group differences were found in severity of psychopathology (PANSS Positive Syndrome, General Psychopathology, Total Score) and FTD (TLC Disorganization, Sum Score), with higher scores in patients with mFTD than patients with sFTD. Full demographic data is shown in Table 1.

Fig. 1 gives the means and standard deviations of the FA, AD, and RD values for the ROIs as well as for the whole brain of the three study groups. In the following, we are going to present the results of our primary analyses concerning FA. For further information regarding our secondary analyses concerning AD and RD, see Supplementary Fig. 6.

3.2. Relationship between FA in ROIs with general psychopathology and FTD, respectively

Multivariate regression analyses revealed that severity of overall FTD (TLC Sum Score) was predicted by decreased FA in the right SLF ($p = 0.042$, uncorrected; see Table 2 and Fig. 2). Further, severity of

Table 2
Relation between fractional anisotropy (FA) and psychopathology.

	b	CI	p		p (FDR corrected)
			2.5%	97.5%	
TLC Total (per 10 points increase)					
Superior longitudinal fasciculus, right	-59.32	-101.64	-2.26	0.042*	0.420
TLC Emptiness (per 10 points increase)					
Arcuate fasciculus, left	7.05	0.61	13.50	0.033*	0.165
Superior longitudinal fasciculus, left	12.67	1.07	24.27	0.033*	0.165
PANSS Total (per 10 points increase)					
Uncinate fasciculus, right	-43.29	-79.19	-7.40	0.020*	0.100
PANSS Positive (per 10 points increase)					
Uncinate fasciculus, right	-14.61	-28.13	-1.09	0.035*	0.350

Notes: TLC, Thought, Language, and Communication scale; PANSS, Positive and Negative Syndrome Scale; PANSS Positive, PANSS Positive Syndrome Scale; b, corresponds to the unstandardized regression coefficient; CI, confidence interval, "per 10 points increase", FA values increase per beta times 10 points on the respective scale.

Multivariate linear regression; Significance at: *, $p < 0.05$.

negative FTD (TLC Emptiness Score) was predicted by increased FA in the left SLF ($p = 0.033$, uncorrected; see Table 2 and Fig. 2) and the left AF ($p = 0.033$, uncorrected; see Table 2 and Fig. 2). Positive FTD (TLC Disorganization Score) was not related to FA in neither of the ROIs (Table 2 and Fig. 2). Severity of overall psychopathology (PANSS Total Score) as well as of positive symptoms (PANSS Positive Syndrome) was predicted by decreased FA in the right UF (Total Score: $p = 0.020$, Positive Syndrome: $p = 0.035$, all uncorrected; see Table 2 and Fig. 2). These results were no longer significant after employing FDR method to adjust for possible biases due to multiple comparisons.

3.3. Whole brain analyses

Voxel-wise comparisons in the whole brain WM skeleton of FA values using the GLM revealed a significant main effect of group (TFCE corrected $p < 0.01$). Patients differed significantly from HC, showing systematically lower FA throughout the whole WM skeleton (see Figs. 1 and 3). In particular, patients compared to HC (HC > sFTD, HC > mFTD) showed significantly lower FA in the ROIs as well as in eleven additional WM tracts including association, projection, and commissural fibres (TFCE corrected $p < 0.01$; HC > sFTD: Table 3; HC > mFTD: Table 4). Yet, patient groups (sFTD > mFTD, mFTD > sFTD) did not differ in FA in the whole WM skeleton (sFTD > mFTD: $p = 0.679$; mFTD > sFTD: $p = 0.639$; see Fig. 3).

4. Discussion

This study used TBSS to examine WM aberrations in language-related tracts (AF, ILF, IFOF, SLF, and UF) as correlates of FTD in patients with schizophrenia. Severity of overall FTD was predicted by decreased FA in the right SLF, and severity of negative FTD was predicted by increased FA in the left SLF and AF, partly supporting our first hypothesis. In addition, severity of overall psychopathology and severity of positive symptoms was predicted by decreased FA in the right UF. Notably, these results were no longer statistically significant after adjustment for multiple comparisons. Whole brain analyses revealed lower FA in patients compared to HC in all the investigated language-related WM tracts, as well as across the whole WM skeleton, with patients with severe FTD and patients with mild FTD showing similar low FA. These results are partly in line with our second hypothesis. Finally, while the main focus of this study was on changes in FA associated with FTD, secondary analyses focusing on AD and RD were conducted (presented in the Supplementary Materials) that revealed no group differences in AD, but significant higher RD throughout the whole WM-skeleton including language-related tracts in both patient groups compared to HC.

4.1. FTD in schizophrenia may be linked to WM aberrations of language areas

Patients with mild and severe FTD did not differ in FA in language-related WM tracts, but showed both significantly lower FA than HC. In the whole patient group, FA in the SLF and AF were significantly associated with FTD severity. Notably, the latter results were no longer statistically significant after adjustment for multiple comparisons. However, our results are consistent with other studies reporting aberrations of language-related WM tracts to be associated with FTD in schizophrenia (Asami et al., 2013; Riguucci et al., 2013; Viher et al., 2018; Zhou et al., 2017). In particular, Viher et al. (2018) found that higher FA values in the bilateral SLF were associated with more negative FTD in patients with schizophrenia and Zhou et al. (2017) reported a positive correlation between FA in the right SLF II, including the rostral AF, and FTD in patients with first-episode psychosis. However, we were not able to replicate recent findings of associations between FTD and FA in the IFOF (Riguucci et al., 2013; Viher et al., 2018), ILF (Riguucci et al., 2013; Viher et al., 2018) and UF (Viher et al., 2018), respectively. This may be due to

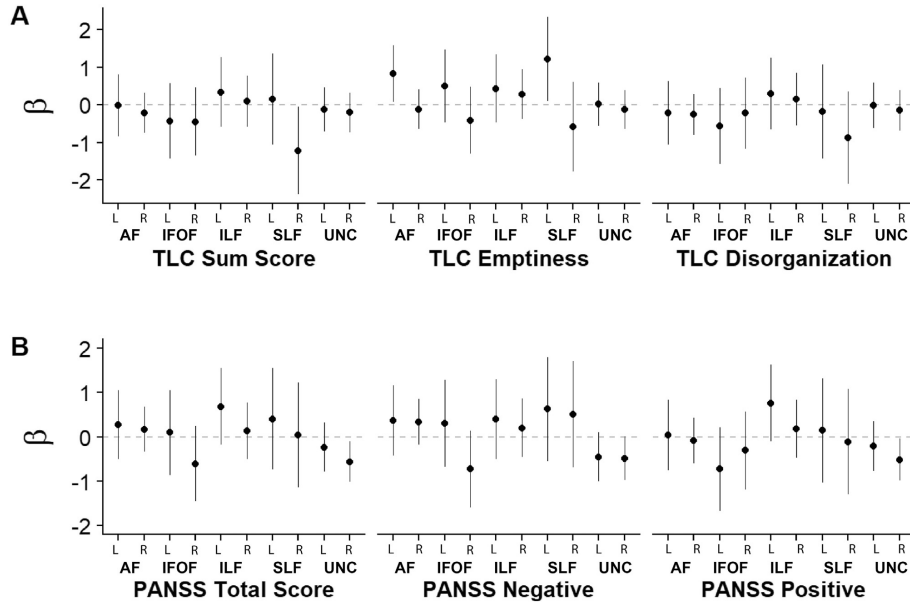


Fig. 2. White matter integrity predicts severity of (A) formal thought disorder and (B) general psychopathology. The dot plots show standardized regression coefficients with 95% confidence intervals. Mean beta values (dots) reflect the partial correlation (positive > 0 ; negative < 0) of fractional anisotropy with FTD. Confidence intervals not touching the zero line indicate an uncorrected significant effect at $p < 0.05$.

differences in the clinical samples with regard to illness duration, age, and medication exposure, which have been found to affect WM integrity (Samartzis et al., 2014), different FTD assessment methods (i.e., Disorganized PANSS factor, Bern Psychopathology Scale, and TLC), and the methods used during image acquisition and analysis. In summary, we found evidence for structural aberrations of the dorsal language pathway (SLF, AF) to be associated with FTD in schizophrenia. Being aware that the SLF/AF is a multi-component structure and that the SLF and AF are anatomically not easily distinguishable (Friederici, 2015), to date the fibre bundle connecting the temporal cortex (i.e. Wernicke's area) to the IFG (i.e., Broca's area), either directly or indirectly via the inferior parietal lobe (IPL), is named the AF, whereas the fibre bundle connecting the temporal cortex with the premotor cortex (PMC) via the IPL is most commonly named the SLF (Friederici, 2015). Thus, our results also correspond with the broader literature reporting FTD in schizophrenia to be associated with aberrations in grey matter (Horn et al., 2009, 2010; Palaniyappan et al., 2015; Sans-Sansa et al., 2013), resting state perfusion (Horn et al., 2009; Sabri et al., 1997; Stegmayer et al., 2017), and blood oxygenation level-dependent (BOLD) activation (Arcuri et al., 2012; Horn et al., 2012; Kircher et al., 2001b, 2002, 2003; McGuire et al., 1998) in the IFG, temporal cortex, and IPL, which are involved in auditory perception and language processing (Friederici, 2015). Considering that the specific functions of the SLF/AF are still under debate, the AF has been found to support the processing of syntactically complex sentences, possibly by providing top-down predictions for the incoming input (Friederici, 2015). Notably, patients with schizophrenia and FTD show impaired comprehension and production of syntactically complex sentences (Covington et al., 2005), and the articulation of syntactically more simple sentences was associated with an absence of activation in the right temporal and left superior frontal cortex (Kircher et al., 2005). The SLF terminating in the PMC has been allocated to auditory-motor-

integration; that is the production and articulation of perceived speech sounds, including verbal self-monitoring (Friederici, 2015; Hickok and Poeppel, 2007). In patients with schizophrenia, the severity of FTD during the production of free speech in the scanner was negatively correlated with BOLD changes in the left temporal cortex and positively correlated with BOLD changes in the right PMC (Kircher et al., 2001b). Also, between-clause pauses as an indicator of deficient speech planning and monitoring has been found to be linked to reduced engagement of the left temporal cortex in patients with schizophrenia and FTD (Matsumoto et al., 2013). Thus, our results of associations between aberrations in the SLF/AF and FTD refer to an altered connectivity between frontal and temporo-parietal language regions, which have been found to be involved in FTD in schizophrenia. To bear in mind, these conclusions have to be considered as preliminary and need further confirmation through replication, as our regression results were no longer significant after adjustment for multiple comparisons.

Interestingly, WM aberrations (both increased and decreased FA) in the SLF/AF have also been found to be associated with auditory hallucinations (AH) in patients with schizophrenia (Geoffroy et al., 2014; Hubl et al., 2004; McCarthy-Jones et al., 2015; Psomiades et al., 2016; Shergill et al., 2007). It has been argued that FTD and AH are both clinical manifestations of abnormal language processing, while the individual pattern of the involved network components might determine the psychopathological features (Strik et al., 2008). As both the SLF and AF consist of multiple subcomponents, which are differently relevant for language processing (Friederici, 2015; Geoffroy et al., 2014), future studies are needed to disentangle the distinct associations of altered SLF/AF subcomponents with FTD and AH in schizophrenia.

In our study, severity of overall psychopathology as well as severity of positive symptoms was predicted by decreased FA in the right UF. The UF was the only investigated language-related WM tract found to

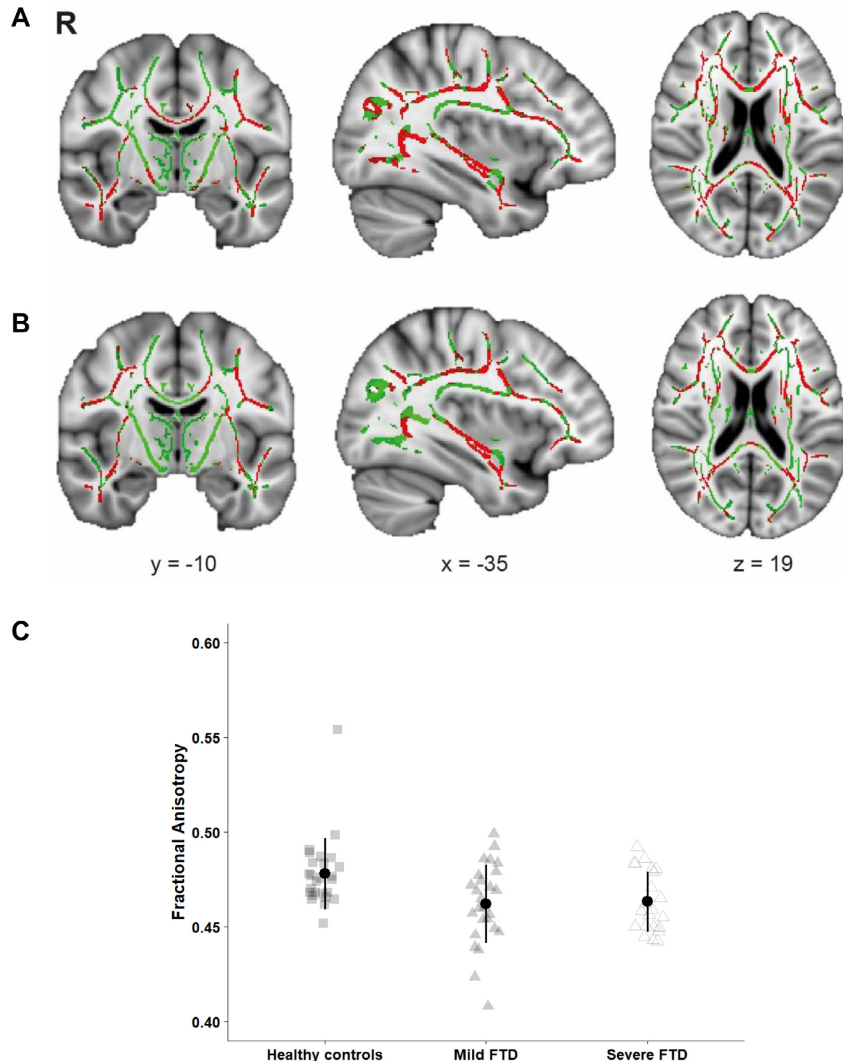


Fig. 3. Reduced white matter integrity in (A) patients with mild frontotemporal disorder (FTD) and (B) patients with severe FTD. Corrected tract-based statistics analysis (TBSS) indicates significantly lower fractional anisotropy (FA) throughout the whole WM-skeleton for both patient groups compared to healthy controls (TFCE corrected $p < 0.01$). TBSS results (red) overlaid on the whole brain FA-skeleton (green) and presented on the Montreal Neurological Institute template. The scatterplots (C) overlaid with the mean (dot) and standard deviation (whiskers) show the distribution of FA for the three groups in the whole brain WM-skeleton. (For interpretation of the references to colour in this figure legend, the reader is referred to the web version of this article.)

be related to overall psychopathology and positive symptoms. Again, the correlations between FA in the right UF and severity of overall psychopathology and of positive symptoms, respectively, were no longer significant after adjustment for multiple comparisons and have, thus, to be interpreted with caution. However, our results correspond

with the literature reporting reduced FA in the UF to be associated with severity of positive (Curcic-Blake et al., 2015; Zhang et al., 2018) symptoms, and may indicate that WM deficits in the UF are not specifically related to FTD, but to psychotic symptoms in general.

Table 3

Whole brain voxel-wise comparison shows higher fractional anisotropy for healthy controls (HC) than for patients with severe formal thought disorder (sFTD). (HC > sFTD).

WM tract	Hemisphere	Voxels	Centre of gravity			t-value	p-value
			x	y	z		
Anterior thalamic radiation	Left	1790	113	124	84	2.02	0.002**
	Right	1065	66	140	86	1.82	0.002**
Corticospinal tract	Left	261	109	107	72	1.76	0.003**
	Right	285	69	104	89	1.83	0.002**
Cingulum (Gingulate gyrus)	Left	868	104	106	101	2.07	0.001***
	Right	298	72	91	105	2.01	0.002**
Forceps major		1236	91	61	89	1.83	0.002*
Forceps minor		3332	92	162	80	2.02	0.001***
Inferior fronto-occipital fasciculus	Left	1906	121	121	73	1.98	0.002**
	Right	2599	59	130	76	1.95	0.001***
Inferior longitudinal fasciculus	Left	1308	128	101	67	1.89	0.003**
	Right	1270	47	104	64	1.82	0.002**
Superior longitudinal fasciculus (SLF)	Left	3319	131	104	93	1.98	0.004**
	Right	3145	50	105	98	1.88	0.004**
Uncinate fasciculus	Left	474	122	144	62	2.01	0.003**
	Right	613	67	146	60	1.96	0.001***
SLF (temporal part)		388	42	87	69	2.04	0.007**
Corpus callosum							
Genu		1540	91	154	81	2.25	0.001***
Body		1824	92	125	100	2.11	0.001***
Splenium		1121	85s	85	93	1.91	0.002**
Cerebral peduncle	Left	106	106	106	63	1.62	0.004**
Internal capsule							
Anterior limb	Right	228	69	134	84	1.77	0.006**
Left	415	109	135	82	2.15	0.002**	
Retro Lenticular part	Right	240	57	101	74	1.80	0.005**
Left	347	122	99	75	1.96	0.002**	
Corona radiate							
Anterior	Right	734	68	155	77	1.90	0.001***
Left	940	110	155	81	1.96	0.001***	
Superior	Right	283	68	118	105	1.75	0.003**
Posterior	Right	346	110	124	103	2.08	0.001***
Left	250	67	82	103	2.31	0.003**	
Posterior thalamic radiation (include optic radiation)	Left	142	112	81	102	1.76	0.002**
External capsule	Right	278	124	70	75	1.77	0.009**
		646	59	124	71	2.05	0.002**

Notes: WM white matter. Voxel-wise statistical analysis indicating significant differences between patients and healthy controls ($p < 0.01$, cluster size ≥ 100 voxels), with clusters labelled using the JHU White Matter Tractography Atlas.

Significant at: **, $p < 0.01$; ***, $p < 0.001$.

4.2. FTD dimensions may have different neurobiological underpinnings

In patients, severity of overall FTD was predicted by reduced FA in the right SLF and severity of negative FTD was predicted by increased FA in the left SLF and AF. While keeping in mind that these results were no longer significant after adjustment for multiple comparisons and need, thus, replication before drawing final conclusions, it could be argued that in patients with schizophrenia relatively lower FA in the right SLF increases vulnerability for overall FTD, while relatively higher FA in the left SLF and AF increases vulnerability for negative FTD. However, even in the patients who showed the most severe FTD, the FA in those regions were lower than in HC. These results support the notion that FTD is a multidimensional entity (Roche et al., 2015), are in line with the literature reporting distinct structural and functional aberrations in the language network to be associated with positive and negative FTD (Arnedo et al., 2015; Kircher et al., 2003; Palaniyappan et al., 2015; Sans-Sansa et al., 2013; Stegmayer et al., 2017; Viher et al., 2018), and highlight the importance of differentiating subtypes of FTD in future studies investigating the neurobiological underpinnings of this syndrome. Further, they contradict the simplistic postulate that higher FA is always better, as reduced FA indicates diminished anatomical connectivity. Alba-Ferrara and de Frausquin (2013) argued that aberrant connectivity, including both increases and decreases in FA, could refer to either a diffuse dysregulation of neural networks underlying

schizophrenia symptoms or possible compensatory changes in response to primary deficits. Which explanation is more likely can only be decided on the basis of longitudinal studies that have been lacking to date.

4.3. WM aberrations in patients with schizophrenia are widespread across the whole brain

WM deficits including reduced FA along with unaltered AD and increased RD in patients with schizophrenia compared to HC were not restricted to language-related tracts, but were found across the whole WM skeleton, including association, projection, and commissural fibres. The combination of reduced FA, unaltered AD, and increased RD in patients compared to HC may indicate demyelination of the affected WM tracts (Feldman et al., 2010). Our results are in line with the literature reporting FA reduction along with RD increases across all major WM tracts in patients with schizophrenia (Ellison-Wright and Bullmore, 2009; Kelly et al., 2017; Vitolo et al., 2017). Recent meta-analyses revealed a (rather weak) relationship between FA alterations and positive and negative symptoms in patients with schizophrenia (Kelly et al., 2017; Yang et al., 2017). Thus, our whole-brain results contribute to the literature suggesting symptoms of schizophrenia are due to disrupted structural connectivity between brain regions (Wheeler and Voineskos, 2014).

Table 4

Whole brain voxel-wise comparison shows higher fractional anisotropy for healthy controls (HC) than for patients with mild formal thought disorder (mFTD). (HC > mFTD).

WM tract	Hemisphere	Voxels	Centre of gravity			t-value	p-value
			x	y	z		
Anterior thalamic radiation	Left	1820	112	125	84	1.88	0.001***
	Right	1253	68	137	83	1.78	0.001***
Corticospinal tract	Left	701	110	104	87	1.79	0.004**
	Right	739	71	105	84	1.85	0.004**
Cingulum (Gingulate gyrus)	Left	914	105	106	101	2.08	0.001***
	Right	298	73	95	103	2.12	0.001***
Forceps major		2215	88	55	86	1.80	0.003**
Forceps minor		3721	91	161	81	2.13	0.001***
Inferior fronto-occipital fasciculus	Left	2069	120	118	75	1.98	0.003**
	Right	3028	59	115	76	1.87	0.002**
Inferior longitudinal fasciculus	Left	1172	126	84	74	1.94	0.003**
	Right	1674	48	96	63	1.94	0.004**
Superior longitudinal fasciculus (SLF)	Left	3504	129	99	99	1.87	0.003**
	Right	2188	52	97	97	1.84	0.004**
Uncinate fasciculus	Left	429	115	148	67	1.87	0.001***
	Right	498	68	145	60	2.02	0.001***
SLF (temporal part)		322	43	88	69	1.88	0.004**
Corpus callosum							
Genu		1642	90	154	81	2.41	0.001***
Body		2260	91	125	100	2.20	0.001***
Splenium		1187	88	84	94	1.96	0.001***
Cerebral peduncle							
Right		307	76	108	61	1.85	0.005**
Left		257	105	106	61	1.75	0.004**
Internal capsule							
Anterior limb		440	71	135	81	1.81	0.004**
Left		420	108	135	81	1.88	0.003**
Retrolenticular part		244	57	100	73	1.80	0.005**
Left		336	122	99	74	2.07	0.004**
Corona radiate							
Anterior		906	69	155	80	1.98	0.001***
Left		1053	110	156	81	1.99	0.001***
Superior		485	68	117	106	1.81	0.001***
Left		472	111	118	105	1.83	0.001***
Posterior		340	66	86	103	1.96	0.004**
Posterior thalamic radiation (include optic radiation)							
Right		189	112	83	103	2.02	0.001***
Left		605	57	70	79	1.85	0.005**
External capsule							
Right		704	123	68	79	2.07	0.003**
Right		478	59	123	71	1.95	0.003**

Notes: WM white matter. Voxel-wise statistical analysis indicating significant differences between patients and healthy controls ($p < 0.01$, cluster size ≥ 100 voxels), with clusters labelled using the JHU White Matter Tractography Atlas.

Significant at: **, $p < 0.01$; ***, $p < 0.001$.

4.4. Limitations

Several limitations ought to be considered in this study. First, in TBSS voxels that contain maximal FA are projected onto the ‘skeleton’. This restricts the analysis to the central part of the WM tracts, but leads to a loss of individual structural variability of the tracts (Bach et al., 2014) and may not correct all remaining misalignments (Bach et al., 2014). Also, to account for the constraint of individual structural variability, we additionally performed the TBSS analysis with a study specific template. Results did not differ independently of which template was used. Second, the anatomical distinction of the SLF and the AF on the basis of the used JHU-atlas is limited. Because of the lack of a specific AF-mask in these atlases, the temporal branch of the SLF was used and is, therefore, more of an approximation to the complex structure of the AF. Third, 48.0% of measurements were conducted on a different scanner. To account for this, scanner type was included as a covariate in the statistical models and the groups were matched with respect to this variable. While FA values obtained from the two scanners differed significantly, we found no evidence for a group-by-scanner interaction, indicating that the group effects did not depend on the scanner type. Fourth, it could be argued that the cut-off of 10 for the TLC Sum Score that was used to stratify patients into a group with mild FTD and a group with severe FTD is arbitrary. Given that there is no

established cut-off for the TLC, a cut-off of 10 was chosen as predefined in the initial study proposal. We repeated the group comparisons using the median of the TLC Sum Score as cut-off for the groups, which did not change the results. Fifth, patients with severe FTD had significantly fewer years of education than HC. Our main interest lay, however, in differences between patients with mild and patients with severe FTD, who did not differ in years of education. Nevertheless, we included years of education as an additional covariate in the linear model (see Supplementary Fig. 5) and found similar results, with the exception that the left AF and SLF did no longer predict negative FTD. Sixth, even if all participants showed good German skills, a minority were not native speaker ($n = 3$) and information on the mother tongue was not available from $N = 15$. Seventh, this study combined the samples of two studies that differed with regard to the diagnostic assessment: In the first study diagnoses were made by an experienced clinician, while in the second study diagnoses were based on a structured clinical interview (i.e., MINI). Lastly, the sample size was relatively small. Small samples lack the power to conclusively decide whether a non-significant finding actually reflects the absence of an effect altogether or whether the effect was relevant but just too small to be detected (Button et al., 2013). The regression results were no longer significant after employing FDR method to adjust for possible biases due to multiple comparisons. While p-value adjustments reduce the risk of making

type I errors (“false positive” finding), they increase the risk of making type II errors (“false negative” finding) and the sample size needed to find an effect (Feise, 2002). Thus, our non-significant findings for the associations between FA in the language-related ROIs and severity in FTD after adjustment for multiple comparisons may be due to the small sample size and lack of power in the current study, calling for replication in larger samples.

4.5. Conclusions

The current study found that in patients with schizophrenia severity of overall FTD was predicted by decreased FA in the right SLF, and severity of negative FTD was predicted by increased FA in the left SLF and AF. These results were no longer significant after adjustment for multiple comparisons, which may be due to a lack of power in the current study. In addition, compared with HC, patients showed lower FA along with unaffected AD and increased RD throughout the whole WM skeleton, including language-related WM tracts (i.e., the AF, IFOF, ILF, SLF, and UF), while no differences in diffusion measures were found between patients with severe FTD and patients with mild FTD. Overall, our results are compatible with earlier studies reporting impairments in widely spread WM tracts, including those related to the language network. The specificity of abnormal structural connections between language-related brain regions for FTD in patients with schizophrenia needs further examination in larger samples.

Contributors

AF, WS, HH, SeW and PH were involved in the design and setup of the study. MC, KS, and KL did the data collection. STW, AF, SG and PH analysed the data. MC and SW wrote the first draft. All authors contributed to and approved the final manuscript version.

Conflict of interest

None.

Funding

This research has been supported by grants from the Swiss National Science Foundation (#320030_146789, #152619, #127359) and a grant from the Bangerter-Rhyner-Foundation to SeW.

Supplementary materials

Supplementary material associated with this article can be found, in the online version, at doi:10.1016/j.psychresns.2018.05.011.

References

- Alba-Ferrara, L.M., de Erausquin, G.A., 2013. What does anisotropy measure? Insights from increased and decreased anisotropy in selective fiber tracts in schizophrenia. *Front. Integr. Neurosci.* 7, 9.
- American Psychiatric Association, 2000. Diagnostic and Statistical Manual of Mental Disorders, fourth ed. text rev. American Psychiatric Association, Washington, D.C.
- Andersson, J.L., Jenkinson, M., Smith, S., 2007a. Non-Linear Optimisation. University of Oxford FMRIB Centre, Oxford, UK FMRIB Technical Report TR07JA1.
- Andersson, J.L., Jenkinson, M., Smith, S., 2007b. Non-Linear Registration, Aka Spatial Normalisation FMRIB Technical Report TR07JA2. FMRIB Analysis Group of the University of Oxford 2.
- Arcuri, S.M., Broome, M.R., Giampietro, V., Amaro Jr., E., Kircher, T.T., Williams, S.C., et al., 2012. Faulty suppression of irrelevant material in patients with thought disorder linked to attenuated frontotemporal activation. *Schizophr. Res. Treat.* 2012, 176290.
- Arnedo, J., Mamah, D., Baranger, D.A., Harms, M.P., Barch, D.M., Svrakic, D.M., et al., 2015. Decomposition of brain diffusion imaging data uncovers latent schizophrenias with distinct patterns of white matter anisotropy. *Neuroimage* 120, 43–54.
- Asami, T., Saito, Y., Whitford, T.J., Makris, N., Niznikiewicz, M., McCarley, R.W., et al., 2013. Abnormalities of middle longitudinal fascicle and disorganization in patients with schizophrenia. *Schizophr. Res.* 143, 253–259.
- Bach, M., Laun, F.B., Leemans, A., Tax, C.M., Biessels, G.J., Stielstra, B., et al., 2014. Methodological considerations on tract-based spatial statistics (TBSS). *Neuroimage* 100, 358–369.
- Bleuler, E., 1958. *Dementia Praecox or the Group of Schizophrenias*. International Universities Press, New York.
- Bopp, M.H.A., Zollner, R., Jansen, A., Dietsche, B., Krug, A., Kircher, T.T.J., 2017. White matter integrity and symptom dimensions of schizophrenia: a diffusion tensor imaging study. *Schizophr. Res.* 184, 59–68.
- Button, K.S., Ioannidis, J.P., Mokrysz, C., Nosek, B.A., Flint, J., Robinson, E.S., et al., 2013. Power failure: why small sample size undermines the reliability of neuroscience. *Nat. Rev. Neurosci.* 14, 365–376.
- Cavelti, M., Homan, P., Vauth, R., 2016. The impact of thought disorder on therapeutic alliance and personal recovery in schizophrenia and schizoaffective disorder: an exploratory study. *Schizophr. Res.* 239, 92–98.
- Cavelti, M., Kircher, T., Nagels, A., Strik, W., Homan, P., 2018. Is formal thought disorder in schizophrenia related to structural and functional aberrations in the language network? A systematic review of neuroimaging findings. *Schizophr. Res.* <http://dx.doi.org/10.1016/j.schres.2018.02.051>.
- Covington, M.A., He, C., Brown, C., Naci, L., McClain, J.T., Fjordbak, B.S., et al., 2005. Schizophrenia and the structure of language: the linguist's view. *Schizophr. Res.* 77, 85–98.
- Curcic-Blake, B., Nanetti, L., van der Meer, L., Cerliani, L., Renken, R., Pijnenborg, G.H., et al., 2015. Not on speaking terms: hallucinations and structural network disconnection in schizophrenia. *Brain Struct. Funct.* 220, 407–418.
- Ellison-Wright, I., Bullmore, E., 2009. Meta-analysis of diffusion tensor imaging studies in schizophrenia. *Schizophr. Res.* 108, 3–10.
- Feise, R.J., 2002. Do multiple outcome measures require p-value adjustment? *BMC Med. Res. Methodol.* 2, 8.
- Feldman, H.M., Yeatman, J.D., Lee, E.S., Barde, L.H., Gaman-Bean, S., 2010. Diffusion tensor imaging: a review for pediatric researchers and clinicians. *J. Dev. Behav. Pediatr.* 31, 346–356.
- First, M.B., Gibbon, M., Spitzer, R.L., 1996. Structured Clinical Interview for DSM-IV Axis I Disorders-Patient Version (SCID-I/P). Biometrics Research Department, New York State Psychiatric Institute, New York, NY.
- Friderici, A.D., 2015. White-matter pathways for speech and language processing. *Handb. Clin. Neurol.* 129, 177–186.
- Gelman, A., Stern, H., 2006. The difference between “significant” and “not significant” is not itself statistically significant. *Am. Stat.* 60, 328–331.
- Geoffroy, P.A., Houenou, J., Duhamel, A., Amad, A., De Weijer, A.D., Curcic-Blake, B., et al., 2014. The Arcuate Fasciculus in auditory-verbal hallucinations: a meta-analysis of diffusion-tensor-imaging studies. *Schizophr. Res.* 159, 234–237.
- Hickok, G., Poeppel, D., 2007. The cortical organization of speech processing. *Nat. Rev. Neurosci.* 8, 393–402.
- Horn, H., Federspiel, A., Wirth, M., Muller, T.J., Wiest, R., Walther, S., et al., 2010. Gray matter volume differences specific to formal thought disorder schizophrenia. *Psychiatry Res.* 182, 183–186.
- Horn, H., Federspiel, A., Wirth, M., Muller, T.J., Wiest, R., Wang, J.J., et al., 2009. Structural and metabolic changes in language areas linked to formal thought disorder. *Br. J. Psychiatry* 194, 130–138.
- Horn, H., Jann, K., Federspiel, A., Walther, S., Wiest, R., Muller, T., et al., 2012. Semantic network disconnection in formal thought disorder. *Neuropsychobiology* 66, 14–23.
- Hua, K., Oishi, K., Zhang, J., Wakana, S., Yoshioka, T., Zhang, W., et al., 2009. Mapping of functional areas in the human cortex based on connectivity through association fibers. *Cereb. Cortex*, 19, 1889–1895.
- Hubl, D., Koenig, T., Strik, W., Federspiel, A., Kreis, R., Boesch, C., et al., 2004. Pathways that make voices: white matter changes in auditory hallucinations. *Arch. Gen. Psychiatry* 61, 658–668.
- Jbabdi, S., Johansen-Berg, H., 2011. Tractography: where do we go from here? *Brain Connect.* 1, 169–183.
- Jenkinson, M., Beckmann, C.F., Behrens, T.E., Woolrich, M.W., Smith, S.M., 2012. Fsl. *Neuroimage* 62, 782–790.
- Jones, S.R., Knösche, T.R., Turner, R., 2013. White matter integrity, fiber count, and other fallacies: the do's and don'ts of diffusion MRI. *Neuroimage* 73, 239–254.
- Kay, S.R., Fiszbein, A., Opler, L.A., 1987. The positive and negative syndrome scale (PANS) for schizophrenia. *Schizophr. Bull.* 13, 261–276.
- Kellmeyer, P., Ziegler, W., Peschke, C., Juliane, E., Schnell, S., Baumgaertner, A., et al., 2013. Fronto-parietal dorsal and ventral pathways in the context of different linguistic manipulations. *Brain Lang.* 127, 241–250.
- Kelly, S., Jahanshad, N., Zalesky, A., Kochunov, P., Agartz, I., Alloza, C., et al., 2017. Widespread white matter microstructural differences in schizophrenia across 4322 individuals: results from the ENIGMA schizophrenia DTI Working Group. *Mol. Psychiatry* 101.1038/mp.2017.170.
- Kircher, T., 2008. Neurobiological foundations of thought and language disorder in schizophrenia. *Fortschr. Neurol. Psychiatr.* 76 (Suppl 1), S24–S32.
- Kircher, T., Liddle, P., Brammer, M., Murray, R., McGuire, P., 2003. Neural correlates of “negative” formal thought disorder. *Der. Nervenarzt.* 74, 748–754.
- Kircher, T.T., Bullmore, E.T., Brammer, M.J., Williams, S.C., Broome, M.R., Murray, R.M., et al., 2001a. Differential activation of temporal cortex during sentence completion in schizophrenic patients with and without formal thought disorder. *Schizophr. Res.* 50, 27–40.
- Kircher, T.T., Liddle, P., Brammer, M., Williams, S., Murray, R., McGuire, P., 2002. Reversed lateralization of temporal activation during speech production in thought disordered patients with schizophrenia. *Psychol. Med.* 32, 439–449.
- Kircher, T.T., Liddle, P., Brammer, M.J., Williams, S.C., Murray, R.M., McGuire, P.K., 2001b. Neural correlates of formal thought disorder in schizophrenia: preliminary findings from a functional magnetic resonance imaging study. *Arch. Gen. Psychiat.*

- 58, 769–774.
- Kircher, T.T., Oh, T.M., Brammer, M.J., McGuire, P.K., 2005. Neural correlates of syntax production in schizophrenia. *Br. J. Psychiatry* 186, 209–214.
- Lecrubier, Y., Sheehan, D.V., Weiller, E., Amorim, P., Bonora, I., Harnett Sheehan, K., et al., 1997. The Mini International Neuropsychiatric Interview (MINI): a short diagnostic structured interview: reliability and validity according to the CIDI. *Eur. Psychiatr.* 12, 224–231.
- Makris, N., Zhu, A., Papadimitriou, G.M., Mouradian, P., Ng, I., Scaccianoce, E., et al., 2017. Mapping temporo-parietal and temporo-occipital cortico-cortical connections of the human middle longitudinal fascicle in subject-specific, probabilistic, and stereotaxic Talairach spaces. *Brain Imaging Behav.* 11, 1258–1277.
- Matsumoto, K., Kircher, T.T., Stokes, P.R., Brammer, M.J., Liddle, P.F., McGuire, P.K., 2013. Frequency and neural correlates of pauses in patients with formal thought disorder. *Front. Psychiatry* 4, 127.
- McCarthy-Jones, S., Oestreich, L.K., Australian Schizophrenia Research, B., Whitford, T.J., 2015. Reduced integrity of the left arcuate fasciculus is specifically associated with auditory verbal hallucinations in schizophrenia. *Schizophr. Res.* 162, 1–6.
- McGuire, P.K., Quested, D.J., Spence, S.A., Murray, R.M., Firth, C.D., Liddle, P.F., 1998. Pathophysiology of ‘positive’ thought disorder in schizophrenia. *Br. J. Psychiatry* 173, 231–235.
- Nagels, A., Fahrmann, P., Stratmann, M., Ghazi, S., Schales, C., Frauenheim, M., et al., 2016. Distinct neuropsychological correlates in positive and negative formal thought disorder syndromes: the thought and language disorder scale in endogenous psychoses. *Neuropsychobiology* 73, 139–147.
- Nagels, A., Stratmann, M., Ghazi, S., Schales, C., Frauenheim, M., Turner, L., et al., 2013. The German translation and validation of the scale for the assessment of thought, language and communication: a factor analytic study. *Psychopathology* 46, 390–395.
- Olffield, R.C., 1971. The assessment and analysis of handedness: the Edinburgh inventory. *Neuropsychologia* 9, 97–113.
- Palaniswami, L., Mahmood, J., Balain, V., Mougin, O., Gowland, P.A., Liddle, P.F., 2015. Structural correlates of formal thought disorder in schizophrenia: an ultra-high field multivariate morphometry study. *Schizophr. Res.* 168, 305–312.
- Psomiades, M., Fontenelle, C., Mondino, M., Luck, D., Haesebaert, F., Suaud-Chagny, M.F., et al., 2016. Integrity of the arcuate fasciculus in patients with schizophrenia with auditory verbal hallucinations: a DTI-tractography study. *Neuroimage Clin.* 12, 970–975.
- Rajarethinam, R.P., DeQuardo, J.R., Nalepa, R., Tandon, R., 2000. Superior temporal gyrus in schizophrenia: a volumetric magnetic resonance imaging study. *Schizophr. Res.* 41, 303–312.
- Rigucci, S., Rossi-Espagnet, C., Ferracuti, S., De Carolis, A., Corigliano, V., Carducci, F., et al., 2013. Anatomical substrates of cognitive and clinical dimensions in first episode schizophrenia. *Acta Psychiatr. Scand.* 128, 261–270.
- Roche, E., Creed, L., MacMahon, D., Brennan, D., Clarke, M., 2015. The epidemiology and associated phenomenology of formal thought disorders: a systematic review. *Schizophr. Bull.* 41, 951–962.
- Sabri, O., Erkwoh, R., Schreckenberger, M., Owega, A., Sass, H., Buell, U., 1997. Correlation of positive symptoms exclusively to hyperperfusion or hypoperfusion of cerebral cortex in never-treated schizophrenics. *Lancet* 349, 1735–1739.
- Samaridis, L., Dima, D., Fusar-Poli, P., Kyriakopoulos, M., 2014. White matter alterations in early stages of schizophrenia: a systematic review of diffusion tensor imaging studies. *J. Neuroimaging* 24, 101–110.
- Sans-Sansa, B., McKenna, P.J., Canales-Rodriguez, E.J., Ortiz-Gil, J., Lopez-Araquistain, L., Sarro, S., et al., 2013. Association of formal thought disorder in schizophrenia with structural brain abnormalities in language-related cortical regions. *Schizophr. Res.* 146, 308–313.
- Shergill, S.S., Kanaan, R.A., Chitnis, X.A., O'Daly, O., Jones, D.K., Frangou, S., et al., 2007. A diffusion tensor imaging study of fasciculi in schizophrenia. *Am. J. Psychiatry* 164, 467–473.
- Sigaudo, M., Crivelli, B., Castagna, F., Giugiaro, M., Mingrone, C., Montemagni, C., et al., 2014. Quality of life in stable schizophrenia: the relative contributions of disorganization and cognitive dysfunction. *Schizophr. Res.* 153, 196–203.
- Silverstein, M.L., Marengo, J.T., Fogg, L., 1991. Two types of thought disorder and lateralized neuropsychological dysfunction. *Schizophr. Bull.* 17, 679–687.
- Smith, S.M., 2002. Fast robust automated brain extraction. *Hum. Brain Mapp.* 17, 143–155.
- Smith, S.M., Jenkinson, M., Johansen-Berg, H., Rueckert, D., Nichols, T.E., Mackay, C.E., et al., 2006. Tract-based spatial statistics: voxelwise analysis of multi-subject diffusion data. *Neuroimage* 31, 1487–1505.
- Smith, S.M., Nichols, T.E., 2009. Threshold-free cluster enhancement: addressing problems of smoothing, threshold dependence and localisation in cluster inference. *Neuroimage* 44, 83–98.
- Stegmayer, K., Stettler, M., Strik, W., Federspiel, A., Wiest, R., Bohlhalter, S., et al., 2017. Resting state perfusion in the language network is linked to formal thought disorder and poor functional outcome in schizophrenia. *Acta Psychiatr. Scand.* 136, 506–516.
- Strik, W., Dierks, T., Hubl, D., Horn, H., 2008. Hallucinations, thought disorders, and the language domain in schizophrenia. *Clin. EEG Neurosci.* 39, 91–94.
- Strik, W., Stegmayer, K., Walther, S., Dierks, T., 2017. Systems neuroscience of psychosis: mapping schizophrenia symptoms onto brain systems. *Neuropsychobiology* 75, 100–116.
- Summer, P.J., Bell, I.H., Rossell, S.L., 2017. A systematic review of the structural neuroimaging correlates of thought disorder. *Neurosci. Biobehav. Rev.* 84, 299–315.
- Tan, E.J., Thomas, N., Rossell, S.L., 2014. Speech disturbances and quality of life in schizophrenia: differential impacts on functioning and life satisfaction. *Compr. Psychiatry* 55, 693–698.
- Team, R.C., 2017. R: A Language and Environment for Statistical Computing. R Foundation for Statistical Computing, Vienna, Austria 2016.
- Viher, P.V., Stegmayer, K., Giezendanner, S., Federspiel, A., Bohlhalter, S., Vanbellingen, T., et al., 2016. Cerebral white matter structure is associated with DSM-5 schizophrenia symptom dimensions. *Neuroimage Clin.* 12, 93–99.
- Viher, P.V., Stegmayer, K., Giezendanner, S., Federspiel, A., Bohlhalter, S., Wiest, R., et al., 2018. White matter correlates of the disorganized speech dimension in schizophrenia. *Eur. Arch. Psychiatr. Clin. Neurosci.* 268, 99–104.
- Vitulo, E., Tata, M.K., Pignolo, C., Cauda, F., Costa, T., Ando, A., et al., 2017. White matter and schizophrenia: a meta-analysis of voxel-based morphometry and diffusion tensor imaging studies. *Psychiatry Res.* 270, 8–21.
- Wakana, S., Jiang, H., Nagae-Poetscher, I.M., van Zijl, P.C., Mori, S., 2004. Fiber tract-based atlas of human white matter anatomy. *Radiology* 230, 77–87.
- Wang, Y., Fernandez-Miranda, J.C., Verstynen, T., Pathak, S., Schneider, W., Yeh, F.C., 2013. Rethinking the role of the middle longitudinal fascicle in language and auditory pathways. *Cereb. Cortex* 23, 2347–2356.
- Wheeler, A.L., Voineskos, A.N., 2014. A review of structural neuroimaging in schizophrenia: from connectivity to connectomics. *Front. Hum. Neurosci.* 8, 653.
- Woods, S.W., 2004. Chlorpromazine equivalent dose for the newer atypical antipsychotics. *J. Clin. Psychiatry* 64, 663–667.
- Yang, X., Cao, D., Liang, X., Zhao, J., 2017. Schizophrenia symptomatic associations with diffusion tensor imaging measured fractional anisotropy of brain: a meta-analysis. *Neuroradiology* 59, 699–708.
- Zhang, X., Gao, J., Zhu, F., Wang, W., Fan, Y., Ma, Q., et al., 2018. Reduced white matter connectivity associated with auditory verbal hallucinations in first-episode and chronic schizophrenia: a diffusion tensor imaging study. *Psychiatry Res.* 273, 63–70.
- Zhou, Y., Liu, J., Driesen, N., Womer, F., Chen, K., Wang, Y., et al., 2017. White matter integrity in genetic high-risk individuals and first-episode schizophrenia patients: similarities and dissociations. *Biomed. Res. Int.* 2017, 3107845.

Supplementary Material for
'Formal thought disorder is related to aberrations in language-related
white matter tracts in patients with schizophrenia'

This file includes:

Supplementary Table 1

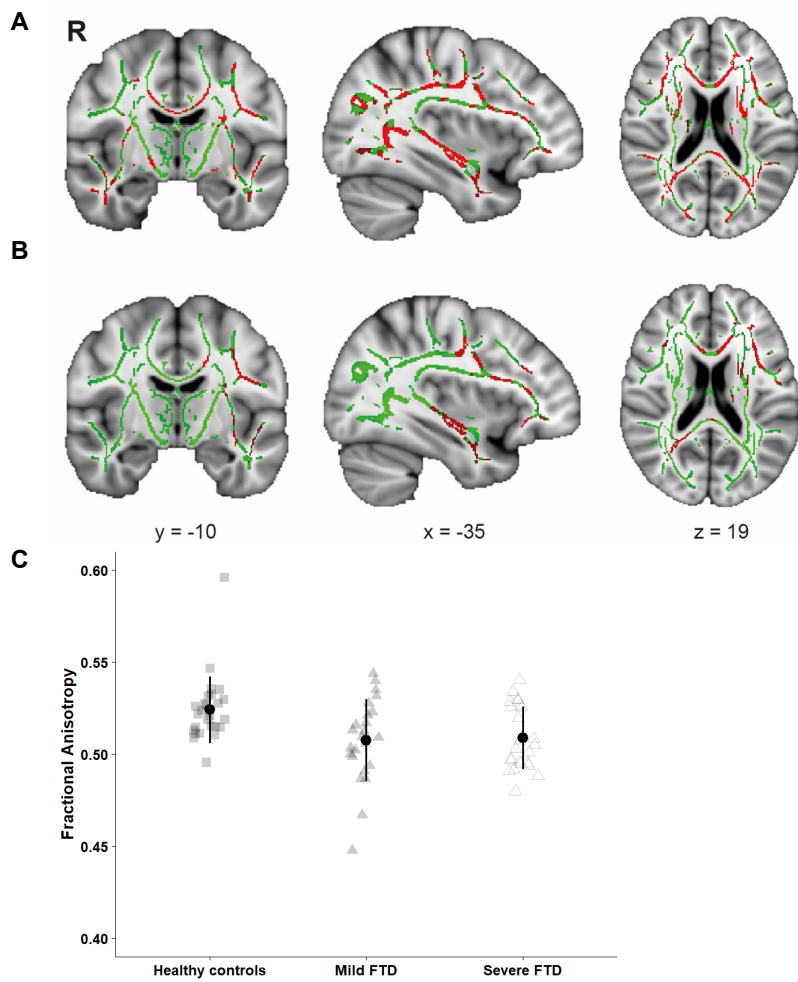
Supplementary Figure 1 - 6

Supplementary Table 1. Mean FA values (\pm SE) from all regions of interest (ROIs) and the whole brain skeleton in healthy controls, patients with mild (mFTD), and patients with severe formal thought disorder (sFTD).

Anatomical regions according to JHU atlas	Controls M (SE) [range] (n=26)	Patients		Group differences ^a			
		Mild FTD M (SE) [range] (n=27)	Severe FTD M (SE) [range] (n=22)	H	df	p	
AF							
	L	0.533 (0.005) [0.506; 0.564]	0.516 (0.006) [0.437; 0.564]	0.514 (0.004) [0.471; 0.554]	7.23	2	0.026*
	R	0.528 (0.005) [0.499; 0.616]	0.515 (0.005) [0.470; 0.582]	0.510 (0.004) [0.470; 0.539]	5.89	2	0.053
IFOF							
	L	0.492 (0.004) [0.454; 0.575]	0.474 (0.005) [0.394; 0.511]	0.474 (0.004) [0.445; 0.509]	10.45	2	0.005*
	R	0.494 (0.004) [0.464; 0.572]	0.478 (0.004) [0.413; 0.513]	0.475 (0.004) [0.443; 0.504]	11.67	2	0.003*
ILF							
	L	0.463 (0.004) [0.428; 0.545]	0.446 (0.005) [0.382; 0.491]	0.447 (0.004) [0.423; 0.481]	8.70	2	0.013*
	R	0.430 (0.005) [0.409; 0.534]	0.414 (0.004) [0.356; 0.447]	0.412 (0.004) [0.387; 0.440]	9.65	2	0.008*
SLF							
	L	0.461 (0.005) [0.438; 0.553]	0.445 (0.005) [0.381; 0.494]	0.445 (0.004) [0.422; 0.478]	9.03	2	0.011*
	R	0.451 (0.004) [0.429; 0.532]	0.438 (0.004) [0.389; 0.486]	0.435 (0.004) [0.412; 0.466]	9.63	2	0.008*
UNC							
	L	0.484 (0.005) [0.450; 0.548]	0.468 (0.005) [0.402; 0.508]	0.464 (0.005) [0.430; 0.511]	6.34	2	0.042*
	R	0.485 (0.004) [0.446; 0.544]	0.471 (0.005) [0.421; 0.520]	0.465 (0.005) [0.423; 0.521]	9.53	2	0.009*
Whole brain							
		0.478 (0.003) [0.452; 0.554]	0.462 (0.004) [0.408; 0.499]	0.463 (0.004) [0.443; 0.492]	9.65	2	0.008*

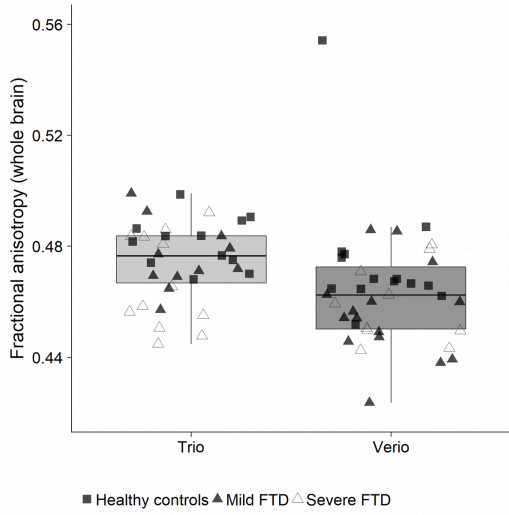
Notes. JHU, Johns Hopkins University; L, left; R, right; AF, arcuate fasciculus; IFOF, inferior fronto-occipital fasciculus; ILF, inferior longitudinal fasciculus; SLF, superior longitudinal fasciculus; UNC, uncinate fasciculus.

*Kruskal-Wallis-Test; Significant at: *, $p < 0.05$.



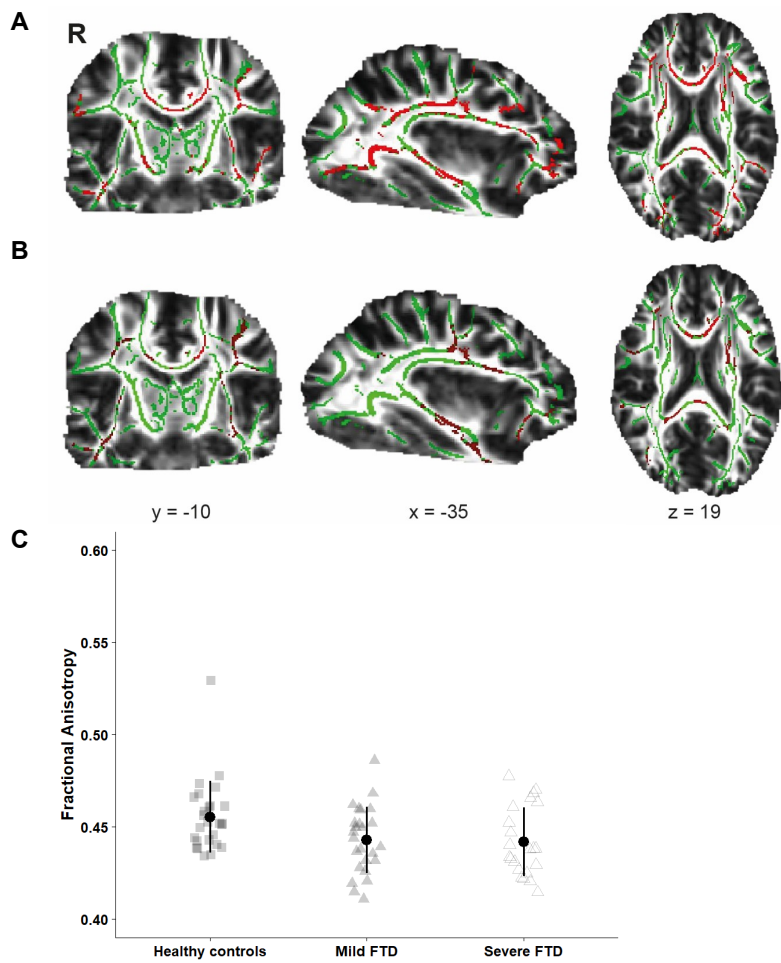
Supplementary Figure 1. Results shown for **(A)** patients with mild formal thought disorder (FTD) and **(B)** patients with severe FTD, when the groups were stratified according to a TLC score of 8 (median split). Corrected tract-based statistics analysis (TBSS) indicates significantly lower fractional anisotropy (FA) throughout the whole WM-skeleton for both patient groups compared to healthy controls (TFCE corrected $p < 0.01$). TBSS results (red) overlaid on the whole brain FA-skeleton (green) and presented on the Montreal Neurological Institute template.

(C) The scatterplots overlaid with the mean (dot) and standard deviation (whiskers) show the distribution of FA for the three groups in the whole brain WM-skeleton.



Supplementary Figure 2. Comparison of whole brain FA values between the two scanners.

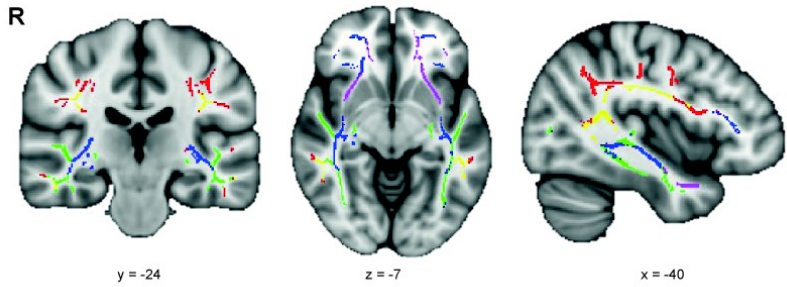
Mean fractional anisotropy values extracted from the whole white matter skeleton for all three groups (healthy controls, patients with mild, and patients with severe formal thought disorder) differed significantly between the Trio and the Verio scanner ($t(73) = 2.12, p = 0.038$). We matched groups and included "scanner" as a covariate in the analyses. In detail, $N = 36$ subjects ($N = 12$ healthy controls, $N = 12$ patients with mFTD, and $N = 12$ patients with sFTD) were measured with the Trio scanner and $N = 39$ subjects ($N = 14$ healthy controls, $N = 15$ patients with mFTD, and $N = 10$ patients with sFTD) were measured with the Verio scanner.



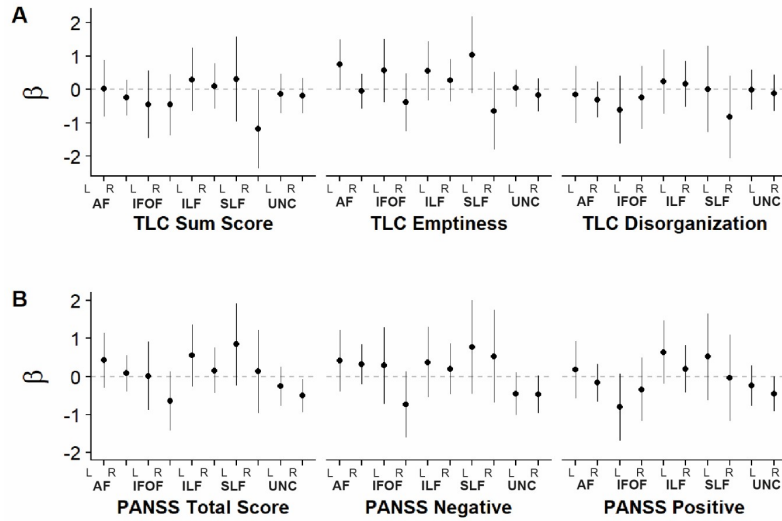
Supplementary Figure 3. Reduced white matter integrity in both (A) patients with mild formal thought disorder (FTD) and (B) patients with severe FTD, when using the study-specific template. Tract-based special statistics (TBSS) revealed significantly lower fractional anisotropy (FA) throughout the whole WM-skeleton for both patient groups compared to healthy controls (TFCE corrected $p < 0.01$). TBSS results (red) are overlaid on the skeletonized study-specific template (green) which is the "most representative" FA image and was used as the target image and affine-

aligned into MNI152 standard space.

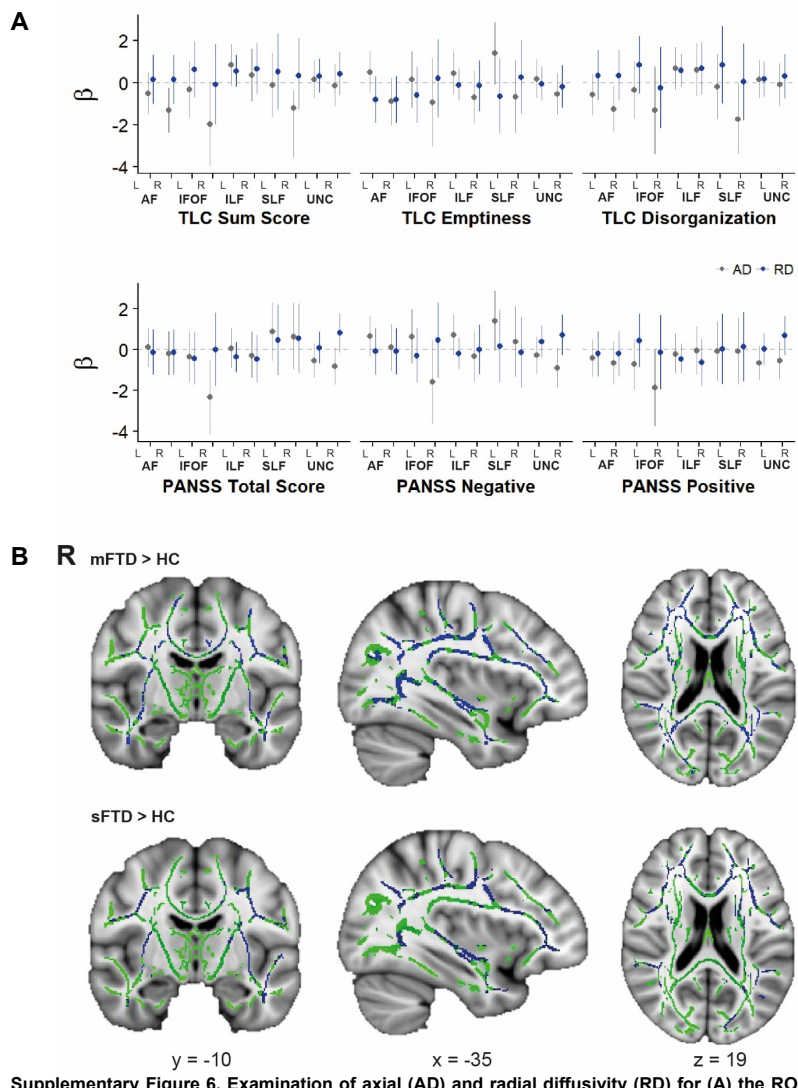
(C) The scatterplots overlaid with the mean (dot) and standard deviation (whiskers) show the distribution of FA for the three groups in the whole brain WM-skeleton.



Supplementary Figure 4. White matter tracts used as regions of interests: arcuate fasciculus (yellow), inferior fronto-occipital fasciculus (blue), inferior longitudinal fasciculus (green), superior longitudinal fasciculus (red), and uncinated fasciculus (rose). Masks are overlaid on the Montreal Neurological Institute template.



Supplementary Figure 5. Results of the ROI and whole brain regression analyses with the additional covariate “education” for (A) formal thought disorder and (B) general psychopathology as outcome variable. The dot plots show the standardized regression coefficients with 95% confidence intervals. Mean beta values (dots) show the partial correlation (positive > 0; negative < 0) of fractional anisotropy with formal thought disorder (FTD). Confidence intervals not touching the zero line indicate an uncorrected significant effect at $p < .05$. FA in the right superior longitudinal fasciculus predicted overall FTD (TLC Sum score) ($p = 0.048$), while FA did neither predict positive nor negative FTD ($p > 0.05$). In line with the model without “education” as covariate, FA in the right uncinate fasciculus predicted overall psychopathology (PANSS Total score) ($p = 0.025$) as well as positive symptoms (PANSS Positive Syndrome scale) ($p = 0.047$).



Supplementary Figure 6. Examination of axial (AD) and radial diffusivity (RD) for (A) the ROIs and (B) the whole brain.

A. Standardized regression coefficients with 95% confidence intervals are shown for severity of formal though disorder (TLC scales) and general psychopathology (PANSS scales). Mean beta

values (dots) show the partial correlation (positive > 0 ; negative < 0) of AD (gray) and RD (blue) with FTD. Confidence intervals not touching the zero line indicate an uncorrected significant effect at $p < .05$. In particular, lower AD in the right arcuate fascicle (AF) ($\beta = -1.33$, $p = 0.016$) and the right superior longitudinal fascicle (SLF) ($\beta = -1.97$, $p = 0.017$) predicted severity of FTD (TLC Sum). Further, lower AD in the right AF ($\beta = -1.27$, $p = 0.024$) and in the right SLF ($\beta = -1.73$, $p = 0.041$) predicted positive FTD (TLC Disorganisation scale). Regarding general psychopathology, lower AD in the right inferior fronto-occipital fasciculus (IFOF) ($\beta = -2.35$, $p = 0.013$) predicted general symptom severity (PANSS Total score). Radial diffusivity did neither predict severity of FTD nor severity of general psychopathology.

B. Corrected tract-based statistics analysis (TBSS) indicates no differences in AD between groups together with significantly higher RD throughout the whole WM-skeleton for both patients with mild FTD (mFTD $>$ HC; TFCE corrected $p = 0.003$) and patients with severe FTD (sFTD $>$ HC; TFCE corrected $p = 0.019$) compared to healthy controls. TBSS results (blue) overlaid on the whole brain RD-skeleton (green) and presented on the Montreal Neurological Institute template.

Reviewer suggestions (Vorschläge für Gutachter)

UZH:

- Prof. Dr. med. Susanne Walitza (susanne.walitza@puk.zh.ch)
- Prof. Dr. phil. Birgit Kleim (birgit.kleim@puk.zh.ch)

External:

- Prof. Dr. med. Stephan Kaiser, Universität Genf (stefan.kaiser@hcuge.ch)
- Prof. Dr. med. Sukwinder Shergill, King's College, London (sukhi.shergill@kcl.ac.uk)

Lecture suggestions (Vorschläge für Probevorlesung)

1. Is there a need for precision medicine in psychiatry?
2. Why clinical research needs to embrace open science and transparency
3. What do we know about placebo response in psychiatry?